THE ROYAL VETERINARY AND AGRICULTURAL UNIVERSITY

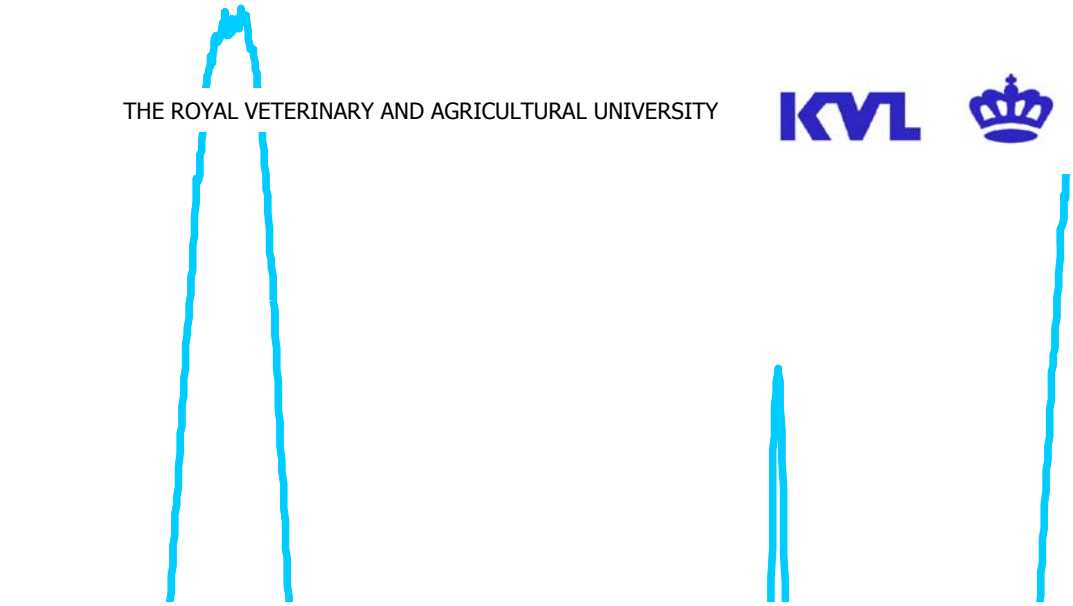

Spectroscopic and chemometric exploration of food quality

- Early prediction of meat quality

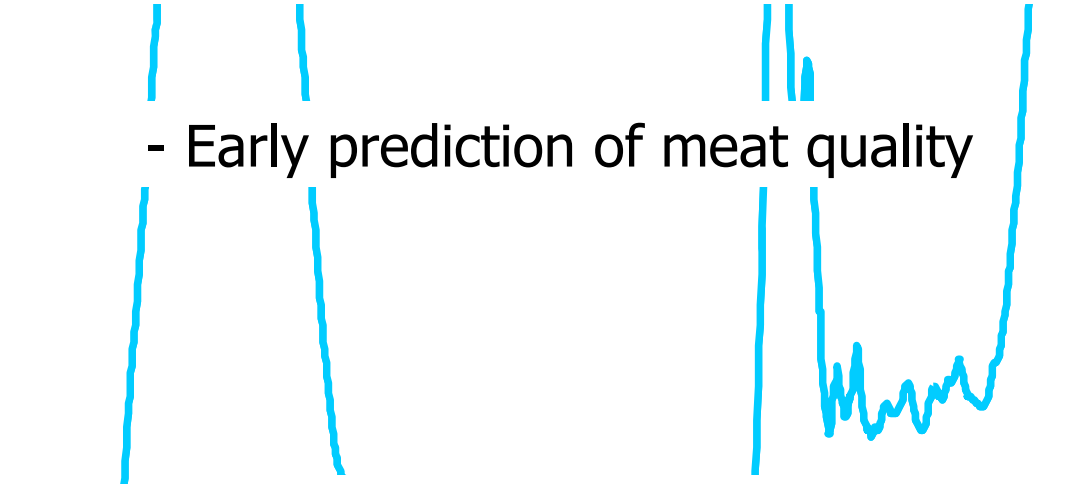

Ph.D. thesis by Dorthe Kjær Pedersen
Department of Dairy and Food Science
Rolighedsvej 30, 1958 Frederiksberg C, Denmark

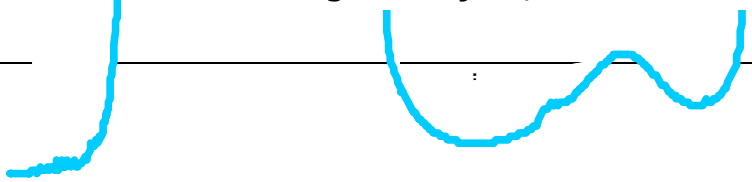

Spectroscopic and chemometric exploration of food quality

- Early prediction of meat quality

Dorthe Kjær Pedersen

Ph.D. Thesis

May 2002

Supervisors:

Associate Professor Søren Balling Engelsen

Professor Lars Munck

Food Technology

Department of Dairy and Food Science

The Royal Veterinary and Agricultural University

Denmark

Development Manager Jan Rud Andersen

Measurements and Chemistry Analyses

Danish Meat Research Institute

Denmark

Preface

This thesis represents three years of research work to fulfil the requirements for a Ph.D. degree at the Royal Veterinary and Agricultural University (KVL), Denmark. The research work was supported by the Ministry of Food, Agriculture and Fisheries and Danske Slagterier during the project 'Early post mortem measurement of WHC (water-holding capacity) and drip loss in fresh pork'. The project was a collaboration between the Food Technology Section of the Department of Dairy and Food Science at KVL, the Danish Meat Research Institute and the Danish Institute of Agricultural Sciences. The supervisors have been Associate Professor Søren Balling Engelsen, KVL, Professor Lars Munck, KVL and Development Manager Jan Rud Andersen, Danish Meat Research Institute.

I am greatly indebted to the Food Technology group, in particular to Lars Nørgaard for introducing me to the world of chemometrics, to Lars Munck for enthusiastic and dedicated discussions, and to Søren Balling Engelsen for introducing me to the possibilities of spectroscopic methods and for educational discussions.

The main part of the experimental work was based on measurements carried out during the slaughter process of pigs and I wish to thank the people at the Research Slaughterhouse in Foulum for making these investigations possible. I especially wish to thank Lars Bager Christensen and Bo Lindberg Jespersen from Danish Meat Research Institute for good collaboration during our commercial slaughterhouse measurements. Thanks also go to Henrik Andersen, Hans Busk, Anders Karlsson and Poul Henckel at the Danish Institute of Agricultural Sciences and to Claus Borggaard, Allan J. Rasmussen and Steffen Holst, Danish Meat Research Institute, for collaboration throughout this study.

During my stay at Matforsk in Ås, Norway, I had the pleasure of working with Gjermund Vogt, Elisabeth Olsen, Frank Lundby and Bjørg Egelandsdal, whom I also want to thank.

Finally, I would like to thank all the people at Food Technology for their help and inspiration and for providing a good working environment. I especially wish to thank Jesper, Harald, Rasmus, Frans, Lisbeth T., Henrik, Charlotte, Åsmund, Allan, Lisbeth H., Anna-Marie and Gilda.

Summary

The desire to develop non-invasive rapid measurements of essential quality parameters in foods is the motivation of this thesis. Due to the speed and non-invasive properties of spectroscopic techniques, they have potential as on-line or at-line methods and can be employed in the food industry in order to control the quality of the end product and to continuously monitor the production. In this thesis, the possibilities and limitations of the application of spectroscopy and chemometrics in rapid control of food quality are discussed and demonstrated by the examples in the eight included publications. Different aspects of food quality are covered, but the focus is mainly on the development of multivariate calibrations for predictions of rather complex attributes such as the water-holding capacity of meat, ethical quality of the slaughtering procedure, protein content of single wheat kernels and contamination of fish oil by toxic environmental substances.

Fourier transform infrared (FT-IR) and Raman spectroscopy proved to be of potential utility for process line measurements of meat quality (water-holding capacity). Preliminary studies revealed a high correlation ($r = 0.89$) between water-holding capacity and FT-IR spectra with prediction errors of 0.85-1.4 % drip loss using Partial Least Squares Regressions. A further development of vibrational spectroscopic methods can be of valuable use in the slaughtering industry, aiming at a better utilization of the raw material through early classification of the meat. Visual and near infrared (VIS/NIR) spectroscopy was evaluated for the ability to assess the depth of CO_2 stunning of slaughter pigs. Near infrared transmittance (NIT) was applied for the assessment of the quality of single wheat kernels. The combination of fluorescence measurements of fish oil and multi-way chemometrics demonstrated the potential for screening of environmental contamination in complex food samples. Significant prediction models were established with correlation coefficients in the range from $r = 0.69$ to $r = 0.97$ for dioxin. Further development of the fluorescence measurements of dioxin in fish oil will, for the fish industry, be a valuable tool for monitoring the quality of their oil products, especially when the EU introduces a limit of 6 ng/kg dioxin later this year.

In order to improve calibrations and model interpretation, methods of spectral pre-transformations, including the recently developed Extended Invented Signal

Correction, and variable region selection were used during the data analysis throughout this study.

The uncertainty of reference analyses and their influence on the subsequent multivariate spectroscopic calibration are discussed throughout the thesis. A general challenge during the development of multivariate calibrations in this study was the accuracy of the reference parameters of interest. It is emphasized that it is of utmost importance to incorporate knowledge of the chemical and biological nature of the samples and of the qualifications of the applied spectroscopic and reference methods during the validation of multivariate calibrations.

Resumé

Motivationen for denne afhandling har været et ønske om at udvikle hurtige og ikke-invasive målinger til vigtige kvalitetsparametre i levnedsmidler. På grund af deres hurtighed og ikke-invasive egenskaber er spektroskopiske teknikker potentielle som on-line eller at-line metoder og kan anvendes i levnedsmiddelindustrien til kvalitetskontrol af slutprodukter og løbende overvågning af produktionen. Forskellige aspekter af levnedsmiddelkvalitet bliver behandlet i denne afhandling, men fokus er hovedsageligt lagt på udviklingen af multivariate kalibreringer til prædiktion af ret komplekse egenskaber som vandbindingsevne af kød, etisk kvalitet under slagteproceduren, proteinindhold af enkelte hvedekerner og forurening med giftige miljøstoffer i fiskeolie.

Fourier transform infrarød (FT-IR) og Raman spektroskopi har vist sig at være af potentiel interesse for proceslinie-målinger af kødkvalitet (vandbindingsevne). Foreløbige undersøgelser har vist en høj korrelation (r = 0,89) mellem vandbindingsevnen og FT-IR spektre med prædiktionsfejl på 0,85-1,4 % dryptab ved anvendelse af Partial Least Squares Regression. Yderligere undersøgelser af vibrationsspektroskopiske metoder er af stor værdi for slagteri-industrien for at opnå en bedre udnyttelse af råvarerne gennem tidlig klassifikation af kødet. Visuel og nær infrarød (VIS/NIR) spektroskopi er blevet evalueret med hensyn til bestemmelse af graden af CO_2-bedøvelse af slagtesvin. Nær infrarød transmission (NIT) blev anvendt til bestemmelse af kvaliteten af enkelte hvedekerner. Kombinationen af fluorescens-målinger på fiskeolie og multivejs kemometri viste sig at have potentiale til screening af miljø-forurening af komplekse levnedsmiddelprøver. Signifikante prædiktionsmodeller viste korrelationskoefficienter til dioxin i området r = 0,69 til r = 0,97. For fiskeindustrien vil yderligere udvikling af fluorescens-målinger af dioxin i fiskeolie blive et værdifuldt redskab til at overvåge kvaliteten af deres olieprodukter, især når EU introducerer en grænse på 6 ng/kg dioxin i løbet året.

Med henblik på at forbedre kalibreringer og model-fortolkning blev metoder til spektral forbehandling, inklusive den nyligt udviklede Extended Invented Signal Correction, og variabeludvælgelse anvendt ved dataanalysen i dette studie.

Usikkerheden af referenceanalyser og indflydelsen på de efterfølgende multivariate spektroskopiske kalibreringer bliver diskuteret igennem hele afhandlingen. En

meget generel udfordring under udviklingen af multivariate kalibreringer i dette studie var nøjagtigheden af de pågældende referenceparametre. Det bliver understreget, at det er yderst vigtigt at indføje viden om prøvernes kemiske og biologiske natur og om begrænsningerne for de anvendte spektroskopiske og referencemetoder under valideringen af multivariate kalibreringer.

List of publications

Paper I

Monitoring Industrial Food Processes Using Spectroscopy & Chemometrics. Dorthe Kjær Pedersen and Søren Balling Engelsen. *New Food* **2** (2001): 9-13.

Paper II

Why high-speed methods never exceed a correlation of 0.9 to drip loss. A chemometric investigation

Dorthe Kjær Pedersen, Harald Martens, Lars Bager Christensen and Søren Balling Engelsen. In prep.

Paper III

Method and apparatus for prediction of the drip loss of a part of a carcass. Dorthe Kjær Pedersen, Jan Rud Andersen, Lars Bager Christensen and Søren Balling Engelsen. *Patent* (2000) **PR 173748**.

Paper IV

Early prediction of water-holding capacity in meat by multivariate vibrational spectroscopy. Dorthe Kjær Pedersen, Sophie Morel, Henrik Jørgen Andersen and Søren Balling Engelsen. *Meat Science*. Submitted.

Paper V

Near-infrared absorption and scattering separated by Extended Inverted Signal Correction (EISC). **Analysis of NIT spectra of single wheat seeds**. Dorthe Kjær Pedersen, Harald Martens, Jesper Pram Nielsen and Søren Balling Engelsen. *Applied Spectroscopy* (2002). Accepted.

Paper VI

Assessment of the depth of CO_2 stunning of slaughter pigs by Visual and Near Infrared spectroscopy on blood. Dorthe Kjær Pedersen, Steffen Holst and Søren Balling Engelsen. In prep.

Paper VII

Development of non-destructive screening methods for single kernel characterisation of wheat. Jesper Pram Nielsen, Dorthe Kjær Pedersen and Lars Munck. *Cereal Chemistry*. Submitted.

Paper VIII

Screening for dioxin contamination in fish oil by PARAFAC and N-PLSR analysis of fluorescence landscapes. Dorthe Kjær Pedersen, Lars Munck and Søren Balling Engelsen. *Journal of Chemometrics* (2002). Accepted.

Table of contents

Abbreviation list

FAD	Flavin Adenine Dinucleotide
FT-IR	Fourier Transform InfraRed
GC-MS	Gas Chromatography-Mass Spectrometry
HPLC-MS	High Performance Liquid Chromatography-Mass Spectrometry
MLR	Multiple Linear Regression
MSC	Multiplicative Signal Correction
NADH	Nicotinamide Adenine Dinucleotide, reduced form
NADPH	Nicotinamide Adenine Dinucleotide Phosphate, reduced form
NIR	Near InfraRed
NIT	Near Infrared Transmittance
PARAFAC	PARAllel FACtor
PCA	Principal Component Analysis
PCB	PolyChlorinated Biphenyls
PCDD	PolyChlorinated Dibenzo-*p*-Dioxin
PCDF	PolyChlorinated DibenzoFuran
PLSR	Partial Least Squares Regression
RMSECV	Root Mean Squared Error of Cross Validation
RMSEP	Root Mean Squared Error of Prediction
TBARS	2-thiobarbituric acid assay
VIS	Visual
WHC	Water-Holding Capacity

1. Introduction

This thesis is motivated by the desire to develop non-invasive rapid measurements of essential quality parameters in foods. Such measurements can be employed in the food industry in order to control the quality of the end product and to continuously monitor the production. The methods and results in this study can be of practical use for the food industry as sampling techniques and spectroscopic instruments improve and become cheaper in the future, and the techniques will be more readily available, allowing simpler and less expensive on-line applications. The current trends in monitoring of food quality are to move the measurements of quality from the laboratories to the process lines, such as the Autofom (SFK Technology, Herlev, Denmark), which is a fully automatic grading system for pork quality using ultrasound, the application of on-line near infrared spectroscopy in the production of sugar (Danisco Sugar, Copenhagen, Denmark) or on-line control of ammonia concentration in pectin amidation liquid by near infrared spectroscopy (CP Kelco, Lille Skensved, Denmark). Such on-line quality controls are made possible due to the continuous development of spectroscopic on-line methods. The spectroscopic methods are fast, non-invasive and highly reproducible, which makes them excellently suited for the on-line challenge. Moreover the output from the spectroscopic methods provides multivariate physical and chemical fingerprinting, which contains a wealth of information concerning the object of measurement, and yields the possibility of simultaneous assessment of several quality parameters.

The aim of this thesis is to discuss the possibilities and limitations for the application of spectroscopy and chemometrics in rapid control of food quality, demonstrated by the examples in the eight included publications. It was the aim to investigate why and how the methods work in order to obtain new or support known understanding of the food processes. The direct applications of the methods as screening methods are investigated, as well as the interpretation and understanding of the attained information from the measurements of the food samples. In Chapter 2 rapid remote spectroscopic methods are presented. Chapter 3 and Paper II discuss the uncertainty of reference analyses and their influence on subsequent multivariate spectroscopic calibration. Chemometric pre-transformation of spectral data is discussed in Chapter 4 and Paper V. In Chapter 5 and Papers III, IV, VI, VII and VIII applications of spectroscopic measurements for investigation of food quality

are presented. Chapter 6 completes the thesis with conclusions and perspectives. The papers in full length are found at the end of the thesis.

Quality of food covers many aspects, such as functional, technological, sensory, nutritional, toxicological, regulatory and ethical aspects. Functional and technological quality is related to the processing and storing of the food and is traditionally measured by physical and chemical methods, while sensory quality is the eating quality as experienced by the consumer. Contamination, environmental or bacterial, of foods or raw materials for food production affect the toxicological quality. A need for ethical quality exists in meat production, where handling of live animals is critical. Different aspects of food quality are treated in this thesis: the functional, technological and sensory quality of porcine meat regarding water-holding capacity (Paper II, III and IV), the technological and nutritional quality as well as the protein content of wheat kernels (Paper V and VII), the toxicological and regulatory quality of dioxin contaminated fish oil (Paper VIII), and the ethical quality concerning the stunning of slaughter pigs (Paper VI).

The major part of this thesis originates from the project 'Early post mortem measurement of WHC (water-holding capacity) and drip loss in fresh pork'. The project was a collaboration between the Food Technology Section of the Department of Dairy and Food Science at KVL, the Danish Meat Research Institute (SF) and the Danish Institute of Agricultural Sciences (DJF). The objective of the project was to obtain knowledge of the meat quality of pig carcasses from physico-chemical measurements carried out early in the slaughter process, i.e. within one hour after sticking. Hence, it would be a remarkable breakthrough if it was possible to predict the meat quality as measured by the water-holding capacity, and thereby be able to classify according to meat quality before the carcasses reach the cooler rooms. The strategy for meeting the objective entailed the screening of model carcasses with different 'engineered' meat qualities by a number of predominantly spectroscopic techniques. On basis of this screening, techniques showing potential for estimating meat quality were selected to undergo further development and testing for the Danish pig slaughter industry.

1.1. Chemometrics in food production

Exploratory multivariate data analysis is applied for investigation of the spectral data measured during this study. The aim of the exploratory approach is to describe the complex multivariate information in the data in simple graphic displays without interference of *a priori* knowledge and let the evaluation based on plots and graphs generate the hypotheses for further interpretation. The tool for exploratory multivariate data analysis is chemometrics, which provides practical problem solving by efficient utilization of experimental data. For complex samples such as food material, data from spectroscopic instruments are typically so complicated that direct interpretation is impossible; peaks overlap to the extent that none are recognizable. That is why chemometric methods need to be applied for the data to be analysed effectively. In addition, chemometrics makes it possible to obtain real-time information from data, which is a clear advantage for the development of on-line methods. The fast, precise and non-destructive spectroscopic methods in combination with chemometrics are suitable for process analysis and optimization leading to improved productivity, efficiency and product quality.

The end quality of food reflects both the quality of the raw ingredients and the actions of the processing unit operations. Food quality is traditionally measured by chemical, physical and sensory methods. Some of these methods are quite time-consuming and all the methods are destructive. Today, it is possible to replace most of these inconvenient methods by instrumental, rapid and non-destructive techniques like near infrared (NIR), Fourier transform infrared (FT-IR) or fluorescence spectroscopy. However, optimum utilization of these techniques requires chemometric data analysis. Multivariate methods such as PCA and PLSR have demonstrated their superior performance when analysing spectroscopic information in quality control measurements. Today, chemometrics is applied in many aspects of the food and feed production, for instance, in the production of cereals, dairy products, meat, fruit, vegetables, oils and alcoholic beverages.

1.2. Complex food data

Multivariate spectroscopic measurements of complex materials like foods are sampled directly from the multivariate and complex world, for example, from a food production chain like a slaughter line or a fish oil factory. The samples applied for

analysis are not constructed in any way, i.e. by mixing a few known components in a controlled laboratory system, and will rarely behave as ideal systems. Usually the samples are not even exposed to any kind of pre-treatment such as separation or dissolution of the constituents. Working with complex food data requires a great deal of emphasis on the nature of the samples and experience with the instrumental and reference methods. In order to decide whether developed models involving complex food data are of any use, it is crucial to apply both chemometric validation of models (described in Chapter 2.3.3.) as well as chemical and biological validation of the methods.

1.3. Chemical and biological validation

In chemometric models carried out on complex food data, chemometric validation is not sufficient for getting an absolute picture of the modelling performance. Chemical and biological validation is necessary in order to estimate if a chemometric model based on spectroscopic data is suitable for the practical purpose it was designed for, for example as a quality control tool in the food industry. Chemical and biological validation includes evaluation of the calibration samples concerning, for instance, important sample characteristics, process conditions and sampling methods. The applied analytical methods, both spectroscopic measurements and reference measurements, must be evaluated with respect to, for instance, detection limits, instrumental noise and influence from the surroundings. Traditional measurements of the quality of foods are often related to significant errors due to lack of homogeneity of complex food materials and to the many steps of analyses often used in the methods of reference analysis.

It is normally considered progress to replace an uncertain and time-consuming chemical method with a more precise and faster spectroscopic method. However, the ‘new’ spectroscopic method relies on the ‘old’ reference method through the calibration step. Hence, an estimation of the uncertainty of the chemical reference methods can be of great value in order to judge whether the ‘new’ method is suited as a practical replacement for the ‘old’ method. In other words, a comparison of the modelling error found by chemometric validation with the uncertainty estimate of the reference method can provide an approach to the ‘true’ error of measurement.

2. Rapid remote spectroscopic measurements of food quality

Spectroscopic techniques are very suitable for the analysis of food characteristics and chemical components. They are considered as sensitive, remote, multivariate sensors and they are non-destructive, rapid, environmentally friendly and non-invasive, which makes the methods suitable for on-line or at-line process control. In the last two decades, rapid spectroscopic measurements have advanced in quality control in many areas of food production as outlined in Paper I. Spectroscopic methods for measurements of food quality include ultraviolet and visual absorption, fluorescence emission, near infrared and mid infrared absorption, Raman scattering, nuclear magnetic resonance, microwave absorption and (ultra)-sound transmission. The spectroscopic methods based on different regions of the electromagnetic spectrum and different physical principles have different sensing capabilities. The methods, however, share the ability to provide rapid multivariate information on the sample being monitored, which in turn makes it possible to simultaneously determine several quality parameters. In this chapter Fourier transform infrared (FT-IR), Raman, near infrared (NIR and NIT) and fluorescence spectroscopy are described.

2.1. Vibrational spectroscopy

Molecules can vibrate only at specific frequencies that correspond to specific energy levels. The energy of most molecular vibrations corresponds to that of the mid infrared region of the electromagnetic spectrum, which is between 4000 cm^{-1} and 400 cm^{-1}. Infrared (IR) and Raman spectroscopy are complementary techniques and have different levels of sensitivity to different types of vibrations, also called ‘selection rules’; thus, different molecules in different environments are measured more accurately with the more appropriate technique. Infrared light is absorbed when the oscillating dipole moment (due to a molecular vibration) interacts with the oscillating infrared beam. In the Raman effect a corresponding interaction occurs between the light and the polarizability of the molecule.

A complex molecule has a large number of vibrational modes (3N-6, where N is the number of atoms). Some of these molecular vibrations can be associated to

vibrations of individual bonds or functional groups, while others are more delocalized and must be considered as vibrations of the whole molecule. The localized vibrations can be stretching, bending, rocking, twisting, or wagging. When the molecule is irradiated with infrared light, the vibrating bond will only absorb energy if the frequencies of the light and the vibration are the same.

A group frequency is a vibrational frequency (usually wavenumber) that is characteristic for a particular chemical functional group. Some group frequencies fall within a restricted range, regardless of the compound in which the group is found, while other group frequencies are highly affected by the matrix, which the group is a part of. Functional groups of special interest in infrared spectroscopy are primarily C=O, O-H, N-H and C-H, mostly originating from the side groups of molecules, while the interesting groups in Raman, for example, are C-C, C=C, C≡N and aromatic groups, mostly originating from the skeleton of molecules.

2.1.1. Infrared spectroscopy

Infrared (IR) spectroscopic instruments are designed to measure the intensity of molecular vibrations as a function of wavelength or wavenumber. IR has been a common qualitative technique for the identification and verification of chemical compounds. The first infrared instruments were dispersive in which radiation is separated spatially into its component wavenumbers by a dispersive element such as a prism or a diffraction grating. But since the early 1970's, Fourier transform infrared (FT-IR) spectroscopy has been available (Griffiths and de Haseth, 1986). FT-IR technology has substantial potential as a quantitative quality control tool for the food industry, because the technique is robust, convenient, rapid and automatable, and in conjunction with attenuated total reflectance (ATR) technology, provides easy sample handling for 'difficult samples' such as food.

FT-IR spectroscopy is based on Michelson interferometry. A diagram of an interferometer is shown in Figure 2-1. A Michelson interferometer uses a beamsplitter to divide the radiation from the source into two parts, one reflected to a fixed mirror and one to a moving mirror. The two beams undergo constructive and destructive interference as they recombine at the beamsplitter due to the varying path difference between the two mirrors. The recorded interference pattern is called an interferogram.

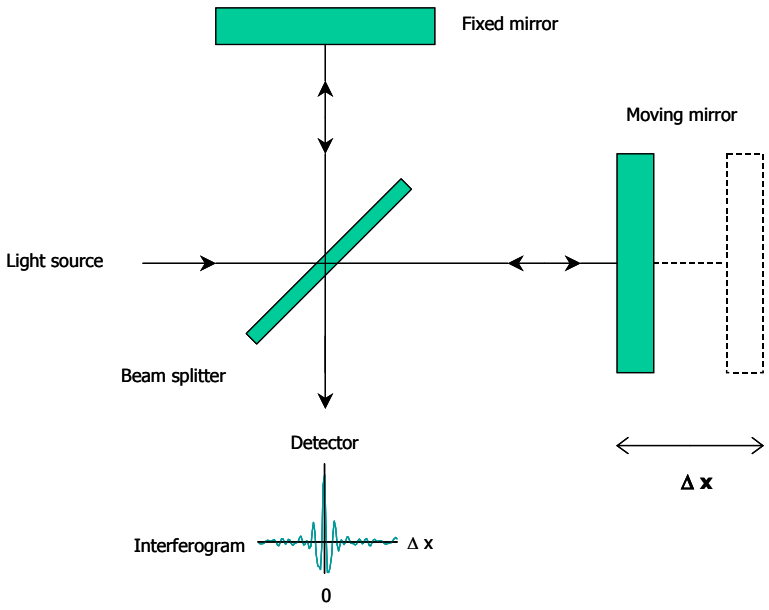

Figure 2-1. Diagram of an interferometer

An interferogram is recorded by measuring the detector signal as a function of the position of the moving mirror during the movement, and is thus a summation of all cosine functions produced by the various wavelengths. It is possible to calculate the contribution of each wavelength from this interferogram by a Fourier transformation from the time domain to the frequency domain. In this way all frequencies are measured simultaneously. This is a considerable advantage compared to the dispersive technique, where the frequencies are measured successively by rotating the grating. Due to the ability of the FT-IR to measure more data points at the same time, it is possible to improve the signal-to-noise ratio by averaging many spectra. Moreover, all the light reaches the detector in the FT-IR instrument, in contrast to a dispersive instrument where energy is lost by the use of slits. Another advantage of the FT-IR technique is that wavenumber calibration is very accurate and robust due to the laser control of the mirror position. All these advantages make FT-IR very

potential as a fast on-line solution for the food industry. One general disadvantage of IR spectroscopy is that IR radiation cannot be transmitted through glass or quartz due to absorption, which restricts the use of optical fibres and thereby on-line installation. Another disadvantage of IR spectrometers is that water absorbs heavily and can hide spectral information of interest, and thus limits the use of IR for foods with high water content.

The most common principle for measurement of a sample by FT-IR is transmittance measurements using different sample cells dependent on the physical state and chemical properties of the sample material. The measurement of transmittance usually involves very small amounts of sample material (mg) and requires that the sample is measured as a liquid or is pressed into a pellet, often with KBr (potassium bromide). Successful FT-IR applications in food systems depend largely on the use of ATR (attenuated total reflectance) technology, as it provides a simple and reproducible means of handling products by being applicable to liquids, solutions, viscous materials and flexible solids. Figure 2-2 **s**hows the principle of ATR.

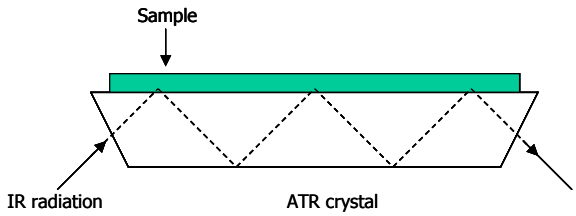

Figure 2-2. The principle of the attenuated total reflection technique showing the penetration of the radiation beam into the sample material pressed closely to the crystal

To obtain a spectrum by using the ATR technique, the sample is brought into optical contact with a crystal. With a properly chosen radiation angle, the beam will strike the flat surfaces at less than the critical angle leading to 'total' internal reflection. In reality, the radiation beam penetrates slightly beyond the surface of the crystal during each reflection, and with sample material pressed closely to the crystal the beam will travel a small distance through the sample at each reflection, thus providing transmission spectra of the outer layers of the sample. The depth of penetration into the sample is a function of the refractive index of the crystal and

sample, the launch angle and the wavelength. Because the depth of penetration also varies with wavelength, ATR/FT-IR spectra exhibit baseline curvature, especially at the lower frequencies. The main advantage of ATR is very easy sampling. Some of the disadvantages are that the spectra are sensitive to the applied pressure, and the spectral intensity depends on contact between crystal and material.

Among the characteristic absorption bands associated with the macrocomponents of foods which contribute to the IR spectrum are the carbonyl ester and CH signals associated with fat, the carbonyl and amide signals for protein, the hydroxyl bands for carbohydrate and the HOH bending absorption of water. Table 2-1 and Figure 2-3 display the characteristic absorption bands of a food product.

Table 2-1. The spectral bands observed in the FT-IR and Raman spectra of porcine meat 30-40 min after slaughter (Paper IV)

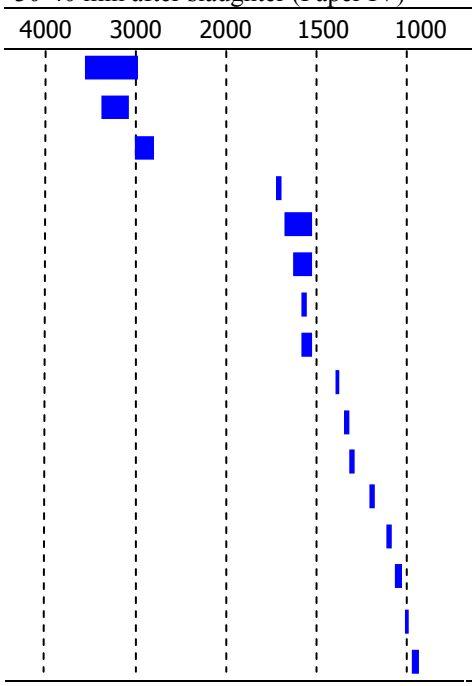

Vibration	IR	Raman	Meat component
OH str.	X		Water
NH str.	X	X	Protein
CH str.	X	X	Fat
C=O	X	X	Fat
HOH bend	X		Water
Amide I	X	X	Protein
C=C str. cis		X	Fat
Amide II	X	X	Protein
C-O str.	X	X	Fat
C-O str.	X	X	Fat
CH bend		X	Protein
Amide III	X	X	Protein
C-O str.	X		Glycogen
C-O-C str.	X		Glycogen
aromatic ring		X	Protein
α-helix		X	Protein

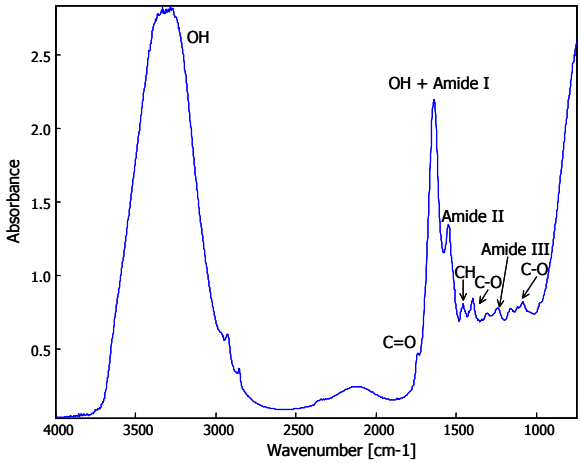

Figure 2-3. FT-IR spectrum (4000-750 cm^{-1}) of porcine meat (Paper IV)

FT-IR has been used in several studies of different foods or food ingredients; e.g., milk (van de Voort *et al.*, 1992; Nathier-Dufour *et al.*, 1995; Hansen, 1998), sugars (Dupuy *et al.*, 1993a,b; Mirouze *et al.*, 1993; Bellon-Maurel *et al.*, 1995a,b; Kameoka *et al.*, 1998a,b), pectins (Engelsen and Nørgaard, 1996), corn starch (Dolmatova *et al.*, 1998), meat (Murcia *et al.*, 1994; Dion *et al.*, 1994; Rannou and Downey, 1997; Al-Jowder *et al.*, 1997, 1999; McElhinney *et al.*, 1999; Iizuka and Aishima, 1999, 2000), edible oils (Ismail *et al.*, 1993; van de Voort *et al.*, 1993, 1994, 1995; Liescheski, 1996; Dahlberg *et al.*, 1997; Engelsen, 1997; Ripoche and Guillard, 2001) and fruit products (Bellon, 1993; Defernez and Wilson, 1995; Defernez *et al.*, 1995, 1997; Ferreira *et al.*, 2001). FT-IR with photoacoustic sampling has recently been applied to low-moisture food products (Irudayaraj *et al.*, 2000, 2001) and to meat (Yang and Irudayaraj, 2001). There have even been a few on-line applications used on sugar solutions and fruit concentrate (Kemsley *et al.*, 1992, 1993) and on olive oil by silver halide fibre probes (Küpper *et al.*, 2001), which showed a great potential for FT-IR as a quality control technique for the food industry. One of the problems with FT-IR as an on-line method is the lack of suitable probes. IR probes are usually made by a toxic halogenide (Wilson and Tapp, 1999; Chatzi *et al.*, 1997; Lowry *et al.*, 1993, 1994), which is not permitted in food production.

2.1.2. Raman spectroscopy

Raman scattering is based on the weak, inelastic scattered side bands which arise when illuminating a sample with a strong monochromatic light, a laser. Like mid-infrared, Raman scatter measures the fundamental molecular vibrations, however, with different selection rules. The Raman effect was discovered in 1928 and described as follows: *When radiation passes through a transparent medium, the species present scatter a fraction of the beam in all directions. The wavelength of a small fraction of the radiation scattered by certain molecules differs from that of the incident beam and the shifts in wavelength depend upon the chemical structure of the molecules responsible for the scattering* (Raman and Krishnan, 1928). The phenomenon results from the same type of vibrational changes that are associated with infrared absorption. Thus, the difference in wavelength between the incident and scattered radiation corresponds to absorbed wavelengths in the mid infrared region.

Raman spectra are obtained by irradiating a sample with a powerful laser source of visible (e.g. 532 nm, 633 nm or 785 nm) or near infrared (e.g. 1064 nm) monochromatic radiation. Most of the scattered light consists of the parent line, the Rayleigh line. Much weaker lines, which constitute the Raman spectrum, occur at lower and higher energies and are due to scatter of light coupled with vibrational excitation or decay, respectively. The difference in frequency between the Rayleigh line and the Raman line is the frequency of the corresponding vibration. At the very most, the intensities of Raman lines are 0.001% of the intensity of the light source (Skoog and Leary, 1992). As a consequence, their detection and measurement are difficult, as the Rayleigh line has to be efficiently filtered from the weak Raman bands. An important advantage of Raman spectra over infrared spectra lies in the fact that water does not cause interference. In addition, glass or quartz cells or optical fibres can be employed, which makes Raman spectroscopy an attractive alternative to the difficult on-line implementation of mid infrared sensors (Dao and Jouan, 1993; Keller *et al.*, 1993; Schrader, 1996). A disadvantage of Raman spectroscopy is the interference by fluorescence of the sample or of impurities in the sample. This problem is largely overcome by the use of a near infrared (λ = 1064 nm) laser source (Keller *et al.*, 1993), which will rarely excite fluorescence.

The near infrared laser, though, provides weaker Raman bands, as the Raman efficiencies depend on the wavelength of the source by $\frac{1}{\lambda^4}$.

Raman is a very powerful technique for food analysis purposes which has been used for studying edible oils (Góral and Zichy, 1990; Sadeghi-Jorabchi *et al.*, 1991; Engelsen, 1997; Davies *et al.*, 2000; Baeten *et al.*, 2001), studying changes of food components (Góral and Zichy, 1990; Ozaki *et al.*, 1992; Belton, 1993; Fontecha *et al.*, 1993; Li-Chan, 1996; Engelsen and Nørgaard, 1996; Bouraoui *et al.*, 1997; Ogawa *et al.*, 1999), analysing dietary fibre in cereal foods (Archibald *et al.*, 1998a,b), identification and quantification of foodborne bacteria (Harhay and Siragusa, 1999), studying muscle fibres (Pezolet *et al.*, 1978a,b, 1980) and predicting meat quality (Paper III). Raman spectroscopy has also been tested in connection to warmed-over flavour in porcine meat (Brøndum *et al.*, 2000a), but without success. The rather few applications of Raman spectroscopy as an on-line method in food production may be owing to tradition or to the fact that the technique is considered quite advanced.

2.1.3. Near infrared spectroscopy

Over the last decade, near infrared (NIR) spectroscopy has been successfully implemented as a fast at-line and on-line quality control method in many areas of the food industry. The vibrational overtone and combination bands appearing in the near infrared spectral region contain an abundance of chemical information comparable to the mid infrared (IR) region, as seen in Figure 2-4. NIR spectroscopy is defined as the spectral area from 780 nm to 2500 nm and primarily involves C-H, O-H and N-H overtones and combinations of the fundamental vibrational transitions in the IR region. Usually, the first overtones are reduced by a factor of 10, and the second overtones are reduced by a factor of 100.

It is common to divide the NIR area in two parts. Light in the range 1200 nm to 2500 nm is absorbed heavily by water and is therefore used for reflection measurements, while the range 780 nm to 1200 nm is also suitable for transmission measurements (NIT), since the water absorption is significantly less. NIR spectroscopy is basically an indirect method, and the spectra are essentially non-specific; hence, different constituents have broad overlapping peaks. For this reason

NIR measurements have to be calibrated against samples of known chemical composition, and the success of the NIR method is therefore closely linked to the use of multivariate regression methods.

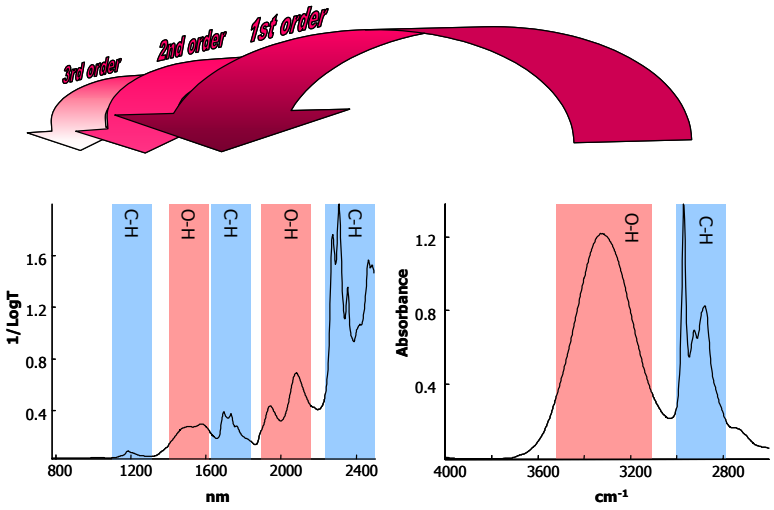

Figure 2-4. The principle of near infrared spectroscopy is demonstrated with a spectrum of ethanol. The motif from the fundamental stretching vibrations in the mid-infrared region (right) is repeated in the near infrared spectrum (first, second and third overtones) and overlaid with combinatorial information (combination tones) (Paper I)

NIR spectroscopy is particularly well-suited for quantification of fats, proteins, carbohydrates and moisture (Osborne *et al.*, 1993). In meat, NIR has also been tested for measuring sensory and functional properties such as warmed-over flavour (Brøndum *et al.*, 2000a), meat tenderness (Mitsumoto *et al.*, 1991; Hildrum *et al.*, 1994; Byrne *et al.*, 1998; Rødbotten *et al.*, 2000; Park *et al.*, 2001) or water-holding capacity (Swatland and Barbut, 1995; Brøndum *et al.*, 2000b; Forrest et al., 2000). Near infrared sensors have the additional advantage that instrumentation is relatively simple and that the radiation may be transmitted through quartz, making the use of optical fibres feasible.

2.2. Fluorescence spectroscopy

In fluorescence spectroscopy, transitions between excited electronic states and the electronic ground state are measured. Excitation is brought about by absorption of photons in the UV and visible area (about 200-600 nm), which have energies sufficient to promote electronic transitions. Some of the excitation energy is instantly lost due to thermal vibrations (typically after 10^{-12} s). The return of an electron in an excited molecule from the excited to ground state (after 10^{-5} to 10^{-8} s) involves the release of a photon of radiation, which can be emitted as fluorescence. Since the light emitted has lower energy than the absorbed, the emission wavelength is longer than that of the excitation light.

Any fluorescent molecule is characterized by the excitation spectrum and the emission spectrum. The maximum excitation-emission wavelength pair is the main feature used to describe a fluorophore. Measuring several emission spectra at different excitation wavelengths creates a landscape, as seen in Figure 2-5.

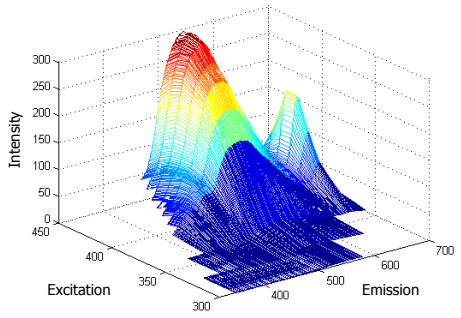

Figure 2-5. Fluorescence excitation-emission landscape measured on fish oil (Paper VIII)

The landscape structure has the advantage that analytes or interferences peaking in different areas are to a large extend discovered by visual inspection. With the use of chemometrics, it has become possible to extract relevant chemical information hidden in the spectral data. The data structure involving the excitation wavelength

and the emission wavelength allows for trilinear data analytical methods, giving the possibility of unique resolution of the underlying components, as discussed in sections 2.3.4. and 5.2.1.

One of the most attractive features of the fluorescence method is its inherent sensitivity. Typical detection limits are in the parts-per-billion range. That is 100-1000 times more sensitive than absorption spectroscopy. In addition, fluorescence is often measured against a dark background, as most substances do not fluoresce. Fluorescent compounds are sensitive to their environment, for example, temperature and pH. Increasing temperature leads to increased molecular movement and collisions, resulting in less fluorescence due to quenching (see below). Moreover, both the wavelength and the emission intensity can be affected by pH, since ionized and nonionized forms of a fluorophore lead to different excited states (Skoog and Leary, 1992). Radiation lower than 250 nm is sufficiently energetic to cause deactivation of the excited states by predissociation or dissociation (Skoog and Leary, 1992). As an example, UV radiation of 200 nm corresponds to about 600 kJ/mol which is more than the dissociation energy for C-H bonds of 414 kJ/mol. Interactions between a fluorophore and other substances can cause quenching, which leads to the reduction of fluorescence. Collisional quenching occurs when an excited-state fluorophore is deactivated upon contact with another molecule in the system. Examples of collisional quenchers include oxygen, halogens and amines (Lakowicz, 1999). Other types of quenching are, for example, formation of nonfluorescent complexes of fluorophores with quenchers or attenuation of the incident light by the fluorophore itself or other absorbing species (Lakowicz, 1999). Quenching may happen in complex food systems usually consisting of many different substances with the possibility of interaction with a fluorophore.

Fluorescence methods are relatively rapid, giving rise to fast collection of large amounts of information. Quartz cells or optical fibres can be employed, which makes fluorescence spectroscopy suitable for on-line implementation. Robust fluorescence sensors based on fibre optics already exist, but their on-line implementation in food processes has not yet been exploited.

The most intense and the most useful fluorescence is found in compounds containing aromatic functional groups, but compounds containing aliphatic and alicyclic carbonyl structures may also exhibit fluorescence. Fluorescence

spectroscopy is widely used as an analytical technique in many fields of science including chemistry, biology, biochemistry, medicine, environmental science and food science (Munck, 1989a; Strasburg and Ludescher, 1995; Rettig *et al.*, 1999). Fluorescence spectroscopy has been applied for several purposes in food science, including control of nutritional quality (Birlouez-Aragon *et al.*, 1998, 2001), investigation of colour impurities of sugar (Baunsgaard *et al.*, 2000), determination of the level of lipid oxidation in meat and fish (Aubourg, 1999; Wold and Mielnik, 2000; Wold and Kvaal, 2000), investigations of fish and fish extracts (Andersen *et al.*, 2002; Andersen and Wold, 2002), quantification of intramuscular fat (Wold *et al.*, 1999a), quantification of connective tissue (Swatland *et al.*, 1993; Swatland, 1997; Swatland and Findlay, 1997; Wold *et al.*, 1999b), replacing expensive digestibility tests for assessing the quality of fish meal (Dahl *et al.*, 2000), determination of deterioration of frying oils (Engelsen, 1997) and detection of plant tissue components (pericarp, aleurone and endosperm) in wheat by using fluorescent indicator substances for monitoring the separation in milling (Munck, 1989b; Pedersen and Martens, 1989).

2.3. Chemometric methods

The spectroscopic methods used in this thesis, FT-IR, Raman, NIR or fluorescence, produce covariant multivariate data containing hundreds or thousands of variables for each sample. A chemometric approach allows qualitative and quantitative information to be obtained from these complex spectral data. Chemometric methods are mathematical and statistical methods which decomposes complex multivariate data into simple and easier interpretable structures that can improve the understanding of chemical and biological information. The bilinear chemometric methods, Principal Component Analysis (PCA) and Partial Least Squares Regression (PLSR) are used for multivariate data overview and multivariate calibrations. The spectroscopic methods provide a data vector (**x**) (FT-IR, Raman and NIR) or a data matrix (**X**) (fluorescence) for each sample.

2.3.1. Exploratory data analysis

In order to explore the multivariate data the most fundamental chemometric algorithm PCA (Pearson, 1901; Wold *et al.*, 1987) was applied. PCA is a

mathematical procedure applied to spectral data to generate new latent variables which are orthogonal and thus uncorrelated to each other. The purpose of PCA is to express the main information contained in the initial variables in a lower number of variables, the so-called principal components (latent variables), which describe the main variations in the data. In PCA the data are projected from the original coordinate system into the new system of principal components, as depicted in Figure 2-6.

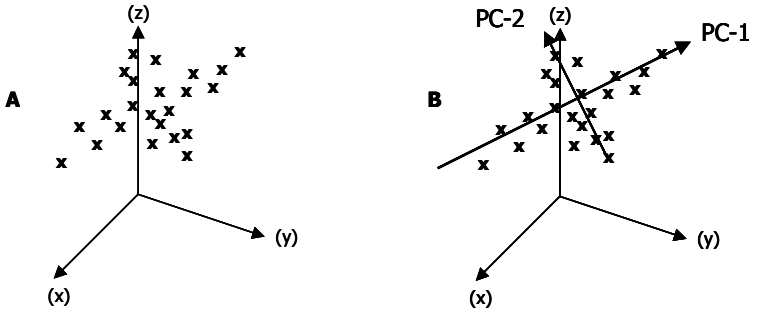

Figure 2-6. Data points (**x**) in the original coordinate system (xyz) (A) and projected on to the two principal components (PC-1 and PC-2) (B)

Each component (each new variable) is a linear combination of the original measurements. In the figure, the principal component lies along the direction of maximum variance in the data set. This projection of data is continued by composing additional, orthogonal principal components, until all latent structures of the data are described. In this way PCA provides an approximation of the data matrix (e.g., near infrared spectra of a number of samples) in terms of the product of two low-dimensional matrices **T** (scores) and **P'** (loadings). These two matrices capture the systematic variation of the data matrix

$$\mathbf{X} = \mathbf{TP'} + \mathbf{E}$$

and leave the unsystematic variation in the residual matrix (**E**). Plots of the columns of **T** (score plots), (Figure 2-7A), provide a picture of the sample concentrations of the principal components, while plots of the rows of **P'** (loading plots) depict the variable contribution to the principal components, (Figure 2-7B).

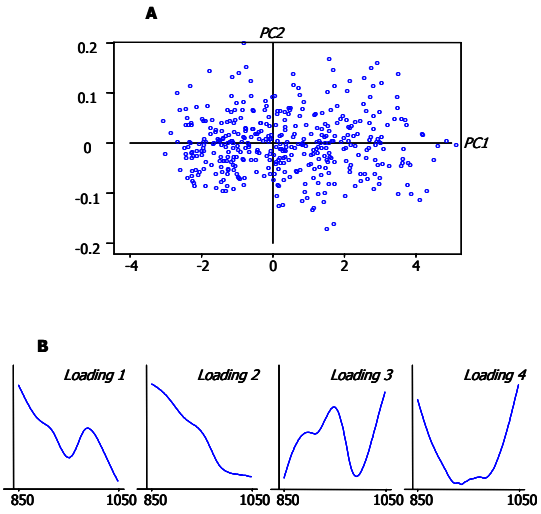

Figure 2-7. Score plot of PC1 versus PC2 (A) and loading plots of PC's 1-4 (B) of near infrared transmittance (NIT) spectra (850-1050 nm) of single wheat kernels (Paper V and VII)

PCA is a powerful and robust tool for obtaining an overview of complex data, such as covarying multivariate spectroscopic measurements of food samples, in order to discover groupings and trends in the data. In the work described in this thesis, PCA was used to form a general view of the data sets with the purpose of revealing deviant objects and to discover unknown trends, such as in Paper VI, in which PCA revealed changes during the day of measurement.

2.3.2. Multivariate regression

Using measured spectral data to predict important quality parameters (**y**) such as drip loss of meat (Paper III and IV), stunning quality of slaughter pigs (Paper VI), protein content in wheat kernels (Paper V and VII) and dioxin content in fish oils (Paper VIII) involves efficient multivariate regression techniques. The multivariate calibration task is to build a relationship between the spectra or landscapes (**x**/**X**) and the reference parameter (**y**) for all the samples in a given data set. The purpose of the

relationship is to predict the **y**'s from the **x**/**X**'s in the future and to interpret the relationships between **x**/**X** and **y**. The multivariate regressions in this thesis were performed by Partial Least Squares Regression (PLSR) (Martens and Næs, 1989), which is a predictive regression method based on estimated latent variables describing the relations between **X** (spectra or landscapes of a sample set) and **y** (corresponding reference measurements of the sample set). The strategy of PLSR is to reduce the dimension of the **X** and **y** space by creating linear combinations of the original variables. These new (latent) variables or components are statistically independent and ideally carry all relevant information. The reference variable, e.g. protein content, to be predicted is used actively in determining these components, and a linear regression model is defined as

$$\mathbf{y} = \mathbf{Xb} + \mathbf{E}$$

where **b** is the corresponding vector of regression coefficients, and **E** their residuals (model errors, noise etc.).

Spectroscopic data consist of spectra within a given wavelength range, depending of the type of instrument used, and often the spectra are composed of broad and overlapping peaks. Such data are highly covariate. One of the important characteristics of PLSR is the ability to model covariate data, in contrast to Multiple Linear Regression (MLR). MLR is the classical and often used method for developing regressions involving several x-variables in linear combinations to the corresponding y-values. MLR is designed for 'independent' x-variables and does thus not cope well with covariate spectral data.

PLSR has become an indispensable tool for the development of regressions between multivariate spectroscopic data and essential quality parameters in foods, since PLSR can provide simple and robust calibrations which are applicable for future predictions. In this thesis, PLSR was used to develop regressions between multivariate spectroscopic measurements such as FT-IR (Paper III and IV), Raman (Paper IV), NIR/NIT (Paper V, VI and VII) and fluorescence (Paper VIII) for the prediction of essential food quality attributes.

Chemometric methods include much more than PCA and PLSR, for example, methods for curve resolution, calibration transfer and classification. However, in the work discussed in this thesis, PCA and PLSR are the key methods. Chemometric

pre-transformation of spectral data and variable selection will be described in Chapter 4.

2.3.3. Chemometric validation

By chemometric validation it is possible to obtain as realistic performance of the models as possible with the available data. There are conceptually two ways to validate chemometric models: test-set and cross-validation. Test-set validation requires two data sets which are similar with respect to their ability to cover future sample variations and sampling conditions. One of the data sets is used for calibration, while the other is used for validation. Test-set validation requires sufficient samples in order to span the existing variation in both sets. It may often occur that it is not possible to collect enough samples for producing usable calibration and test sets. In the absence of a test set, it is necessary to apply cross-validation, where several sub-calibrations are made with single samples (full cross-validation) or segments of samples (segmented cross-validation) kept out of the calibration alternately, until all samples have been kept out once. The samples kept out are then used for validation, and the average of the validation results is calculated. Such methods will at their best provide a robust consistent estimation of the prediction error. The measure of model performance is usually given by the correlation coefficient (r), which is the correlation between the measured reference (y) and the predicted reference ($\hat{y}$), and by the prediction error RMSECV (root mean square error of cross-validation) or RMSEP (root mean square error of prediction):

$$\text{RMSECV or RMSEP} = \sqrt{\frac{1}{N}\sum_{i=1}^{N}(y_i - \hat{y}_i)^2}$$

where $\hat{y}_i$ is the predicted value for sample i, y_i is the corresponding reference value, and N is the total number of samples. The validation results of PLSR modelling are often displayed in predicted versus measured plots, as shown in Figure 2-8, where the **y**-values as predicted by the PLSR model are plotted against the originally measured **y**-values for the validation samples.

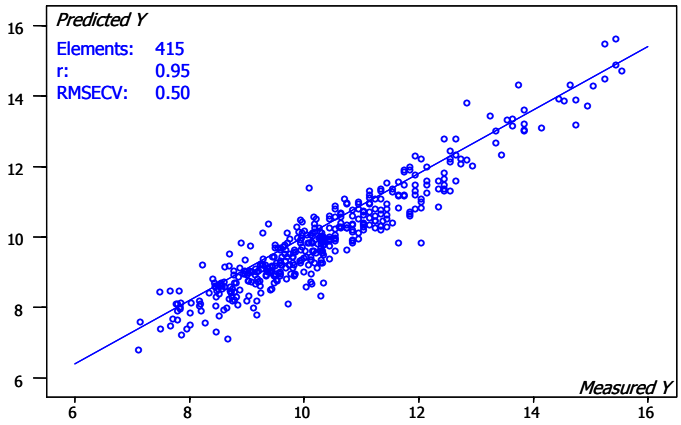

Figure 2-8. Predicted versus measured plot of a PLSR prediction of protein content of single wheat kernels by near infrared transmittance (NIT). Full cross-validation was applied, and the number of samples (Elements), the correlation coefficient (r) and the prediction error (RMSECV) are shown (Paper V and VII).

The calibration models in this study are mainly validated by cross-validation (Paper II, III, IV, V, VI, VII and VIII) due to limited number of samples, but test-set validation is also applied (Paper V and VII).

2.3.4. Multi-way methods

In fluorescence spectroscopy, two-dimensional spectra (landscapes) are generated for each sample. As mentioned earlier, the landscape structure has the advantage that analytes or interferences emitting in different spectral areas are revealed, and unique resolvation of fluorophores is possible because of the trilinear data structure (Ho *et al.*, 1978). With the PARAFAC (PARAllell FACtor analysis) algorithm (Harshman, 1970) it is possible to perform 'mathematical chromatography' and resolve the complex fluorescence landscapes into excitation and emission profiles of the underlying fluorophores (Bro, 1997) and thus obtain their relative concentrations. Unique resolution of the underlying components has been demonstrated by the application of PARAFAC to fluorescence landscapes in the sugar industry (Munck *et al.*, 1998; Andersson, 2000; Baunsgaard, 2000).

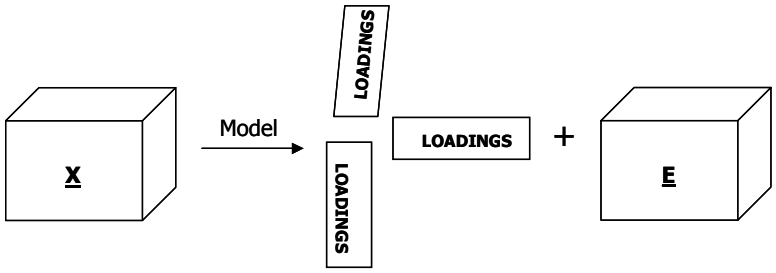

Figure 2-9. Three-way PARAFAC model of fluorescence landscapes resulting in three sets of loadings (concentration in the samples, emission and excitation profiles)

PARAFAC is a trilinear decomposition method which conceptually can be regarded as the multi-way analog to the bilinear PCA (Principal Component Analysis), but without the orthogonal constraints. The principle of PARAFAC is shown in Figure 2-9. For a data matrix consisting of i samples, j emission wavelengths and k excitation wavelengths, three loading matrices with elements a_{in}, b_{jn}, and c_{kn} give a PARAFAC model of a three-way array (x_{ijk}). The trilinear model is found to minimize the sum of squares of the residuals, e_{ijk} in the model, where n is the number of components:

$$x_{ijk} = \sum_{n=1}^{N} a_{in} b_{jn} c_{kn} + e_{ijk}$$

The reason for using PARAFAC instead of PCA is rarely to obtain a better fit, but rather to obtain a more adequate and interpretable model due to its mathematically unique resolvation. If the data is indeed trilinear and provided that the right number of components is used, the underlying spectra of fluorescent analytes including their relative concentration will be found (Bro, 1997). Thus, the analyte concentration may be obtained directly after scaling, but without the need of a regression.

The general multi-way PLSR model (N-PLSR) is considered superior to the unfolded PLSR method for regression purposes, owing to stabilisation of the decomposition by respecting the original structure of the fluorescence data (Bro, 1996). In the three-way version of PLSR, the three-way array of independent variables is decomposed into a trilinear model similar to the PARAFAC model.

However, in N-PLSR, the model is not a least squares fit of the independent data, but seeks in accordance with the philosophy of PLSR to maximize the covariance of the spectral (**X**) and reference (**y**) variables. The advantage of using N-PLSR instead of unfolding methods is that N-PLSR is more parsimonious, i.e. simple, and hence easier to interpret. N-PLSR will also be less prone to noise, because the information across all modes is used for the decomposition (Bro, 1996).

3. Uncertainty of reference analyses for multivariate spectroscopic calibration

In order to validate developed multivariate regression models based on spectroscopic measurements, as those developed during the project 'Early post mortem measurement of WHC (water-holding capacity) and drip loss in fresh pork', it is valuable to have experience with the instrumental and reference methods used for the regressions. In this project, the multivariate spectroscopic measurements of porcine meat were acquired early after slaughter with the purpose of development of regression models for prediction of the water-holding capacity (WHC) of the meat. Traditional chemical or physical measurements of the quality of foods are often prone to significant analytical errors due to inhomogeneity of complex samples and to the large number of analytical steps often required for the methods of analysis. Estimation of the uncertainty of the chemical reference methods can be of great value in order to judge whether the 'new' spectroscopic method is suited as a practical replacement for the 'old' chemical method.

Spectroscopic measurements are usually quite accurate and highly reproducible, but one must still be aware of possible errors such as the inhomogeneity of the sample, which is of great importance with respect to the method of sampling. Other sources of error in spectroscopic measurements are scatter interferences and unstable process variables like humidity, pH and temperature (Wülfert *et al.*, 1998). The uncertainty of spectroscopic methods can be estimated simply by making additional measurements without moving the sample (uncertainty of the spectroscopic measurement) or by replacing the sample by another representative sample and make additional measurements (uncertainty of the sampling method + the spectroscopic measurement). This is possible, because spectroscopic measurements are fast (a few seconds or minutes per measurement) and non-destructive (re-use of the sample is possible).

With regard to most reference measurements, replicate measurements can be much more difficult to produce. The reference measurements are usually destructive, which makes the requirement of true, representative replicates very critical. Food samples are often inhomogeneous, for which reason the production of good replicates might be difficult.

The reference measurements for water-holding capacity of porcine meat as described in Papers III and IV are disadvantaged by the impossibility of producing true replicates. Water-holding capacity is traditionally measured as drip loss by several available methods. In the Honikel (1998) method a large sample (80-100 g) is cut out of, for instance, the loin and used as a whole for the measurement to represent the drip loss of the entire carcass. Due to the variation between samples taken from different parts of the carcass, a large sampling error will be introduced. In another method suggested by Rasmussen and Andersson (1996), several smaller samples (25 mm in diameter and 25 mm in length) across a slice of the loin are used. This is expected to give more detailed information about the drip loss from the muscle, but it is still not possible to produce true replicates, as it is not possible to homogenize the material, which would result in destruction of the structure and loss of information concerning the water-holding capacity. The sources of errors of these methods are related to the nature of the meat samples and the processing of the samples during the analysis. Orientation of the fibres with respect to cut is important when measuring the drip loss, as the expelled fluid accumulates between fibre bundles (Offer and Knight, 1988). Surface evaporation or squeezing of the samples during handling can cause unwanted loss of water during the measurement (usually 24 or 48 hours). Different levels and distributions of fat and connective tissue, which influence the amount of drip, also cause inhomogeneity.

The purpose of Paper II was to investigate alternative ways of approximation of the level of the error of the reference parameter 'drip loss' in order to assess the requirements for a multivariate calibration predicting drip loss in porcine meat by fast and non-destructive spectroscopic measurements. The level of the error of the reference parameter is required to evaluate the practical use for calibrations to more indirect methods such as those performed in several studies (Paper III and IV; Forrest *et al.*, 2000; Brøndum *et al.*, 2000b; Brown *et al.*, 2000; Bertram *et al.*, 2001, 2002). The obtained prediction errors in these investigations were in the range of 0.8-2.6 % drip loss, and the question whether this is satisfactory, or if there is room for improvement of the spectroscopic calibration. The estimates of uncertainty of the measurement of drip loss of porcine meat from Paper II are in the range of 0.6-0.9 % drip loss. These uncertainty estimates indicate the error arising from the reference methods of drip loss measurements of porcine meat and can be utilized in the chemical/biological validation of the methods. Whether or not the obtained

prediction errors are satisfactory concerning the individual purposes of the spectroscopic calibrations, has to be evaluated against the actual ranges of drip loss in the populations of future predictions.

One way to use the uncertainty estimates of reference methods for evaluation of multivariate models based on spectroscopic data is demonstrated in Figure 3-1.

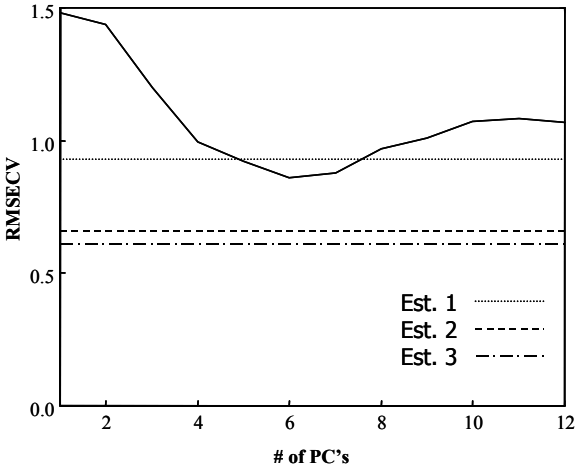

Figure 3-1. The prediction error (RMSECV) of a PLSR model based on FT-IR spectra for prediction of drip loss for 41 pigs from a research slaughterhouse plotted versus the number of components (PC's) used in the model. The uncertainty estimates calculated according to three approaches are plotted as horizontal lines (Paper II).

In the figure, the prediction error (RMSECV) from one of the PLSR models applied in Paper III is plotted versus the number of components used for the modelling. The PLSR model is based on FT-IR spectra of porcine meat from 41 of the animals. The drip loss measured by the method described by Honikel (1998) is applied as the reference measurement. The uncertainty estimates for the reference method calculated as % drip loss according to three approaches presented in Paper II (Est. 1, Est. 2 and Est. 3) are displayed as horizontal lines in the figure. These estimates can be used to show the amount of the error associated with the PLSR model, which is caused by the method of measurement of the reference parameter. When using the optimal number of components (6) for the PLSR prediction of the drip loss

reference, the reference method accounts for 0.61-0.93 % drip loss of the total modelling error.

Another situation, in which true replicates are impossible to produce, is the spectroscopic single seed quality control applied in Paper V and VII. Single seed quality analyses contribute to an increased understanding of the variation of the single seeds in order to evaluate sorting performance and thereby be able to optimize the choice of variety, grading conditions and end use. In order to get enough sample material for the reference method, the whole kernel was needed for determination of the protein content in single wheat kernels by the Kjeldahl method (Kjeldahl, 1883). Obviously, this approach leaves no possibility for making replicates, as the Kjeldahl method is destructive. Instead, 20 replicates of a wheat flour sample (i.e. excluding the grain structure) were used for an estimation of the uncertainty of the reference method (Paper V and VII). For the chemical/biological validation, the uncertainty estimate of these 20 replicates of 0.16 % protein could be compared to the prediction errors of the multivariate near infrared transmittance calibrations of the protein content of the single wheat kernels, which were in the area of 0.5-0.8 % protein.

These examples of reference methods with no or poor possibilities of making replicates emphasize the need for rapid and non-destructive methods for measurements of complex, inhomogeneous food samples.

4. Chemometric pre-transformation of spectral data

Spectral data usually contain non-relevant information, interferences and instrumental noise, in addition to the exact chemical, physical or biological information of interest. For example, the offsets between the near infrared (NIT) spectra of wheat kernels, displayed in Figure 4-1**,** are not associated to the information of interest in this case, the protein content of the wheat kernels, but instead express different scatter properties of the kernels, including kernel size, water content and texture. Scatter is a common phenomenon in spectral data. Among other sources of spectral interferences are instrumental artefacts, which might affect specific parts of the spectra. In order to reduce the impact of non-relevant spectral information, pre-transformations of the spectra prior to modelling can be applied. Besides elimination of non-relevant information, the advantages of using pre-transformations of spectral data, include simplification of the multivariate model, better linear correlation between spectra (**X**) and the reference parameter (**y**), more interpretable and robust models, and reduction of the number of calibration samples leading to cheaper and easier modelling (Martens, 2001). However, the scatter information reflecting the physics of the sample such as kernel hardness, may also be a relevant quality parameter.

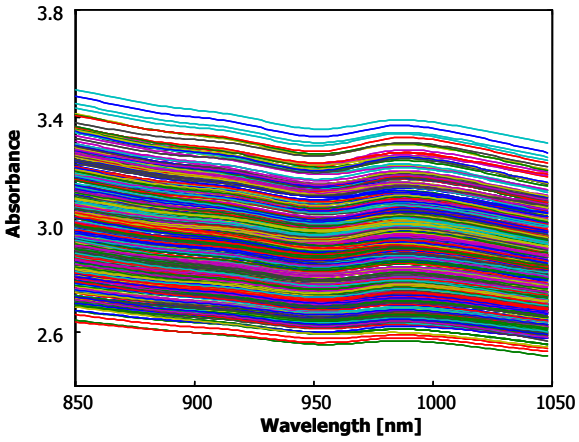

Figure 4-1. Raw near infrared transmittance (NIT) spectra (850-1050 nm) of 415 single wheat kernels (Paper V)

Two categories of pre-transformations of spectral data are described in this chapter: 1) physical and chemical pre-transformation of spectra and 2) variable region selection. Physical and chemical pre-transformation is used for correction of, for example, non-relevant scatter effects or non-relevant chemical interference. Multiplicative signal correction (MSC) (Geladi *et al.*, 1985), inverted signal correction (ISC) (Helland *et al.*, 1995; Martens *et al.*, 2002) or derivatives are examples of methods applied for this type of corrections. The other category covers methods for variable region selection which are used in order to emphasize especially informative regions of the spectra or to completely eliminate non-relevant regions of the spectra.

4.1. Physical and chemical pre-transformation of spectra

Even though linear calibration methods such as PLSR have the ability to model non-linear relationships by increasing the multivariate complexity, simpler and more robust models are desirable. Especially for industrial applications of multivariate calibration, the robustness of the models is of utmost importance (de Noord, 1994). Physical interference in reflectance spectroscopy could, as mentioned earlier, be light scatter and non-linearity of instrument response. The physical interference is often affected by the physical condition of the sample. Chemical interferences are caused by chemical components in the sample structure, other than those of direct interest, i.e. the analyte in question. Complex samples like food materials are composed of many different chemical and biological components, which all contribute to the spectra resulting from most instruments. An exception is fluorescence spectroscopy which only detects components with fluorescent characteristics.

A commonly applied technique for scatter correction of spectral data is the calculation of second derivatives (Savitzky and Golay, 1964). The second derivative of NIT spectra, as shown in Figure 4-2, often leads to more simple and better predictive multivariate models, because simple offsets and linear trends are removed. In this case of prediction of protein in wheat kernels, equal prediction errors were yielded for an 11-component model based on raw spectra and a 5-component model based on second derivatives of the spectra; see Table 4-1. The second derivative pre-transformation usually results in a reduction of the scatter-

related offsets and reveals more spectral features compared to the raw spectra (Fig. 4-1).

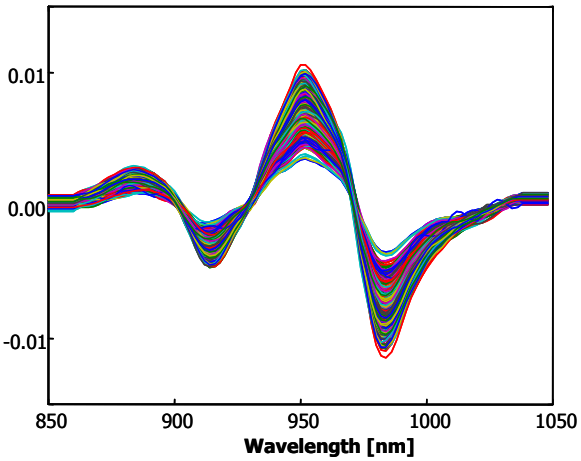

Figure 4-2. Second derivative of near infrared transmittance (NIT) spectra (850-1050 nm) of 415 single wheat kernels (Paper V)

Table 4-1. Performance statistics of the PLSR models for single seed protein predictions using single seed NIT spectra from the calibration set (415 kernels) and the subsequent test set (108 kernels) (Paper V).

Pre-	# of PLSR	Correlation		Prediction error (% protein)	
transformation	Components	Cal.set	Test set	Cal.set	Test set
Raw	11	0.93	0.96	0.55	0.70
2nd	5	0.93	0.96	0.56	0.52
MSC	9	0.93	0.95	0.57	0.78
ISC	9	0.93	0.95	0.58	0.69
EIMSC	7	0.95	0.98	0.49	0.49
MSC	9	0.93	0.95	0.57	0.78
2nd+MSC	5	0.95	0.98	0.47	0.48

Another well-tested concept is the multiplicative signal correction (MSC) (Geladi *et al.*, 1985). The basis of the MSC is the fact that light scatter's wavelength dependency is different from that of chemically based light absorption. By using data from many wavelengths, it is possible to distinguish between absorption and scatter (Geladi *et al.*, 1985). The MSC involves correcting each input spectrum in a set of related samples towards an ideal spectrum, where the influence of physical scattering variations has been removed from the effects of chemical absorbance. Two coefficients, the additive offset a_i and the multiplicative slope b_i, which ideally contain all the physical information in the input spectra, are estimated by:

$$\mathbf{z}_i = a_i + b_i\mathbf{m} + \boldsymbol{\varepsilon}_i$$

where $\mathbf{m}$ is a common reference spectrum and $\boldsymbol{\varepsilon}_i$ are the residuals that ideally contain all the chemically relevant information in the input spectra ($\mathbf{z}_i$), plus other unmodelled effects and random noise. After parameters a_i and b_i have been estimated, reversing the equation from the estimates of a_i and b_i then generates the corrected spectrum $\mathbf{z}_i$:

$$\mathbf{z}_{i,\text{corrected}} = (\mathbf{z}_i - a_i) / b_i$$

Corrected spectra, as exemplified by the MSC-corrected NIT spectra in Figure 4-3, can then be used in the subsequent multivariate modelling as applied in Papers V and VII.

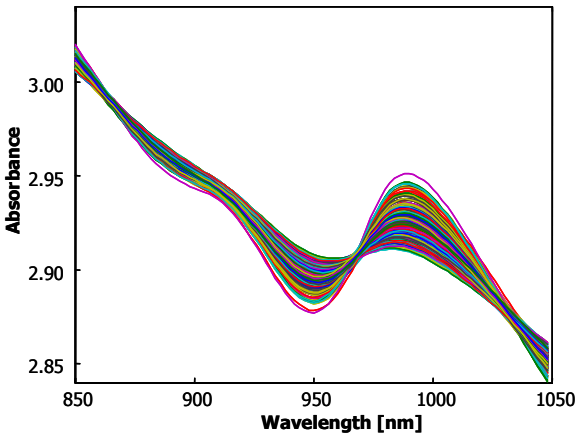

Figure 4-3. MSC-corrected near infrared transmittance (NIT) spectra (850-1050 nm) of 415 single wheat kernels (Paper V)

To obtain maximal understanding and maximal predictive reliability it is important to combine *a priori* knowledge and empirical data in a balanced way (Martens, 2001). In order to attain a more effective separation of chemical and physical effects the extended multiplicative signal correction (EMSC) was developed (Martens and Stark, 1991). The EMSC method employs *a priori* knowledge about the spectra of the non-relevant analytes by including information about the major analyte spectra in the estimation of a_i and b_i to avoid multiplicative correction of analyte information.

Spectral pre-transformations include many techniques not described in this chapter. Examples are Standard Normal Variate (Barnes *et al.*, 1989), path length correction with chemical modelling (Miller and Næs, 1990), piece-wise multiplicative scatter correction (Isaksson and Kowalski, 1993) and Orthogonal Signal Correction (Wold *et al.*, 1998).

4.1.1. Extended Inverted Signal Correction (EISC)

A new extended method, named Extended Inverted Signal Correction (EISC), for separating scattering from absorbance in spectroscopic measurements is described theoretically by Martens *et al.* (2002) and applied on single seed NIT spectra in Paper V. EISC can be applied in a general form, including additive terms, multiplicative terms, wavelengths dependency of the scatter coefficient and simple polynomial terms. In the general form, the additive offset and the multiplicative slope is corrected (Helland *et al.*, 1995). By application of polynomial terms, non-linear behaviour can be corrected, and additive and multiplicative characteristics of chemical influence can be corrected in the extended version.

The EISC method was originally developed with chemical analyte extensions (Martens *et al.*, 2002), and has subsequently been applied with spectroscopic extensions (Paper V) to NIT spectra of single wheat kernels prior to multivariate calibration for protein content. The NIT spectra, displayed in Figure 4-4, are corrected by EISC including a quadratic term c_i and wavelength dependent terms d_i and e_i, in addition to the 'usual' additive offset a_i and the multiplicative slope b_i:

$$\mathbf{z}_{i,\text{corrected}} = a_i + b_i\,\mathbf{z}_i + c_i\,\mathbf{z}_i^2 + d_i\,\boldsymbol{\lambda} + e_i\,\boldsymbol{\lambda}^2$$

where $\mathbf{z}_{i,corrected}$ is the corrected version of the input spectra ($\mathbf{z}_i$), and $\boldsymbol{\lambda}$ is the wavelength vector. The primary purpose of the extension terms $\mathbf{z}_i^2$, $\boldsymbol{\lambda}$ and $\boldsymbol{\lambda}^2$ is to improve the estimation of the basic interference effects, a_i and b_i. If the coefficient estimates c_i, d_i and e_i are found to pick up irrelevant information from the data, the subsequent calibration modelling may be simplified.

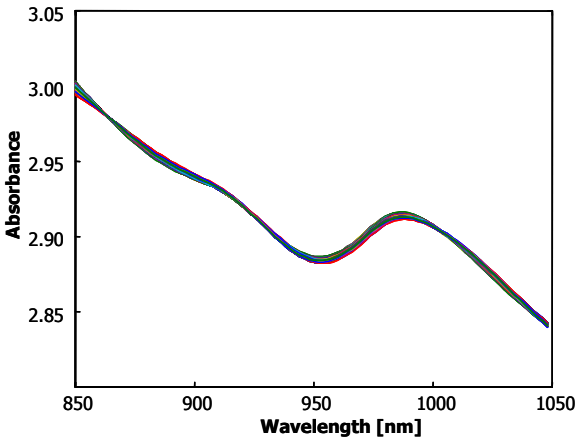

Figure 4-4. EISC corrected near infrared transmittance (NIT) spectra (850-1050 nm) of 415 single wheat kernels (Paper V)

The EISC with the general (physical) extensions (Paper V) performed equally as well as the two-step 'second derivatives followed by MSC, as earlier used by Delwiche (1995) and Paper VII, in the multivariate calibration for protein content of wheat kernels; see Table 4-1. In this data set, the two methods of pre-transformation can correct for spectra interferences that are not corrected by the more 'classical' pre-transformations MSC or second derivatives.

4.2. Variable region selection

It can often be advantageous to select significant variables during a multivariate regression in order to improve the predictive ability of the model. Spectral regions of specific interest, e.g. absorption of a well-defined component, can in some cases possess improved predictive ability compared to regressions using whole spectra as

defined by the instrument properties. Useless or unreliable variables, caused, for example, by non-relevant chemical information, noise or instrumental artefacts, can be eliminated, in order to simplify the final model and make it more robust. Several types of methods for variable selection exist; a few examples include principal variables (Höskuldsson, 1994), forward stepwise selection (Höskuldsson, 1996) and significance testing by jack-knife estimation of parameter uncertainty (Martens and Martens, 2000), while interval PLSR (Nørgaard *et al.*, 2000) is a method for variable region selection. Principal variables is a method where the spectral variables that co-vary the most with the reference variable are selected (Höskuldsson, 1994). Forward stepwise selection is a forward selection method, which is based on finding the spectral variable that gives the lowest prediction error, and then try all combinations with the other spectral variables in the selection of the next variable that gives the lowest prediction error, using multiple linear regression. Interval PLSR is suitable for spectral data and is based on dividing the spectrum into intervals of suitable size and selecting the interval with the best prediction ability (Nørgaard *et al.*, 2000). In order to study synergy between different spectral intervals, a synergy interval PLSR algorithm was developed by Nørgaard (www.models.kvl.dk) and applied by Munck *et al.* (2001) and in Paper IV.

Jack-knife estimates of the uncertainty of model parameters can automatically eliminate useless or unreliable variables in order to simplify the final model and make it more reliable (Martens and Martens, 2000; Westad and Martens, 2000).

In paper IV variable selection by iPLSR was applied in order to find the best predictive regions of FT-IR and Raman spectra of porcine meat for the prediction of water-holding capacity. The chemometric selection of the best predictive spectral regions was evaluated by chemical interpretation of the spectra, as IR and Raman spectra, to some extent, are interpretable. A considerable improvement in prediction error was found by employing only informative regions of the spectra, which demonstrated the importance of selecting especially informative spectral regions prior to PLSR modelling. It was found to be especially important to avoid the regions in the spectra with very high absorption, as they are noisy and will disturb the regressions (Paper IV).

5. Applications of rapid remote spectroscopic measurements for investigation of food quality

The aim of this thesis is to develop rapid measurements of essential quality parameters in foods. This will be exemplified in this chapter by several investigations of vibrational and fluorescence spectroscopic methods developed for the exploration and prediction of food quality. It remains to be seen if the developed methods are interesting enough for implementation in industry for monitoring of quality in the production of foods.

5.1. Vibrational spectroscopic investigations of food quality

Vibrational spectroscopy is suitable for the analysis of food quality, as food systems are mainly composed of fats, proteins, carbohydrates and moisture, which all contain characteristic functional groups with stable group frequencies. In addition, a very useful feature of the vibrational spectroscopic techniques is their potential as on-line or at-line methods in the food industry.

5.1.1. Technological and eating quality of porcine meat

The quality of porcine meat is very complex, and covers functional characteristics such as intramuscular fat, tenderness and water-holding capacity (WHC). WHC is probably the most important technological property of porcine meat. Approximately 75 % of the weight of lean muscle tissue immediately after slaughter is water. If a muscle has a poor ability to retain water, exudates or drip will come from cut surfaces. The reduction of pH post mortem normally results in a reduction in water holding, so that exudates leak out of cut muscle surfaces during post-mortem storage. The water content of meat is important for two reasons. Firstly, meat is sold by weight, so the water loss is an important economic factor. In the Danish meat industry, a decrease by 1 % of the water of the meat in all pigs produced annually (23 million pigs per year) represents an economic loss to the industry in excess of 50 million DKK. Secondly, the water content of meat determines to a large extent the juiciness of meat and thereby the eating quality. The WHC of the meat determines the use of the meat. For this reason, the slaughterhouses have a desire to be able to

classify the carcasses according to their level of water-holding capacity, preferably before the carcasses reach the cold storage room.

As the WHC of meat is a complicated phenomenon, it is difficult to measure. To date, it has not been possible to assess the meat quality until the carcass has gone through rigor mortis and has fully temperature equilibrated to cold storage conditions, i.e. the day after slaughter. With regard to the possibility of early prediction of meat quality, a method suitable for on-line measurements is required. With an on-line method, the slaughter industry can gain knowledge regarding the meat quality early after sticking in order to facilitate sorting before further use.

FT-IR in combination with chemometrics has proved to be a possibility for early post-mortem prediction of drip loss in porcine meat (Paper III and IV). The method is characterized by the fact that measurements are carried out while the carcass is still warm from slaughter, i.e. while the muscles undergo the transformation from living tissue in a recently slaughtered animal to chilled, edible meat, which makes it possible to measure the carcasses at the rate, at which they are advanced on a common slaughter line, typically 350-400 carcasses per hour. The inaccuracy of the FT-IR method is sufficiently small to make it realistic to sort the carcasses in quality classes already before the carcasses are chilled in the slaughterhouse. Then it is possible to use carcasses with a very low drip loss or a high drip loss for the manufacture of suitable types of products, whereas carcasses with a normal drip loss may be used for the production of fresh cuts (Paper III).

Multivariate modelling based on FT-IR spectra of meat of pig carcasses from a research trial ranging from 0.7-8.0 % drip loss showed prediction errors (RMSECV) of 0.85-1.4 % drip loss, while the corresponding prediction error for commercial pigs (0.5-8.3 % drip loss) were 1.0-1.2 % drip (Paper IV). These results were found to be acceptable for the purpose of suggesting an on-line method for sorting out the carcasses with low and high drip loss. When comparing the prediction errors to the uncertainty estimate of the traditional reference measurement of drip loss, which was found to be 0.6-0.7 % drip loss (Paper II), the majority of the prediction errors can be explained by the uncertainty of the reference measurement.

A major difficulty encountered with the FT-IR analysis of meat is the sample presentation. For analysis in the transmission mode, samples must be converted to a milk-like emulsion in which the globule sizes are smaller than the analytical

wavelengths (2-8 μm), in order to avoid scattering effects (Dion *et al.*, 1994). A possibility for direct measurement of food by FT-IR is the attenuated total reflection (ATR) technology described in Chapter 2, which simplifies sample handling. The application of ATR for measurements on meat described in Papers III and IV is depicted in Figure 5-1.

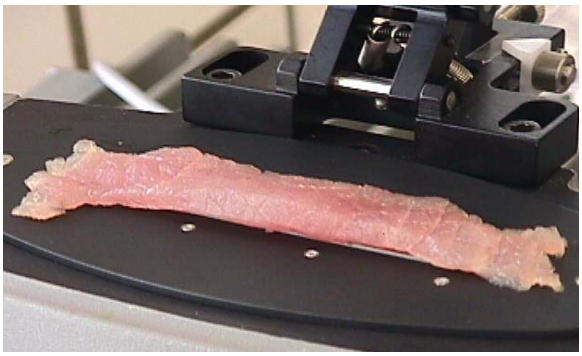

Figure 5-1. A piece of recently cut-out porcine meat placed on an ATR crystal

Among the disadvantages of ATR are that the spectra are sensitive to applied pressure and that spectral intensity depends on the contact between crystal and material. Satisfactory contact between the crystal of the ATR and the meat was difficult to obtain due to the inhomogeneous nature of the meat, for which reason the spectroscopic method itself must be expected to contribute to the prediction errors associated with the multivariate models. In addition, the development of satisfactory optical fibres for FT-IR is at present not very promising, as IR radiation cannot be transmitted through materials like glass or quartz due to absorption. On the other hand, optical fibres are available for the Raman technique, as it uses visual or near infrared radiation, and moreover, water does not interfere the spectra, as is the case of FT-IR and NIR. This is a very important attribute, as meat contains mostly water. A PLSR model based on Raman spectra was employed in Paper IV, but included a limited number of samples. The resulting prediction error, though, was found to be encouragingly low. Such an extraordinary good PLSR model based on the Raman spectra is probably unrealistic, due to the low number of samples. Nevertheless, it

deserves further attention in future studies, especially because Raman measurements can be performed using insertion probes and fibres that provide good contact with the meat and having the spectrometer in a remote location far from the harsh environment at the slaughter line.

Prediction of WHC by vibrational spectroscopic methods has earlier been investigated by application of near infrared spectroscopy (Swatland and Barbut, 1995; Byrne *et al.*, 1998; Forrest *et al.*, 2000; Brøndum *et al.*, 2000b). Apart from Forrest *et al.* (2000) these investigations have applied the spectroscopic measurements post rigor, which in the slaughtering process is too late for efficient classification of carcasses. Forrest *et al.* (2000) measured NIR (900-1800 nm) through a fibre optic probe 30-36 min after sticking. In combination with multivariate data analysis they predicted drip loss with a correlation of approximately 0.8 for a trial of 99 carcasses measured at a commercial slaughterhouse. The prediction error was estimated to be 1.8 % drip loss, which is considerably higher than the prediction error obtained in Paper IV, which also includes measurements made at a commercial slaughterhouse.

In order to decide whether FT-IR should be recommended as a method for early classification of carcasses in the slaughterhouses according to WHC, measurement of many more samples is necessary, so that all kinds of biological variations in the meat material can be included in the model. It must also be taken into consideration, if the method is technically robust enough to be able to work in a rather rough environment at the slaughterhouses with changing temperatures and humidity.

The information on food quality, which can be acquired by FT-IR and Raman spectroscopy has not yet been sufficiently investigated, and the potential in the meat industry deserves more attention. In particular, Raman spectroscopy possesses desirable characteristics for measurement of food quality due to its ability to measure samples having high water content and, the fact that it is fast and easy to use. The highly interpretable vibrational techniques in combination with exploratory multivariate data analysis can be valuable tools for scientists in the effort to understand functional properties of foods.

5.1.2. Ethical quality of the slaughtering procedure

Animal welfare is a major concern in meat production due to the fact that meat consumers increasingly demand that animals are produced, transported and slaughtered in a humane way (Appleby and Huges, 1997). Pre-slaughter stunning is used to ensure that animals do not suffer needlessly and are unconscious and insensible to the slaughter procedure. According to proper animal welfare, it is important to expose pigs to CO_2 for a long enough time to ensure they remain unconscious during post-stun handling until death intervenes by debleeding. It is possible to assess the depth of CO_2 stunning of pigs under slaughterhouse conditions by using practical guidelines established by the Danish Meat Research Institute (Holst, 2001). The assessment is based on absence or presence of a number of reflexes characterizing the depth of stunning.

Blood consists mainly of water, haemoglobin, cholesterol, urea, albumin and globulin, and CO_2 is transported in the blood both in solution in plasma and in chemical combination (Robinson, 1997). NIR has been applied on blood for determination of haemoglobin content (Kuenstner *et al*., 1994), lactate content in plasma (Lafrance *et al.*, 2000) and total protein, albumin, globulin, triglycerides, cholesterol, urea, glucose, and lactate in serum (Hazen *et al.*, 1998).

In Paper VI visual and near infrared (VIS/NIR) spectroscopy was evaluated for the ability to assess the depth of CO_2 stunning of slaughter pigs. The study was based on observations made during the investigation of early post mortem quality prediction of porcine meat performed at a research slaughterhouse. In this investigation blood from pigs was measured with VIS/NIR spectroscopy (400-2500 nm) immediately after sticking. The spectra showed significant differences apparently related to the method of stunning and to the state of the animal in the CO_2 chamber. In Figure 5-2 three spectra are shown, one from a pig that was electrically stunned and two from pigs that were stunned in CO_2. One of the CO_2-stunned pigs was gasping during sticking, while the other one did not show gasping during sticking and was apparently very deeply stunned or may even have died during stunning. The spectrum of blood from the electrically stunned pig differs distinctively in shape from the spectra of the CO_2 stunned pigs, while the difference between the two CO_2 stunned pigs is expressed as intensity differences in certain parts of the spectra. The

objective of the investigation in Paper VI was to evaluate the ability of VIS/NIR spectroscopy to assess the depth of CO_2 stunning of slaughter pigs.

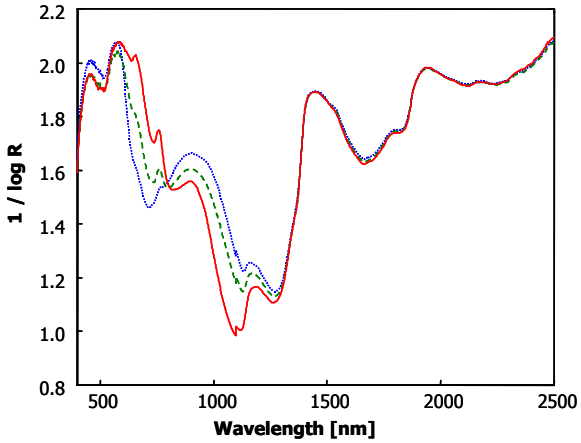

Figure 5-2. VIS/NIR spectra (400-2500 nm) of blood from three pigs measured immediately after sticking: one from an electrically stunned pig (·····) and two from CO_2 stunned pigs. One CO_2 stunned pig was gasping during sticking (----), the other one was apparently completely stunned (—) (Paper VI).

The investigation was carried out at three commercial slaughterhouses, chosen in the light of previous knowledge of the CO_2 stunning 'quality'. One slaughterhouse with a relatively high occurrence of corneal reflex, one with a medium occurrence and one with a very low to no occurrence were chosen. During debleeding, blood was collected from each animal for subsequent spectroscopic measurement by VIS/NIR spectroscopy, and depth of the CO_2 stunning was assessed immediately before and after sticking, in accordance with guidelines established by the Danish Meat Research Institute (Holst, 2001). The reflexes assessed were corneal reflex, breathing and excitation, and the assessments were converted to a quantitative scoring system in order to be applied as reference measurements for the calibration of the depth of stunning (Paper VI).

The acquired spectra contain features related to the water content of the samples and to the presence and level of oxygenated and deoxygenated haemoglobin. The spectra from the three slaughterhouses were quite similar in shape, but the spectra from the

one slaughterhouse with no occurrence of reflexes differed from the spectra from the other two slaughterhouses in regions of the spectra that pointed in the direction of a more powerful CO_2 stunning. The spectral data revealed systematic variations according to different levels of the assessed reflexes. Besides the effect of stunning, the spectra also contain information on biological properties of the blood and probably environmental effects from the slaughterhouses. For this reason complete interpretation of the spectra was impossible and the relevant information concerning depth of stunning was difficult to separate, especially because the level of influence of the interfering effects (biology and environment) was not assessed.

It was possible to roughly classify the spectra according to slaughterhouse, and PLSR predictions by the spectra indicated that the VIS/NIR method was able to distinguish blood from well-stunned and the less well stunned pigs. The method might not be reliable for an exact estimate of the depth of stunning; but the VIS/NIR spectroscopic method still deserves further investigation for its potential as a rapid and objective estimate of the depth of CO_2 stunning in slaughter pigs. However, this requires that different slaughterhouses are involved in further investigations and that the environmental effects are controlled or measured in order to eliminate them from the regressions.

5.1.3. Single kernel quality of wheat

Until recently, nearly all grain quality analyses were performed on bulk samples consisting of hundreds or thousands of kernels, most often in ground form. In doing so, information was lost on the characteristics of the individual kernel. Analyses of homogeneity of wheat samples are allowed by using single kernel analyses. Single seed quality analyses thus contribute to an increased understanding of the variation of the single seeds in a seed lot in order to evaluate sorting performance and thereby be able to optimize the choice of variety, grading conditions and end use. Fast and non-destructive single kernel quality analyses would be valuable tools in plant breeding for quality selection in early generations and for single kernel quality evaluation within the spikes.

Protein content largely determines the end use quality, and premiums are often offered on high protein wheat. Single kernel near infrared transmittance (NIT) spectroscopy has shown excellent ability to determine protein content (Papers V and

VII). The NIT spectra cover the spectral region from 850 nm to 1050 nm containing primarily the second overtones of O-H (carbohydrates and water) and N-H (protein) stretching vibrations and the third overtone of the C-H (fats) stretching vibration. The fundamental N-H, C-H and O-H stretchings and the corresponding theoretical second and third overtones expected in the 850-1050 nm region are listed in Table 5-1, while NIT/NIR spectra of gluten, starch and water in the spectral region of 850-1050 nm are shown in Figure 5-3. This relative narrow window underlines the holographic nature of NIR as all the relevant information is found but in new combinations from that of the fundamental vibrations in IR. Moreover, the absorbencies in this region are a factor 10-100 less as compared to the fundamental which facilitate transmission of samples 10-100 times thicker. NIT spectra were acquired for single wheat kernels from different varieties, and nitrogen content was determined directly for each single kernel by a modified Kjeldahl method (Kjeldahl, 1883). A prediction model for protein content was developed on the basis of the NIT spectra of a calibration set and validated by an independent test set. The prediction error (RMSEP) of 0.5 % protein was comparable to results reported earlier using near infrared transmittance (850-1050 nm) (Delwiche, 1995) and near infrared reflectance (1100-2498 nm) (Delwiche, 1998). The development of non-destructive screening methods for other single seed characteristics, such as vitreousness, density and hardness, would be of great value for routine homogeneity analysis (Paper VII).

Table 5-1. Group frequencies of fundamental N-H, C-H and O-H stretchings and wavelength values for the corresponding theoretical second and third overtones expected in the 850-1050 nm region.

Group	Compound	Fundamental (IR) [cm^{-1}]	Second overtone (NIR) [nm]	Third overtone (NIR) [nm]
N-H	Protein	3300	1010	
C-H	Protein / Carbohydrate	3000-2800		900-930
O-H	Carbohydrate / Water	3400-3300	980-1010	

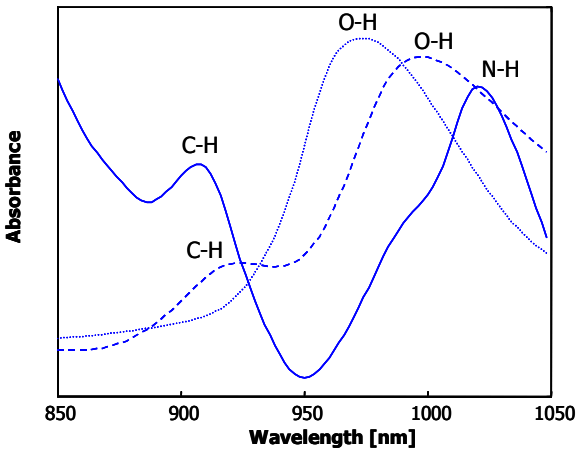

Figure 5-3. Near infrared spectra of the main components of wheat: gluten (—), starch (---) and water (·····).

5.2. Fluorescence spectroscopic analysis of food quality

Fluorescence spectroscopy is a very sensitive technique able to measure trace substances. However, the method naturally requires that the trace substance to be analysed contain one or more fluorescent chemical groups. Important fluorophores of relevance to foods include proteins (containing the amino acids tryptophane, tyrosine and phenylalanine), coenzymes (NADH, NADPH and FAD), vitamins (A, B_1, B_2, B_6, B_{12}, D_2, E and folic acid), caffeine, chlorophyll, polyphenols, flavanoids, aflatoxins, and some nucleic acids (Lakowicz, 1999). In addition, fluorescence spectroscopy has the potential of direct or indirect measurement of contaminants present in very small concentrations in complex matrices like foods due to the sensitivity of the technique and the presence of background fluorescence in most food materials. Indirect measurement means that the fluorescence signal does not arise directly from the substance in question, but is due to, for example, quenching or fluorescent indicator substances.

5.2.1. Screening for environmental contamination of fish oil

Food and feed often contain trace amounts of environmental contaminants, and monitoring programmes are therefore required to analyse the presence of toxic substances. Dioxins (polychlorinated dibenzo-*p*-dioxins (PCDD's) and

polychlorinated dibenzofurans (PCDF's)) are widely encountered toxic substances. In general, the dioxin levels found in food and feed are very low (ppt-level), the detection of which requires sophisticated and hypersensitive (sub-ppb) physicochemical separation techniques such as GC-MS and HPLC-MS. In the case of complex organic molecules such methods are often laborious and very expensive; a typical dioxin analysis takes two weeks and costs approximately $1,000 (Belgian Government, 1999). For this reason, only limited environmental monitoring is performed.

In a preliminary investigation of fish oils, the use of fluorescence excitation-emission landscapes evaluated by 3-way chemometric methods (see section 2.3.4.) was demonstrated as a candidate for an inexpensive screening method to indicate the level of contamination by dioxin and PCB's (PolyChlorinated Biphenyls) (Paper VIII). Fluorescence landscapes of fish oils were investigated and showed great variation due to species, season and treatment, depicting a variation in natural fluorescent components. The fluorescence landscapes were analysed by PARAFAC. Figure 5-4 shows the plot of PARAFAC score 1 versus PARAFAC score 2.

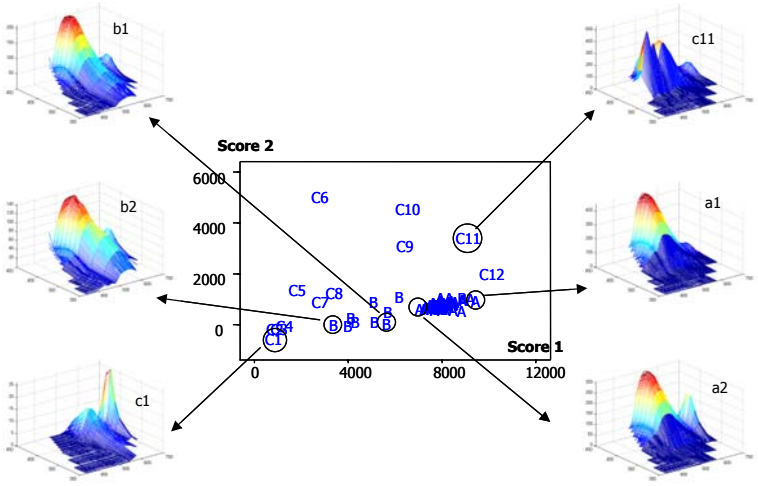

Figure 5-4. Score plot of PARAFAC component 1 versus component 2 from a 3-component PARAFAC model of sample sets A (one batch from factory 1), B (different batches from factory 1) and C (different batches from factory 2). Selected fluorescence landscapes of two set A samples (a1 and a2), two set B samples (b1 and b2) and two set C samples (c1 and c2) are shown (Paper VIII).

The figure reveals different fluorescence properties related to the nature of the different fish oil samples and connected to the origin of the samples (Paper VIII).

Application of PARAFAC/MLR (Multiple Linear Regression) and N-PLSR to the fluorescence landscapes resulted in local regression models for dioxin determination with prediction errors below 1 ng/kg, which is comparable to the error of the reference method. In the PARAFAC model, two of the modes gave the excitation and emission spectra of the pure underlying fluorophores and the third mode their individual concentrations. Excitation and emission optima for 3-4 PARAFAC components in each data set were identified, representing both positive and negative (quenching) correlation components (Paper VIII).

The encouraging results in the paper should, however, be taken with precaution, since dioxins do not fluoresce, so the correlations must be related to complex chemical covariate objects in the fish oil matrix. However, a few hypotheses regarding the fluorescence screening method for dioxin to be further tested are presented in the paper, and further research could give profitable results based on the hypotheses generated in this exploratory investigation. This exploratory multivariate approach has great potential as a strategy for solving other environmental problems, for example, by using environmental indicator substances, which are accumulated in the biological chain. The environmental issue is indeed multivariate and complex, and therefore difficult to manage with traditional statistical methods (Vega *et al.*, 1998).

5.2.2. Oxidative quality of poultry meat

Several authors have demonstrated that fluorescence is a good indicator of lipid oxidation in biological materials. Numerous fluorophores have been obtained following reactions between primary and secondary lipid peroxidation products and primary amines, and a majority of the unsaturated aldehydes formed by lipid peroxidation have been found to be precursors of fluorescent compounds (Melton, 1983; Esterbauer *et al.*, 1986). Through investigations on formation of fluorescent oxidation products, a variety of excitation and emission peaks have been reported (Chio and Tappel, 1969; Tappel, 1970; Dillard and Tappel, 1971; Kikugawa *et al.*, 1981; Kikugawa *et al.*, 1985; Beppu *et al.*, 1986; Kikugawa and Beppu, 1987; Hasegawa *et al.*, 1992, 1993; Wold *et al.*, 1999b; Wold and Mielnik, 2000). These

vary in types of matrices, extraction techniques and whether measurements are performed on solid state or on the organic or aqueous phase. The development of fast methods for determination of lipid oxidation based on fluorescence spectroscopy is currently in progress (Wold *et al.*, 1999b; Wold and Mielnik, 2000).

In order to further investigate the suitability of fluorescence spectroscopy as a method for fast determination of the oxidation level of meat, fluorescence landscapes and spectra have been collected on breasts and legs from chickens with varying oxidation levels affected by different storage periods of the meat (0, 4, 10 or 16 weeks) and different feeds for the chickens (feed containing fish oils with varied levels of oxidation); see Figure 5-5. The oxidative rancidity was determined by the TBARS assay. This method is the most widespread procedure for estimating the oxidative changes of meat and meat products (Shahidi, 1994). The assay measures the quantity of 2-thiobarbituric acid reactive substances (TBARS), among them malondialdehyde which is an oxidative breakdown product formed mainly from oxidized polyunsaturated fatty acids. Dynamic headspace GC-MS measured volatile oxidation products of the meat samples, e.g. aldehydes, ketones, alcohols and acids. The composition of these compounds is related to the oxidative state of the sample.

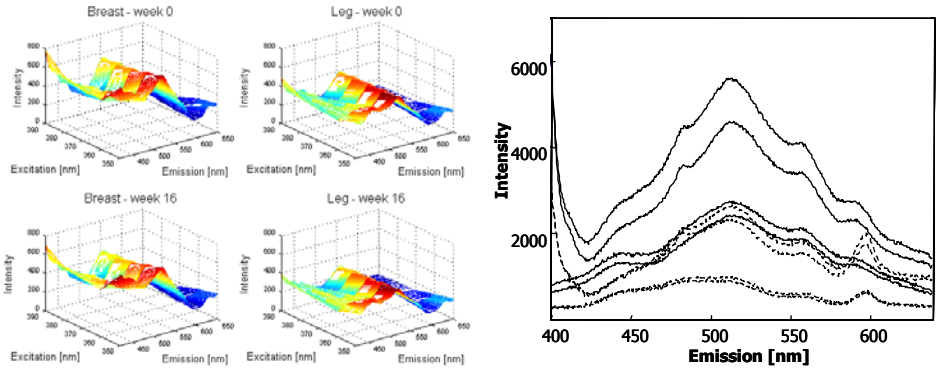

Figure 5-5. Fluorescence excitation-emission landscapes from an LS50B spectrofluorometer (Perkin-Elmer) and fluorescence spectra (excitation 350 nm and 382 nm) from an optical bench system using a 512*512 charge-coupled device (CCD) (Princeton) as detector. Breasts (——) and leg (------)

Early unpublished results of this study showed high correlations between the fluorescence spectra and the time of storage. The fluorescence spectra were acquired using the same method as described in Wold and Mielnik (2000). The MSC-corrected fluorescence emission spectra produced by excitation at 382 nm were modelled in PLSR calibrations for prediction of the storage time (weeks of storage) of the meat samples. A total calibration model of 61 breast samples and 63 leg samples covering all storage times and feeds were tested on a validation set consisting of 32 breast samples and 30 leg samples. The predicted values (weeks) versus the actual values of the validation samples are shown in Figure 5-6.

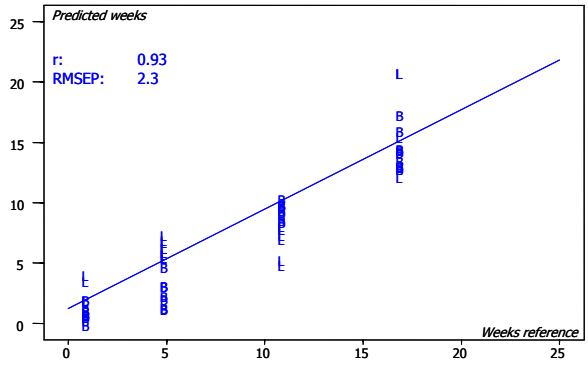

Figure 5-6. Predicted versus measured plot for the validated prediction of the time of storage (weeks) by fluorescence spectra (excitation 382 nm) of the validation set consisting of 32 chicken breast samples and 30 leg samples based on a PLSR involving 61 chicken breast samples and 63 leg samples. The correlation coefficient (r) and the prediction error (RMSEP) are reported.

Breast and leg samples were modelled and validated separately. The correlation coefficient (r) and prediction error (RMSEP) for each test of the validation sets are displayed in Table 5-2, along with the corresponding results for predictions based on the MSC-corrected fluorescence spectra produced by excitation at 350 nm. The modelling and predictions of the breast samples seem to perform considerably better than of the leg samples. This is possibly due to the more homogeneous appearance of the breast samples compared to the leg samples. The requirement of a relatively

large number of components (4-8) for the PLSR models may be due to the fact that the fluorescence spectra are quite complex, so that the noise correction is using some of the components.

Table 5-2. PLSR predictions of storage time (weeks) and TBARS (mg/kg) of chicken samples by MSC-corrected fluorescence spectra. Three sample sets are employed: breast and leg samples (All), only breast samples (Breast) or only leg samples (Leg). The number of calibration and validation samples (cal / val) are displayed. The results are shown as correlation coefficient (r) and prediction error (RMSEP).

Reference	Sample set	# of samples	Excitation λ	# of components	r	RMSEP	Range
Weeks	All	124 / 62	382 nm	8	0.93	2.3	0-16
Weeks	Breast	61 / 32	382 nm	8	0.98	1.3	0-16
Weeks	Leg	63 / 30	382 nm	7	0.89	2.6	0-16
Weeks	All	124 / 62	350 nm	6	0.92	2.4	0-16
Weeks	Breast	61 / 32	350 nm	5	0.97	1.6	0-16
Weeks	Leg	63 / 30	350 nm	4	0.88	2.8	0-16
TBARS	Breast	61 / 32	382 nm	6	0.71	0.12	0.12-0.82
TBARS	Breast	61 / 32	350 nm	5	0.72	0.13	0.12-0.82

The MSC-corrected fluorescence spectra of the breast samples produced by excitation at 382 nm and at 350 nm, respectively, were modelled in PLSR calibrations for prediction of TBARS. A calibration model of 61 breast samples covering all storage times and feeds were tested by a validation set consisting of 32 breast samples; see Table 5-2. The correlation coefficients around 0.7 found in this study were considerably lower than those found by Wold and Mielnik (2000) (correlations coefficients higher than 0.8), while the prediction errors (RMSEP = 0.12-0.13) in this study were slightly higher than those in the Wold and Mielnik study (RMSECV = 0.15-0.22). The reason for the lower correlation coefficients in this study may be due to the lower range of TBARS (0.1-0.8) compared to the TBARS range (0.1-1.3) in the Wold and Mielnik study. Combination of the two spectra (excitation 350 nm and 382 nm) did not improve the predictions. The

prediction errors found in this study and in the Wold and Mielnik study seem to correspond, which implies that there is basis for further development of a fluorescence method for rapid assessment of lipid oxidation in poultry meat. A paper including these results is under preparation.

6. Conclusions and perspectives

This project has employed vibrational spectroscopic techniques, FT-IR, Raman and NIR, as well as fluorescence spectroscopy in combination with chemometrics for the exploration of food quality during the production of food. The speed and non-invasive properties of spectroscopic techniques make them potential on-line or at-line methods and hence very useful for process monitoring and control in the food industry. NIR probes are already utilized for innumerable quality measurements in the food industry, while FT-IR and Raman are less widespread. In this project FT-IR and Raman spectroscopy demonstrated to be of potential interest for process line measurements of meat quality (water-holding capacity). PLSR models of meat samples from a research slaughterhouse and from a commercial slaughterhouse showed prediction errors acceptable for classification of the carcasses at an early stage after slaughter (45 min). A further development of vibrational spectroscopic methods for process line measurements can be of valuable use in the slaughtering industry with the purpose of better utilization of the raw materials through early classification of the meat. In order to facilitate the use of FT-IR as an on-line method in food production, the development of robust and efficient probes is needed, as IR radiation cannot be transmitted through standard materials like glass or quartz. In contrast, Raman signals can be transmitted through quartz, but here the main difficulties are the inherent poor signal-to-noise ratio and sample fluorescence.

The role of chemometrics in future scientific data analysis is promoted by its ability to solve many different data analytical problems. A change in the approach to problem solving from univariate to multivariate thinking is one of the requirements for making chemometrics an indispensable tool for the food industry. In order to optimize a process with optimal utilization of chemometrics, it is first necessary to measure the process without restrictive hypotheses, then to analyse and model the data, test the model and finally reach an understanding of the process. In this way chemometrics has the potential to solve urgent problems by providing parsimonious solutions. One example is the efforts to monitor environmental problems, where a multivariate approach is absolutely necessary due to the multivariate nature of the environmental mechanisms. Even though it has not yet been confirmed exactly which compounds were detected during the fluorescence measurements of fish oil, the investigation demonstrated the potential of the combination of fast spectroscopic measurements and chemometric data analysis for screening of environmental

contamination in complex food samples. The measurement of dioxin in fish oil represents a great benefit for the fish industry, as EU has introduced a 6 ng/kg limit and because laboratory measurements cost approximately 10000 DKK per sample. Further study of the fish oil measurements will give profitable results based on the hypotheses generated during the explorative investigation. The fluorescence and multi-way approach has the potential to provide direct chemical fingerprinting of a range of natural and polluting molecules in a variety of biological matrices.

Different aspects of food quality were covered in this thesis. The focus was mainly on the development of multivariate calibrations based on spectroscopic measurements for predictions of rather complex attributes such as the water-holding capacity of meat, ethical quality of the slaughtering procedure and contamination by toxic environmental substances. The investigations treat quality attributes that are traditionally difficult to measure due to requirement of labour-intensive and time-consuming analytical methods. The depth of CO_2 stunning assessed as the presence or absence of reflexes during sticking and debleeding of slaughter pigs is an example of an attribute that is difficult, if not impossible, to measure. Thus, the desire to develop new methods was also motivated by the possibility of finding more precise methods, in addition to the fast and non-invasive advantages of the spectroscopic methods.

A general challenge during the development of multivariate calibrations in this study was the accuracy of the reference parameters of interest which are often established methods based on very pragmatic principles developed decades ago. The approximation of the uncertainty of the reference methods is important for the final validation of multivariate calibration methods in order to provide better understanding and interpretation of the methods. The estimation of the uncertainty can be difficult, as in the case of inhomogeneous samples which prevent the use of true representative subsamples or if the time perspective is crucial due to, for example, biological processes. It is therefore of utmost importance to incorporate knowledge of the chemical and biological nature of the samples and of the qualifications of the applied spectroscopic and reference methods during the validation of multivariate calibrations.

References

Al-Jowder O., Kemsley E.K. and Wilson R.H. 1997. Mid-infrared spectroscopy and authenticity problems in selected meats: a feasibility study. *Food Chemistry* **59**: 195-201.

Al-Jowder O., Defernez M., Kemsley E.K. and Wilson R.H. 1999. Mid-infrared spectroscopy and chemometrics for the authentication of meat products. *Journal of Agricultural and Food Chemistry* **47**: 3210-3218.

Andersen C.M., Jørgensen B.M. and Bro R. 2002. Investigation of the fluorescence from cod extracts. In prep.

Andersen C.M. and Wold J.P. 2002. On the fluorescence of muscle and connective tissue from cod and salmon. *Journal of Agricultural and Food Chemistry*. Submitted.

Andersson C. 2000. Exploratory multivariate data analysis with applications in food technology. Ph.D. thesis, The Royal Veterinary and Agricultural University, Denmark.

Appleby M.C. and Huges B.O. 1997. Introduction. In *Animal Welfare.* Edited by M.C. Appleby and B.O. Huges, CAB International, Wallingford, UK.

Archibald D.D., Kays S.E., Himmelsbsch D.S. and Barton F.E. 1998a. Raman and NIR spectroscopic methods for determination of total dietary fiber in cereal foods: A comparative study. *Applied Spectroscopy* **52**: 22-31.

Archibald D.D., Kays S.E., Himmelsbsch D.S. and Barton F.E. 1998b. Raman and NIR spectroscopic methods for determination of total dietary fiber in cereal foods: Utilizing model differences. *Applied Spectroscopy* **52**: 32-41.

Aubourg S.P. 1999. Recent advances in assessment of marine lipid oxidation by using fluorescence. *Journal of the American Oil Chemists Society* **76**: 409-419.

Baeten V., Dardenne P. and Aparicio R. 2001. Interpretation of Fourier transform Raman spectra of the unsaponifiable matter in a selection of edible oils. *Journal of Agricultural and Food Chemistry* **49**: 5098-5107.

Barnes R.J., Dhanoa M.S. and Lister S.J. 1989. Standard normal variate transformation and de-trending of near-infrared diffuse reflectance spectra. *Applied Spectroscopy* **43**: 772-777.

Baunsgaard D. 2000. Analysis of color impurities in sugar processing using fluorescence spectroscopy and chemometrics. Ph.D. thesis, The Royal Veterinary and Agricultural University, Denmark.

Baunsgaard D., Munck L. and Nørgaard L. 2000. Analysis of the effect of crystal size and color distribution on fluorescence measurements of solid sugar using chemometrics. *Applied Spectroscopy* **54**: 1684-1689.

Belgian Government, Federal Ministry of Agriculture and Federal Ministry of Health. 1999. PCB and dioxin contamination in the feed and food chain in Belgium. http://dioxin.fgov.be/pe/ene00.htm.

Bellon V. 1993. Fermentation control using ATR and an FT-IR spectrometer. *Sensors and Actuators B* **12**: 57-64.

Bellon-Maurel V., Vallat C. and Goffinet D. 1995a. Quantitative analysis if individual sugars during starch hydrolysis by FT-IR/ATR spectrometry. Part I: Multivariate calibration study – repeatability and reproducibility. *Applied Spectroscopy* **49**: 556-562.

Bellon-Maurel V., Vallat C. and Goffinet D. 1995b. Quantitative analysis if individual sugars during starch hydrolysis by FT-IR/ATR spectrometry. Part II: Influence of external factors and wavelength parameters. *Applied Spectroscopy* **49**: 563-598.

Belton P.S. 1993. New methods for monitoring changes in proteins. *Food Reviews International* **9**: 551-573.

Beppu M., Murakami K., Kikugawa K. 1986. Fluorescent and cross-linked proteins of human erythrocyte ghosts formed by reaction with hydroperoxylinoleic acid, malonaldehyde and monofunctional aldehydes. *Chemical & Pharmaceutical Bulletin.* **34**: 781-788.

Bertram H.C., Andersen H.J. and Karlsson A.H. 2001. Comparative study of low-field NMR relaxation measurements and two traditional methods in the determination of water holding capacity of pork. *Meat Science* **57**: 125-132.

Bertram H.C., Dønstrup S., Karlsson A.H. and Andersen H.J. 2002. Continuous distribution analysis of T_2 relaxation in meat – an approach in the determination of water-holding capacity. *Meat Science* **60**: 279-285.

Birlouez-Aragon I., Nicolas M., Metais A., Marchond N., Grenier J. and Calvo D. 1998. A rapid fluorimetric method to estimate the heat treatment of liquid milk. *International Dairy Journal* **8**: 771-777.

Birlouez-Aragon I., Leclere J., Quedraogo C.L., Birlouez E. and Grongnet J.F. 2001. The FAST method, a rapid approach of the nutritional quality of heat-treated foods. *Nahrung* **45**: 201-205.

Bouraoui M., Nakai S. and Li-Chan E. 1997. *In situ* investigation of protein structure in Pacific whiting surimi and gels using Raman spectroscopy. *Food Research International* **30**: 65-72.

Bro R. 1996. Multiway calibration. Multi-linear PLS. *Journal of Chemometrics* **10**: 47-61.

Bro R. 1997. PARAFAC. Tutorial and applications. *Chemometrics and Intelligent Laboratory Systems* **38**: 149-171.

Brown R.J.S., Capozzi F., Cavani C., Cremonini M.A., Petracci M. and Placucci G. 2000. Relationships between ^{1}H NMR relaxation data and some technological parameters of meat: A chemometric approach. *Journal of Magnetic Resonance* **147**: 89-94.

Brøndum J., Byrne D.V., Bak L.S., Bertelsen G. and Engelsen S.B. 2000a. Warmed-over flavour in porcine meat – a combined spectroscopic, sensory and chemometric study. *Meat Science* **54**: 83-95.

Brøndum J., Munck L., Henckel P., Karlsson A., Tornberg E. and Engelsen S.B. 2000b. Prediction of water-holding capacity and composition of porcine meat by comparative spectroscopy. *Meat Science* **55**: 177-185.

Byrne C.E., Downey G., Troy D.J. and Buckley D.J. 1998. Non-destructive prediction of selected quality attributes of beef by near-infrared reflectance spectroscopy between 750 and 1098 nm. *Meat Science* **49**: 399-409.

Chatzi E.G., Kammona O. and Kiparissides C. 1997. Use of a midrange infrared optical-fiber probe for the on-line monitoring of 2-ethylhexyl acrylate/styrene emulsion copolymerisation. *Journal of Applied Polymer Science* **63**: 799-809.

Chio K.S. ans Tappel A.L. 1969. Synthesis and characterization of the fluorescent products derived from malonaldehyde and amino acids. *Biochemistry* **8**: 2821-2832.

Dahl P.L., Christensen B.M., Munck L., Larsen E.P. and Engelsen S.B. 2000. Can spectroscopy in combination with chemometrics replace minks in digestibility tests? *Journal of the Science of Food and Agriculture* **80**: 365-374.

Dahlberg D.B., Lee S.M, Wenger S.J. and Vargo J.A. 1997. Classification of vegetable oils by FT-IR. *Applied Spectroscopy* **51**: 1118-1124.

Dao N.Q. and Jouan M. 1993. The Raman laser fiber optics (RLFO) method and its applications. *Sensors and Actuators B-Chemical* **11**: 147-160.

Davies A.N., McIntyre P. and Morgan E. 2000. Study of the use of molecular spectroscopy for the authentication of extra virgin olive oils. Part I: Fourier transform Raman spectroscopy. *Applied Spectroscopy* **54**: 1864-1867.

Defernez M. and Wilson R.H. 1995. Mid-infrared spectroscopy and chemometrics for determining the type of fruit used in jam. *Journal of the Science of Food and Agriculture* **67**: 461-467.

Defernez M., Kemsley E.K. and Wilson R.H. 1995. Use of infrared spectroscopy and chemometrics for the authentication of fruit purees. *Journal of Agricultural and Food Chemistry* **43**: 109-113.

Defernez M., Kemsley E.K. and Wilson R.H. 1997. Mid-infrared as a new tool for detecting adulteration in fruit products. *Microchimica Acta* Suppl. **14**: 181-182.

Delwiche S.R. 1995. Single wheat kernel analysis by Near Infrared Transmittance: Protein content. *Cereal Chemistry* **72**: 11-16.

Delwiche S.R. 1998. Protein content of single kernels of wheat by near-infrared reflectance spectroscopy. *Journal of Cereal Science* **27**: 241-254.

De Noord O.E. 1994. The influence of data preprocessing on the robustness and parsimony of multivariate calibration models. *Chemometrics and Intelligent Laboratory Systems* **23**: 65-70.

Dillard C.J. and Tappel A.L. 1971. Fluorescent products of lipid peroxidation of mitochondria and microsomes. *Lipids* **6**: 715-721.

Dion B., Ruzbie M., van de Voort F.R., Ismail A.A. and Blais J.S. 1994. Determination of protein and fat in meat by transmission Fourier transform infrared spectrometry. *Analyst* **119**: 1765-1771.

Dolmatova L., Ruckebusch C., Dupuy N., Huvenne J.P. and Legrand P. 1998. Identification of modified starches using infrared spectroscopy and artificial neural network processing. *Applied Spectroscopy* **52**: 329-338.

Dupuy N., Huvenne J.P., Sombret B. and Legrand P. 1993a. Quantitative analysis by mid-infrared spectrometry in food and agro-industrial fields. *Journal of Molecular Structure* **294**: 223-226.

Dupuy N., Meurens M., Sombret B., Legrand P. and Huvenne J.P. 1993b. Multivariate determination of sugar powders by attenuated total reflectance infrared spectroscopy. *Applied Spectroscopy* **47**: 452-457.

Engelsen S.B. 1997. Explorative spectrometric evaluations of frying oil deterioration. *Journal of the American Oil Chemists Society* **74**: 1495-1508.

Engelsen S.B. and Nørgaard L. 1996. Comparative vibrational spectroscopy for determination of quality parameters in amidated pectins as evaluated by chemometrics. *Carbohydrate Polymers* **30**: 9-24.

Esterbauer H., Koller E., Slee R.G. and Koster J.F. 1986. Possible involvement of the lipid-peroxidation product 4-hydroxynonenal in the formation of fluorescent chromolipids. *Biochemical Journal* **239**: 405-409.

Ferreira D., Barros A., Coimbra M.A. and Delgadillo I. 2001.Use of FT-IR spectroscopy to follow the effect of processing in cell wall polysaccharide extracts of a sun-dried pear. *Carbohydrate Polymers* **45**: 175-182.

Fontecha J., Bellanato J. and Juarez M. 1993. Infrared and Raman spectroscopic study of casein in cheese: Effect of freezing and frozen storage. *Journal of Dairy Science* **76**: 3303-3309.

Forrest J.C., Morgan M.T., Borggaard C., Rasmussen A.J., Jespersen B.L. and Andersen J.R. 2000. Development of technology for the early post mortem

prediction of water holding capacity and drip loss in fresh pork. *Meat Science* **55**: 115-122.

Geladi P., MacDougall D. and Martens H. 1985. Linearization and scatter-correction for near-infrared reflectance spectra of meat. *Applied Spectroscopy* **39**: 491-500.

Góral J. and Zichy V. 1990. Fourier transform Raman studies of materials and compound of biological importance. *Spectrochimica Acta* **46A**: 253-275.

Griffiths P.R. and Haseth J.A. de. 1986. *Fourier Transform Infrared Spectroscopy*. John Wiley and Sons, New York.

Hansen P.W. 1998. Urea determination in milk using Fourier transform infrared spectroscopy and multivariate calibration. *Milchwissenschaft* **53**: 251-255.

Harhay G.P. and Siragusa F.R. 1999. Hydrogen-deuterium exchange and ultraviolet resonance Raman spectroscopy of bacteria in a complex food matrix. *Journal of Rapid Methods and Automation in Microbiology* **7**: 25-38.

Harshman R.A. 1970. Foundations of the PARAFAC procedure: models and conditions for an 'explanatory' multi-modal factor analysis. *UCLA Working Paper. Phonetics* **16**: 1-84.

Hasegawa K., Endo Y., Fujimoto K. 1992. Oxidative detoriation in dried fish model systems assessed by solid sample fluorescence spectrophotometry. *Journal of Food Science* **57**: 1123-1126.

Hasegawa K., Endo Y., Fujimoto K. 1993. Assessment of lipid oxidation in freeze-dried pork and egg yolk by solid sample spectrofluorometry. *Nippon Shokuhin Kogyo Gakkaishi* **40**: 150-153.

Hazen K.H., Arnold M.A. and Small G.W. 1998. Measurement of glucose and other analytes in undiluted human serum with near-infrared transmission spectroscopy. *Analytica Chimica Acta* **371**: 255-267

Helland I.S., Næs T. and Isaksson T. 1995. Related versions of the multiplicative scatter correction method for preprocessing spectroscopic data. *Chemomometrics and Intelligent Laboratory Systems* **29**: 233-241

Hildrum K.I., Nilsen B.N., Mielnik M. and Næs T. 1994. Prediction of sensory characteristics of beef by near-infrared spectroscopy. *Meat Science* **38**: 67-80.

Ho C.N., Christian G.D. and Davidson E.R. 1978. Application of the method of rank annihilation to quantitative analyses of multicomponent fluorescence data from the video fluorometer. *Analytical Chemistry* **50**: 1108-1113.

Holst S. 2001. CO2 stunning of pigs for slaughter – practical guidelines for good animal welfare. *Proceedings 47th International Congress of Meat Science and Technology*, Krakow, Poland, Vol. I: 48-54.

Honikel K.O. 1998. Reference methods for the assessment of physical characteristics of meat. *Meat Science* **49**: 447-457.

Höskuldsson A. 1994. The H-principle: new ideas, algorithms and methods in applied mathematics and statistics. *Chemometrics and Intelligent Laboratory Systems* **23**: 1-28

Höskuldsson A. 1996. In *Prediction Methods in Science and Technology*. *Vol 1. Basic Theory*. Thor Publishing, Denmark.

Iizuka K. and Aishima T. 1999: Tenderization of beef with pineapple juice monitored by Fourier Transform infrared spectroscopy and chemometric analysis. *Journal of Food Science* **64**: 973-977.

Iizuka K. and Aishima T. 2000. Comparing beef digestion properties of four proteolytic enzymes using infrared spectrometry and chemometric analysis. *Journal of the Science of Food and Agriculture* **80**: 1413-1420.

Irudayaraj J. and Yang H. 2000. Analysis of cheese using step-scan Fourier transform infrared photoacoustic spectroscopy. *Applied Spectroscopy* **54**: 595-600.

Irudayaraj J., Sivakesava S., Kamath S. and Yang H. 2001. Monitoring chemical changes in some foods using Fourier Transform photoacoustic spectroscopy. *Journal of Food Science* **66**: 1416-1421.

Isaksson T. and Kowalski B. 1993. Piece-wise multiplicative scatter correction applied to near-infrared diffuse transmittance data from meat products. *Applied Spectroscopy* **47**: 702-709.

Ismail A.A., van de Voort F.R., Emo G. and Sedman J. 1993. Rapid quantitative determination of free fatty acids in fats and oils by Fourier Transform infrared spectroscopy. *Journal of the American Oil Chemists Society* **70**: 335-341.

Kameoka T., Okuda T., Hashimoto A., Noro A., Shiinoki Y. and Ito K. 1998a. FT-IR analysis of sugars in aqueous solution using ATR method. *Nippon Shokuhin Kagaku Kogaku Kaishi* **45**: 192-198.

Kameoka T., Okuda T., Hashimoto A., Noro A., Shiinoki Y. and Ito K. 1998b. A rapid FT-IR/ATR method for sugar content determination in food. *Nippon Shokuhin Kagaku Kogaku Kaishi* **45**: 199-204.

Keller S., Löchte T., Dippel B. and Schrader B. 1993. Quality-control of food with near-infrared-excited Raman-spectroscopy. *Fresenius Journal of Analytical Chemistry* **346**: 863-867.

Kemsley E.K., Wilson R.H. and Belton P.S. 1992. Potential of Fourier-transform infrared-spectroscopy and fiber optics for process-control. *Journal of Agricultural and Food Chemistry* **40**: 435-438.

Kemsley E.K., Wilson R.H., Poulter G. and Day L.L. 1993. Quantitative analysis of sugar solutions using a novel fiber-optic-based sapphire ATR accessory. *Applied Spectroscopy* **47**: 1651-1654.

Kikugawa L. and Beppu M. 1987. Involvement of lipid oxidation products in the formation of fluorescent and cross-linked proteins. *Chemistry and Physics of Lipids* **44**: 277-296.

Kikugawa K., Machida Y. Kida M., Kurechi T. 1981. Studies on peroxidized lipids. III. Fluorescent pigments derived from the reaction of malonaldehyde and amino acids. *Chemical & Pharmaceutical Bulletin* **29**: 3003-3011.

Kikugawa L., Takayanagi K., Watanabe S. 1985. Polylysines modified with malonaldehyde, hydroxylinoleic acid and monofunctional aldehydes. *Chemical & Pharmaceutical Bulletin* **33**: 5437-5444.

Kjeldahl J. 1883. *Analytical Chemistry* **22**: 366.

Kuenstner J.T., Norris K.H. and McCarthy W.F. 1994. Measurement of hemoglobin in unlysed blood by near-infrared spectroscopy. *Applied Spectroscopy* **48**: 484-488.

Küpper L., Heise H.M., Lampen P., Davies A.N. and McIntyre P. 2001. Authentication and quantification of extra olive oils by attenuated total reflectance infrared spectroscopy using silver halide fiber probes and partial least-squares calibration. *Applied Spectroscopy* **55**: 563-570.

Lafrance D., Lands L.C., Hornby L. and Burns D.H. 2000. Near-infrared spectroscopic measurement of lactate in human plasma. *Applied Spectroscopy* **54**: 300-304.

Lakowicz J.R. 1999. *Principles of Fluorescence Spectroscopy*. 2nd edition, Kluwer Academic / Plenum Publishers, New York, USA.

Li-Chan E.C.Y. 1996. The applications of Raman spectroscopy in food science. *Trends in Food Science and Technology* **7**: 361-370.

Liescheski P.B. 1996. Supercritical fluid extraction coupled to infrared spectroscopy for iodine number analysis of edible oils. *Journal of Agricultural and Food Chemistry* **44**: 823-828.

Lowry S.R., May T.E. and Bornstein A. 1993. Signal enhancement technique for internal reflection spectroscopy. *Applied Spectroscopy* **47**: 30-34.

Lowry S., May T., Bornstein A., Weissman Y., Harman R. and Tugenthaft I. 1994. New accessory for characterizing optical fibers with an FT-IR spectrometer. *Applied Spectroscopy* **48**: 852-856.

Martens H. 2001. Personal communications

Martens H. and Martens M. 2000. Modified jack-knife estimation of parameter uncertainty in bilinear modelling by partial least squares regression (PLSR). *Food quality and preference* **11**: 5-16.

Martens H. and Næs T. 1989. *Multivariate Calibration*. John Wiley and Sons, Chichester, UK.

Martens H. and Stark E. 1991. Extended multiplicative signal correction and spectral interference subtraction: new preprocessing methods for near infrared spectroscopy. *Journal of Pharmaceutical & Biomedical Analysis* **9**: 625-635.

Martens H., Nielsen J.P. and Engelsen S.B. 2002. Light scattering and light absorbance separated by extended multiplicative signal correction (EMSC). Application to NIT analysis of binary powder mixtures. *Analytical Chemistry*. Submitted.

McElhinney J., Downey G. and O'Donnell C. 1999. Quantitation of lamb content in mixtures with raw minced beef using visible, near and mid-infrared spectroscopy. *Journal of Food Science* **64**: 587-591.

Melton S.L. 1983. Methodology for following lipid oxidation in muscle food. *Food Technology* **37**: 105-111.

Miller C.E. and Næs T. 1990. A pathlength correction method for near-infrared spectroscopy. *Applied Spectroscopy* **44**: 895-898.

Mirouze F.D., Boulou J.C., Dupuy N., Meurens M., Huvenne J.P. and Legrand P. 1993. Quantitative analysis of glucose syrups by ATR/FT-IR spectroscopy. *Applied Spectroscopy* **47**: 1187-1191.

Mitsumoto M., Maeda S., Mitsuhashi T. and Ozawa S. 1991. Near-infrared spectroscopy determination of physical and chemical characteristics in beef cuts. *Journal of Food Science* **56**: 1493-1496.

Munck L. 1989a. *Fluorescence Analysis in Foods*. Longman Singapore Publishers Ltd., Singapore.

Munck L. 1989b. Practical experiences in development of fluorescence analysis in an applied food research laboratory. In *Fluorescence Analysis in Foods*. Ed. L. Munck, Longman Singapore Publishers Ltd., Singapore.

Munck L., Nørgaard L., Engelsen S.B., Bro R. and Andersson C.A. 1998 Chemometrics in food science - a demonstration of the feasibility of a highly exploratory, inductive evaluation strategy of fundamental scientific significance. *Chemometrics and Intelligent Laboratory Systems* **44**: 31-60.

Munck L., Pram Nielsen J., Møller B., Jacobsen S., Søndergaard I., Engelsen S.B., Nørgaard L. and Bro R. 2001. Exploring the phenotypic expression of a regulatory proteome-altering gene by spectroscopy and chemometrics. *Analytica Chimica Acta* **446**: 171-186.

Murcia M.A., Cano C. and Bretón J. 1994. FT-IR spectroscopy as a tool for the study of the quality of processed meat-products. *Grasas y Aceites* **45**: 297-299.

Nathier-Dufour N., Sedman J. and van de Voort F.R. 1995. A rapid ATR/FTIR quality control method for the determination of fat and solids in sweetened condensed milk. *Milchwissenschaft* **50**: 462-466.

Nørgaard L., Saudland A., Wagner J., Nielsen J.P., Munck L. and Engelsen S.B. 2000. Interval partial least-squares regression (iPLS): A comparative chemometric study with an example from near-infrared spectroscopy. *Applied Spectroscopy* **54**: 413-419.

Offer G. and Knight P. 1988. The structural basis of water-holding in meat. Part 2: Drip losses. In *Developments in Meat Science, Vol. 4*. Edited by R.A. Lawrie, Elsevier, London, UK.

Ogawa M., Nakamura S., Horimoto Y., An H., Tsuchiya T. and Nakai S. 1999. Raman spectroscopic study of changes in fish actomyosin during setting. *Journal of Agricultural and Food Chemistry* **47**: 3309-3318.

Osborne B.G., Fearn T. and Hindle P.H. 1993. *Practical NIR Spectroscopy with Applications in Food and Beverage Analysis*. 2nd edition, Longman, Scientific & Technical, Essex, UK.

Ozaki Y., Cho R., Ikegaya K., Muraishi S. and Kawauchi K. 1992. Potential of near-infrared Fourier transform Raman spectroscopy in food analysis. *Applied Spectroscopy* **46**: 1503-1507.

Park B., Chen Y.R., Hruschka W.R., Shackelford S.D. and Koohmaraie M. 2001. Principal component regression of near-infrared reflectance spectra for beef tenderness prediction. *Transactions of the ASAE* **44**: 609-615.

Pearson K. 1901. On lines and planes of closest fit to systems of points in shape. *Philosophical Magazine* **2**: 559-572.

Pedersen B. and Martens H. 1989. Multivariate calibration of fluorescence data. In *Fluorescence Analysis in Foods*. Ed. L. Munck, Longman Singapore Publishers Ltd., Singapore.

Pezolet M., Pigeon-Gosselin M. and Caille J.P. 1978a. Laser Raman investigation of intact single muscle fibers protein conformations. *Biochimica et Biophysica Acta* **533**: 263-269.

Pezolet M., Pigeon-Gosselin M., Savoie R. and Caille J.P. 1978b. Laser Raman investigation of intact single muscle fibers on the state of water in muscle tissue. *Biochimica et Biophysica Acta* **544**: 394-406.

Pezolet M., Pigeon-Gosselin M., Nadeau J. and Caille J.P. 1980. Laser Raman scattering – A molecular probe of the contractile state of intact single muscle-fibers. *Biophysical Journal* **31**: 1-8.

Raman C.V. and Krishnan K.S. 1928. A new type of secondary radiation. *Nature* **121**: 501.

Rannou H. and Downey G. 1997. Discrimination of raw pork, chicken and turkey meat by spectroscopy in the visible, near- and mid-infrared ranges. *Analytical Communications* **34**: 401-404.

Rasmussen A.J. and Andersson M. 1996. New method for determination of drip loss in pork muscles. *Proc. 42nd International Congress of Meat Science and Technology*, Lillehammer, Norway: 286-287.

Rettig W., Strehmel B., Schrader S. and Seifert H. 1999. *Applied Fluorescence in Chemistry, Biology and Medicine*. Springer-Verlag, Berlin.

Ripoche A. and Guillard A.S. 2001. Determination of fatty acid composition of pork fat by Fourier transform infrared spectroscopy. *Meat Science* **58**: 299-304.

Robinson N.E. 1997. Gas transport in the blood. In *Textbook of Veterinary Physiology*. Ed. J.G. Cunningham, 2nd edition, W.B. Saunders Company, Philadelphia, USA.

Rødbotten R., Nilsen B.N. and Hildrum K.I. 2000. Prediction of beef quality attributes from early post mortem near infrared reflectance spectra. *Food Chemistry* **69**: 427-436.

Sadeghi-Jorabchi H., Wilson R.H., Belton P.S., Edwards-Webb J.D. and Coxon D.T. 1991. Quantitative analysis of oils and fats by Fourier transform Raman spectroscopy. *Spectrochimica Acta* **47A**: 1449-1458.

Savitzky A. and Golay M.J.E. 1964. Smoothing and differentiation of data by simplified least squares procedures. *Analytical Chemistry* **36**: 1627-1639.

Schrader B. 1996. Raman spectroscopy in the near infrared – A most capable method of vibrational spectroscopy. *Fresenius Journal of Analytical Chemistry* **355**: 233-239.

Shahidi F. 1994. Assessment of lipid oxidation and off-flavour development in meat and meat products. In *Flavour of meat and meat products*. Edited by F. Shahidi. Blackie Academic & Professional, Glasgow, UK: 247-266.

Skoog D.A. and Leary J.J. 1992. *Principles of Instrumental Analysis*. Forth edition. Harcourt Brace College Publishers, Orlando, USA: 296-309.

Strasburg G.M. and Ludescher R.D. 1995. Theory and applications of fluorescence spectroscopy in food research. *Trends in Food Science and Technology* **6**: 69-75.

Swatland H.J. 1997. Relationships between the back-scatter of polarised light and the fibre-optic detection of connective tissue fluorescence in beef. *Journal of the Science of Food and Agriculture* **75**: 45-49.

Swatland H.J. and Barbut S. 1995. Optical prediction of processing characteristics of turkey meat using UV fluorescence and NIR birefringence. *Food Research International* **28**: 227-232.

Swatland H.J. and Findlay C.J. 1997. On-line probe prediction of beef toughness, correlating sensory evaluation with fluorescence detection of connective tissue and dynamic analysis of overall toughness. *Food Quality and Preference* **8**: 233-239.

Swatland H.J., Warkup C. and Cuthbartson A. 1993. Testing a UV fluorescence probe for beef carcass connective tissues. *Computers and Electronics in Agriculture* **9**: 255-267.

Tappel A.L. 1970. Biological antioxidant protection against lipid peroxidation damage. *American Journal of Clinical Nutrition* **23**: 1137-1139.

van de Voort F.R., Sedman J., Emo G. and Ismail A.A. 1992. Assessment of Fourier Transform infrared analysis of milk. *Journal of AOAC International* **75**: 780-785.

van de Voort F.R., Sedman J. and Ismail A.A. 1993. A rapid FTIR quality-control method for determining fat and moisture in high-fat products. *Food Chemistry* **48**: 213-221.

van de Voort F.R., Ismail A.A., Sedman J., Dubois J. and Nicodemo T. 1994. The determination of peroxide value by Fourier Transform infrared spectroscopy. *Journal of the American Oil Chemists Society* **71**: 921-926.

van de Voort F.R., Ismail A.A. and Sedman J. 1995. A rapid, automated method for the determination of *cis* and *trans* content of fats and oils by Fourier Transform infrared spectroscopy. *Journal of the American Oil Chemists Society* **72**: 873-880.

Vega M., Pardo R., Barrado E. and Debán L. 1998. Assessment of seasonal and polluting effects on the quality of river water by exploratory data analysis. *Water Research* **32**: 3581-3592.

Westad F. and Martens H. 2000. Variable selection in near infrared spectroscopy based on significance testing in partial least squares regression. *Journal of Near Infrared Spectroscopy* **8**: 117-124.

Wilson R.H. and Tapp H.S. 1999. Mid-infrared spectroscopy for food analysis: recent new applications and relevant developments in sample presentation methods. *Trends in Analytical Chemistry* **18**: 85-93.

Wold J.P. and Kvaal K. 2000. Mapping lipid oxidation in chicken meat by multispectral imaging of autofluorescence. *Applied Spectroscopy* **54**: 900-909.

Wold J.P. and Mielnik M. 2000. Nondestructive assessment of lipid oxidation in minced poultry meat by autofluorescence spectroscopy. *Journal of Food Science* **65**: 87-95.

Wold J.P., Kvaal K. and Egelandsdal B. 1999a. Quantification of intramuscular fat content in beef by combining autofluorescence spectra and autofluorescence images. *Applied Spectroscopy* **53**: 448-456.

Wold J.P., Lundby F. and Egelandsdal B. 1999b. Quantification of connective tissue (hydroxyproline) in ground beef by autofluorescence spectroscopy. *Journal of Food Science* **64**: 377-383.

Wold S., Esbensen K. and Geladi P. 1987. Principal Component Analysis. *Chemometrics and Intelligent Laboratory Systems* **2**: 37-52.

Wold S., Antti H., Lindgren F. and Öhman J. 1998. Orthogonal correction of near-infrared spectra. *Chemometrics and Intelligent Laboratory Systems* **44**: 175-185.

Wülfert F., Kok W.T. and Smilde A.K. 1998. Influence of temperature on vibrational spectra and consequences for the predictive ability of multivariate models. *Analytical Chemistry* **70**: 1761-1767.

Yang H. and Irudayaraj J. 2001. Characterization of beef and pork using Fourier-transform infrared photoacoustic spectroscopy. *Lebensmittel-Wissenschaft und Technologie* **34**: 402-409.

Paper I

Monitoring Industrial Food Processes Using Spectroscopy & Chemometrics

D.K. Pedersen and S.B. Engelsen

In the last decade rapid spectroscopic measurements have revolutionized quality control in practically all areas of primary food and feed production. Near-infrared spectroscopy (NIR & NIT) has been implemented for monitoring quality of millions of samples of cereals, milk and meat with unprecedented precision and speed. The key to this success is the extraordinary synergy that lies in the merging of spectroscopy and the new data technology called chemometrics. A true paradigm shift has occurred in the food industry where engineers are now exploring their processes using soft models and spectroscopic sensors to complement traditional hard models and univariate measurements. The new exploratory, multivariate spectroscopic methods of observing nature and processes are non-destructive, rapid and environmentally friendly compared to the traditionally used univariate and slower physico-chemical methods (Fig. 1).

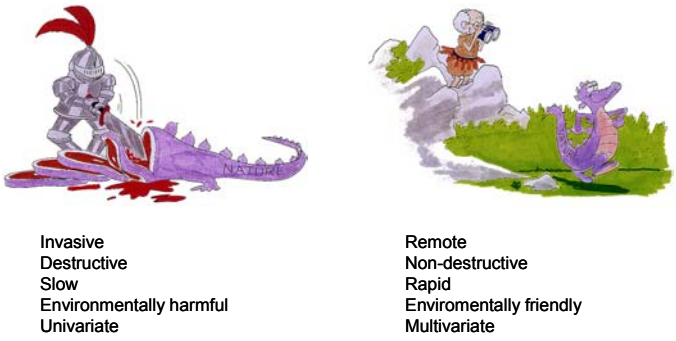

Figure 1. Two ways of handling the "dragon" (nature). The advantages of explorative multivariate spectroscopic measurements compared to traditional deductive univariate measurements. © Munck & Newlin

However, the most significant advantage of the spectroscopic methods is their remote sensing capabilities. In contrast to most other methods spectroscopic sensors can be implemented directly in the process line for real-time quality monitoring of the continuous stream of raw products, semi-processed reaction products or final products. This revolution appears to transform the food industry from a traditionally low-technology industry into a high-technology industry alongside with the quality control in the pharmaceutical industry.

Why chemometrics:

One of the main advantages of chemometric data analysis is the possibility of projecting multivariate data into few dimensions in a graphical interface. Chemometrics is able to handle large data sets and deal efficiently with real-world multivariate data, taking advantage of the previously feared colinearity of spectral data. With chemometrics it is possible with advantage to analyse whole spectra in real time. The basis of most chemometric algorithms is Principal Component Analysis (PCA) which this year can celebrate its 100-year anniversary in splendid shape. PCA can be considered as the first amendment in exploratory analysis due to its extraordinarily robust data reduction and data-overviewing capabilities. In PCA the multivariate (spectral) data set is resolved into orthogonal components whose linear combinations approximate the original data set in a least squares sense. Partial Least Squares Regression (PLSR), built on PCA technology, is its counterpart for regression analysis. PLSR is a predictive two-block regression method based on estimated latent variables and applies to the simultaneous analysis of two data sets (e.g. spectra and physical/chemical tests) of the same objects [1]. The purpose of PLSR is to build a linear model that enables prediction of a desired characteristic from a measured spectrum. PLSR is used routinely to correlate spectroscopic data (rapid measurements) with related chemical/physical data (slow measurements). Both PCA and PLSR are bi-linear methods able to utilize the multivariate advantage when applied to co-linear first order data (Table 1); i.e., they facilitate inference compensation and outlier detection when abnormal or erroneous signals are measured. In addition, chemometrics covers methods for spectral variable or interval

selection [2] aimed at improving regression models and at developing dedicated fast spectroscopic instruments.

Table 1. Data structures

Graphical example	Data	Advantage	Spectroscopic data example
×	0th order	-	UV abs. at 330nm
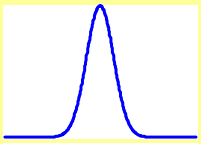	1st order	Outlier detection, interference compensation, noise reduction	UV spectrum
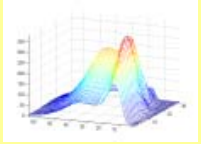	2nd order	All of the above plus **unique solution**	Fluorescence excitation-emission landscape

Why spectroscopy:

Increased demands by the consumers, legislators and competition have been the impetus for the development of new quality-monitoring tools in the food industry. On-line non-contact spectroscopic measurements are the only measuring techniques that can meet these demands. Spectroscopic measurements can be performed remotely and in combination with chemometrics analysed practically real time (in a matter of seconds), which gives a great potential for installment on-line/at-line for process control. When introducing a spectroscopic method in industry the key question "*What would be the appropriate choice of spectroscopic sensor?"* arises. The answer will not only depend on the quality parameter to be measured, but also on the possible sample presentation, the need for non-destructiveness, robustness and, last but not least, possible spin-off in terms of other relevant quality parameters to be measured (Fig. 1). In this context spectroscopic sensors are a handful of methods based on interactions between sample and electromagnetic radiation, including ultraviolet and visual absorption, fluorescence emission, near-infrared and infrared absorption, Raman scattering, nuclear magnetic resonance, microwave

absorption and (ultra)-sound transmission. The spectroscopic methods based on different regions of the electromagnetic spectrum and different physical principles have naturally different sensing capabilities, but share the ability to provide rapid multivariate information on the sample being monitored, which in turn makes it possible to simultaneously determine several quality parameters.

Spectroscopic sensors

One of the most fascinating spectroscopic methods is near-infrared spectroscopy, which over the last decade has been successfully implemented as a fast at-line/on-line quality control in almost all parts of the food industry. It was recognized early that the almost holographic vibrational overtone and combination bands residing in the near-infrared spectral region (780-2500 nm) contain an abundance of chemical information comparable to the mid-infrared region (see Fig. 2).

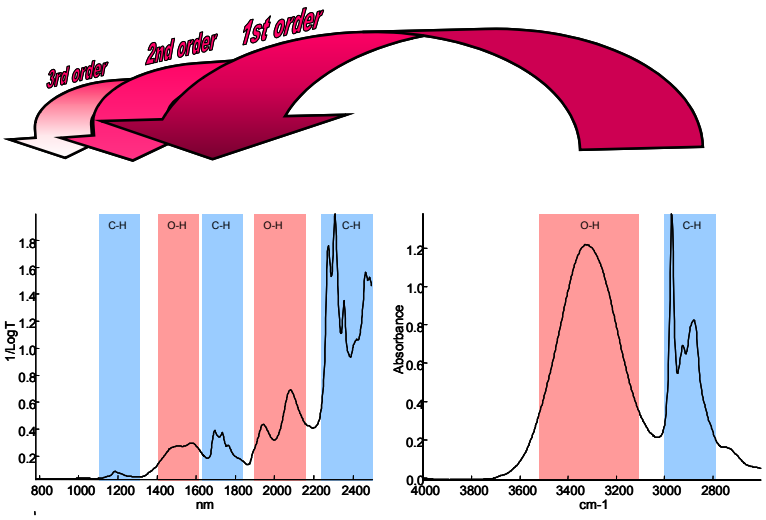

Figure 2. In this figure the holographic principle of near-infrared spectroscopy is demonstrated with a spectrum of ethanol. The motif from the fundamental stretching vibrations in the mid-infrared region (right) is repeated in the near-infrared spectrum (first, second and third overtones) and overlaid with combinatorial information (combination tones)

Moreover, near-infrared sensors have the additional advantage that instrumentation is relatively simple and that the radiation may be transmitted through quartz, making the use of optical fibres feasible. One instrument and an optical switch can thus monitor several measuring points hundred of meters apart. In the food industry near-infrared spectroscopy is implemented to monitor traditional quality parameters such as moisture, protein and fat content as well as product-specific attributes. The trend in on-line near-infrared application goes in the direction of fingerprinting raw materials, end products and optimal reaction end-stage utilising the full holographic potential of near-infrared spectroscopy.

Like sensors built on near-infrared technology, Fourier transform infrared (FT-IR) sensors have substantial potential as a quantitative quality control tool for the food industry, but this far has mainly found use in off-line liquid analyses of especially milk, edible oils and wine. The main objection to implementation of mid-infrared for industrial quality control has been the requirement of sophisticated optical materials prohibiting the use of practical fibres and the lack of optimal sampling methods. Liquids (and gasses), however, can be optimally measured with transmission or attenuated total reflectance (ATR) cells adapted for off-line measurements. Fig. 3 demonstrates the combined performance of mid-infrared spectroscopy and chemometrics.

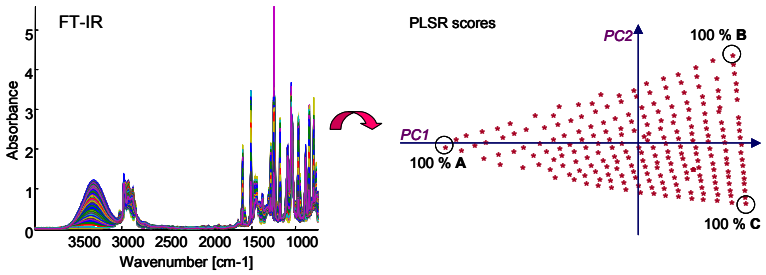

Figure 3. (left) Superimposed mid-infrared spectra of a ternary mixture in the confectionary industry and (right) PLSR score plot with almost perfect recovery of the mixture design

A full-design ternary mixture of extracts in the confectionary industry was measured with the ATR principle and related to consumer sensory attributes. The design was

fully recovered in the PLSR score plot, promising excellent prediction performance for the spectroscopic at-line method. More recently, a small revolution in sampling techniques for infrared has occurred. The ATR principle has been extended to solids through the so-called diamond ATR by which infrared spectra of samples softer than diamond can be measured with high precision and reproducibility.

Raman scattering, based on weak, inelastic scattered side bands arising when illuminating a sample with a strong monochromatic light, appears to be an attractive alternative to the in-practice impossible on-line implementation of mid-infrared sensors. Like mid-infrared, Raman scatter measures the fundamental molecular vibrations, albeit with different selection rules (relative selectivity), and like near-infrared radiation, Raman scattering can be transmitted in optical quartz fibres. To date, a small number of customised on-line Raman applications have been developed in the petrochemical, polymer and harddisk industries. However, in contrast to mid-infrared and near-infrared, the high sensitivity of Raman to C=C, C≡C and C≡N bonds, low sensitivity to water and high selectivity to inorganic substances (salts) can be of potential interest for niche-applications in the food industry.

The vibrational spectroscopies: near-infrared, mid-infrared and Raman have in common that practically all substances will give rise to substantial absorption/scattering effects for which reason information on trace substances and/or detailed conformational information is normally hidden in spectra of complex samples such as food. Trace substance sensitivity can be obtained by fluorescence emission sensors, as most substances do not fluoresce and emission spectra can therefore be measured against a black background. However, a trace substance sensitive measuring method naturally requires that the trace substance to be analysed contain one or more fluorophores. Important fluorophores of relevance to foods include proteins (containing the amino acids tryptophane, tyrosine and phenylalanine), coenzymes (NADH, NADPH and FAD), vitamins (A, B_1, B_2, B_6, B_{12}, D_2, E and folic acid), caffeine, chlorophyll, polyphenols, flavanoids and aflatoxins. Robust fluorescence sensors based on fibre optics already exist, but their on-line implementation in the food processes have not yet been exploited. Fluorescence sensors have great potential for monitoring fermentation reactors, and fingerprinting with fluorescence spectroscopy is a powerful technique which is highly complementary to vibrational fingerprinting.

Fluorescence spectra has the attractive property (see later) that it is measured as a function of two variables, namely, the excitation wavelength and the emission wavelength, thus providing two-dimensional spectra (landscapes). As an example, Fig. 4 displays fluorescence landscapes of the frying oil from the beginning and end of a commercial spring roll frying process [3].

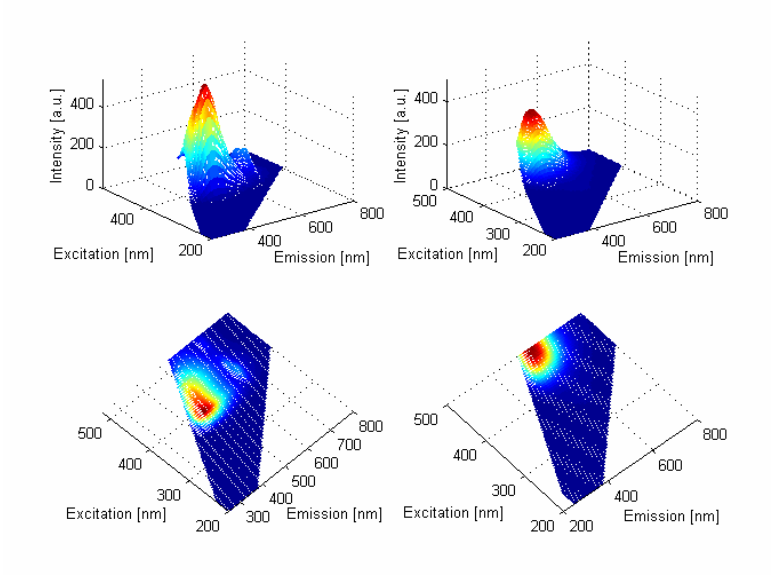

Figure 4. Fluorescence excitation-emission landscapes measured on frying oil samples from a commercial frying operation. To the left the fluorescence landscape of the new unused frying oil and to the right the used oil to be discarded after four weeks of deep-frying spring rolls.

In the beginning, clear evidences of plant pigment (emission 660 nm) which are still present in the (rapeseed/palm) oil have completely vanished in the used oil. Moreover, the complex broad peak has completely changed character and position. This demonstrates that a fluorescence sensor has great potential to follow the deterioration of frying oils during an industrial frying operation. By employing PLSR a number of classical fat- and oil-related quality attributes, such as anisidine value, oligomer content, iodine value and vitamin E content, can be

predicted/measured. With regard to fluorescence sensors the Food Technology group at The Royal Veterinary and Agricultural University has been pioneering the field of fluorescence analysis of sugar and sugar juices. It was discovered early that fluorescence measured from sugar samples dissolved in water could "fingerprint" different sugar factories and identify not-optimally run factories [4]. Although the sugar (sucrose) itself does not fluoresce, the sugar refining process "labels" the product with indicator-substance fluorescence distinct to the process conditions which in turn may be used to optimize the process. However, for the industry to realize the potential for such indirect methods based on trace amount of indicator substances a new paradigm shift is required.

Mathematical chromatography

Bi-linear chemometric methods ($x_{ij} = \sum_{n=1}^{N} a_{in} b_{jn} + e_{ij}$) such as PCA and PLSR have amply demonstrated their superior performance when analysing spectroscopic information in quality control sensors. The advantages of such methods are that when analyzing 1st order multivariate data (Table 1) they can facilitate outlier detection, interference compensation and noise reduction, resulting in more efficient and robust calibration models. When second order data are available (e.g. fluorescence landscapes), tri-linear data analytical methods ($x_{ijk} = \sum_{n=1}^{N} a_{in} b_{jn} c_{kn} + e_{ijk}$) furthermore give the possibility of unique resolution of the underlying components. This has been beautifully demonstrated by the application of the multi-way PCA analog PARAFAC (PARAllell FACtor analysis) to fluorescence landscapes of 268 sugar samples [4]. In this application excitation and emission spectra of 4 fluorophores were directly identified by this deconvolution procedure, two of which could directly be found in the chemical literature as the spectra for the amino acids tryptophane and tyrosine. The other two could later be identified as complex high molecular melanoidines. Moreover, the tri-linear method provides real analyte concentrations, rendering calibration models superfluous. This breakthrough in "mathematical chromatography" naturally has a great impact on application specialists and spectroscopists, creating a quest for

"upgrading" traditional spectroscopies with an extra (tri-linear) dimension (pressure, temperature etc.).

Future trends

The potential advantages of implementing spectroscopic sensors for quality control directly in the food process will create a continuous quest for still more informative and multivariate sensors to be developed. High resolution nuclear magnetic resonance is probably the most successful and versatile spectroscopic technique yet to be developed and although its implementation as an on-line monitoring tool is severely hampered by the requirement of a strong homogeneous magnetic field, we foresee this technique will also invade the more advanced segments of the food and medical industries for quality control. Among many other reasons nuclear magnetic resonance is such a versatile technique which absolutely non-invasively can monitor samples and process streams with spatial resolution or as a volume measure. Nuclear magnetic resonance is capable of measuring very detailed molecular information such as substitution patterns on triglycerides of prime importance to digestion and metabolism as well as and to measure types and amounts of, for example, polyunsaturated fatty acids, some of which have significant potential of being functional fatty acids for preventing myocardial infarction, psoriasis, bronchial asthma and other diseases. Last but not least, nuclear magnetic has the capability to provide complex multivariate and multiway information on food samples that allows application of tri-linear data analytical methods to recover pure analyte concentrations and to explore the covariances with food quality. To this end we have kick-started with low-field nuclear magnetic resonance relaxation decays normally used in the industry to analyse solid fat, total fat and moisture content. By a fascinating approach in which the data as a pre-transformation is upgraded to become pseudo second order data, we have demonstrated the utility of applying the tri-linear methods for analysing nuclear magnetic resonance relaxation decays [5].

Process chemometrics is worth little without high-quality data. Spectroscopic sensors are able to furnish the process engineers with such data. We therefore foresee a growing interest for advanced fingerprinting methods (with and without indicator substances) including spectroscopic sensors from microphones to high-resolution nuclear magnetic resonance sensors.

Literature:

1. Martens H. & Næs T. (1989) Multivariate Calibration. Wiley, UK.

2. Nørgaard L., Saudland A., Wagner J., Nielsen J.P., Munck L. and Engelsen S.B. (2000) Interval partial least-squares regression (*i*PLS): A comparative chemometric study with an example from near-infrared spectroscopy. *Applied Spectroscopy* **54**(3): 413-419.

3. Engelsen S.B. (1997) Explorative Spectrometric Evaluations of Frying Oil Deterioration. *Journal of the American Oil Chemist' Society* **74**(12): 1495-1508.

4. Munck L., Nørgaard L., Engelsen S.B., Bro R. and Andersson C.A. (1998) Chemometrics in food science - a demonstration of the feasibility of a highly exploratory, inductive evaluation strategy of fundamental scientific significance. *Chemometrics and Intelligent Laboratory Systems* **44**(1): 31-60.

5. Pedersen H.T., Bro R. and Engelsen S.B. (2001) Slicing – A novel approach for unique deconvolution of NMR relaxation decays, In *Magnetic Resonance in Food Science: A View to the Future* (Eds. Webb, G.A., Belton, P.S., Gil, A.M. and Delgadillo, I.), The Royal Society of Chemistry, UK, pp. 202-209.

Multi-way chemometric algorithms are available from the Food Technology site www.models.kvl.dk

Paper II

Why high-speed methods never exceed a correlation of 0.9 to drip loss. A chemometric investigation

D.K. Pedersen, H. Martens, L.B. Christensen and S.B. Engelsen

Abstract

This study establishes that drip loss in porcine meat is measured by vague methods which at their best interrelate with a prediction error in the range 0.6-0.9 % drip loss and intercorrelations only slightly above 0.8. For this reason multivariate calibrations from indirect methods such as NIR, IR, Raman, NMR, ultrasound, pH and temperature gradients to classical drip loss measurements cannot be expected to exceed an apparent prediction error of less than approximately 0.6 % drip loss and a correlation higher than approximately 0.85.

The purpose of this study is to calculate the approximate uncertainty of drip loss measurements and to suggest methods for uncertainty estimates for situations where it is not possible to produce true replicates. This study places special emphasis on estimation of the level of the error of the reference parameter 'drip loss' with respect to evaluation of the predictive ability of multivariate calibrations by fast spectroscopic measurements. The different approaches of uncertainty approximation in this study seem to yield similar results. The error of drip loss was found to be highly heteroscedastic, which hinders detailed statistical analysis. However, these uncertainty estimates do give an indication of the level of the error arising from the drip loss measurements. That reference error is similar to the obtained prediction errors of the multivariate calibrations from spectroscopic measurements.

Introduction

The water-holding capacity (WHC) of meat is important for two reasons. Firstly, meat is sold by weight, thus any water loss is economically undesirable. Secondly, the WHC influences the appearance of fresh meat during retail and might affect the

sensory properties of cooked meat, as high cooking loss has been reported to make meat be perceived less juicy (Martens, Stabursvik and Martens, 1982).

In quality control of food production it is often of great practical value to replace an uncertain and time-consuming chemical method with a more precise and ultra-rapid method, such as near infrared (NIR), Fourier transform infrared (FT-IR), Raman spectroscopy, nuclear magnetic resonance (NMR), ultrasound, pH or temperature gradients. For this purpose appropriate multivariate calibrations are required. In multivariate calibration, a relationship between the spectra from the fast spectroscopic method and the reference parameter from the time-consuming chemical method, such as the drip loss measurements, is built for the samples of interest. Estimation of the uncertainty of the chemical reference methods can be of great value in order to estimate if the 'new' spectroscopic method based on chemometric regression is suited as a practical replacement for the 'old' chemical reference method and secondly to estimate if further refinement of the 'new' method is possible on the basis of the data provided by the 'old' reference method. In our recent work (Pedersen, Morel, Andersen and Engelsen, 2002) and in several other studies (Forrest, Morgan, Borggaard, Rasmussen, Jespersen and Andersen, 2000; Brøndum, Munck, Henckel, Karlsson, Tornberg and Engelsen, 2000; Brown, Capozzi, Vavani, Cremonini, Petracci and Placucci, 2000; Bertram, Andersen and Karlsson, 2001; Bertram, Dønstrup, Karlsson and Andersen, 2002) the reference parameter for water-holding capacity (WHC) or drip loss in meat is applied in multivariate calibrations based on spectroscopic measurements. The obtained prediction errors in all these fairly different investigations fall in the range of 0.8-2.6 % drip loss, and the questions whether the spectroscopic calibration is satisfactory for replacing the reference method.

All measurements, fast spectroscopic measurements as well as chemical or physical reference measurements, have errors. Spectroscopic measurements are usually quite accurate, but one must still be aware of possible errors such as the homogeneity of the sample, which is of great importance to the sampling method. Meat is usually very inhomogeneous, so in this case the sampling error is a great contributor. Other sources of error in spectroscopic measurements are scatter interferences and unstable process variables like humidity and temperature (Wülfert, Kok and Smilde, 1998). The uncertainty of spectroscopic methods can be estimated simply by making additional measurements without moving the sample from the instrument

(uncertainty of the spectroscopic measurement) or by replacing the sample by another representative sample and make additional measurements (uncertainty of the sampling method + uncertainty of the spectroscopic measurement). This is possible, because spectroscopic measurements are fast and non-destructive (re-use of the sample is possible).

The methods for determination of drip loss (Honikel, 1998; Rasmussen and Andersson, 1996) are associated with several sources of error related to the nature of the meat samples and the processing of the samples during the analysis. The reduction in water holding during conversion of muscle to meat is primarily due to pH-induced protein denaturation and the ongoing rigor development, which result in shrinkage of the myofilament lattice spacings and hereby becomes the driving force for transfer of water into potential drip channels (Offer *et al.*, 1989). When a muscle is cut, the fluid will drain from the surface due to gravity, given that the viscosity of the fluid is sufficiently low and that capillary forces do not retain it (Offer and Knight, 1988). Therefore, orientation of the fibres with respect to cut is very important when measuring the drip loss. Surface evaporation or squeezing of the sample during handling are other ways of losing water which can occur during the time of measurement (usually 24 or 48 hours). Inhomogeneity is obviously a problem with these methods, as fat and connective tissue in different levels and different distribution across the samples can influence the amount of drip. Another major challenge is that accurate replicates of the reference method are impossible to perform. In the Honikel method a large sample (80-100 g) is cut out of, for example, the loin and used as a whole for the measurement. Due to the variation between samples taken from different parts of the carcass, a large sampling error will be introduced and true replicates are impossible to produce. In the method proposed by Rasmussen and Andersson (1996) several smaller samples (25 mm in diameter and 25 mm in length) across the loin are used. This is expected to give more detailed information about the drip loss from the muscle, but it is still not possible to produce true replicates, as it is not possible to homogenize the material, which would result in destruction of the structure and loss of information about the water-holding capacity.

The purpose of this study is to calculate the approximate uncertainty of drip loss measurements and to suggest methods for uncertainty estimates for situations where it is not possible to produce true replicates. This study places special emphasis on

estimation of the level of the error of the reference parameter 'drip loss' with respect to evaluation of the predictive ability of multivariate calibrations for drip loss in porcine meat by fast spectroscopic measurements.

Materials and methods

Research meat samples. 117 pigs were slaughtered at the research abattoir at The Danish Institute of Agricultural Sciences, Foulum, Denmark. In order to obtain a large variation in meat quality (water-holding capacity) the rates and extents of pH decrease *post mortem* were manipulated through pre-conditioning of the pigs. Adrenaline affects glycogenolysis and thereby represents a tool for manipulating of ultimate pH and probably also the rate of pH decrease, as described by Henckel, Karlsson, Oksbjerg and Petersen (2000). Another way of manipulating energy levels in the live muscle is treadmill exercise. In the present study the pigs were subjected to three different treatments prior to slaughtering: (1) 27 pigs were injected with 0.3 mg adrenaline / kg live weight 16 hours prior to slaughter; (2) 51 pigs were subjected to 14-20 min treadmill exercise immediately prior to slaughter; (3) 39 pigs served as controls. *Longissimus dorsi* from the carcasses were subjected to measurements of WHC, measured as drip loss.

Water-holding capacity according to Honikel (1998) was measured as drip loss, whereby the loss of water was registered from a 2.5 cm thick slice of muscle taken 24 hours post mortem placed hanging in a net and suspended in a plastic bag for 48 hours at +4°C (the bag method). The sample was cut out at the 6th lumbar vertebra of the left loin. In addition, water-holding capacity according to Rasmussen *et al.* (1996) was measured, whereby the loss of water was registered from two or three pieces of muscle taken 24 hours post mortem hanging for 24 hours in a plastic cup with a removable container at +4°C (the EZ (easy) method). The sample was cut out at the 5th lumbar vertebra of the left loin. For 95 of the 117 animals three cylindrical cuts were made for each measurement. The three cuts were named A, B and C (Figure 1). The position of the three cuts where maintained at all measurements. For the remaining 22 of the 117 animals only two cuts were made for each measurement, more or less covering the same area as the A, B and C cuts.

Loin samples. From two industrial slaughterhouses 34 pigs were selected by measurements with the MQM (Meat Quality Marbling)-probe (Borggaard, Andersen and Barton-Gade, 1989) in order to ensure a broad range of drip loss (Christensen, 2002). This constitutes 'the loin data set'. From the 34 pigs a piece of approximately 40 cm from the left and the right *longissimus dorsi* muscles were excised, starting at the joint between third and fourth lumbar vertebra. After 4 hours of rest at 7°C, the *longissimus dorsi* from the right and the left side were cut into slices (11 to 15 slices for all 34 muscles), each with a thickness of 2.5 cm.

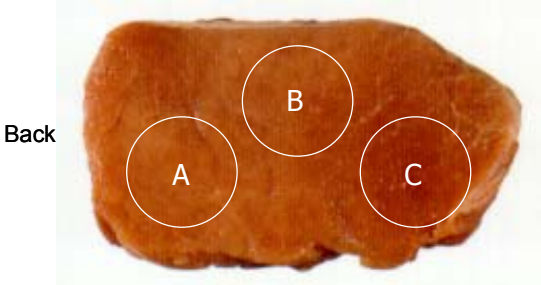

Figure 1. A slice of the loin with definition of the three cylindrical cuts, A, B and C, applied for the measurement of drip loss by the EZ method

The water-holding capacity was measured using the bag method for the slices from the right *longissimus dorsi* as for the research meat samples, except that the slices were hanging in a net and suspended in a plastic bag for only 24 hours at +4°C. From the slices from the left *longissimus dorsi* the water-holding capacity was measured using the EZ method employing three cylindrical cuts (A, B and C) per slice (Christensen, 2002).

Statistical analysis. Chemical data are usually heteroscedastic in the way that high values are related to a larger error of measurement than low values. Since statistical methods assume that data are homoscedastic in the way that all values are related to an equal amount of error, the statistical calculations applied in this study will only be approximations.

The difference (f) between values of measurements performed by the two methods (the EZ method (x) and the bag method (y)) is investigated:

$$f = y\text{-}x \quad (1)$$

The one method (y) can be simulated by the other (x) as $\hat{y}$ by the following equation:

$$\hat{y} = b_0 + b_1 x \quad (2)$$

where b_0 is the offset and b_1 is the slope of the linear relationship between the values of the two methods. Then the difference ($\hat{f}$) is:

$$\hat{f} = y\text{-}\hat{y} \quad (3)$$

Simple correlations between data sets were performed, and the root mean squared error was calculated as:

$$\text{RMSE} = \sqrt{\frac{1}{N-2}\sum_{i=1}^{N}(y_i - \hat{y}_i)^2} \quad (4)$$

where y_i is a reference value for the sample i, $\hat{y}_i$ is a corresponding reference value for the sample i and N is the total number of samples.

The total variation (S^2_{Total}) of a data set can, in simple situations, be calculated as the summation of the different independent sources of variation in the data set (S^2_a), (S^2_b) and (S^2_c):

$$S^2_{Total} = S^2_a + S^2_b + S^2_c \quad (5)$$

where a, b and c refer to the source of variation. This simple variance component model will be used for characterizing various sources. The variances were calculated by:

$$S^2 = \frac{n\sum x^2 - (\sum x)^2}{n(n-1)} \quad (6)$$

where x is the data values and n is the number of samples.

Partial Least Squares Regression (PLSR) (Martens and Næs, 1989), which is a predictive method based on estimated latent variables, will be applied as a

multivariate approach to the simultaneous analysis of the two types of reference measurements on the same samples. The purpose of the PLSR is to build a linear model enabling prediction of a desired reference value (**y**), e.g., drip loss measured according to the bag method, from a number of data (**x**), e.g., the A-, B- and C-values measured according to the EZ method. In matrix notation the linear model is **y** = **Xb**, where **b** contains the regression coefficients that are determined during the calibration step, and **X** is the matrix of collected data for the applied samples. The measure of model performance is usually given by r, which is the correlation between the measured reference (y) and the predicted reference ($\hat{y}$), and by the prediction error RMSECV (root mean square error of cross-validation):

$$\text{RMSECV} = \sqrt{\frac{1}{N}\sum_{i=1}^{N}(y_i - \hat{y}_{i,-i})^2} \qquad (7)$$

where y_i is the measured reference value of sample i, $\hat{y}_{i,-i}$ is its value predicted by a model obtained without sample i, and N is the total number of samples.

Results and Discussion

The two drip loss methods; the bag method and the EZ method, are compared for the two data sets; the research data set and the loin data set. The means and ranges of drip loss measured by the two methods are shown in Table 1.

Table 1. Mean, standard deviation (S.D.), minimum (Min.) and maximum (Max.) values for the measurements of drip loss (%) by the two methods, the bag method (Bag) and the EZ method (EZ), for the two data sets, the research data set (Research) and the loin data set (Loin).

Data set	Method	Mean	S.D.	Min.	Max.
Research	Bag	5.63	3.48	0.71	13.77
Research	EZ	3.09	2.65	0.04	11.13
Loin	Bag	5.07	2.39	0.81	12.61
Loin	EZ	3.80	2.19	0.10	13.09

In Figure 2 the correlations between the drip loss values measured by the two methods for the research data set (1) and the loin data set (2) are shown. RMSE is the error in % drip loss between the two methods, and is found to be 2.82 % drip loss for the research data set and 1.40 % drip loss for the loin data set.

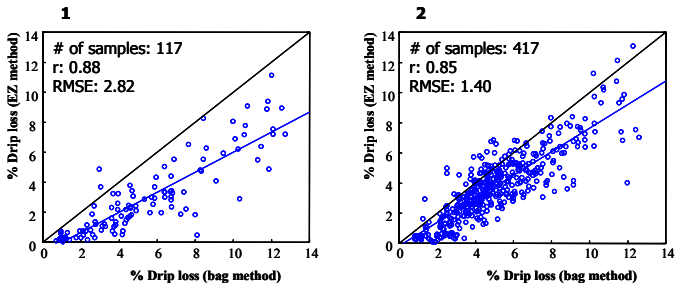

Figure 2. Measured EZ drip loss versus measured bag drip loss for the research data set (1) and the loin data set (2). The regression lines and the target lines are added.

The calculated difference between the two methods is twice as great for the research data set as for the loin data set. In principle, the two methods are expected to produce comparable results, so the rather poor correlations need to be investigated. It is known (Christensen, 2002) that there is an offset between the two methods. Judging from the mean values reported in Table 1, there appears to be a larger offset between the two methods in the research data set than in the loin data set. This might be partly due to the difference in 'hanging time' used in the bag method applied in the two data sets; 24 hours was used for the loin data set, while 48 hours was used for the research data set.

The better correlation between the methods for the loin data set might be explained by the inclusion of several measurements (11-15) per animal, which reduces the contribution of variance concerning the animals in relation to the number of measurements. The research data set shows the poorest correlation between the two methods, even though the samples were taken from the 5th and the 6th lumbar vertebra on the same side of the loin, and it has been shown that the drip variation in that area is not significantly different (Christensen, 2002). For the measurements of the loin data set, all 'bag method' measurements were carried out on the right loin

and all 'EZ method' measurements were carried out on the left loin. That might influence the correlation between the two methods, as differences in meat quality between the two sides can be found (Lundström and Malmfors, 1985). A further difference between the two data sets is the treatments applied to the animals in the research data set. The artificial way of producing different stress levels may interact with the biological properties of the meat in ways that are unpredictable. This might be of particular concern with regard to the exercised pigs, as it involves a greater risk of 'producing' uneven and high drip losses along the loin than for the non-exercised pigs.

Uncertainty estimates can be produced in many ways. A very common method is to employ representative replicates and calculate the standard deviation between them. That is not possible when working with whole meat samples in which case there is no possibility of producing true, representative subsamples. Instead alternative ways of estimating the uncertainty are suggested in this study.

The total variation (S^2_{Total}) of the loin data set is calculated in accordance with equation 5 as the summation of the biological variation between the animals (S^2_{Animal}), the inhomogeneity variation along the loin (S^2_{Slice}), the inhomogeneity within slices ($S^2_{Inhomomogeneity}$) and the variation due to the method of measurement (S^2_{Method}):

$$S^2_{Total} = S^2_{Animal} + S^2_{Slice} + S^2_{Inhomogeneity} + S^2_{Method}$$

Statistical estimates. In a variance component approach, the estimations of the defined variances were calculated by equation 6, applying the drip loss measured by the bag method and by the EZ method. S^2_{Animal} was calculated as the variance between the animals, where the average of all drip loss measurements for each animal was used as x. S^2_{Slice} was calculated as the average of the variances between all slices within each animal of the data set, where the average of drip loss measurements within each slice were used as x. $S^2_{Inhomogeneity}$ was calculated as the average of the variance between the three measurement points A, B and C of within each slice (see Figure 1), where the individual drip loss measurements in the

measurement points A, B and C were used as x. As this is only possible for the EZ method, the calculated value for that method is applied for further calculation concerning both methods, as the $S^2_{Inhomogeneity}$ is assumed to be equal for both methods. In Table 2, the calculated variations are listed. The variation due to the method of measurement (S^2_{Method}) is a part of the calculated variations:

$$S^2_{Amimal,real} = S^2_{Animal} + S^2_{Method}$$

Table 2. The uncertainty estimates calculated by the 'statistic' method with the purpose of calculating the variance of the methods (S^2_{Method}). The total variance (S^2_{Total}), the biological variance of the animals (S^2_{Animal}), the inhomogeneity variance along the loin (S^2_{Slice}), the inhomogeneity variance across the slices ($S^2_{Inhomomogeneity}$).

Estimate	Bag method	EZ method
S^2_{Total}	5.69	4.81
S^2_{Animal}	4.91	4.11
S^2_{Slice}	0.91	0.86
$S^2_{Inhomomogeneity}$	1.59	1.59

When S^2_{Total} was calculated as the variance of all measurements, where the individual drip loss measurements for each slice were used as x for the bag method and the average of the average of the A, B and C drip loss measurements for each slice were used as x for the EZ method, it was possible to calculate S^2_{Method} for the bag method and for the EZ method (see Table 3), by the following equation:

$$S^2_{Total} = (S^2_{Animal} - S^2_{Method}) + (S^2_{Slice} - S^2_{Method}) + (S^2_{Inhomogeneity} - S^2_{Method}) + S^2_{Method}$$

Table 3. The type of uncertainty estimate (Estimate – see text) and the value of the uncertainty estimates for different the different approaches (see text) employing the two data sets, the research data set (Research) and the loin data set (Loin), and the two methods for measurement of drip loss, the bag method (Bag) and the EZ method (EZ).

Study	Data set	Method	Estimate	Value [%]
Statistical	Loin	Bag	S_{Method}	0.93
Statistical	Loin	EZ	S_{Method}	0.94
Neighbour	Loin	Bag	RMSE	0.66
Neighbour	Loin	EZ	RMSE	0.49
Slices 2-5	Loin	Bag	S.D.	0.61
Slices 2-5	Loin	EZ	S.D.	0.50
PLSR	Research	Bag by EZ	RMSECV	2.11
PLSR	Loin	Bag by EZ	RMSECV	1.29

It is an approximation to use the same $S^2_{Inhomogeneity}$ for both methods, since the bag method measures a larger area (the whole slice) than the EZ method (three sub samples). For this reason, it might be more correct to take the random variation within a slice into account. The larger area applied in the bag method corresponds to approximately 8 subsamples of the size of the A, B and C subsamples applied in the EZ method, so the volume factor is 8/3. If it is assumed that the drip loss property is randomly distributed within each slice, i.e. normally distributed, no additional restrictions between subsamples (such as diffusion barriers to the water, total pressure variations or partial water pressures towards evaporation) exist. Then $S^2_{Inhomogeneity}$ can be calculated to 4.24, and further calculations lead to S_{Method} = 1.48 % drip loss. But in practice, the drip loss is not randomly distributed within the slice, and additional restrictions between subsamples have to be reduced by an equivalence factor, compared to the simple volume factor. Diffusion barriers and edge effects are considered to reduce the volume factor by a factor between 0.5 and

0.8. Hence, $S^2_{Inhomogeneity}$ can be calculated to be between 2.12 and 3.39, and further calculations lead to S_{Method} = 1.06-1.33 % drip loss.

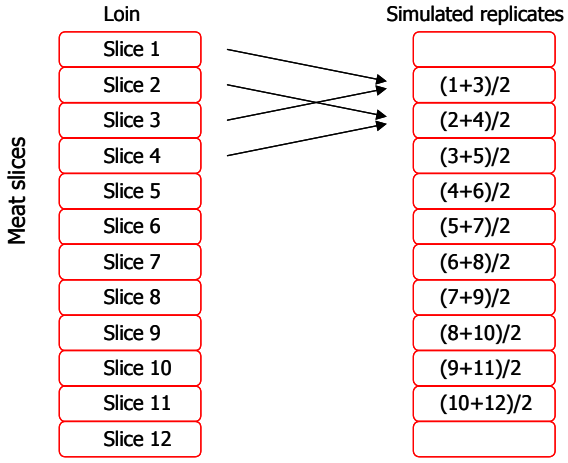

Figure 3. Schematic presentation of the production of the simulated replicates made by averages of sample-slice-neighbours

Neighbour measurements. In another approach neighbour measurements were applied from the loin data set, where measurements of drip loss were performed along the loin (11-15 points of measurement per loin) for each of the 34 animals. By using the average of the two sample neighbours of a certain sample, it was possible to produce a simulated replicate; see Figure 3. This was carried out for all the sample slices, except the first and the last, for each animal. The correlations between the original samples and the simulated replicates for the two drip loss methods, the bag method (1) and the EZ method (2), are shown in Figure 4. There is quite a high correlation for both methods, especially for the low values of drip loss. The uncertainty estimates, the drip loss errors (RMSED) in percent, are 0.66 for the bag method and 0.49 for the EZ method; see Table 3. This way of calculating uncertainty estimates might yield a quite realistic estimate concerning methods of drip loss measurements, since the whole loin was used and several samples (11-15)

from each animal were applied in the comparison. In this way, some of the sources of variation related to different sampling points are decreased.

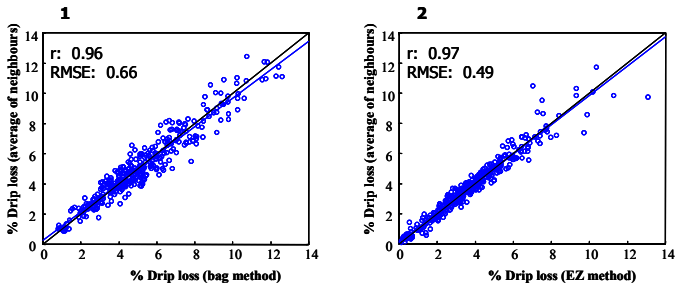

Figure 4. Drip loss values calculated as the average of the two neighbour values versus the drip loss value in question for the loin samples (417) for the bag method (1) and the EZ method (2). The regression lines and the target lines are added.

Slices 2-5. From earlier investigations (Christensen, 2002) it is known that the area around the slices 2-5 is equal with regard to the drip loss of the meat. The 4 slices (2-5) from each of the 34 animals in the loin data set are then considered as replicates, the variation within each animal is calculated, and the standard deviation (S.D.) results are reported as 0.61 for the bag method and 0.50 for the EZ method (Table 3). These uncertainty estimates are rather close to the uncertainty estimates found by the correlations using all slices through whole loins. This approach is, of course, only possible for the loin data set and not for the research data set, where only one measurement per animal was carried out.

PLSR. The three previous approaches for estimation of the uncertainty only employ the loin data set, which contains attempts of replicates. By constructing PLSR models (1 component) using the three drip loss results (A, B and C) from the EZ method (**X**) to predict the drip loss obtained from the bag method (**y**) for both data sets, the research data set (one measurement per animal) and the loin data set (one measurement per slice), can be applied. The predicted versus measured plots for 95 of the research samples (1) and for the loin samples (2) are shown in Figure 5. The uncertainty estimates, the root mean squared error of cross validation (RMSECV), are 2.11 for the research data set and 1.29 for the loin data set (Table 3).

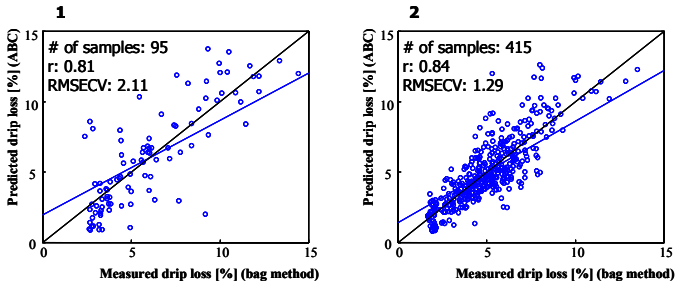

Figure 5. Predicted drip loss based on ABC measurements from the EZ method versus measured drip loss (the bag method) performed by PLSR modelling (1 component) for the research data set (1) and the loin data set (2). The regression lines and the target lines are added.

The research data set again displayed the lowest correlation between the methods, and the resulting uncertainty estimates are considerably higher than the previous attempts at estimation of the samples from the loin data set. The regression coefficients for variable A, B and C, displayed in Figure 6, all have significant influence on the PLSR models for both data sets.

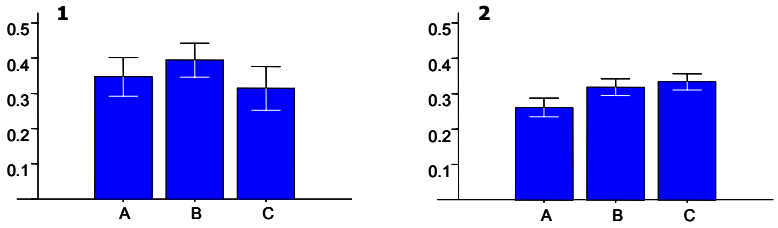

Figure 6. Regression coefficients for the PLSR models (1 component) based on A, B and C measurements from the EZ method for prediction of the drip loss measured by the bag method for the research data set (1) and the loin data set (2).

The extent of the influence of the three variables A, B and C seems to be different for the two models based on the two data sets, the research data set and the loin data set. All three measurements, A, B and C, almost equally influenced the model for

the research data set, while the B and C measurements influenced the model significantly more than the A measurement for the loin data set. No apparent explanation for the difference can be found.

The uncertainty estimates of reference methods are needed for evaluation of multivariate models based on spectroscopic data for prediction of essential quality parameters of complex samples. Early prediction of water-holding capacity in meat by multivariate vibrational spectroscopy as described by Pedersen *et al.* (2002) is this type of a situation. In Figure 7, the prediction error (RMSECV) from one of the PLSR models applied in this study is plotted versus the number of components applied for the modelling.

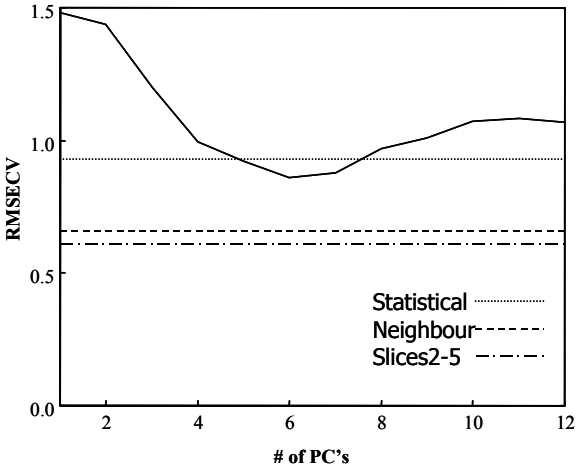

Figure 7. The prediction error (RMSECV) of a PLSR model based on FT-IR spectra for prediction of drip loss (the bag method) for 41 pigs from a research slaughterhouse plotted versus the number of components (PC's) applied for the model. The uncertainty estimates calculated according to three approaches: the statistical, the neighbour and the slices 2-5, are plotted as horizontal lines.

The PLSR model is based on FT-IR spectra of porcine meat from 41 of the animals applied in the research data set used in the current study. The drip loss measured by the bag method is applied as the reference measurement. The uncertainty estimates of the bag method calculated as % drip loss according to the three approaches the

statistical (0.93) without corrections, the neighbour (0.66) and the slices 2-5 (0.61) are plotted as horizontal lines in Figure 7. These estimates can be used to display the amount of the error connected to the PLSR model, which is caused by the method of measurement of the reference parameter. When using the optimal number of components (6) for the PLSR prediction of the drip loss reference, the reference method accounts for 0.61-0.93 % drip loss of the total modelling error. Moreover, there are instrumental errors from the spectroscopic measurement, sampling errors related to the attempt of measuring representative samples and modelling errors due to the lack of fit between the spectroscopic measurement and the reference measurement.

Conclusion

When looking at the approaches of estimation of the uncertainty by employing the loin data set, which contains attempts of replicate measurements, there seems to be a fair agreement about uncertainty estimates of the methods around 0.6-0.9 % drip loss (mean = 5.1 % drip loss) for the bag method and around 0.5-0.9 % drip loss (mean = 3.8 % drip loss) for the EZ method. These uncertainty estimates indicate the error arising from the reference methods of drip loss measurements of porcine meat. These uncertainty estimates can be compared to the obtained prediction errors in the previously reported investigations (Forrest *et al.*, 2000; Brøndum *et al.*, 2000; Brown *et al.*, 2000; Bertram *et al.*, 2001, 2002; Pedersen *et al.*, 2002) in the range of 0.8-2.6 % drip loss. In addition to the error from the reference measurements, errors from the spectroscopic methods and modelling errors will affect the final prediction error, when calibrations are performed. It might be concluded that the investigations which obtained the lowest prediction errors (around 0.8 %) have obtained nearly optimal calibrations concerning the drip loss measurement, while the investigations reporting the highest prediction errors (around 2.6 %) have room for improvement, as they are probably affected by other sources of interfering variations or suffering from low modelling fit. Whether the obtained prediction errors are satisfactory for the individual purposes of the spectroscopic calibrations has to be evaluated against the actual ranges of drip loss in the populations of future predictions, in addition to the quality of the reference parameter.

More precise reference methods than the drip loss methods described in this study might be desired for references for multivariate calibrations with the purpose of future predictions. One way to improve the reference methods could be to routinely introduce 'replicates' along the loin. Often only one slice of the loin is used for the measurement of drip loss. In situations of extensive inhomogeneity of the object of measurement, as the loin of a pig carcass, the introduction of 'replicates' will provide a truer estimate of the drip loss of the whole loin than just one single measurement can provide. Alternatively, it may be better to introduce more samples to improve the robustness of the calibration, as suggested by Sørensen (2002). A mathematical alternative to cope with heteroscedastic data could be to apply weighted least squares of objects in the PLSR.

References

Bertram, H.C., Andersen, H.J. & Karlsson, A.H. (2001). Comparative study of low-field NMR relaxation measurements and two traditional methods in the determination of water holding capacity of pork. *Meat Science, 57*, 125-132.

Bertram, H.C., Dønstrup, S., Karlsson, A.H. & Andersen, H.J. (2002). Continuous distribution analysis of T_2 relaxation in meat – an approach in the determination of water-holding capacity. *Meat Science, 60*, 279-285.

Borggaard, C., Andersen, J.R. & Barton-Gade, P. (1989). Further development of the MQM-equipment for measuring water holding capacity and intramuscular fat on-line. In *Proceedings: 35th International Congress of Meat Science and Technology* (pp. 212-219), Copenhagen, Denmark.

Brown, R.J.S., Capozzi, F., Cavani, C., Cremonini, M.A., Petracci, M. & Placucci, G. (2000). Relationships between ^{1}H NMR relaxation data and some technological parameters of meat: A chemometric approach. *Journal of Magnetic Resonance, 147*, 89-94.

Brøndum, J., Munck, L., Henckel, P., Karlsson, A., Tornberg, E. & Engelsen, S.B. (2000). Prediction of water-holding capacity and composition of porcine meat by comparative spectroscopy. *Meat Science, 55*, 177-185.

Christensen, L.B. (2002). Drip loss sampling in porcine m. longissimus dorsi. *Meat Science*. Submitted.

Forrest, J.C., Morgan, M.T., Borggaard, C., Rasmussen, A.J., Jespersen, B.L. & Andersen, J.R. (2000). Development of technology for the early post mortem prediction of water holding capacity and drip loss in fresh pork. *Meat Science, 55*, 115-122.

Henckel, P., Karlsson, A., Oksbjerg, N. & Petersen, J.S. (2000). Control of post mortem pH decrease in pig muscles: experimental design and testing of animal models. *Meat Science, 55*, 131-138.

Honikel, K.O. (1998). Reference methods for the assessment of physical characteristics of meat. *Meat Science, 49*, 447-457.

Lundström, K. & Malmfors, G. (1985). Variation in light scattering and water-holding capacity along the porcine *longissimus dorsi* muscle. *Meat Science, 15*, 203-214.

Martens, H. & Næs, T. (1989). *Multivariate Calibration*. Chichester: Wiley.

Martens, H., Stabursvik, E. & Martens M. (1982). Texture and colour changes in meat during cooking related to thermal denaturation of muscle proteins. *Journal of Texture Studies*, *13*, 291-309.

Offer, G., Knight, P., Jeacocke, R., Almond, R., Cousins, T., Elsey, J., Parsons, N., Starr, R. & Purslow, P. (1989). The structural basis of the water-holding, appearance and toughness of meat and meat products. *Food Microstructure, 8*, 151-170.

Offer, G. & Knight, P. (1988). The structural basis of water-holding in meat. Part 2: Drip losses. In R.A. Lawrie *Developments in Meat Science* (Vol. 4). London: Elsevier.

Pedersen, D.K., Morel, S., Andersen, H.J. & Engelsen, S.B. (2002). Early prediction of water-holding capacity in meat by multivariate vibrational spectroscopy. *Meat Science*. Submitted.

Rasmussen, A.J. & Andersson, M. (1996). New method for determination of drip loss in pork muscles. *Proceedings 42nd International Congress of Meat Science and Technology* (pp. 286-287), Lillehammer, Norway.

Sørensen, L.K. 2002. True accuracy of near infrared spectroscopy and its dependence on precision of reference data. *Journal of Near Infrared Spectroscopy, 10*, 15-25.

Wülfert, F., Kok, W.T. & Smilde, A.K. (1998). Influence of temperature on vibrational spectra and consequences for the predictive ability of multivariate models. *Analytical Chemistry, 70*, 1761-1767.

Paper III

Method and apparatus for prediction of the drip loss of a part of a carcass

D.K. Pedersen, J.R. Andersen, L. B. Christensen and S.B. Engelsen

---

The present invention relates to a method and an apparatus for prediction of the drip loss of a part of a carcass by measuring a muscle in the part of the carcass after slaughtering.

DK 163.382 B (Slagteriernes Forskningsinstitut) discloses a method of determining the quality of individual meat pieces, in which method a reflection measuring probe is introduced into the meat piece and a number of measurements of the light reflectivity along the scanning line of the probe is recorded. The data set of reflection values obtained is subjected to a statistical analysis computing how many times each reflection value appears, and the degree of frequency is inserted in a multivariable algorithm expressing a quality property. The reflection is measured in a wavelength band in the border range between the visible and the near-infrared range, for instance at 950 nm.

One of the quality properties, which can be determined, is the juice holding capacity, which is the capability of the meat to retain water, for instance during storage. This capability may be determined with high accuracy in chilled meat (post rigor) by means of the method described. When measuring slaughter-warm meat (pre rigor), no correlation as to juice holding capacity has been found.

It is, however, desirable to be able to determine the juice holding capacity early in the slaughter process, as the part carcass may then be subjected to treatments which are more optimally adapted to the actual quality properties of the individual carcass or meat.

DK 172.774 B1 (Slagteriernes Forskningsinstitut) discloses a method of predicting the drip loss of a meat piece or determining its juice holding capacity. In the method two sets of light reflectivity measurements with timing difference are recorded on a slaughter-warm muscle in the carcass, for instance with a timing difference of 1-20 minutes. The change of the reflection values are inserted in an algorithm

expressing the juice holding capacity of the meat. Measurements are made in the near-infrared area from 900 to 1800 nm. A drawback of the method is that it takes a long time, seen in relation to the advancing tempo of carcasses on a modern slaughter line. Moreover, a higher accuracy than the one found (1.8%) is desirable. It is the object of the invention to provide a method and an apparatus for prediction of the drip loss of a part of a carcass by measuring a muscle in the part carcass after slaughtering, said method and apparatus obviating the above drawbacks.

The method according to the invention is characterized in that measurements are carried out while the part carcass is still warm from slaughter, that the light reflectivity of the muscle is measured in at least one wave range with a wave number below 1500 cm^{-1}, that the resulting, possibly processed measurement data are inserted as a variable in an algorithm expressing a prediction of the drip loss as a function of the light reflectivity in one or more wave ranges with a wave number below 1500 cm^{-1}, and that the prediction of the drip loss is automatically calculated in a calculation unit by means of the algorithm.

The method according to the invention is based on the surprising observation that by carrying out a reflection measurement on a muscle in a carcass, while the carcass is still warm after the slaughtering, in at least one wave range with a wave number below 1500 cm^{-1}, a quick measurement can be made predicting the drip loss, which makes it possible to measure the carcasses in the tempo, in which they are advanced on a common slaughter line, and it has moreover been found that the measurement is able to predict the drip loss with an accuracy which is substantially higher than the one obtained by the method using measurements with timing difference.

The wave range in question with a wave number below 1500 cm^{-1} (corresponding to a wavelength band with a wavelength of more than 6,667 nm) lies preferably in which corresponds to the middle-infrared range, i.e. very far from the above wavelengths of 950 and 900 - 1800 nm used up till now.

A preferred embodiment of the method according to the invention is characterized in that measurements are carried out in one or more wave ranges with a wave number in the interval 900-1500 cm^{-1}. In this connection a very good correlation between the reflection ability and the prediction of the drip loss has been found.

Preferably, measurements are carried out in one or more wave ranges with a wave number in the interval 900-1200 cm^{-1}.

Preferably, measurements are carried out in more than one wave range, and the algorithm is preferably multivariable. Preferably, measurements are made in less than 100 wave ranges and/or an algorithm having less than 100 variables is used. In particular, measurements are carried out in less than 10 wave ranges and/or an algorithm having less than ten variables is used.

It is preferred to use only one piece of measuring equipment per slaughter line. The piece of equipment may be a fully automatic device or a semi-automatic, operator controlled instrument. The piece of equipment may be adapted to measure each carcass passing the equipment, but may possibly only carry out random measurements if conditions so require. The equipment may moreover be designed for measuring chilled meat.

The time required for recording measurement data may vary in accordance with the specifications of the equipment and will thus typically lie from below one second and up to 10 seconds, thus making it possible for one single piece of equipment to measure in the tempo of the slaughter line. Preferably, measurement data are used which have been recorded within less than 1 minute, for instance less than 10 seconds.

In the method according to the invention, measurements are carried out while the part carcass is still in slaughter-warm condition, i.e. while the muscles undergo the transformation from living tissue in a recently slaughtered animal to chilled, edible meat. The measuring is therefore preferably carried out while the muscle is in pre rigor condition, in particular before the chilling of the part carcass.

The measuring is preferably carried out within two hours from the slaughtering (drainage of blood), for instance 0.5 to 2 hours after slaughtering.

The apparatus according to the invention is characterized in comprising

- a light reflection meter adapted to measure the light reflectivity of a muscle in at least one wave range with a wave number below 1500 cm^{-1},

- a calculation unit with a program and/or memory part adapted to automatically record measured, possibly processed light reflectivity data in an algorithm and to calculate the algorithm value,

- an algorithm contained in the program and/or memory part expressing a prediction of the drip loss as a function of the light reflectivity in one or more wave ranges with a wave number below 1500 cm^{-1}, measured on a muscle in a part carcass after slaughtering, while the part carcass is still warm (pre rigor), and

- a signal unit which after the insertion of light reflectivity data in the algorithm and calculation of the algorithm value emits a signal depending on the calculated prediction.

The apparatus may be stationary or portable and may be adapted to measure directly on a visible meat surface or on a cut surface in the meat provided by insertion of a measurement probe with a pointed end. The measurement head of the apparatus is preferably in contact with the muscle during measurement. If desired, measurements may be performed in various different muscles.

By a slaughter part carcass is in the present case preferably to be understood a whole carcass, in particular a carcass from which the bowels have been removed, a half carcass produced by backsplitting of a whole carcass, or a part carcass or a cut-out piece, for instance a fore-end, a middle piece or a ham of a pig carcass. Measurements are preferably carried out on a muscle in a whole or backsplit carcass.

A carcass is in particular a pig carcass.

By drip loss is in the present connection also to be understood the juice holding capacity.

In a wave range with a wave number below 1500 cm^{-1} is in the present connection to be understood what corresponds to a wavelength band with a wavelength of more than 6667 nm.

Example

This example illustrates that the drip loss of slaughter carcasses can be predicted with high accuracy already on the slaughter line by measurement of the reflection of the meat at several wave ranges with a wave number below 1500 cm^{-1}. The measuring is carried out within a so short period of time that no transformation of the meat takes place during the period of measurement.

In a test slaughterhouse 1/3 of a group of 46 pigs are exercised to provide a higher share than normal of carcasses having a high drip loss after chilling. Then all pigs are given an anaesthetic and slaughtered. 35 minutes after sticking, a hot meat sample (cutlet) is taken from the back muscle (longissimus dorsi). The temperature is 37 to 41°C. An ATR-IR spectrum is obtained with 64 scans in an interval from 900 to 1500 cm^{-1} (ATR = Attenuated Total Reflectance). The definition is 4 cm^{-1}. A spectrometer of the type Arid-Zone MB155S from Bomem, Canada, with an InAs detector, single-plate beamsplitter and SiC radiation source.

The drip loss of the meat from the same 46 pigs is recorded in a laboratory by measuring of the weight of a meat sample by cutting out after 24 hours and again after 72 hours (K.O. Honikel 1987. How to measure the water-holding capacity of meat? Recommendation of standardized methods. Evaluation and Control of Meat Quality in Pigs. Edited by P.V. Tarrangt, G. Eikelenboom & G. Monin. Martinus Nijhoof Publishers, Holland: p. 129-142). The drip losses measured lie between 0.7 and 8.0 %.

PLS regressions (PLS = Partial Least Squares) between the IR measurement values and the drip loss measured in the laboratory are determined in respect of the 46 pigs, partly directly on the IR measurement values of the spectrum and partly on the first and second derivative of the spectrum. On basis of this a multivariable algorithm is developed of the type

$$W_{dryp} = k_0 + k_1 \,.\, a_1 + k_2 \,.\, a_2 + k_n \,.\, a_n$$

in which

W_{dryp} is the predicted drip loss (in %)

k_0, k_1, k_2 ….. k_n are constants,

a_1, a_2 ….. a_n are reflection measurement values or the first or second derivative in a range with a given wave number, and

n is an integer, for instance 100.

Data from the four outliers do not form part of the development.

On basis of the algorithm and the two data sets the correlation R and the accuracy of the prediction RMSEP (% drip loss) can be calculated, which will appear from the table below.

Spectral range (cm^{-1})	Data pre-processing	R	RMSEP
900-1100		0.90	0.82
1000-1200		0.91	0.78
1000-1200	1st derived	0.94	0.64
1000-1200	2nd derived	0.92	0.73

It will be seen that the drip loss can be determined with an inaccuracy of less than 1% by measuring of the reflection capability of the meat in several wave ranges in the interval from 900 to 1200 cm^{-1} and by insertion of the measurement values in a multivariable algorithm developed with a standard measuring method as reference. This inaccuracy is sufficiently small for making it realistic to sort the carcasses in quality classes already before the carcasses are chilled in the slaughterhouse, which makes it possible to use carcasses with a very low drip loss or a high drip loss for the manufacture of types of products suitable therefore, whereas carcasses with a normal drip loss for instance may be used for the production of fresh cut-outs.

By the development of production equipment the reflection measurement and the calculation can be carried out in the same tempo as the advancing of the carcasses on a slaughter line, i.e. without any need to wait for transformation processes of the meat like in the method according to Danish Patent No. 172.774 B1.

The correlation between the spectroscopically measured drip loss and the drip loss measured in the laboratory of the 42 samples is shown in Fig. 1. In the calculation of the drip loss by spectroscopy the 1st derived of the IR spectra is used.

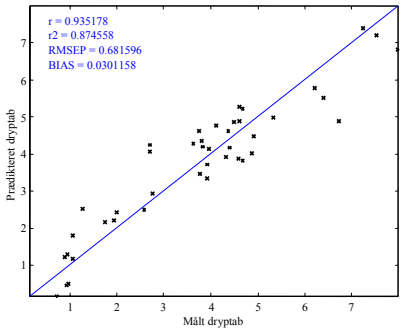

Figure 1

The IR spectra in the interval 900-1500 cm^{-1} for meat from all 46 pigs are shown in Fig. 2. In particular about 1000 cm^{-1}, the spectra contain much information which is correlated to the drip loss.

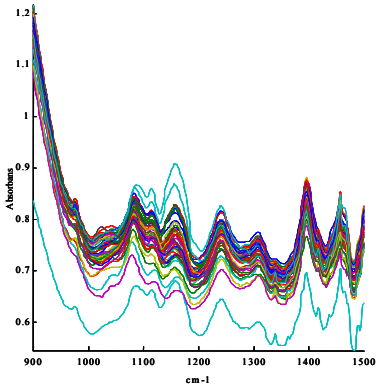

Figure 2

Above 1500 cm^{-1} no correlation between drip loss and reflection in slaughter-warm meat has been found.

Patent claims

1. A method for prediction of the drip loss of a part of a carcass by measuring a muscle in the part of the carcass after slaughtering, characterized in that measurement is carried out while the part carcass is still warm from slaughter, that the light reflectivity of the muscle is measured in at least one wave range with a wave number below 1500 cm^{-1} that the resulting, possibly processed measuring data are inserted as variables in an algorithm expressing a prediction of the drip loss as a function of the light reflectivity in one or more wave ranges with a wave number below 1500 cm^{-1} and that the prediction of the drip loss is automatically calculated in a calculation unit by means of the algorithm.

2. A method according to claim 1, characterized in that measurements are carried out in one or more wave ranges with a wave number in the interval 900-1500 cm^{-1}.

3. A method according to claim 2, characterized in that measurements are carried out in one or more wave ranges with a wave number in the interval 900-1200 cm^{-1}.

4. A method according to claim 1, characterized in that measurements are made in less than 100 wave ranges and/or an algorithm having less than 100 variables is used.

5. A method according to claim 1, characterized in that measurements are made in less than 10 wavelength bands and/or an algorithm having less than 10 variables is used.

6. A method according to claim 1, characterized in that measuring data are used which have been recorded within less than 1 minute, such as within less than 10 seconds.

7. A method according to claim 1, characterized in that the measuring is carried out while the muscle is in pre rigor condition.

8. A method according to claim 1, characterized in that the measuring is carried out prior to the chilling of the part carcass.

9. A method according to claim 1, characterized in that the measuring is carried out within two hours after the slaughtering (drainage of blood).

10. An apparatus for prediction of the drip loss of a part of a carcass by measuring a muscle in the part carcass after slaughtering, characterized in comprising:

- a light reflection meter adapted to measure the light reflectivity of a muscle in at least one wave range with a wave number below 1500 cm^{-1},

- a calculation unit with a program and/or memory part adapted to automatically record measured, possibly processed light reflectivity data in an algorithm and to calculate the algorithm value,

- an algorithm contained in the program and/or memory part expressing a prediction of the drip loss as a function of the light reflectivity in one or more wave ranges with a wave number below 1500 cm^{-1}, measured on a muscle in a part carcass after slaughtering, while the part carcass is still warm from slaughter, and

- a signal unit which after the insertion of light reflectivity data in the algorithm and calculation of the algorithm value emits a signal depending on the calculated prediction.

Abstract

To predict the drip loss of a part of a carcass a measuring is made on a muscle of a part of a carcass after slaughtering, while the part carcass is still warm from slaughter. The light reflectivity of the muscle is measured in at least one wave range with a wave number below 1500 cm^{-1}, preferably in the interval 900-1500 cm^{-1}. The measuring data obtained are inserted as variables in an algorithm expressing a prediction of the drip loss as a function of the light reflectivity in one or more wave ranges with a wave number below 1500 cm^{-1}. The prediction in respect of the drip loss is automatically calculated in a calculation unit by means of the algorithm.

The measurement may be carried through quickly, which means that carcasses may be measured by means of equipment concurrently with their advancing on a slaughter line. Through the measurement it becomes possible to predict the drip loss with high accuracy.

Paper IV

Early prediction of water-holding capacity in meat by multivariate vibrational spectroscopy

D.K. Pedersen, S. Morel, H.J. Andersen and S.B. Engelsen

Abstract

This study had the dual purpose of (a) investigating the feasibility of measuring fundamental vibrational information in fresh porcine meat using infrared (IR) absorption and Raman scattering, and (b) investigating if the vibrational spectra obtained within 1 hour after slaughter contained information about the water-holding capacity (WHC) of the meat. Preliminary studies performed at a research slaughterhouse revealed a high correlation between WHC and both IR (r = 0.89) and Raman spectra using Partial Least Squares Regressions (PLSR). The good results were confirmed under industrial conditions using FT-IR at-line spectroscopy. However, the latter experiment yielded a somewhat lower correlation (r = 0.79). This result is, however, promising for the purpose of finding a method for classification of carcasses with regard to WHC at the slaughter line. The IR region 1800-900 cm^{-1} contains the best predictive information according to WHC of the porcine meat. This region covers functional group frequencies of water, protein, fat and glycogen, including the carbonyl and amide groups.

Keywords: Early prediction; Quality; Vibrational spectroscopy; FT-IR; Raman; Water-holding capacity; Porcine meat; Chemometrics; PLSR; PCA

Introduction

Vibrational spectroscopy has been widely adopted as an analytical technique for the identification and verification of chemical compounds. However, it's full potential as a rapid method for quality control in the food industry remains largely to be elucidated. Recent successful applications of Fourier transform infrared (FT-IR) spectroscopy for milk and wine quality control (Andersen, Hansen & Andersen,

2002) points in the direction that FT-IR is most useful for liquid quality control. Moreover, near infrared (NIR) spectroscopy is thus far the most successful technique and has been applied for a variety of quality attribute determinations in food and feeds. NIR applications to meat quality include determination of fat, moisture, protein and sodium chloride (Osborne, Fearn & Hindle, 1993). The application of mid-IR spectroscopy to food systems has mainly been limited because of the strong absorption of water across most of the mid-IR spectrum.

An extended use of FT-IR in the food industry could be through introduction of the attenuated total reflection (ATR) technology, which simplifies sample handling of very viscous or very strongly absorbing materials normally difficult to analyse by transmission spectroscopy. The disadvantage of ATR is that the spectra are sensitive to the contact between the ATR crystal and the sample, and that the IR radiation will only penetrate a few microns of the sample. More recently, the ATR principle has been further developed to solids through the diamond ATR by which infrared spectra of solid samples can be measured with high precision and reproducibility. A major obstacle to the implementation of mid-infrared spectroscopy for industrial quality control has been the need for sophisticated optical materials, which prohibits the use of practical fibres. A complement to FT-IR is Raman spectroscopy, which has not been appreciated in agricultural and food sciences, because it is not easily applicable to materials that exhibit fluorescence, especially when using visible excitation. Water, on the other hand, is only weakly polarizable and does not create disturbing interferences, as in mid-IR and NIR spectroscopy. Optical fibres are applicable in Raman spectroscopy, which together with the ongoing developments makes the technique interesting as a tool for industrial quality control in the food industry (Li-Chan, 1996). Its potential in meat context was already exposed in the late seventies, when Raman spectroscopy was applied for investigations of intact muscle fibres (Pezolet, Pigeon-Gosselin & Caille, 1978; Pezolet, Pigeon-Gosselin, Savoie & Caille, 1978; Pezolet, Pigeon-Gosselin, Nadeau & Caille, 1980).

Meat is a complex biological system consisting mainly of water (~ 75 %), protein (~ 19 %) and fat (~ 2.5 %), but it also contains minor components such as glycogen, phosphorous compounds (e.g. creatine phosphate and ATP), metabolites (e.g. lactate and creatine) and trace amounts of vitamins (Figure 1). The rate and extent of the *post mortem* pH-fall trigger mechanisms that affect the water holding of meat (Bate-Smith, 1948; Bendall, 1979). The WHC of meat is important for two reasons.

Firstly, meat is sold by weight, thus any water loss is economically undesirable. Secondly, the WHC influences the appearance of fresh meat during retail and might affect the sensory properties of cooked meat, as high cooking loss has been reported to make meat be perceived less juicy (Martens, Stabursvik & Martens, 1982).

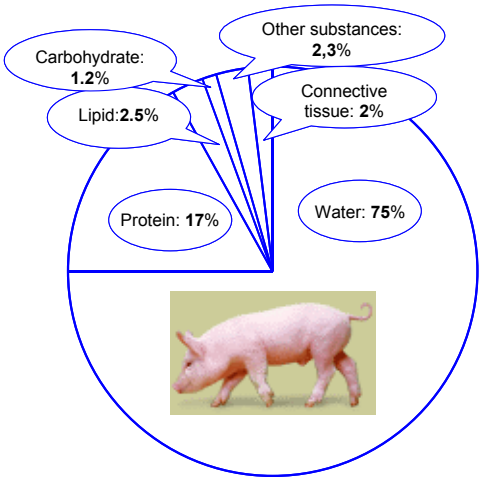

Figure 1. Chemical composition of meat. Protein consists of myofibrillar (e.g. myosin and actin) and sarcoplasmic proteins. Carbohydrates are mainly glycogen. Other substances include lactic acid, creatine, inorganics and vitamins (Lawrie, 1991).

The reduction in water holding during conversion of muscle to meat is primarily due to both pH induced protein denaturation (Bendall & Wismer-Pedersen, 1962; Penny, 1969) and the ongoing rigor development (Honikel, Kim & Hamm, 1986; Bertram, Purslow & Andersen, 2002) which result in shrinkage of the myofilament lattice spacings and hereby becomes the driving force for transfer of water into potential drip channels (Offer *et al.*, 1989).

As *post mortem* progress in pH affects WHC, many of the *post mortem* metabolism-associated compounds, e.g. glycogen, lactate, creatine and ATP, are indirectly associated to the water-holding capacity of meat (Offer & Knight, 1988). However, they are all present in relatively low levels in the porcine meat 30-40 min after slaughter and difficult, if not impossible, to detect in vibrational spectra of meat. Glycogen and lactate, though, are expected in concentrations in the lower ranges of

the detection levels of the FT-IR or Raman techniques (0.1 %) for this type of difficult complex samples.

Molecular absorption of mid-IR radiation (4000-400 cm^{-1}) results in the excitation of the fundamental vibrational modes. Accordingly, the mid-IR spectrum of a compound contains a wealth of chemical and structural information such as the structure of meat associated to the water-holding capacity. In addition, the intensities of the bands in the absorption spectrum are proportional to concentration, obeying Lambert-Beer's law, making mid-IR spectroscopy amenable to quantitative analysis applications. Raman spectroscopy, which is another technique for detection of the same molecular vibrations, but with different selectivity, can potentially be useful for detecting certain functional groups of foodstuffs. For example, vibrations involving C=C are weak in IR, but strong in Raman and proposed for measurement of iodine number in foods by e.g. Sadeghi-Jorabchi, Hendra, Wilson & Belton (1990). C≡N is another group (Micklander, Brimer & Engelsen, 2002) that is strongly Raman active, and in general Raman can be said to be more sensitive to backbone structure of macromolecules in contrast to the functional side groups that are usually more intense in IR.

Prediction of WHC by vibrational spectroscopic methods has previously been investigated by application of near infrared spectroscopy (Swatland & Barbut, 1995; Byrne, Downey, Troy and Buckley, 1998; Forrest, Morgan, Borggaard, Rasmussen, Jespersen & Andersen, 2000; Brøndum, Munck, Henckel, Karlsson, Tornberg & Engelsen, 2000). Apart from Forrest *et al.* (2000) these investigations have applied the spectroscopic measurements post rigor, which according to modern slaughtering processes is too late for efficient classification of carcasses. Forrest *et al.* (2000) measured NIR (900-1800 nm) during a 6 min period 30 min after sticking by using a fibre optic probe. In combination with multivariate data analysis they predicted drip loss 24 h after slaughter with a prediction error of 1.8 % drip loss.

The objective of this study was to investigate the fundamental vibrational information in meat within 1 hour after slaughter and simultaneously evaluate the applicability of FT-IR and Raman to meat and if possible build a predictive model for assessment of the quality parameter WHC of porcine meat through multivariate calibrations (Pedersen, Andersen, Christensen & Engelsen, 2000). FT-IR and Raman spectroscopy and subsequent analysis were carried out on selected pure meat

components, meat samples from a research slaughterhouse and meat samples from a commercial slaughterhouse, respectively. Interpretation of obtained spectra was attempted, despite major difficulties due to the complex and amorphous nature of whole meat causing many broad and overlapping peaks. This study was a part of a larger experimental setup in which the metabolic state of the *post mortem* meat, impedance and NIR was also measured, but it holds the most promising results.

Materials and methods

Pure meat components, including glycogen (BioChemika 50571), lactate (Chemika 71720), hydroxyproline (BioChemika 56250), fat (4 days after slaughtering of the pig), myoglobin (Sigma M-0630), myofibrils (prepared as described by Møller, Vestergaard & Wismer-Pedersen (1973)), creatine (Aldrich Chem. Co. 29,119-6), creatine phosphate (BioChemika 27920) and ATP (Aldrich Chem. Co. A26209) were acquired for recording of FT-IR and Raman spectra.

Research meat samples. Initially, 41 pigs were slaughtered at the research abattoir at The Danish Institute of Agricultural Sciences, Foulum, Denmark. In order to obtain a large variation in meat quality (water-holding capacity) the rates and extents of pH decrease *post mortem* were manipulated through pre-conditioning of the pigs. Adrenaline affects glycogenolysis and thereby represents a tool to manipulate ultimate pH and probably also the rate of pH decrease, as described by Henckel, Karlsson, Oksbjerg & Petersen (2000). Another way of manipulating energy levels in the live muscle is by treadmill exercise. In the present study the pigs were subjected to three different treatments prior to slaughtering: (1) 16 pigs were injected with 0.3 mg adrenaline / kg live weight 16 hours prior to slaughter; (2) 12 pigs were subjected to 14-20 min treadmill exercise immediately prior to slaughter; (3) 13 pigs served as the control. All pigs were stunned by 85 % CO_2 for three min, exsanguinated, scalded at 62°C for three min, cleaned and eviscerated within 30 min. At 45 min *post mortem* the carcasses were placed in a chill room at 4°C. FT-IR and Raman spectra as well as WHC measured as drip loss were recorded on *M. longissimus dorsi* from the carcasses.

Commercial meat samples. An additional 66 pigs were slaughtered at a commercial Danish slaughterhouse. At-line FT-IR and WHC measured as drip loss were recorded on *M. longissimus dorsi* from these carcasses.

Measurement of drip loss. For the 'research meat samples' water-holding capacity was measured as drip loss according to Honikel (1998), i.e. loss of water was registered from a 2.5 cm thick slice of muscle taken 24 hours *post mortem* and placed hanging in a net and suspended in a plastic bag for 48 hours at +4°C.

For the 'commercial meat samples' water-holding capacity was measured as drip loss according to Rasmussen & Andersson (1996) whereby the loss of water was registered from two cylindrical cuts (25 mm in diameter and 25 mm in length) of muscle taken 24 hours *post mortem* and then hanging for 24 hours in a plastic cup with a removable container at +4°C. The average of the drip loss from the two pieces was used for subsequent data analysis.

FT-IR spectroscopy. The Arid-Zone MB100 FT-IR (Bomem, Quebec, Canada) was used for measurement of IR spectra of the 'pure meat components' (4000-600 cm^{-1}) of the 'research meat samples' (4000-750 cm^{-1}) and the 'commercial meat samples' (4000-750 cm^{-1}). Prior to FT-IR measurements the 'research meat samples' from *longissimus dorsi* were cut out 35 min after sticking from the right loin of the 5th vertebra, and 40 min after sticking from the right loin at the 8th vertebra, while the 'commercial meat samples' from *longissimus dorsi* were cut out immediately after the classification centre, approximately 45 min after sticking, and measured by an instrument placed close to the slaughter line. The two spectral recordings of the 'research meat samples' are treated as replicates; thus, the average of the two measurements for each sample was used for further exploration.

Sampling of the 'pure meat components' was performed using an Attenuated Total Reflectance (ATR) device with a diamond crystal (Durascope, SensIR Technologies), while the meat samples were squeezed directly onto an ATR crystal (ZnSe, 45°, Tr-Plate, ARK 0055-603, Spectra-Tech Inc., CT, USA). The 'pure meat component' samples were squeezed against the ATR window with equal pressure (Force = 6 (a.u.)). A resolution of 4 cm^{-1} was employed, and 64 spectra were accumulated, averaged, and ratioed against a single-beam spectrum of the clean ATR crystal and converted into absorbance units.

Raman spectroscopy. A LabRam Infinity spectrograph (Jobin-Yvon, Lille, France) equipped with a 785-nm laser diode (30 mW reaching the sample) was used for the measurement of Raman spectra (3400-200 cm^{-1}) of the 'pure meat components', while a LabRam spectrograph (Jobin-Yvon, Lille, France) with a HeNe laser (632 nm) (5 mW reaching the sample) was employed for the measurement of Raman spectra (3200-500 cm^{-1}) of the 'research meat samples' 10-30 min after sticking. A microscope was used for sample presentation. A 'long-working-distance' objective was used for the measurement of the 'pure meat components', while a 'short-working-distance' objective was used for the measurement of the 'research meat samples'. The 'long-working-distance' objective is less sensitive to focus drifts, although it has a lower numerical aperture than the 'short-working-distance' objective. This can be an important feature when measuring meat samples at an early stage after slaughter, since the meat is still 'alive' and is 'moving' under laser illumination. A 600 (1/mm) grating and a confocal hole of 200 μm for the 'pure meat components' and 300 μm for the 'research meat samples' were employed. Four Raman scatter spectra were recorded and averaged for each sample, except for the research meat samples, where the average of Raman spectrum 1 and spectrum 2 of the four recorded spectra for each sample were used for further investigation, due to the critical time perspective in measuring the samples at such an early stage after slaughtering. The individual spectra were acquired using 60 sec (glycogen, lactate, hydroxyproline, creatine, ATP and 'research meat samples'), 45 sec (creatine phosphate) or 30 sec (fat and myofibrils) integration time on the CCD. Only meat samples from 14 of the 41 available research animals were measured. The reason for the limited number of samples is that the Raman equipment was only available at the research facilities for a part of the period of research slaughtering.

Other measurements. Measurement of the 'research meat samples' was performed during an experiment in which near infrared reflectance (NIR), impedance, pH, temperature, colour, glycogen and other metabolites and enzymes were also measured. pH measurements were taken at fixed intervals *post mortem*: 1 min, 15 min, 30 min, 1 h, 2 h, 3 h, 6 h, 9 h and 24 h. Temperature was measured at the same intervals up to 2 h and at 24 h. Colour measurements were made on loin samples excised at 24 h *post mortem*. Biopsies were used for analyses of glycogen, lactate and the phosphorous compounds creatinephosphate, ATP and ADP.

Chemometrics. Principal Component Analysis (PCA) (Wold, Esbensen & Geladi, 1987) was applied to the spectral data to obtain an overview. Calibrations and predictions of drip loss in meat based on spectral information were performed with Partial Least Squares Regression (PLSR) (Martens & Næs, 1989) and by interval Partial Least Squares Regression (iPLSR) (Nørgaard, Saudland, Wagner, Nielsen, Munck & Engelsen, 2000). Full cross-validation (leave one out) was applied throughout this study and only validated results are presented. The multivariate data analysis was performed with the chemometric programs The Unscrambler 7.6 (CAMO, Trondheim, Norway) and Matlab 6.1 (The Mathworks Inc., Natick, MA, USA).

Principal Component Analysis (PCA) (Wold *et al.*, 1987) is the most fundamental chemometric algorithm. In PCA the spectra are resolved into orthogonal principal components whose linear combinations approximate the original data set in a least squares sense. PCA provides an approximation of the data matrix (e.g., FT-IR spectra of porcine meat) in terms of the product of the two low dimensional matrices **T** (scores) and **P'** (loadings). These two matrices capture the systematic variation of the data matrix. Plots of the columns of **T** (score plots) provide a picture of the sample concentrations of the latent variables, while plots of the rows of **P'** (loading plots) depict the variable contribution to the latent variables (Wold *et al.*, 1987).

Partial Least Squares Regression (PLSR) (Martens *et al.*, 1989) is a predictive regression method based on estimated latent variables and is applied to the simultaneous analysis of two data sets (e.g., spectra (**X**) and WHC measurements (**y**)) on the same samples. The purpose of the PLSR is to build a linear model enabling prediction of a desired characteristic (**y**) from a measured spectrum (**x**).

Interval PLSR (iPLSR) (Nørgaard *et al.*, 2000) is simply PLSR models developed on spectral subintervals, which together with the full-spectrum PLSR model gives a superb overview of spectral correlation and additionally reduces interference problems and thus simplifies models. The comparison between iPLSR and the full-spectrum PLSR is mainly based on the validation parameter RMSECV (root mean squared error of cross-validation):

$$\text{RMSECV} = \sqrt{\frac{1}{N}\sum_{i=1}^{N}(y_i - \hat{y}_i)^2}$$

where $\hat{y}_i$ is the predicted value for sample i, y_i is the corresponding reference value, and *N* is the total number of samples. The number of intervals in this study is varied using 10, 20, 30 or 40 subintervals. Synergy amongst iPLSR models as earlier applied by Munck *et al.* (2001) was subsequently investigated.

Results and discussion

Meat components. Figure 2 shows the vibrational spectra of pure meat components that are characterized in terms of characteristic group frequencies and specific (intense) bands in the fingerprint region (1500 cm^{-1} – 200 cm^{-1}). Strong differences between IR and Raman selection rules are also indicated. Many bands of the different components may be shifted in both position and intensity as a result of matrix effects. Therefore, the spectra of meat may be considerably different from the simple summation spectrum of the individual compounds. Still, they can be explanatory for the aim of interpretation of the meat spectra.

Glycogen is an α-glucan and the principal storage carbohydrate in muscles. The IR spectrum (Fig. 2A) displays stable group frequencies at 3300 cm^{-1} due to OH stretching from hydroxyl groups in the α-glucan skeleton and adsorbed water, and at 2900 cm^{-1} caused by CH stretching from the α-glucan skeleton. The fingerprint region is dominated by very intense peaks in the region 1150-1020 cm^{-1} due to complex C-O-C ether stretchings found in glucopyranose rings and in the glycosidic linkages. The Raman spectrum includes a characteristic peak at 850 cm^{-1} exclusive to α anomeric glucans as opposed to the corresponding β-anomers. In addition, an intense and characteristic peak at 490 cm^{-1} is found, which is due to a low frequency skeleton mode in the primarily α-1,4 linked glucan and is common with the corresponding storage carbohydrate in plants, starch. The increasing baseline in the Raman spectrum is caused by fluorescence from trace components.

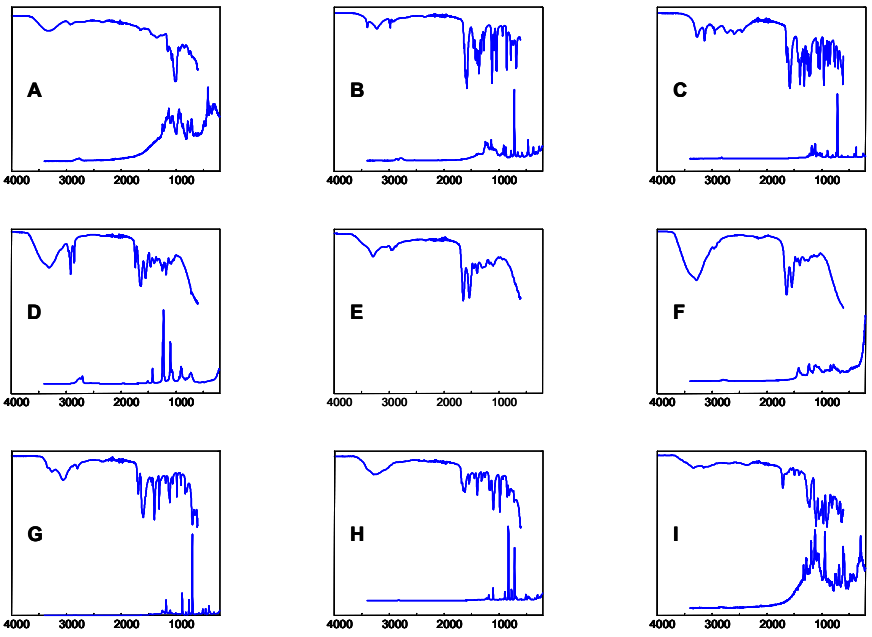

Figure 2. FT-IR (upper) (showed as transmittance spectra) and Raman (lower) spectra of meat components: glycogen (A), lactate (B), hydroxyproline (C), fat (D), myoglobin (E), myofibrils (F), creatine (G), creatine phosphate (H) and ATP (I)

Lactate (Fig. 3) is the major end product of anaerobic glycolysis (of glycogen) that causes the pH decrease in the muscle *post mortem*. The IR spectrum (Fig. 2B) of lactate shows a sharp band at 3400 cm^{-1} and a broad band centred at 3200 cm^{-1} due to OH stretching. Aliphatic CH stretching shows as peaks in the IR and Raman spectra at 2980 cm^{-1}, 2930 cm^{-1} and 2900 cm^{-1}. The strong IR bands at 1580 cm^{-1} and 1360 cm^{-1} are due to carbonyl stretching of the carboxylate group. In the fingerprint region the spectra of lactate exhibit a complex CH bending pattern between 1460 cm^{-1} and 1330 cm^{-1}. The IR spectrum shows characteristic strong bands near 1100 cm^{-1} due to CO vibrations. In the Raman spectrum the strongest peak is located at 850 cm^{-1}, which is IR active as well.

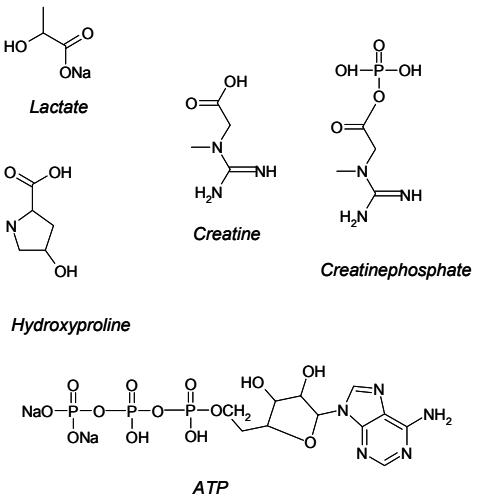

Figure 3. Structure images of some simple meat components: lactate, hydroxyproline, creatine, creatinephosphate and ATP

Hydroxyproline (Fig. 3) is a chemical component of the connective tissue. The IR spectrum (Fig. 2C) shows characteristic group frequencies at 3270 cm^{-1} and 3140 cm^{-1} due to OH and NH stretching, respectively. Aliphatic CH stretching is displayed in the Raman spectrum around 2950 cm^{-1} and as IR bands in the region 3000-2400 cm^{-1}. Strong carbonyl IR bands are located at 1580 cm^{-1} and at 1360 cm^{-1} due to the carboxylic group. The intense IR peaks in the region 1300-1000 cm^{-1} are due to complex vibrations involving CO stretching and OH deformation. The, by far, most intense Raman band is found at 850 cm^{-1}, probably due to a symmetric ring breathing in the pyrrolidine ring.

Fat constitutes around 2.5 % of the meat (Fig. 1). The IR spectrum of fat (Fig. 2D) displays a strong and broad peak centred at 3300 cm^{-1} due to OH stretching from the glycerol backbone. Saturated aliphatic CH stretching is found at 2920 cm^{-1} and 2850 cm^{-1}, while olefinic CH stretching is found slightly above 3000 cm^{-1}. The characteristic C=O peak due to the carbonyl group in the ester linkages of fat molecules at 1740 cm^{-1} is present in both the IR (medium) and the Raman (weak) spectra. *Cis* C=C shows as a characteristic band at 1660 cm^{-1} in the Raman spectrum, while the dual peak at 1630 cm^{-1} and 1550 cm^{-1} in the IR spectrum is due

to carbonyl stretching from secondary amides from connective tissue. Peaks due to CO stretching at 1300-1000 cm^{-1} dominate the fingerprint region of the IR spectrum. The strongest band in the Raman spectrum is the sharp 1440 cm^{-1} peak.

Myoglobin is the main muscle pigment that stores oxygen and facilitates oxygen transport within the muscle. OH stretching due to absorbed water and NH stretching from secondary amides cause the broad band at 3300 cm^{-1} in the IR spectrum (Fig. 2E). Aliphatic CH stretching appears as peaks in the spectrum at 2960 cm^{-1}, 2930 cm^{-1} and 2870 cm^{-1}. The amide I band is located at 1650 cm^{-1}, and the amide II band appears around 1540 cm^{-1}. In the fingerprint region the amide III band is found at 1240 cm^{-1} (Bellamy, 1975) along with well-defined peaks at 1450 cm^{-1}, 1390 cm^{-1}, 1300 cm^{-1}, 1170 cm^{-1} and 1100 cm^{-1}. It was not possible to measure a Raman spectrum of myoglobin due to its absorbance characteristics (high absorbance in the Raman region).

Myofibrils consist mainly of the contractile proteins actin and myosin. The broad peak at 3300 cm^{-1} in the IR spectrum of myofibrils (Fig. 2F) is mostly due to the OH stretching of solvent water and NH stretching of the polypeptides. Aliphatic CH stretching appears in the IR spectrum at 2960 cm^{-1}, 2930 cm^{-1} and 2880 cm^{-1}. The most prominent bands of the spectra of the myofibrils are carbonyl absorption from the secondary amide bands at 1650 cm^{-1} (amide I overlapped with OH bending) and the mixture of CN and NH vibrations at 1540 cm^{-1} (amide II). In the Raman spectrum the bands at 1450 cm^{-1} (the symmetric methylene bending) and at 1320 cm^{-1} (CH bending) are quite strong. In the Raman spectrum a characteristic sharp peak at 1000 cm^{-1} is caused by aromatic ring vibration from aromatic amino acids like phenylalanine, and the band at 940 cm^{-1} can be assigned to peptide α-helix conformation (Frushour & Koenig, 1974).

Creatine, *creatine phosphate* and *ATP* (adenosine triphosphate) (Fig. 3) are involved in the energy metabolism of the muscle. ATP is gradually depleted in the muscle cells *post mortem*, even though some ATP is temporarily regenerated by the conversion of creatine phosphate to creatine and the transfer of its phosphate to ADP (adenosine diphosphate). The most pronounced bands in the spectra (Fig. 2GHI) of these compounds are the Raman peak at 840 cm^{-1} in creatine, 860 cm^{-1} in creatinephosphate and 820 cm^{-1} in ATP due to phosphate groups.

Table 1. The spectral bands observed in the FT-IR and Raman spectra of porcine meat 30-40 min after slaughter

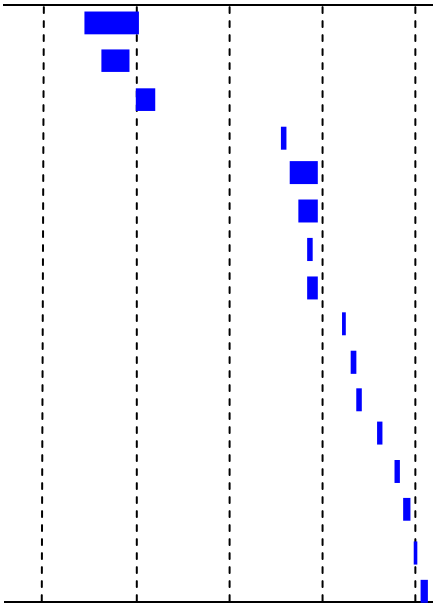

Vibration	IR	Raman	Meat component
OH str.	X		Water
NH str.	X	X	Protein
CH str.	X	X	Fat
C=O	X	X	Fat
HOH bend	X		Water
Amide I	X	X	Protein
C=C str. cis		X	Fat
Amide II	X	X	Protein
C-O str.	X	X	Fat
C-O str.	X	X	Fat
C-H bend		X	Protein
Amide III	X	X	Protein
C-O str.	X		Glycogen
C-O-C str.	X		Glycogen
aromatic ring		X	Protein
α-helix		X	Protein

Research meat samples. Table 1 based on the above-mentioned spectra lists the most important vibrational bands observed in porcine meat between 4000 cm^{-1} and 750 cm^{-1}. The spectra are shown in Figure 4 and can roughly be described as myofibril/myoglobin spectra overlapped with a small amount of fat spectrum. They clearly stress the difficulty of performing thorough assignment of complex biological matrices due to the strong and complex background. The amide I band at 1650 cm^{-1} is mixed with HOH bending (1640 cm^{-1}) from water in the IR spectrum and with *cis* C=C stretching (1660 cm^{-1}) of fat in the Raman spectrum. The amide II band appears around 1550 cm^{-1} in both spectra and the amide III band is found at 1240 cm^{-1}. These observed amide bands of meat spectra were also reported by Al-Jowder, Kemsley & Wilson (1997) who studied ATR-FT-IR spectra of meat (chicken, turkey and pork) for solving authenticity problems, and by Yang & Irudayaraj (2001) who compared ATR-FT-IR and PAS (photoacoustic spectroscopy)-FT-IR spectra of whole and ground beef. Contribution from proteins is also found as NH stretching in the broad IR band centred at 3300 cm^{-1} overlapping with OH stretching from the water content of the meat, which also

contributes to the IR band near 1640 cm^{-1} due to HOH bending. The band at 1740 cm^{-1} due to the carbonyl stretching of the ester group is related to the intramuscular fat present in the meat samples. The bands at 1460 cm^{-1}, 1400 cm^{-1} and 1310 cm^{-1} are recognised from the protein spectra of myofibrils (Fig. 2F) and myoglobin (Fig. 2E), while the CO stretching bands at 1160 cm^{-1} and 1080 cm^{-1} can be recognised from the IR spectrum of glycogen (Fig. 2A).

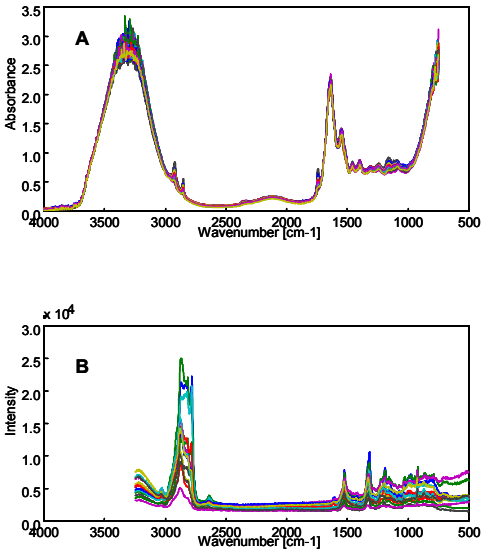

Figure 4. FT-IR spectra of the 41 research pig carcasses measured 35-40 min after slaughter (A) and Raman spectra of the 14 pig carcasses measured 10-30 min after slaughter (B)

In order to get an overview of the multivariate spectral data, a PCA was performed on the FT-IR spectra of the 41 research meat samples. Score plots of the principal components (not shown) revealed no spectral differences according to the three types of treatment applied to the pigs prior to slaughter; injection with adrenaline, subjection to exercise and non-treated control pigs. In other words, no obvious information of the applied stress levels of the pigs is imbedded in the FT-IR spectra. In agreement with this observation, other investigations (Henckel *et al.*, 2000) have not been able to find significant difference in ultimate pH and in the rate of pH

decrease *post mortem* for meat samples from exercised pigs contrary to control pigs. For the same reason it might not be reasonable to expect clear differences in WHC between the different types of treatment.

In order to investigate possible spectral correlations to WHC, PLSR models were developed (Table 2). First, a PLSR model based on the FT-IR spectra (4000-750 cm^{-1}) of the 41 research meat samples ranging from 0.7-8.0 % drip loss was developed. The PLSR model yielded a prediction error (RMSECV) of 1.35 % drip loss. Such prediction error is not considered sufficiently low for a method to perform early sorting of carcasses into groups with high and low drip losses. The prediction error was obtained by a 3-component PLSR model, which is considered to be too few components for solving a rather complex problem, but underlines the concealment of relevant information in vibrational spectra of complex biological samples.

Table 2. Regression results for PLSR models based on FT-IR and Raman spectra of research samples and industrial samples for prediction of water-holding capacity (WHC). The number of PLSR components (PC's), the correlation coefficients (r), the prediction errors (RMSECV) and the range of WHC are presented.

Samples	Instrument	Spectra [cm^{-1}]	# of PC's	r	RMSECV [%]	WHC range [%]
Research	FT-IR	4000-750	3	0.68	1.35	0.7-8.0
Research	FT-IR	1072-993	5	0.84	1.00	0.7-8.0
Research	FT-IR	1396-1317+1072-993	5	0.89	0.85	0.7-8.0
Research	FT-IR	1800-900	5	0.89	0.86	0.7-8.0
Research	Raman	3200-500	3	0.98	0.27	0.7-8.0
Research	Raman	3128-3071	3	0.95	0.38	0.7-8.0
Research	Raman	3128-3071+951-876	3	0.98	0.23	0.7-8.0
Industrial	FT-IR	4000-750	4	0.73	1.17	0.5-8.3
Industrial	FT-IR	1800-900	7	0.79	1.06	0.5-8.3
Industrial	FT-IR	1396-1317	4	0.82	0.97	0.5-8.3
Industrial	FT-IR	1396-1317+1072-993	6	0.81	1.02	0.5-8.3

When applying chemometric calibration techniques to complex spectra consisting of many variables, usually not all parts of the spectra are equally relevant for the calibration purpose. There are two obvious ways of finding relevant parts of the spectra for calibration purposes: 1) by using *a priori* knowledge about the spectra or

2) by using chemometric variable selection tools for finding the best predictive areas of the spectra. Interval PLSR (iPLSR) (Nørgaard *et al.*, 2000) is an example of the latter, which develops local PLSR models on subintervals of the full-spectrum region. Figure 5 displays the result of iPLSR models based on the FT-IR spectra (4000-750 cm^{-1}) of the 41 research meat samples. The number of intervals was 40, and the prediction errors (RMSECV) for each of the 40 subintervals are presented as bars for a 5-component-model superimposed with the average FT-IR spectrum and with the global prediction error presented as a horizontal line (1.35 % drip loss, see above). The subinterval reaching the lowest prediction error (Figure 5) was found to be subinterval 37 (1072-993 cm^{-1}). A PLSR performed using that narrow spectral region alone provides a 5-component model with a correlation of 0.84 and a prediction error of 1.00 % drip loss. Usually, fewer components due to lesser complexity of the spectra are expected when applying iPLSR. However, in this case, the number of components in the full-spectrum model is suspiciously low, perhaps due to unresolved complexity. In Figure 5 the prediction errors (shown as bars) are quite high when applying the noisy parts of the spectra, subintervals 7-11 and 40, which imply PLSR modelling problems when using those parts of the spectra. Consequently, the application of more components in the iPLSR models with low prediction errors, such as subinterval 37, facilitates improved modelling, when the noisy parts of the spectra are kept out.

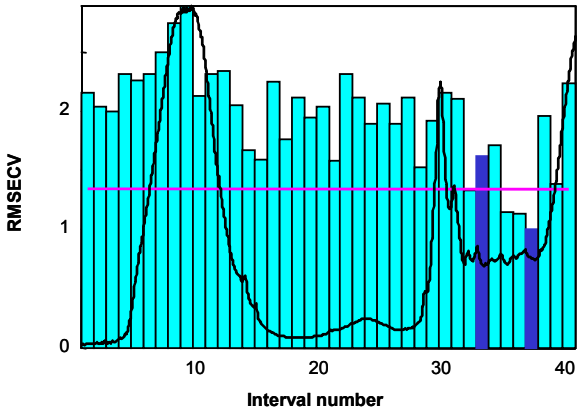

Figure 5. iPLSR plot of a 5-component model based on 40 subintervals of the full FT-IR spectra (4000-750 cm^{-1}) of the 41 research pig carcasses. The prediction errors (RMSECV) for each subinterval are presented as bars. The global prediction error presented as a horizontal lines is based on a 3 component model.

Instead of using one single subinterval at a time, it might be advantageous to use two subintervals in the PLSR modelling. By combining all possible iPLSR pairs, synergy models were identified. By combining subintervals 33 (1396-1317 cm^{-1}) and 37 (1072-993 cm^{-1}), represented as the two dark bars in Figure 5, a prediction error of 0.85 % drip loss was obtained, which is a significant improvement compared to the global prediction error of 1.35 % drip. It is also interesting to notice that subinterval 33 in synergy with subinterval 37 provides better regression, irrespective of the relatively poor prediction ability of subinterval 33 alone (RMSECV = 1.6). In order to obtain a robust model, it is preferable to work with continuous spectra compared to discrete subintervals of spectra. Figure 5 shows that the lowest iPLSR prediction errors are found in the fingerprint region, especially subintervals 32-37 covering the region 1477-993 cm^{-1}. A PLSR model based on a part of the FT-IR spectra (1800-900 cm^{-1}) covering the fingerprint region as well as the important amide bands (1650 cm^{-1} and 1550 cm^{-1}) of the 41 research meat spectra was performed and yielded a prediction error of 0.86 % (Figure 6A), only slightly inferior to the 'optimised' synergy model. This underlines the importance in the PLSR modelling of applying only the parts of the spectra, which contain systematic information free from excessive noise.

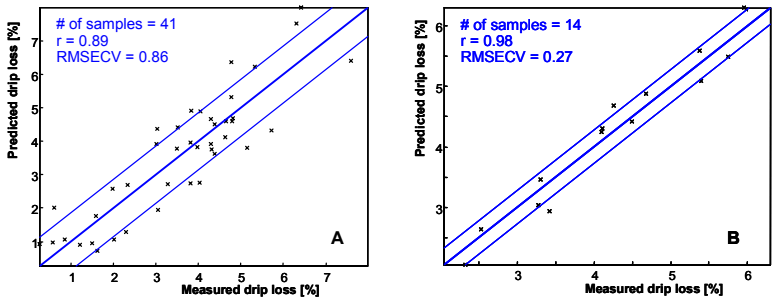

Figure 6. Predicted drip loss versus measured drip loss for PLSR models based on the FT-IR spectra (1800-900 cm^{-1}) (A) employing 5 components for the 41 research pig carcasses and on Raman spectra (3200-500 cm^{-1}) (B) employing 3 components for 14 research pig carcasses. The prediction errors, root mean square error of cross-validation (RMSECV), are reported.

A PLSR model based on Raman spectra (3200-500 cm^{-1}) of the 14 research meat samples (ranging from 0.7-8.0 % drip loss) covering all treatments (injection with adrenaline, subjection to exercise and non-treated control pigs) was also performed. The resulting prediction error (RMSECV) for a 3-component model was found to be 0.27 % drip (correlation = 0.98), as shown in Figure 6B. Such an extraordinary good PLSR model based on the Raman spectra is perhaps unrealistic, due to the low number of samples (14), but it certainly deserves further attention in future studies. When working with only 14 samples in a 3-component model, there is a serious risk of over fitting.

iPLSR models based on the Raman spectra (not shown) showed that subinterval 3 (3128-3071 cm^{-1}) gave the lowest prediction error. PLSR performed using that interval alone provides a 3-component-model with a correlation of 0.95 and a prediction error of 0.38 % drip loss. This is still very good, but considerably higher than the full-spectrum model, and it shows that more than just a small part of the spectra is necessary for the modelling in order to obtain the best prediction of the drip loss. For synergy iPLSR, a 3-component model of the subintervals 3 (3128-3071 cm^{-1}) and 35 (951-876 cm^{-1}) yielded a prediction error of 0.23 % drip loss, which is a small improvement compared to the global prediction error of 0.27 % drip loss. This result shows that the combination of those two subintervals of the spectra contains sufficient information for prediction of the drip loss in this data set.

Commercial meat samples. The FT-IR spectra of the 'commercial meat samples' measured 45 min after sticking have the same spectral characteristics as the FT-IR spectra of the 'research meat samples' measured 35 and 40 min after sticking. However, the spectra of the 'commercial meat samples' seem to contain more variation compared to the spectra of the 'research meat samples', especially the parts of the spectra containing the fat information vary considerably. The 'commercial meat spectra' appear to contain less noise in the regions of high absorption compared to the 'research meat spectra'. The reason for the difference might be that the instrument employed for the commercial experiment was another, however the same type, Arid-Zone MB100, than the instrument used for the initial experiment.

PLSR models based on the full FT-IR spectra (4000-750 cm^{-1}) and on a reduced part of the spectra (1800-900 cm^{-1}) of the 66 'commercial meat samples' ranging from

0.5-8.3 % drip loss were developed. The prediction error (RMSECV) of the PLSR model (4 PC) based on the full FT-IR spectra was calculated to 1.17 % drip loss (r = 0.73), while the prediction error of the PLSR model (7 PC) based on 1800-900 cm^{-1} was 1.06 % (r = 0.79), as listed in Table 2. The full-spectrum PLSR model of the 'commercial meat samples' yielded a slightly lower prediction error than the full-spectrum model of the 'research meat samples'. The reason might be that the commercial model requires an extra PLSR component, which contributes to the explanation of the coherence between the spectra and the drip loss. On the other hand, the reduced-spectrum model of the 'commercial samples' has a slightly higher prediction error than the reduced-spectrum model of the 'research samples', even though more components (7) are applied. This could perhaps be explained by the larger biological variation present in the 'commercial meat samples'.

Not all the measured samples from the 'commercial experiment' were included in the PLSR models. More samples were measured during the experiment, but had to be removed prior to PLSR modelling due to (a) missing reference values, (b) unrealistically high reference values, (c) FT-IR spectra low on information resulting from poor contact to the ATR crystal, (d) strong interference information in the spectra caused by high fat content or (e) simple PLSR modelling outliers such as lack of coherence between spectra and reference values. Basically, the large number of outliers reflects the difficulties connected to measurements using laboratory equipment in the harsh process environment. For example, due to the speed of the measurements close to the slaughter line it was not possible to re-measure samples with poor spectra. For that reason the majority of the outlier measurements were lost.

The synergy PLSR on subintervals 33 (1396-1317 cm^{-1}) and 37 (1072-993 cm^{-1}) found by the iPLSR of the research samples yielded a prediction error of 1.02 % drip loss (r = 0.81) on the industry samples (Table 2). The improvement of the synergy PLSR is again significant when compared to the full-spectrum model. By using subinterval 33 (1396-1317 cm^{-1}) alone a 4-component-model with a correlation of 0.82 and a prediction error of 0.97 % was obtained. In the 'commercial example' the subinterval 37 alone provided a rather poor prediction ability (RMSECV = 1.5 %).

Interpretation. The vibrational spectral regions of interest to WHC according to iPLSR are the IR regions 1396-1317 cm^{-1} and 1072-993 cm^{-1} and the Raman regions 3128-3071 cm^{-1} and 951-876 cm^{-1}. The IR regions cover spectral information about carbonyl vibrations of the deprotonated carboxylic group (1360 cm^{-1}), which would be expected to be correlated to the pH of the sample, CO stretching of glycogens (1020 cm^{-1}) connected to the level of glycogen at the time of measurement, and the presence of an 'internal standard' represented by the sharp aromatic ring vibration at 1000 cm^{-1}. The Raman regions contain NH stretching of primary amides in proteins (3140 cm^{-1}), which might indicate protein denaturation. Secondary structure information of proteins is represented by the α–helical 940 cm^{-1} band and again the presence of an 'internal standard' represented by the sharp aromatic ring vibration at 1000 cm^{-1}, which is very strong in Raman spectroscopy. These observations suggest coherence between water-holding capacity and pH, glycogen level and protein conformations, which supports earlier developed theories in this area, as investigated by among others, Offer *et al.* (1989), Warner, Kauffman & Greaser (1997), den Hertog Meischke, van Laack & Smulders (1997), Kristensen & Purslow (2001), Bertram *et al.* (2002) and Schäfer, Rosenvold, Purslow, Andersen & Henckel (2002).

Conclusion

PLSR models based on FT-IR spectra of meat samples from a research slaughterhouse ranging from 0.7-8.0 % drip loss showed prediction errors (RMSECV) of 0.85-1.4 % drip loss, while the corresponding prediction error for industry pigs (0.5-8.3 % drip loss) were 1.0-1.2 % drip loss. These results are acceptable for the purpose of finding a method for sorting out the carcasses with very low and very high drip losses at an early stage after slaughter (45 min).

In this study an exploratory strategy for finding important regions of spectra, which best predict the reference quality parameter (without using *a priori* knowledge), namely iPLSR has been used. The considerable improvement in prediction error employing only informative regions of the spectra demonstrates the importance of selecting spectral regions prior to PLSR modelling. It is especially important to avoid the regions in the FT-IR spectra with very high absorption (in this case water absorptions in the region between 3500-3100 cm^{-1} and the region 800-750 cm^{-1},

where the instrumental setup loses sensitivity), as they are noisy and will disturb the regressions. The predictive importance of the intervals was validated by the 'commercial samples', which demonstrated a low prediction error (1.0 % drip) by employment of one of the two intervals (1396-1317 cm^{-1}) for PLSR calibration using four components.

Vibrational spectroscopic methods for early prediction of WHC have also been investigated by Forrest *et al.* (2000) who predicted drip loss early after slaughter by NIR with a correlation of approximately 0.8 for a trial of 99 carcasses measured at a commercial slaughterhouse. The prediction error was estimated to be 1.8 % drip loss, which they compared with the repeatability of the laboratory reference method of approximately 0.7 %. The prediction error for commercial slaughter pigs in this study of 1.0 % drip loss (0.5-8.3 % range) is considerably lower and more promising for the purpose of finding a method for early classification of pig carcasses based on the WHC of the meat.

In order to assess possible applications of these spectroscopic methods in the slaughterhouses with the purpose of early classification of the carcasses according to WHC, measurement of many more samples is necessary to include all kinds of biological variations in the meat material. It must also be taken into consideration whether the methods are technically robust enough to be able to work in a rough environment at the slaughterhouses with changing temperatures and humidity. In particular, FT-IR instruments are vulnerable to those conditions, and the development of satisfactory optical fibres is at present not very promising. Optical fibres are available for the Raman technique, as it uses visual or near infrared radiation. Moreover, water does not interfere with the spectra, as is the case with FT-IR and NIR. This is a very important attribute, as meat contains mostly water. The main difficulties with the Raman technique are the inherent poor signal-to-noise ratio and sample fluorescence; however, technological solutions to these might be under way for example in form of time-resolved Raman scattering.

Part of the strategy of this investigation was to, if possible, interpret important regions of FT-IR and Raman spectra according to the quality parameter WHC of porcine meat. The strategy included an attempt to assign the characteristic bands in the meat spectra and estimate the importance of the observed functional groups according to the WHC of porcine meat. The IR region 1800-900 cm^{-1} contains the

best predictive information according to WHC of the porcine meat. The spectral region covers the carbonyl group frequencies from esters and amides and the fingerprint region including information from the functional groups of water (1640 cm^{-1}), protein (1650, 1550 and 1240 cm^{-1}), fat (1740, 1660, 1630, 1455, 1310 and 940 cm^{-1}) and glycogen (1160 and 1080 cm^{-1}).

Acknowledgements

The authors wish to thank Danske Slagterier and the Ministry of Food, Agriculture and Fisheries for financial support through the project "Early *post mortem* measurement of WHC and drip loss in fresh pork". The Centre for Advanced Food Studies is acknowledged for co-financing the Raman spectrometer. Gilda Kischinovsky is acknowledged for assistance with the manuscript.

References

Al-Jowder, O., Kemsley, E.K. & Wilson, R.H. (1997). Mid-infrared spectroscopy and authenticity problems in selected meats: a feasibility study. *Food Chemistry, 59*, 195-201.

Andersen, S.K., Hansen, P.W. & Andersen, H.V. (2002). Vibrational spectroscopy in the analysis of dairy products and wine. In J.M. Chalmers, & P.R. Griffiths, *Handbook of Vibrational Spectroscopy* (Vol. 5) (pp. 3672-3681). Chichester: John Wiley & Sons Ltd.

Bate-Smith, E.C. (1948). Observations on the pH and the related properties of meat. *Journal of the Society of Chemical Industry-London*, 67, 83-90.

Bellamy, L.J. (1975). *The Infra-red Spectra of Complex Molecules*. Third edition. London: Chapman and Hall LTD.

Bendall, J.R. (1979). Relations between muscle pH and important biochemical parameters during the post-mortem changes in mammalian muscles. *Meat Science*, *3*, 143-157.

Bendall, J.R. & Wismer-Pedersen J. (1962). Some properties of the fibrillar proteins of normal and watery pork muscle. *Journal of Food Science*, *27*, 144-159.

Bertram, H.C., Purslow, P.P. & Andersen, H.J. (2002). Relationship between meat structure, water mobility, and distribution: A low-field nuclear magnetic resonance study. *Journal of Agriculture and Food Chemistry, 50*, 824-829.

Brøndum, J., Munck, L., Henckel, P., Karlsson, A., Tornberg, E. & Engelsen, S.B. (2000). Prediction of water-holding capacity and composition of porcine meat by comparative spectroscopy. *Meat Science, 55*, 177-185.

Byrne, C.E., Downey, G., Troy, D.J. & Buckley, D.J. (1998). Non-destructive prediction of selected quality attributes of beef by near-infrared reflectance spectroscopy between 750 and 1098 nm. *Meat Science, 49*, 399-409.

den Hertog Meischke, M.J.A., van Laack, R.J.L.M. & Smulders, F.J.M. (1997). The water-holding capacity of fresh meat. *Veterinary Quarterly, 19*, 175-181.

Forrest, J.C., Morgan, M.T., Borggaard, C., Rasmussen, A.J., Jespersen, B.L. & Andersen, J.R. (2000). Development of technology for the early *post mortem* prediction of water holding capacity and drip loss in fresh pork. *Meat Science, 55*, 115-122.

Frushour, B.G. & Koenig, J.L. (1974). Raman Spectroscopic study of tropomyosin denaturation. *Biopolymers, 13*, 1809-1819.

Henckel, P., Karlsson, A., Oksbjerg, N. & Petersen, J.S. (2000). Control of post mortem pH decrease in pig muscles: experimental design and testing of animal models. *Meat Science, 55*, 131-138.

Honikel, K.O. (1998). Reference methods for the assessment of physical characteristics of meat. *Meat Science, 49*, 447-457.

Honikel, K.O., Kim, C.J., Hamm, R. (1986). Sarcomere shortening of prerigor muscles and its influence on drip loss. *Meat Science*, *16*, 267-282.

Kristensen, L. & Purslow, P.P. (2001). The effect of ageing on the water-holding capacity of pork: role of cytoskeletal proteins. *Meat Science, 58*, 17-23.

Lawrie, R.A. (1991). *Meat Science*. Fifth edition. Oxford: Pergamon Press.

Li-Chan, E.C.Y. (1996). The applications of Raman spectroscopy in food science. *Trends in Food Science and Technology, 7*, 361-370.

Martens, H. & Næs, T. (1989). *Multivariate Calibration*. Chichester: Wiley.

Martens, H., Stabursvik, E. & Martens M. (1982). Texture and colour changes in meat during cooking related to thermal denaturation of muscle proteins. *Journal of Texture Studies*, *13*, 291-309.

Micklander, E., Brimer, L. & Engelsen, S.B. (2002). Non-invasive assay for cyanogenic constituents in plants by Raman spectroscopy: Content and distribution of amygdalin in bitter almond (*Prunus amygdalus*). *Applied Spectroscopy*, Accepted.

Munck, L., Pram Nielsen, J., Møller, B., Jacobsen, S., Søndergaard, I., Engelsen, S.B., Nørgaard, L. & Bro, R. (2001). Exploring the phenotypic expression of a regulatory proteome-altering gene by spectroscopy and chemometrics. *Analytica Chimica Acta, 446*, 171-186.

Møller, A.J., Vestergaard, T. & Wismer-Pedersen, J. (1973). Myofibril fragmentation in bovine Longissimus dorsi as an index of tenderness. *Journal of Food Science, 38*, 824-825.

Nørgaard, L., Saudland, A., Wagner, J., Nielsen, J.P., Munck, L. & Engelsen, S.B. (2000). Interval partial least-squares regression (iPLS): A comparative chemometric study with an example from near-infrared spectroscopy. *Applied Spectroscopy, 54*, 413-419.

Offer, G., Knight, P., Jeacocke, R., Almond, R., Cousins, T., Elsey, J., Parsons, N., Starr, R. & Purslow, P. (1989). The structural basis of the water-holding, appearance and toughness of meat and meat products. *Food Microstructure, 8*, 151-170.

Offer, G. & Knight, P. (1988). The structural basis of water-holding in meat. Part 2: Drip losses. In R.A. Lawrie, *Developments in Meat Science* (Vol. 4) (pp. 173-243). London: Elsevier.

Osborne, B.G., Fearn, T. & Hindle, P.H. (1993). Practical NIR spectroscopy with applications in food and beverage analysis. Second edition. Essex: Longman Scientific & Technical.

Pedersen, D.K., Andersen, J.R., Christensen, L.B. & Engelsen, S.B. (2000). Method and apparatus for prediction of the drip loss of a part of a carcass. *Patent no. DK 173748 B1*.

Penny, I.F. (1969). Protein denaturation and water-holding capacity in pork muscle. *Journal of Food Technology*, *4*, 269-273.

Pezolet, M., Pigeon-Gosselin, M. & Caille, J.P. (1978). Laser Raman investigation of intact single muscle fibers protein conformations. *Biochimica et Biophysica Acta, 533*, 263-269.

Pezolet, M., Pigeon-Gosselin, M., Savoie, R. & Caille, J.P. (1978). Laser Raman investigation of intact single muscle fibers on the state of water in muscle tissue. *Biochimica et Biophysica Acta, 544*, 394-406.

Pezolet, M., Pigeon-Gosselin, M., Nadeau, J. & Caille, J.P. (1980). Laser Raman scattering – A molecular probe of the contractile state of intact single muscle fibers. *Biophysical Journal, 31*, 1-8.

Rasmussen, A.J. & Andersson, M. (1996). New method for determination of drip loss in pork muscles. In *Proceedings 42nd International Congress of Meat Science and Technology* (286-287), 1-6 September 1996, Lillehammer, Norway.

Sadeghi-Jorabchi, H., Hendra, P.J., Wilson, R.H. & Belton, P.S. (1990). Determination of the total unsaturation in oils and margarines by Fourier transform Raman spectroscopy. *Journal of the American Oil Chemists Society, 67*, 481-486.

Schäfer, A., Rosenvold, K., Purslow, P.P., Andersen, H.J. & Henckel, P. (2002). Physiological and structural events post mortem of importance for drip loss in pork. *Meat Science*, Accepted.

Swatland, H.J. & Barbut, S. (1995). Optical prediction of processing characteristics of turkey meat using UV fluorescence and NIR birefringence. *Food Research International, 28*, 227-232.

Warner, R.D., Kauffman, R.G. & Greaser, M.L. (1997). Muscle protein changes *post mortem* in relation to pork quality traits. *Meat Science, 45*, 339-352.

Wold, S., Esbensen, K. & Geladi, P. (1987). Principal Component Analysis. *Chemometrics and Intelligent Laboratory Systems, 2*, 37-52.

Yang, H. & Irudayaraj, J. (2001). Characterization of beef and pork using Fourier-transform infrared photoacoustic spectroscopy. *Lebensmittel-Wissenschaft und Technologie*, *34*, 402-409.

Paper V

Near infrared absorption and scattering separated by Extended Inverted Signal Correction (EISC).

Analysis of NIT spectra of single wheat seeds

D.K. Pedersen, H. Martens, J.P. Nielsen and S.B. Engelsen

Abstract

A new extended method for separating e.g. scattering from absorbance in spectroscopic measurements, Extended Inverted Signal Correction (EISC) is presented and compared to the Multiplicative Signal Correction (MSC) and existing modifications of this. EISC pre-processing is applied to Near Infrared Transmittance (NIT) spectra of single wheat kernels with the aim of improving the multivariate calibration for protein content by Partial Least Squares Regression (PLSR). The primary justification of the EISC method is to facilitate removal of spectral artifacts and interferences that are uncorrelated to target analyte concentration. In this study EISC is applied in a general form, including additive terms, multiplicative terms, wavelengths dependency of the light scatter coefficient and simple polynomial terms. It is compared to conventional MSC and derivative methods for spectral pre-processing. Performance of the EISC was found to be comparable to a more complex dual-transformation model obtained by first calculating the second derivative NIT spectra followed by MSC. The calibration model based on EISC pre-processing performed better than models based on the raw data, second derivatives, MSC, and MSC followed by second derivatives.

INDEX HEADINGS: additive, multiplicative, interference, inverted scatter correction, ISC, EISC, multiplicative signal correction, MSC, near infrared, NIT, PLSR, protein, single seed, light scattering

Introduction

The Extended Inverted Signal Correction (EISC) method, originally developed with chemical analyte extensions[1], is here presented with spectroscopic extensions. This new method is then applied to Near-Infrared Transmission (NIT) spectra of single wheat kernels prior to multivariate calibration[2] for protein content, with the calibration model estimated by cross-validated Partial Least Squares Regression (PLSR)[3,4]. The most basic version of EISC, ISC, was originally called "Inverted Scatter Correction" (ISC)[5]. Martens *et al*.[1] explains the rationale behind the EISC method and its chemically based extensions, in relation to its heritage, the Multiplicative Signal Correction (MSC)[67] and the Extended MSC (EMSC)[8]. In the present study, the EISC method is extended with some general physical approximation parameters (wavelength dependency and curvatures), and compared to derivative-based pre-processing.

Today, near infrared (NIR) spectroscopy in combination with multivariate calibration has become the established method for protein determination in cereal breeding as well as for quality determination in the cereal industry, relieving the more than 100-year old, slow, chemical analysis invented at the Carlsberg Laboratories by the Danish chemist Johan G. Kjeldahl in 1883[9]. The advantages of using NIR spectroscopic methods for cereal quality are mainly the speed of the analysis and their non-invasive character, which is essential if seed fertility is the aim in breeding programmes. As an important spin-off, NIR methods provide possibilities for simultaneous determination of additional quality parameters such as moisture, starch and fibre content.

In low-cost / high-speed analysis of complex systems such as whole-wheat grain, the pattern of optical paths is very complex, and several physical phenomena may contribute to the apparent pattern of "light scatter". The information in NIR spectra usually result from both diffuse light scatter and chemically (vibrationally) absorbed light by the sample, and the NIT spectra of single seeds can be considered a worst case with large additive and multiplicative scatter effects due to differences in kernel size, structure and presentation angle. It is not uncommon to see more than 95% of the variance in NIR *log*(1/T) or *log*(1/R) data caused by uncontrolled light scattering variations, which usually will dominate the first latent variable in PCA (Principal Component Analysis) or PLSR modelling. In some cases this is desirable, when the

quality to be calibrated for is physical and related to light scattering, e.g. hardness variation of wheat kernels, or particle size variation in powders. However, in most cases light scattering creates selectivity and linearity problems for simple quality attributes related to chemical concentrations. In such cases it is imperative that scatter is isolated from the NIT spectra prior to calibration in order to provide a robust and accurate quantitative method.

The single seed protein system has been studied in depth by Delwiche[10] who found that an optimal data transformation prior to PLSR calibration was obtained by first calculating the second derivative spectra and then correcting them by MSC. The performance of this double transformation model is confirmed by this study[11], but such a complex pre-transformation naturally calls for the development of more general and powerful pre-transformations. In the present study it is demonstrated that a general form of EISC is able to provide a quantitative protein model with a precision equal to Delwiche's doubly pre-transformed model.

Theory

In its most basic "ISC" form, the EISC data transformation can correct a combination of additive and multiplicative interference effects in measured spectra, analogous to the original MSC method[6,7]. Both the MSC and the ISC/EISC adjust the input spectrum of each sample, $\mathbf{z}_i$ in a set of samples, i=1,2,..., towards a common reference spectrum, **m**, in order to separate possible physical effects from possible chemical absorption effects. The difference between the methods is that the ISC simply reverses regressor and regressand in each sample's regression model between $\mathbf{z}_i$ and **m**. Like the conventional MSC, the ISC ("basic EISC") pre-processing method estimates and isolates two presumably physical effects for each sample: an *additive* baseline offset effect and a *multiplicative* scaling effect. If the input information $\mathbf{z}_i$ represents absorbance ($A = log(I_o/I) = log(1/T)$) values, the additive baseline offset is intended to model an unknown, fixed amount of absorbance lost at every wavelength, e.g. due to light failing to reach the detector because of dispersion of light in the sample. Multiplicative scaling is intended to model an unknown amplification of the absorbance at every wavelength, e.g. due to a change in the effective optical path length because of light scattering effects in the sample.

In the original EISC paper[1] the basic version of EISC was extended with chemical information known *a priori* to represent absorbance spectra from interfering constituents. In the present paper the EISC is instead extended with physical information representing wavelength and polynomial extensions when compared to MSC.

Multiplicative Signal Correction

The multiplicative signal correction, originally named Multiplicative Scatter Correction, MSC, involves correcting each input spectrum $\mathbf{z}_i = [z_{i1}, z_{i2},..., z_{ik},..., z_{iK}]$ in a set of related samples i=1,2... towards an ideal spectrum **m** where the influence of physical scattering variations has been removed from the effects of chemical absorbance (K is the number of variables in the spectrum). The basic MSC consists of estimating two coefficients, a_i and b_i that ideally contain all the physical information in $\mathbf{z}_i$, based on the linear regression model

$$\mathbf{z}_i = a_i + b_i\mathbf{m} + \boldsymbol{\varepsilon}_i \quad (1)$$

where $\boldsymbol{\varepsilon}_i = [\varepsilon_1, \varepsilon_2,..., \varepsilon_k,..., \varepsilon_K]$ are the residuals that ideally contain all the chemically relevant information in $\mathbf{z}_i$, plus other unmodelled effects and random noise. Vector $\mathbf{m} = [m_1, m_2,..., m_k,..., m_K]$ is a common reference spectrum. After parameters a_i and b_i have been estimated, the corrected spectrum $\mathbf{z}_{i,corrected}$ for this sample is then generated by reversing equation 1, from the estimates of a_i and b_i, in an analogy to the univariate "reverse"[2] calibration:

$$\mathbf{z}_{i,corrected} = (\mathbf{z}_i - a_i) / b_i \quad (2)$$

These corrected spectra may be used as regressors in the subsequent mulivariate calibration modelling of the analyte y_i from $\mathbf{x}_i = \mathbf{z}_{i,corrected}$ over a set of samples, $y_i = f(\mathbf{x}_i)$, i=1,2,... .

The common reference spectrum **m** in equation 1 may, for example, be defined as the mean of a set of N spectra of calibration samples:

$$\mathbf{m} = \frac{\sum_{i=1}^{N} \mathbf{z}_i}{N} \quad (3)$$

This reference spectrum **m** from the spectra of the N calibration samples $\mathbf{z}_i$, i=1,2,...,N may also be applied to MSC of new spectra $\mathbf{z}_i$, i=1,2,3,... e.g. from future prediction samples; equations 1 and 2 are the same for both kinds of samples.

In each calibration or prediction sample i, the unknown additive and multiplicative MSC coefficients a_i and b_i in equation 1 may be estimated by ordinary least squares regression of $\mathbf{z}_i$ on **m**, minimising the sum of squared residuals in $\boldsymbol{\varepsilon}_i$.

$$[a_i \;\; b_i] = ([\mathbf{1}\;\mathbf{m}']'\;[\mathbf{1}\;\mathbf{m}'])^{-1}[\mathbf{1}\;\mathbf{m}']'\mathbf{z}_i' \qquad (4)$$

However, the process for estimating and correcting for scattering parameters a_i and b_i is only safe, if the effects of chemical variation between $\mathbf{z}_i$ and **m** can be ignored; otherwise, the coefficients a_i and b_i may be contaminated with information about, e.g., the analyte, which will then be partially lost in $\mathbf{z}_{i,corrected}$ (equation 2). If applied to pure baseline separated absorbance bands, MSC (and basic EISC) will remove all relevant chemical information, as concentration will have a simple multiplicative effect on the spectral band. For this reason it is good practice to test the scatter coefficients a_i and b_i for information about the analyte or quality to be calibrated for. If a_i and b_i are found to be informative, they may even be included as additional regressor variables in the subsequent multivariate calibration models.

The problem of mixing chemical and physical information in the MSC may alternatively be reduced by down-weighting wavelength regions that carry chemical information. However, in some applications, like NIT of single wheat grains in the 850-1050 nm range, it is difficult to find wavelength regions that are sufficiently informative about the light scattering, but which do not carry chemical information. A more elegant approach would be an MSC model which includes information about the spectra of the chemical constituents[1,2,8]. However, in some applications like the present one, the in situ constituent spectra are not known and difficult to measure.

Basic Extended Inverted Signal Correction

The basic form of the EISC, ISC, is similar to MSC, but it may be more flexible and easier to understand for spectroscopists using multivariate calibration modelling by, for instance, PLSR. MSC, like its extensions, is based on a "reverse"[8] correction in equation 2, compared to the model in equation 1. In contrast, the basic EISC, like its

extensions, uses a "forward"[8] model: The same direction of the relationship between spectrum $\mathbf{z}_i$ and reference spectrum **m** is kept, both in the model specification

$$\mathbf{m} = a_i + b_i\mathbf{z}_i + \boldsymbol{\varepsilon}_i \quad (5)$$

and in the final correction of the spectra

$$\mathbf{z}_{i,corrected} = a_i + b_i\,\mathbf{z}_i \quad (6)$$

Hence, instead of regressing $\mathbf{z}_i$ on **m** in the model (equation 1) and then reversing this model in the signal correction step (equation 2), the inversed MSC (ISC/EISC) regresses **m** on $\mathbf{z}_i$ and uses this "forward" model directly in the signal correction step 6.

The estimation of the parameters a_i and b_i may be done by ordinary least squares regression

$$[a_i \;\; b_i] = ([\mathbf{1}\;\mathbf{z}_i]'\,[\mathbf{1}\;\mathbf{z}_i])^{-1}[\mathbf{1}\;\mathbf{z}_i]'\,\mathbf{m} \quad (7)$$

Like in MSC, weighted least squares regression may be used instead, if certain wavelengths are to be eliminated because of too strong overlap between constituent spectra and light scattering effects.

The rationale behind this model is explained by Martens et al.[1]. The statistical difference between EISC and MSC in their basic form, discussed more theoretically by Helland et al.[5] is illustrated in Figure 1. In the plot of reference spectrum **m** vs. a sample's input spectrum $\mathbf{z}_i$ the residuals ε_{ik} are minimised horizontally in MSC (noise modelled on the individual spectra) and vertically in ISC/EISC (noise modelled on the average/reference spectrum).

General spectroscopic extensions of EISC

Just as the MSC can be extended into Extended Multiplicative Signal Correction (EMSC)[8], the basic EISC can be extended to accommodate various types of physical or chemical a priori knowledge.

In the present case, it is impossible to find wavelength ranges that distinguish the physical light scattering information from the chemical absorbance information. That must be expected to create problems for the MSC or basic EISC methods, but

EMSC as well as EISC extended with chemical constituent spectra might solve the problems. However, contrary to the case in Martens et al.[1], the present in situ chemical constituent spectra are not known. In the grain, water is probably bound to a greater or lesser extent to the protein, starch and cellulosis biopolymers, and the NIR in situ spectral contributions from the constituents may therefore be rather different from those of isolated constituents in a pure state.

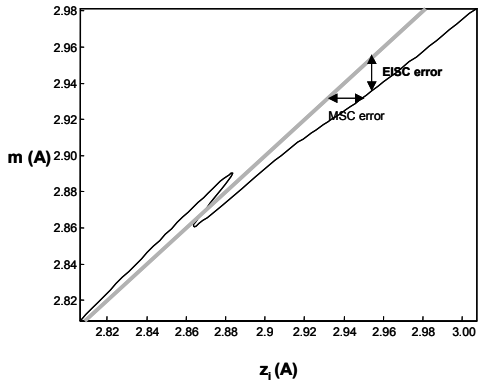

Figure 1. Plot of a wheat kernel sample's input spectrum $\mathbf{z}_i$ versus the mean ($\mathbf{m}$) spectrum of the NIT wavelength range (850-1050 nm). While the MSC models the error horizontally on the individual spectra the EISC models the error vertically on the average spectrum.

On the other hand, the heterogeneity of the intact wheat grains may cause rather complex optical phenomena that are difficult to model explicitly, but which may be approximated in more detail by polynomial extension of equation 5, e.g.

$$\mathbf{m} = a_i + b_i\mathbf{z}_i + c_i\mathbf{z}_i^2 + \boldsymbol{\varepsilon}_i \qquad (8)$$

Moreover, we expect the light scattering coefficient to have some dependency on the wave number. The exponent of this dependency depends on particle size, which is unknown. A first order approximation of this is to include the wavelength vector $\boldsymbol{\lambda}$, with polynomial terms, e.g. :

$$\mathbf{m} = a_i + b_i\,\mathbf{z}_i + c_i\,\mathbf{z}_i^2 + d_i\,\boldsymbol{\lambda} + e_i\,\boldsymbol{\lambda}^2 + \boldsymbol{\varepsilon}_i \qquad (9)$$

The parameters a_i, b_i, c_i, d_i, e_i may be estimated by some sort of linear regression that makes the residual elements in $\boldsymbol{\varepsilon}_i$ small, with one separate model for each sample i=1,2,... . To ensure statistical and numerical stability, regression on standardised regressors was used, with a small ridge parameter[1].

The primary purpose of the EISC extension terms $\mathbf{z}_i^2$, $\boldsymbol{\lambda}$ and $\boldsymbol{\lambda}^2$ in equation 9 is to improve the estimation of the basic interference effects, the Additive offset a_i (reflecting "baseline differences") and the Multiplicative slope b_i (reflecting "relative scatter coefficient differences"). But the extensions may also be used explicitly in the subsequent correction. Depending on whether or not one expects the corresponding coefficient estimates c_i, d_i and e_i to carry information about the analyte, one may choose whether or not to use them in the subsequent correction. If they are thought (or found) to pick up irrelevant complexity from the data, the subsequent calibration modelling may be simplified after the EISC correction

$$\mathbf{z}_{i,corrected} = a_i + b_i \mathbf{z}_i + c_i \mathbf{z}_i^2 + d_i \boldsymbol{\lambda} + e_i \boldsymbol{\lambda}^2 \qquad (10)$$

This is the EISC correction used in the present paper. Alternatively, if the extension coefficients d_i and e_i for the wavelength are expected to have picked up variation in the analyte that one does not want to lose, the effects $d_i \boldsymbol{\lambda}$ and $e_i \boldsymbol{\lambda}^2$ may be retained in the spectra by reducing the correction to

$$\mathbf{z}_{i,corrected} = a_i + b_i \mathbf{z}_i + c_i \mathbf{z}_i^2 \qquad (11)$$

Note that equation 8 is still a simple, linear (additive) model, but equation 9 works as a mixed additive/multiplicative pre-processing, in the sense that b_i is a multiplier that may reflect the relative scatter coefficient, while a_i may represent its additive baseline offset. In that sense the EISC correction (eq. 10 or 11) is analogous to the correction by MSC (eq. 2) and its extension[1].

Material and Methods

Samples: Wheat kernels (415) representing 43 different varieties or variety mixtures from two different locations in Denmark made up the calibration set, while wheat kernels (108) representing 11 different varieties from one location made up the test set[11]. All kernels were randomly chosen from bulk samples. The test samples were acquired with the calibration samples, but stored for about 2 additional months

before measurement in order to provide a check for temporal drift in the samples and instrumentation. The NIT single seed data set is made available on WWW (Pedersen, Pram Nielsen, Munck & Engelsen, NITSingleSeed, www.models.kvl.dk)

Spectra recordings: The single kernel transmittance spectra were collected on an Infratec 1255 Food and Feed Analyzer (Tecator AB, Höganäs, Sweden). Each kernel was placed in a single seed sample cassette, and transmittance spectra in the range 850-1050 nm were recorded. A tungsten lamp (50 W) and a diffraction grading were used to create monochromatic light. The light passed through the kernel reaching the silicon detector in a diffuse pattern. Spectra were recorded three times for each kernel and the average of the three spectra was used for the calibrations. The time required for scanning (single scan) 23 single kernels in the cassette was about 90 Sec.

Protein determination in single kernels: After the spectral recording of the intact wheat kernels each kernel was crushed in the Single Kernel Characterization System (SKCS 4100, Perten Instruments Inc., Reno, NV, USA) and the moisture content necessary for calculation of protein content in dry matter determined. Subsequently, single kernel nitrogen content was determined directly by a modified Kjeldahl method[12]. Nitrogen in single kernel grits was transformed into ammonium sulphate by digestion (410^{o}C for 1 hour) with 6 ml sulphuric acid (98%). The solution was then alkalised (25 ml 35% NaOH and 75 ml H_2O) and distilled into 25 ml boric acid (0.2%) with methyl red and bromcresol green indicator. The amount of resulting ammonia produced was determined by titration (0,0050 M HCl). The method is based on the assumptions that proteins contain 16 percent nitrogen and that non-protein nitrogen content can be neglected. The protein content is reported as 5.7 times the total nitrogen content for wheat kernels. This unusual calculation factor is due to the high nitrogen content of glutamine. Based on previous experience with samples of 30-40 mg wheat flour, the analytical error of the analyte was expected to have an absolute standard uncertainty of 0.16 % (percent protein content in dry matter).

Data analysis: Multivariate data analysis was carried out using The Unscrambler version 7.6 (www.camo.com), except for EISC calculations, which were programmed and carried out using MatLab version 6.1 (The Matworks, Inc., Natick, MA, USA). Conventional multivariate calibration models were developed from the

415 calibration samples using PLSR for protein content (**y**) from NIT spectra (**X**), after different types of spectral pre-transformation (MSC, basic EISC (eq. 6), EISC with physically extensions (eq. 10), second derivatives, and combinations of MSC and second derivatives). Optimal numbers of PLSR components (PCs), A_{Opt}, as well as apparent root mean square error of Y-prediction, RMSECV, were estimated by cross-validation within the calibration set. To ensure robust and representative segmentation in the cross-validation, the 415 calibration samples were sorted for increasing value of protein content (**y**), and then split systematically into 10 cross-validation segments. Performance of calibration models was validated by predicting the protein content in the 108 samples (validation set), yielding the root mean square error of Y-prediction, RMSEP.

Results and Discussion

Protein content: The statistics of the Kjeldahl protein determination of the two sample sets are listed in Table I.

Table I. Means and standard deviations (SD) of single kernel protein data in the calibration and test sets

Sample set	# of kernels	Mean Protein [%]	SD [%]	Min. [%]	Max. [%]
Calibration	415	10.0	1.56	6.8	15.2
Test	108	9.8	1.75	7.0	17.0

The protein concentration in the calibration set ranges from 6.8% to 15.2%, while the concentration in the test set ranges from 7.0% to 17.0%. As indicated by the standard deviations in Table I, relatively few kernels have extreme protein content; however, a certain degree of extrapolation is required for the PLSR calibration model to cover the protein range of the test set. The higher protein content in the test samples is probably the result of a certain loss of moisture during the additional storage period.

NIT spectra: The NIT spectra of the single wheat kernels presented in this study cover the spectral region from 850 nm to 1050 nm in 2 nm steps containing primarily the second overtones of O-H (carbohydrates and water) and N-H (protein) stretching vibrations and the third overtone of the C-H (fats) stretching vibration.

The fundamental O-H stretch for hydrogen-bonded systems is typically found between 3400 and 3300 cm^{-1} (IR), corresponding to 2940-3030 nm, which will ideally give second overtones in the NIR region 980-1010 nm. Secondary amides (proteins) give rise to a fundamental N-H stretching vibration located near 3300 cm^{-1} (IR), corresponding to an ideal second NIR overtone near 1010 nm. Aliphatic C-H stretching vibrations are located between 3000 and 2840 cm^{-1}, corresponding to 3333-3521 nm, which will ideally give rise to third overtones in the VIS/NIR region between 833 and 880 nm. This spectral region is thus of outmost importance to food-related samples, as most important functional components are represented. The electromagnetic radiation is relatively high in energy, yet still absolutely non-destructive. Moreover, the absorption of the second and third overtones is much lower than the fundamental and first overtone vibrations, enabling larger sample volumes to be measured, which is very important when measuring heterogeneous systems.

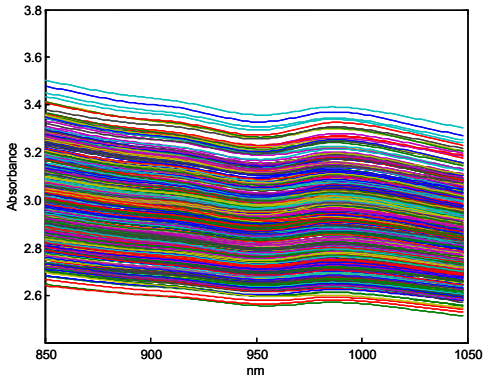

Figure 2. Raw NIT spectra (850-1050 nm) of the 415 wheat kernels from the calibration set

Figure 2 displays raw NIT absorbance spectra of the 415 samples in the calibration set. From the figure, large additive offset and multiplicative scaling effects are readily observed. These are probably due to dispersive loss of light and changes in optical path length, caused by variations in kernel size and texture as well as kernel orientation in the sample cassette. These observed differences in light lost due to

physical effects probably overshadow the absorbance changes due to concentration variations in the chemical constituent like starch, water and protein.

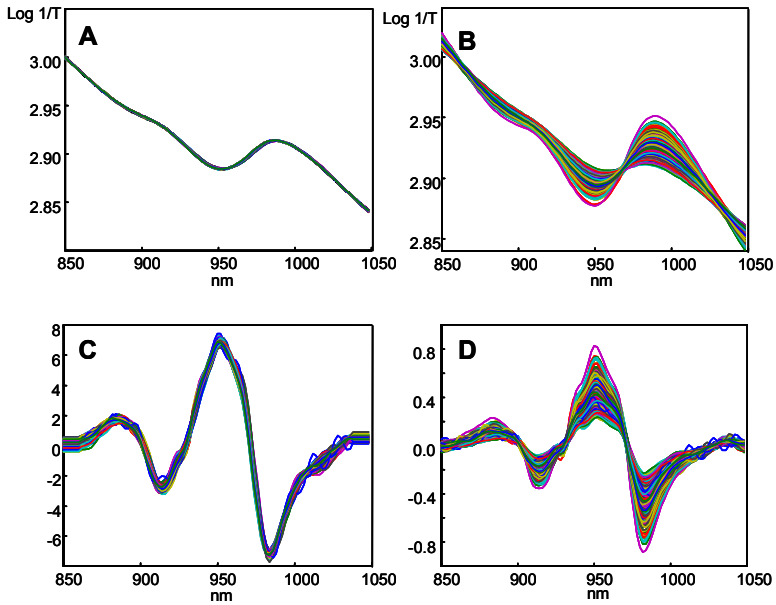

Figure 3. NIT spectra (850-1050 nm) of the 415 wheat kernels from the calibration set; (**A**) EISC transformed (eq. 10), (**B**) MSC transformed (eq. 2), (**C**) Second derivatives followed by MSC and (**D**) MSC followed by second derivatives.

Figure 3A displays the same NIT spectra after EISC pre-transformation according to equation 10. In comparison, Figure 3B shows MSC pre-transformed spectra (equation 6), Figure 3C shows second derivatives of the spectra followed by MSC and Figure 3D shows MSC-transformed spectra followed by second derivatives. Compared to the raw spectra in Figure 2, all the calibration samples appear almost identical after the EISC.

However, Figure 4A shows that after mean centring to remove average spectral pattern in the NIT data, the EISC pre-transformed spectra are quite different. Likewise, the mean-centred MSC pre-transformed spectra (4B), mean-centred second derivatives of the spectra followed by MSC (4C) and mean-centred MSC-transformed spectra followed by second derivatives (4D) show clear differences

between the samples. The question is whether these differences relate to variations in the protein content.

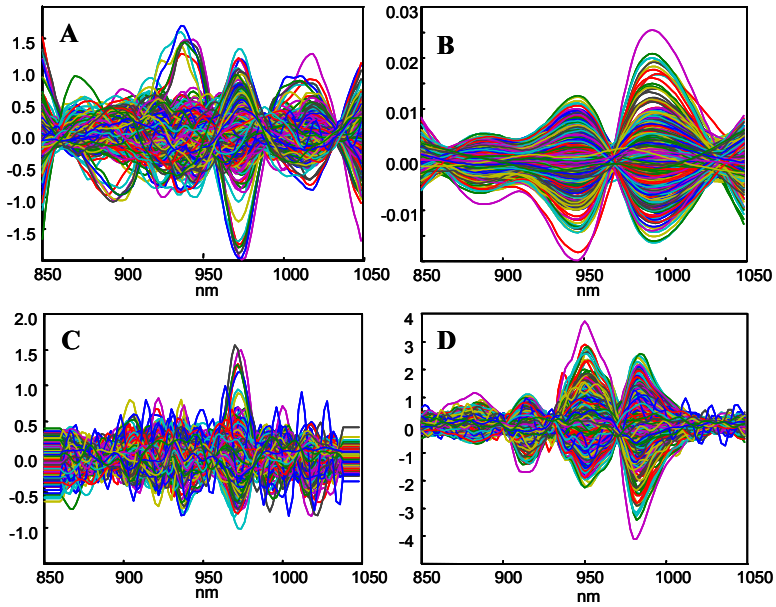

Figure 4. Mean-centred NIT spectra (850-1050 nm) of the kernels from the calibration set; (**A**) EISC transformed, (**B**) MSC transformed, (**C**) Second derivatives followed by MSC and (**D**) MSC followed by second derivatives.

Figure 5 compares the calibration models from the raw (dotted) spectra (Figure 2) and the EISC-transformed (solid) spectra (Figure 3A), both after mean centring. It shows the regression coefficient summary for the two models obtained at a conservative model rank (i.e. 9 and 6 PCs, 5A) and at the number of PCs that appeared to be near optimal (11 and 7 PCs, 5B), judging from the cross-validation. In general, the EISC has reduced the number of PCs required. Particularly in Figure 5B, the two predictors are relatively similar, although some differences can be observed. At the slightly lower rank in Figure 5A the models are even more distinct.

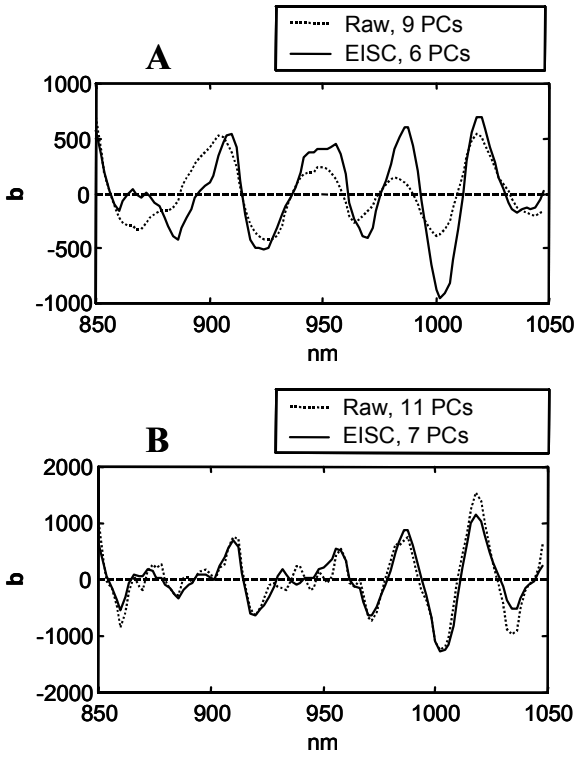

Figure 5. The regression coefficients for the calibration of raw input spectra (-----) for 9 PCs (A) and the optimal 11 PCs (B), and for the calibration of EISC-transformed spectra (——) for 6 PCs (A) and the optimal 7 PCs (B)

Figure 6 compares the apparent performance of the raw NIT-data and the EISC pre-transformation to various other pre-transformations for the single seed protein calibration models. The prediction errors (RMSECV) are plotted against the number of PLSR components. The figure reveals a significant reduction in the number of PLSR components needed, from the raw spectra to the pre-transformed spectra. Secondly and most interestingly, the plot reveals that only the EISC pre-transformation (solid) and the second derivative followed by MSC pre-transformation (densely dotted) are able to provide an optimal model according to the level of the prediction error in the calibration set.

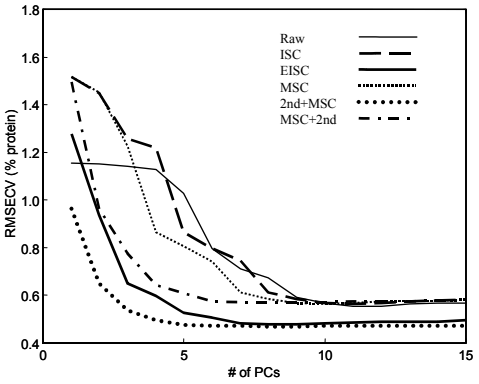

Figure 6. RMSECV versus PLSR components (PCs) for models based on different pre-transformed NIT spectra; Raw spectra, ISC-corrected spectra, EISC-corrected spectra, MSC corrected spectra, spectra transformed to the second derivative followed by MSC correction (2^{nd}+MSC) and MSC correction followed by second derivative (MSC+2nd)

The prediction error in the calibration set for the PLSR model based on EISC-transformed spectra was estimated by cross-validation to 0.49% protein (7 PC's). The corresponding prediction error for the PLSR model based on the second derivatives followed by MSC-transformed spectra was also estimated to 0.47% protein (5 PC's), while PLSR models based on raw, differentiated, basic EISC or MSC-treated spectra never reached a prediction error less than 0.55% protein, regardless of the number of PLSR components applied. The improved prediction performance agrees with the findings of Delwiche[10] who showed that the two-step procedure of using second derivatives followed by MSC gave a better single seed NIT model for prediction of protein content. The most significant result of this comparison is that the single-step EISC performs equally as well as the double transformation, but it is perhaps also noteworthy that basic EISC performs just as the sister algorithm MSC on the calibration set, but with a significantly better result on the test set.

The two-step method based on second derivatives followed by MSC corrected spectra performs considerably better than the opposite two-step method - MSC followed by second derivatives (Figure 6). This emphasises that the order of the applied pre-transformations is important and that conventional MSC is a poor model when the scatter is not linear[13]. In the MSC it is assumed that the scatter is linear

throughout the spectral range, since the whole spectrum is linearly adjusted by one slope and one offset. However, if the loss of light due to light scattering and other effects is not this simple, the MSC correction is not suitable and, consequently, a model based on MSC followed by the second derivatives will not be optimal. On the contrary, by using the second derivatives, it appears that the spectra are successfully corrected for local offsets and linear trend variations.

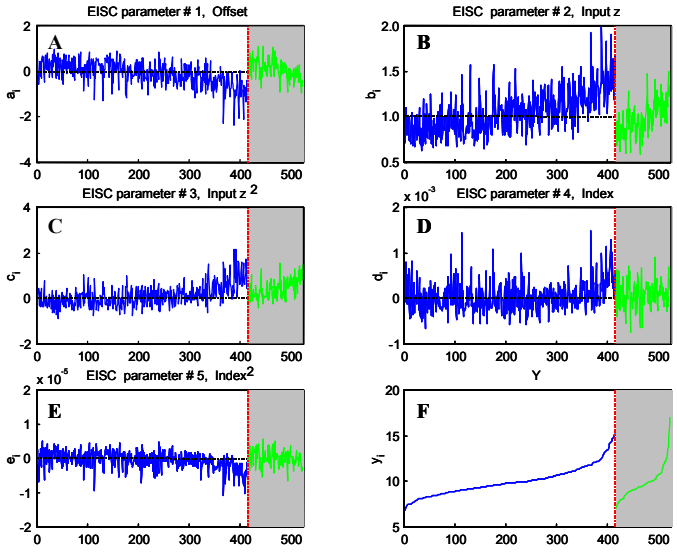

Figure 7. The estimated EISC parameters (eq. 9) plotted against sample # *i* for the 415 calibration samples (black) as well as for the 108 test samples (grey), sorted according to increasing protein content in the two data sets; EISC parameter # 1: a_i (additive/offset) (A), EISC parameter # 2: b_i (Multiplicative/relative scatter scaling of input spectrum) (B), EISC parameter # 3: c_i (effect of squared spectrum) (C), EISC parameter # 4: d_i (effect of wavelength) (D) and e_i (effect of squared wavelength) (E). The increasing protein content y_i within each of the two sample sets is shown in subplot F.

Validation: The test set (108 single wheat kernels representing 11 of the varieties included in the calibration, but stored for an additional 2 months) was measured on the same NIT instrument, analysed for protein content by the same method and used for testing the (long-term) stability of various calibration models. Figure 7 shows the EISC parameter estimates, the coefficients a_i (additive offset), b_i (multiplicative scaling), c_i (for squared spectrum), d_i (for wavelength) and e_i (for squared

wavelength). See equation 10, for the 415 calibration samples as well as for the 108 test samples. Figure 7F illustrates that the samples have been sorted for increasing protein content (**y**) within each of the two sample sets, for simpler cross-validation in the calibration set and simpler visual interpretation of the EISC parameters in both sets. The EISC parameters (7A-7E) show highly erratic variations, especially b_i (multiplicative scaling) and d_i (wavelength). But some systematic changes with the protein content may be observed in both sets, particularly at the highest protein levels (>11%). This is an indication that the EISC may have picked up and removed some variation related to the analyte. The cause and nature of this lost analyte information is unclear, but needs to be studied in more detail.

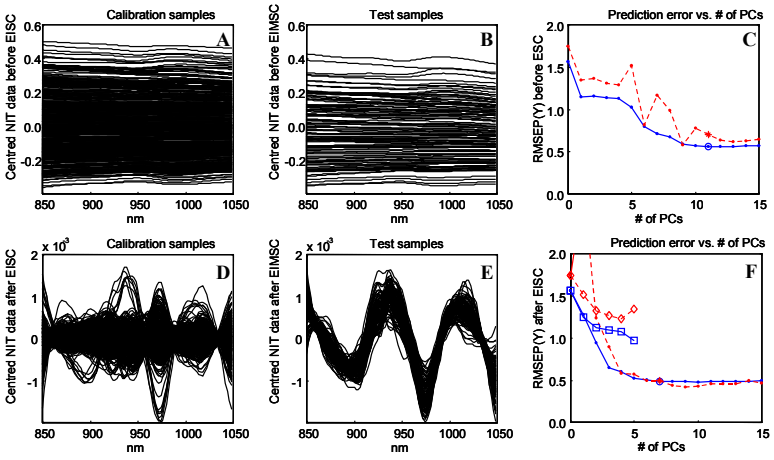

Figure 8. The mean-centred NIT spectra for (A) the calibration samples and(B) the test samples, and the EISC transformed mean-centred NIT spectra for (D) the calibration samples and (E) the test samples. Prediction error versus the number of PCs for the calibration samples (—) and the test samples (- - -) before EISC transformation (C) and after EISC transformation (F). The two short curves in subplot F shows the prediction errors calibrating only with the 5 EISC parameters (eq. 9), **X**= [a_i, b_i, c_i, d_i, e_i]: the calibration samples (—) and the test samples (- - -).

Figure 8 compares the calibration set and the test set, before and after the EISC. Spectroscopically, the mean-centred spectra of the test samples appear normal in the raw data (Figure 8B), compared to the calibration set (Figure 8A), while they show a very distinct pattern after the EISC (Figure 8E vs. Figure 8D). This is an indication

that all test samples deviate in the same systematic way from the calibration mean spectrum **m**. If this type of deviation is also present among the calibration samples, it may be modelled and corrected for in the calibration model; if not, the systematic deviations will cause grave errors in the predicted % protein in the test set. The peaks just below 950 nm in Figure 7D indicate that some of the calibration samples indeed display the same general pattern, but this needs to be verified in the prediction of protein.

Figures 8C and 8F compare the predictive performance before and after EISC. The long curves show the estimated error for protein content **y** predicted from the 100 NIT wavelength channels **X** for PLSR calibration models using between 0 and 15 PCs, for the cross-validated calibration set (RMSECV, solid) and the test set (RMSEP, dashed). When using the raw spectra in Figure 8C as **X**, the cross-validation shows that several of the first PCs (2,3,4,5) have little or no predictive relevance for the protein content; hence, they must reflect very strong covariance structures in the NIT spectra. More importantly, the predictive ability in the test set changes erratically with the increasing number of PCs; obviously, a wrong choice in the number of PCs to be used for prediction may cause very high prediction errors in the test set.

In contrast, when using the spectra after EISC in Figure 8F as **X**, the cross validation curve falls smoothly, as desired. The model is shown to require at least 4 PCs. The test set curve is very similar to the cross-validation curve after 4 PCs.

The two short curves in Figure 8F show the estimated prediction errors using instead the 5 EISC parameters $[a_i, b_i, c_i, d_i, e_i]$ (eq. 10) from the different samples as **X**, instead of the 100 wavelengths channels. Some predictive ability for the protein content (**y**) is evident in the cross-validation curve (squares). Hence, the EISC may have removed Y-relevant information. However, in the test set (diamonds) the predictive ability for **y** is not as good. Attempts (not shown here) at joining the NIT data with the EISC parameters as extra variables, $\mathbf{X}= [\mathbf{z}_{i,corrected}, a_i, b_i, c_i, d_i, e_i]$, using weighted least squares PLSR, gave a slight, but insignificant improvement in RMSECV (calibration set), but no improvement in RMSEP (test set). So it appears that the "physical" information apparently removed by the EISC in these data was not important or reliable for the prediction of chemical protein content: The errors

that they contribute to the calibration model is greater than the otherwise un-modelled Y-variation that they can remove.

The calibration and the test set results for all the tested pre-transformation methods are summarized in Table II in terms of the RMSECV (calibration set) and RMSEP (test set) read at the optimal number of PCs, and of the correlation coefficients based thereon. Compared to the untransformed raw data, the basic EISC/ISC did not affect the results very much. However, there is an improved correlation, both for the calibration set (from 0.93 to 0.95) and for the test set (0.96 to 0.98), after applying the EISC to the NIT spectra. The protein calibration model predicts the test kernels well throughout the protein range: The prediction error (RMSECV and RMSEP) ends as low as 0.49 % protein in a protein range of 7 to 17 %. This RMSE level approaches the sampling- and measurement error on the single seed protein determination (0.16 % determined for samples of 30-40mg flour), and the results demonstrate a very good and robust protein calibration on single wheat kernels.

Table II. Performance statistics of the PLSR models for single seed protein predictions using single seed NIT spectra from the calibration set (415 kernels) and the subsequent test set (108 kernels). CV is cross validation. RMSECV is the root mean square error of cross validation and RMSEP is the root mean error of prediction.

Pre-transformation	# of PLS Components	Correlation		Prediction error (% protein)	
		Cal. set (CV)	Test set	Cal. Set RMSECV	Test set RMSEP
Raw	11	0.93	0.96	0.55	0.70
ISC	9	0.93	0.95	0.58	0.69
EISC	7	0.95	0.98	0.49	0.49
MSC	9	0.93	0.95	0.57	0.78
2nd+MSC	5	0.95	0.98	0.47	0.48
MSC+2nd	7	0.92	0.93	0.60	0.66

The conclusion is that the new, extended ISC performs equally as well as the traditional MSC, perhaps even slightly less aggressive on the calibration set, resulting in an improved test set prediction. Both the EISC with general (physical) extensions and the two-step “second derivatives followed by MSC” in this data set can correct for spectra interferences that are not corrected by the more “classical” pre-transformations MSC or second derivatives. The EISC is particularly promising,

because it is more flexible and easier to understand than the "classical" MSC and two-step methods. In this study we have emphasized a general applicable version of the EISC, but its flexible approach allows simple implementation of system specific interferences such as known analytes[1]. In a future implementation we work on a version where the correction coefficients are constrained to be orthogonal to the reference value **y**, with the aim of optimising subsequent regression models with even less loss of analyte information.

Acknowledgements

The authors wish to thank Danish Slaughteries and the Ministry of Food, Agriculture and Fisheries for financial support through the project "Early post mortem measurement of WHC (water-holding capacity) and drip loss in fresh pork" and to the Ministry of Food, Agriculture and Fisheries through the Danish Cereal Network (B4). Gilda Kischinovsky is acknowledged for assistance with the manuscript.

Reference List

1. H. Martens, J. P. Nielsen, and S. B. Engelsen, *Anal. Chem.* submitted (2002).

2. H. Martens and T. Næs, *Multivariate Calibration*, Wiley, New York (1993).

3. S. Wold, H. Martens, and H. Wold. Lecture Notes in Mathematics. Ruhe, A. and Kågström, Eds., (Springer Verlag, Heidelberg. 1982), p. 286.

4. H. Martens and M. Martens, *Multivariate Analysis of Quality. An Introduction*, John Wiley and Sons Ltd., Chichester, UK (2001).

5. I. S. Helland, T. Næs, and T. Isaksson, *Chemom. Intell. Lab. Syst.* **29**, 233 (1995).

6. P. Geladi, D. McDougall, and H. Martens, *Appl. Spectrosc.* **39**, 491 (1985).

7. H. Martens, S. A. Jensen, and P. Geladi, "Multivariate linearity transformation for near-infrared reflectance spectro-metry" in *Symposium on Applied Statistics*. Christie, O. H. J., Ed. (Stokkand Forlag Publ. Nordic., Stavanger, Norway, N-4000, 1983) p. 208.

8. H. Martens and E. Stark, *Journal of Pharmaceutical and Biomedical Analysis* **9**, 625-635 (1991).

9. J. Kjeldahl, *Anal. Chem.* **22**, 366 (1883).

10. S. R. Delwiche, *Cereal Chemistry* **72**, 11-16 (1995).

11. J. P. Nielsen, D. K. Pedersen, and L. Munck, *Cereal Chemistry,* submitted (2002).

12. American Association of Cereal Chemists, AACC Method 46-12. Crude Protein - Kjeldahl Method, Boric Acid Modification. *Approved Methods of the American Association of Cereal Chemists* (1995).

13. H. Martens and T. Næs, Multivariate calibration by data compression. In *Near-Infrared Technology in the Agriculturel and Food Industries*, 2nd Edn, P. C. Williams and K. H. Norris, Eds., American Association of Cereal Chemists, St. Paul (2001).

Paper VI

Assessment of the depth of CO_2 stunning of slaughter pigs by visual and near infrared spectroscopy on blood

D.K. Pedersen, S. Holst and S.B. Engelsen

Abstract

The ability of VIS/NIR (visual/near infrared) spectroscopy to assess the depth of CO_2 stunning of slaughter pigs was evaluated. In this study VIS/NIR spectra of blood were acquired and the depth of CO_2 stunning assessed during sticking and debleeding of 145 slaughter pigs from three Danish slaughterhouses. Partial Least Squares Regression (PLSR) based on VIS/NIR spectra (700-1300 nm) to the assessed depth of stunning indicated that it is possible to predict the well stunned and the less well stunned slaughter pigs with an error around 1.4 for the total range of 0-7 (quantitative score of the depth of stunning assessments). Multivariate analysis of the VIS/NIR spectra further revealed a systematic pattern amongst the three slaughterhouses investigated related to the general quality of CO_2 stunning.

Keywords: NIR, near infrared, VIS, blood, preslaughter CO_2 stunning, chemometrics, PCA, PLSR

Introduction

Preslaughter stunning is used to ensure that animals do not suffer needlessly and that they are unconscious and insensible to the slaughter procedure. The stunning method should provide a duration of unconsciousness and insensibility which ensures that death from subsequent slaughter intervenes before recovery of sensibility. Today, concern for animal welfare is a major concern in meat production. Scientific interest in farm animal welfare has rapidly grown in recent years. This has largely been due to meat consumers' increasing demand that animals are produced, transported and slaughtered in a humane way (Appleby and Huges, 1997). In the European Union as well as in other countries, all animals destined for

meat consumption must be rendered insensible instantaneously and remain insensitive to pain until there is a complete loss of brain responsiveness due to exsanguinations (Council Directive 93/119/EC of 22 December 1993).

At all Danish slaughterhouses preslaughter CO_2 stunning of slaughter pigs is applied to induce a state of unconsciousness which prevents the ability to perceive pain. According to acceptable animal welfare it is important to expose slaughter pigs to CO_2 for long enough to ensure they remain unconscious during post-stun handling until death intervenes by debleeding.

Evaluation of insensibility from an effective CO_2 stunning of slaughter pigs can be done by a skilled veterinarian using the methods normally employed to judge the effect of a chemical anaesthetic used for surgical procedures (Blackmore and Newhook, 1983). Brain stem reflexes such as absence of rhythmic breathing and absence of corneal reflex have been used to assess the effectiveness of CO_2 stunning of slaughter pigs (Gregory, Moss and Leeson, 1987; Raj, 1999). These brain stem reflexes may, if positive, indicate that the animal is beginning to regain consciousness after the stun, but there is no indication of the speed at which the animal is recovering. One method to assess the depth of CO_2 stunning of slaughter pigs under slaughterhouse conditions is by using practical guidelines established by the Danish Meat Research Institute (Holst, 2001). The assessment is based on absence or presence of a number of reflexes characterizing the depth of stunning. To ensure that no slaughter pigs regain consciousness during post-stun handling and debleeding, the safe depth of anaesthesia at the time of sticking can be evaluated by the following criteria (Holst, 2001):

- No pig shows deep or regular respiration except for irregular abdominal gasping
- No pig shows excitation or kicking except for slow movements of legs
- No pig shows natural blinking of the eye
- Maximum 5% of the pigs have a corneal reflex

Using these criteria just before sticking not only takes into consideration animal welfare concerns, but also the safety of slaughterhouse workers during post-stun handling of pigs. Presence of corneal reflex at a high frequency, deep rhythmic breathing and excitation at the time of sticking may be indicative of an inadequate stunning. In order to comply with legislation on animal welfare and marked

requirements it may be necessary in the future to document adequate anaesthesia of pigs prior to slaughter. An objective on-line measurement technique for assessment of the depth of stunning would meet this requirement.

Inhalation of high-concentration CO_2 rapidly leads to dramatic changes in the partial pressure of CO_2 and O_2 and of pH in the blood (Martoft *et al.*, 2002). In that way, the depth of CO_2 stunning can thus be revealed by measurement of the blood.

The visual (VIS, 400-780 nm) and Near InfraRed (NIR, 780-2500 nm) regions of the electromagnetic spectrum contain absorption bands corresponding to overtones and combinations of fundamental vibrations mainly of the bonds C-H, O-H and N-H. NIR spectra of aqueous systems such as blood show strong, broad and overlapping bands. The position and intensity of the signals are dominated by the water vibrations but may vary according to secondary chemical composition. By the ability to rapidly and non-destructively analyse a wide range of chemical and physical properties of various samples, the NIR technique appears well suited for process control, particularly for on-line and at-line applications. NIR has been applied for a variety of quality attribute determinations in meat including determination of fat, moisture, protein and sodium chloride (Osborne, Fearn and Hindle, 1993). In blood, NIR has been applied for determination of haemoglobin content (Kuenstner, Norris and McCarthy, 1994; Vályi-Nagy, Kaffka, Jákó, Gönczöl and Domján, 1997), hematocrit level (Zhang, Soller, Kaur, Perras and van der Salm, 2000), lactate content in plasma (Lafrance, Lands, Hornby anf Burns, 2000), cholesterol in serum (Peuchant, Salles and Jensen, 1987), total protein in serum (van Toorenenbergen, Blijenberg and Leijnse, 1988) and total protein, albumin, globulin, triglycerides, cholesterol, urea, glucose, and lactate in serum (Hazen, Arnold and Small, 1998).

This study was based on observations made during an exploratory spectral investigation of early post mortem quality of porcine meat performed at a research slaughterhouse. Blood from slaughter pigs was measured with VIS/NIR spectroscopy (400-2500 nm) immediately after sticking. The spectra showed significant differences apparently related to the method of stunning. In Figure 1 three spectra are shown, one from a pig that was electrically stunned and two from pigs that were stunned by CO_2. By a process we call ‘interview validation’, in which spectral variation are sought explained by consulting the journal of the responsible

stunning expert, it was revealed that the two CO_2 stunned animals had behaved differently during inhalation of the CO_2 high atmosphere. One of the CO_2 stunned pigs was excited during stunning, while the other one just fell into sleep in the CO_2 chamber, the result being that the excited pig was heavily stunned and probably dead at the time of slaughter, while the sleepy pig was only mildly stunned. By simple inspection, the differences in the spectra appear between 400 nm and 1300 nm. The notch at 1100 nm is due to instrumental shift of detector. The spectrum of blood from the electrically stunned pig differs distinctively in shape from the spectra of the CO_2 stunned pigs, while the difference between the two CO_2 stunned pigs is expressed as intensity differences in certain parts of the spectra apparently related to deoxygenated haemoglobin peaking around 760 nm (Wray, Cope, Delpy, Wyatt and Reynolds, 1988; Baykut *et al.*, 2001).

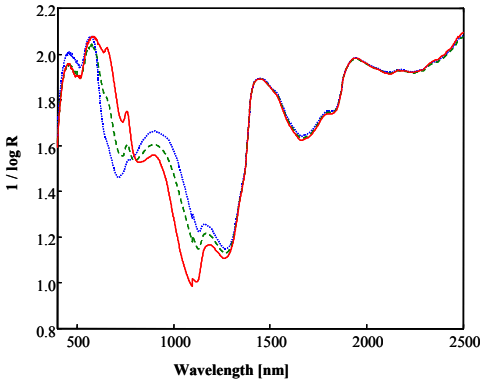

Figure 1. VIS/NIR spectra (400-2500 nm) of blood from three slaughter pigs measured immediately after sticking. One from an electrically stunned pig (·····) and two from CO_2 stunned pigs. One CO_2 stunned pig was excited during stunning (----), the other one just fell into sleep in the CO_2 chamber, the result being that the excited pig was heavily stunned and probably dead at the time of slaughter (—).

The objective of this investigation was to evaluate the ability of VIS/NIR spectroscopy to assess the depth of CO_2 stunning of slaughter pigs. The

spectroscopic data is evaluated by multivariate chemometric methods in an attempt to build a predictive model of the depth of CO_2 stunning.

Methods

The investigation was carried out at three commercial slaughterhouses (labelled S1, S2 and S3). They were chosen in the light of previous knowledge on the CO_2 stunning 'quality'. One slaughterhouse with a relatively high occurrence of corneal reflex (S1), one with a medium occurrence (S2) and one with a very low to no occurrence (S3) were chosen. During debleeding, blood was collected from each animal for subsequent spectroscopic measurement. The measurements were carried out over three consecutive days, with the same instrument and the same operator.

Physiological assessment of the depth of stunning

Depth of the CO_2 stunning was assessed immediately before and after sticking (time = 0 and 15 sec) in accordance with guidelines established by the Danish Meat Research Institute (Holst, 2001). In order to judge the depth of stunning, the absence or presence of the following reflexes was measured: corneal reflex, breathing and excitation. If breathing was present, it was assessed whether it was superficial gasping or deep and rhythmic. If excitation was present, it was assessed whether it was weak or strong. The assessments are shown in Table 1.

In order to obtain a quantitative graduation, a scoring system was developed. Absence of corneal reflex yields score 0, while presence of corneal reflex yields score 2. Absence of gasping yields score 0, while presence of superficial gasping yields score 1, and deep regular breathing yields score 2. Absence of excitation yields score 0, while presence of weak excitation yields score 2, and strong excitation yields score 4. The reason for the higher score is that presence of excitation is regarded as a stronger indication of insufficient stunning than corneal reflex and gasping breathing.

Besides the parameters of the actual assessed reflexes, three combined parameters were constructed. These combined parameters express the depth of CO_2 stunning at 0 sec and 15 sec and both times in one parameter. The constructed parameters are

called Respons0, Respons15 and ResponsTotal. The constructed parameters are produced by summing up the scores of the assessments of the three reflexes (corneal reflex, breathing and excitation) at 0 sec (Respons0), 15 sec (Respons15) and at 0 sec and 15 sec in combination (ResponsTotal) for each pig.

Table 1. The reflexes appearing during debleeding and the time of assessment for each parameter. The mean (Mean) and the standard deviation (SD) for each parameter assessed for the 145 pigs from the three slaughterhouses; S1 (45), S2 (49) and S3 (51).

Reflex	Time (sec)	Mean				SD			
		S1	S2	S3	All	S1	S2	S3	All
Corneal	0	1.64	0.90	0	0.81	0.77	1.01	0	0.99
Corneal	15	1.47	0.65	0	0.68	0.89	0.95	0	0.95
Breath	0	0.98	0.76	0	0.56	0.26	0.43	0	0.51
Breath	15	0.42	0.41	0	0.27	0.50	0.50	0	0.45
Excitation	0	1.56	0.53	0	0.66	1.03	0.89	0	1.00
Excitation	15	0.84	0.37	0	0.39	1.24	0.97	0	0.95
Cor 0 + Bre 0 + Exc 0	0	2.67	1.65	0	1.39	0.83	1.25	0	1.48
Cor 15 + Bre 15 + Exc 15	15	1.93	1.06	0	0.96	1.07	1.16	0	1.20
Cor 0 + Bre 0 + Exc 0 + Cor 15 + Bre 15 + Exc 15	0 + 15	4.60	2.71	0	2.34	1.62	1.96	0	2.38

VIS/NIR measurements

Blood. During debleeding 1-2 litres of blood from each animal was collected in a container. Immediately thereafter, a wash bottle (½ litre) containing 5 ml EDTA (10 %) anticoagulation was filled with the blood. A cuvette (thickness = 3 mm) for NIR-Systems 6500 spectrophotometer (FOSS NIRSystems, Inc., Silver Spring, Maryland, USA) with a Transport Module (NR-6511) was filled with the blood sample, and the reflectance spectra from 400 nm to 2500 nm were recorded. The average of 32 scans was used.

Single components. VIS/NIR spectra (400-2500 nm) of haemoglobin (Sigma H-4131), in the methaemoglobin form, was recorded on another NIR-Systems 6500 spectrophotometer (FOSS NIRSystems, Inc., Silver Spring, Maryland, USA) using a small ring cup and a Spinning Module (NR-6506). Water (distilled) was recorded by using a cuvette (thickness = 10 mm) and a Transport Module (NR-6511).

Chemometrics

A chemometric approach allows qualitative and especially quantitative information to be revealed from complex VIS/NIR spectra. Principal Components Analysis (PCA) (Wold, Esbensen, and Geladi, 1987) is a mathematical procedure applied to spectral data to generate eigenvectors, which are orthogonal and thus uncorrelated. The purpose of PCA is to express the main information contained in the initial variables (the spectra) in a lower number of variables, the so-called principal components, which describe the main variations in the data. The regression approach Partial Least Squares Regression (PLSR) (Martens and Næs, 1989) defines factors, which are linear combinations of the original spectral data. PLSR extracts a small number of factors carrying most of the variable information, and the reference variable to be predicted is used actively in determining these factors.

One of the main advantages of chemometric data analysis is the possibility of projecting multivariate data into few dimensions and visualizing the results through a graphic interface. Principal Component Analysis (PCA) (Wold *et al.*, 1987) and interval Principal Component Analysis (iPCA) (Nørgaard, 2002) were applied for gaining an overview of the spectroscopic VIS/NIR data. Predictions of the depth of stunning of slaughter pigs based on spectral information were performed be means of Partial Least Squares Regression (PLSR) (Martens *et al.*, 1989) and interval Partial Least Squares Regression (iPLSR) (Nørgaard, Saudland, Wagner, Nielsen, Munck and Engelsen, 2000). Full cross-validation (leave one out) was applied throughout this study and only validated results are presented. The multivariate data analysis was performed with the chemometric program The Unscrambler 7.6 (CAMO, Trondheim, Norway) and Matlab 6.1 (The Mathworks Inc., Natick, MA, USA).

Results and discussion

VIS/NIR spectra and assessments of the depth of stunning on 45 slaughter pigs from slaughterhouse S1 with assumed ‘relatively low’ stunning quality, on 49 slaughter pigs from slaughterhouse S2 with assumed ‘medium’ stunning quality and on 51

slaughter pigs from slaughterhouse S3 with assumed 'relatively high' stunning quality (in total 145 animals) were analysed using chemometric tools.

Assessments of the depth of stunning

The scores of the physiological assessment of the depth of CO_2 stunning are overviewed in Table 1. All the means of the assessed reflex parameters are relatively low (< 30 % of maximum). This is due to the complete lack of reflexes for the pigs from slaughterhouse S3 (51 pigs). The range of the score of the combined parameter ResponsTotal is 0-7. This parameter will be applied as the overall level of the stunning quality.

VIS/NIR spectra

The recorded spectra of pig blood were applied for development of prediction models of the depth of CO_2 stunning. The spectra (400-2500 nm) are shown in Figure 2.

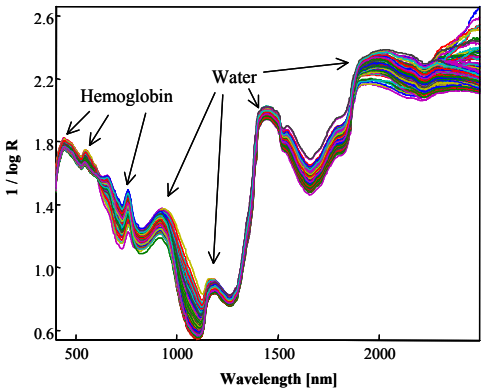

Figure 2. VIS/NIR spectra (400-2500 nm) of blood (145 slaughter pigs from three slaughterhouses) measured immediately after sticking.

Peaks were observed at 440 and 550 nm in the visual part of the spectra. These peaks are caused by the oxygenated form of haemoglobin (Kim, Kim, Kim and Yoon, 2001), as also seen in Figure 3A. The peak at 760 nm is related to

deoxygenated haemoglobin (Wray *et al.*, 1988; Baykut *et al.*, 2001). When the O_2 concentration in the blood is low, the 760 nm peak is more intense (Baykut *et al.*, 2001). The O-H stretching and bending from water causes the broad peaks at 970 nm (O-H stretch, second overtone), 1190 nm (O-H stretch and bend, combination tone), 1450 nm (O-H stretch, first overtone) and 1940 nm (O-H stretch and bend, combination tone), as seen in Figure 3B.

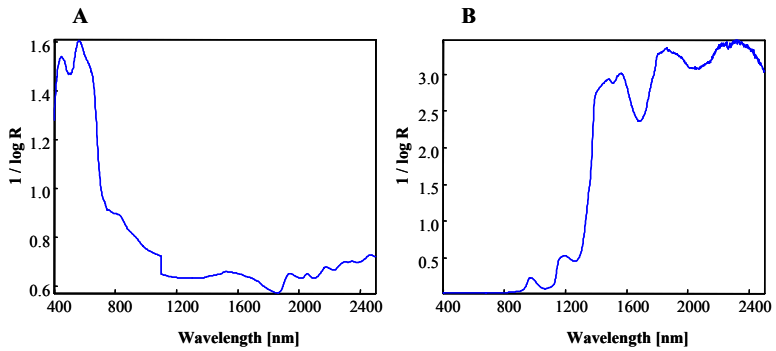

Figure 3. VIS/NIR spectra (400-2500 nm) of pure haemoglobin (methaemoglobin) (A) and water (B).

In Figure 4A the averages of the spectra of all samples from each of the three slaughterhouse S1 (·····), S2 (----) and S3 (—) are displayed. By simple inspection the average spectra from slaughterhouse S1 and S2 appear very similar, while the average spectrum from slaughterhouse S3 is markedly different. Even in the supposed CO_2 indicative peak at 760 nm (inserted enlargement in Fig. 4A), the average spectrum from S3 differs from that of S1 and S2. Slaughterhouse S1 was expected to show a relatively high occurrence of reflexes, while slaughterhouse S2 was expected to show a medium occurrence and slaughterhouse S3 was expected to show very low to no occurrence of reflexes. If the peak at 760 nm can be regarded as an indication of the CO_2 stunning, then slaughterhouse S3 appears to perform a more powerful CO_2 stunning than slaughterhouses S1 and S2. In addition to information on the effect of stunning, the spectra contain information on biological properties of the blood and environmental effects from the slaughterhouses.

However, it is beyond the scope of this study to investigate the influence of these factors, including the influence of breed upon the assessment of stunning.

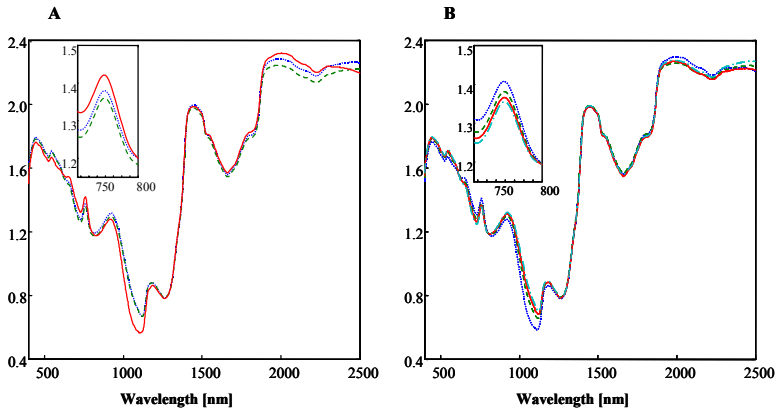

Figure 4. VIS/NIR spectra (400-2500 nm) of blood (145 slaughter pigs from three slaughterhouses) measured immediately after sticking. A) Averages of all samples from slaughterhouse S1 (·····), S2 (----) and S3 (—). B) Averages of all samples with ResponsTotal 0-1 (·····), 2-3(----), 4-5 (—) and 6-7 (-·-·-·).

In Figure 4B the averages of the spectra of all samples with ResponsTotal 0-1 (·····), 2-3 (----), 4-5 (—) and 6-7 (-·-·-·) are displayed. The average spectrum of samples with ResponsTotal 0-1 seems to differ most from the other average spectra, and indeed very much in the same way as the average spectrum from slaughterhouse S3 (Fig. 4A). The average spectrum of ResponsTotal 0-1 is dominated by samples from slaughterhouse S3, where all the assessed pigs lacked reflexes (ResponsTotal = 0). In the supposed CO_2 indicative peak at 760 nm (inserted enlargement), the average spectra are decreasing according to the assessed depth of stunning. The average spectrum of ResponsTotal 0-1 shows the highest intensity, while the average spectrum of ResponsTotal 6-7 shows the lowest intensity. This is in agreement with the expected relationship between the effect of stunning and the presence of reflexes. The variations seen in the spectra of different levels of reflexes in this investigation is considerably smaller than the extreme variations shown in Figure 1 between the different types of stunning of slaughter pigs.

Data overview

Principal Component Analysis (PCA) was applied to obtain an overview of the data to find possible trends and clusters. The spectral area between 400 nm and 2200 nm was applied in the analysis. The spectral area above 2200 nm was judged too noisy (see Fig. 2), for which reason it was kept out of the analysis. Score plots of the principal components showed weak trends tending to group the three slaughterhouses (plots not shown). In order to find parts of the spectra, which were especially good at separating the samples from each of the three slaughterhouses, iPCA was performed using subintervals of 200 nm of the spectra, 9 intervals in total. The score plot of principal component 2 versus principal component 3 of the PCA of a subinterval covering the spectral region 1200-1400 nm is shown in Figure 5A. The plot displays good separation of the samples from the slaughterhouses S1 (∇), S3 (O) and most of the samples from S2 (◊), while 16 samples from S2 (♦) are located with the samples from S1. Information from the experimental notes revealed that the S2 samples located with the S1 samples were all measured before a break in the measurements during the day, while all the separated S2 samples were measured after the break. There were no significant differences in the scorings of the evaluation of the depth of stunning for the animals assessed before the break and the animals assessed after the break. This indicates that environmental factors like temperature and humidity, which probably change during a day of slaughter, have considerable influence on the spectra.

By moving the spectral interval in question only 10 nm to apply the region 1190-1390 nm in a new PCA model, a new score plot of principal component 2 versus principal component 3 was produced (Fig. 5B). The plot displays reasonable groupings in the spectra from the three slaughterhouses, including the 16 samples from S2 measured before the break. This shows that the spectra contain information on stunning quality as well as on environmental effects of the surroundings. The environmental effects were not accurately monitored through this investigation, but it is a well-known fact that humidity and especially the temperature of the samples and surroundings influence spectroscopic measurements (Thygesen and Lundqvist, 2000; Wülfert, Kok and Smilde, 1998).

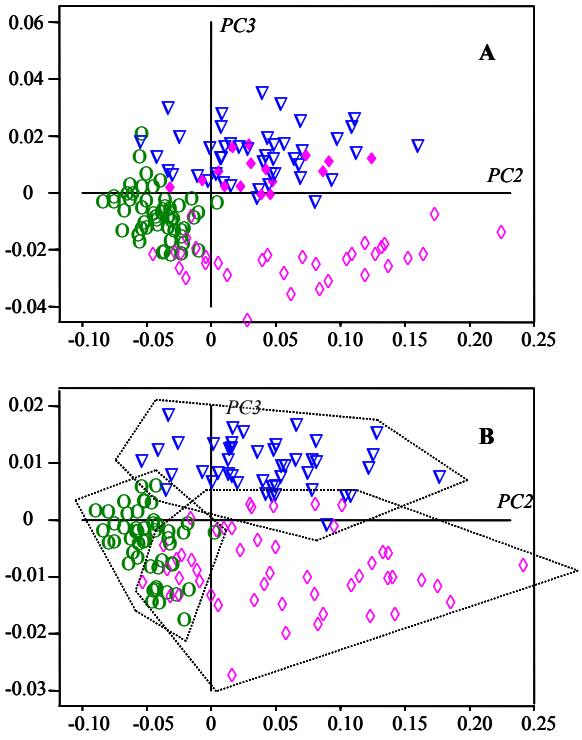

Figure 5. PCA on intervals of the NIR spectra, 1200-1400 nm (A) and 1190-1390 nm (B), of blood (145 slaughter pigs from three slaughterhouses; S1(∇), S2(◊) and S3(O)) measured immediately after sticking; Principal Component 2 (PC2) versus Principal Component 3 (PC3).

Regressions

The results of the physiological assessments of the depth of CO_2 stunning were used for the development of models for prediction of the depth of stunning by VIS/NIR spectra. The full spectral region between 400 nm and 2500 nm was applied for a preliminary modelling of ResponsTotal covering all the assessed reflexes. The correlation (r) for an 8-component model was 0.8 and the prediction error RMSECV was 1.5. This is a fairly good regression result, but the complex model applying many components might indicate that the model will be unstable for future predictions. A look at the regression coefficient (not shown) reveals noise problems in the spectral region 400-700 nm and to some degree in the region above 1300 nm.

Due to these noise problems and in the light of the information in Figure 1, which showed that the region up till 1300 nm displayed most information reflecting the differences in stunning quality, only the spectral region between 700 nm and 1300 nm was applied for further analysis.

PLSR models were performed on the VIS/NIR spectra (700-1300 nm) versus each of the 9 reflex parameters; Corneal reflex (time = 0 and 15 sec), Breathing (time = 0 and 15 sec), Excitation (0 and 15 sec) and Respons0, Respons15 and ResponsTotal. The data set applied for PLSR consisted of 145 samples. All PLSR models were validated by full cross validation, and the validated results are shown in Table 2. The PLSR results show relatively large prediction errors when predicting the individual reflex references, Corneal, Breath and Excitation, and in some cases proved impossible (Breath 15 and Excitation 15). Regressions based on individual slaughterhouses (S1 and S2) were especially difficult to fit. These difficulties are partly due to the low ranges of the scores of the individual reflexes. The summation of the reflex scores in the ResponsTotal is the most interesting parameter covering all the assessed responses. It shows a good correlation ($r = 0.80$) to the VIS/NIR spectra and the prediction error, root mean square error of cross validation, is 1.42 for the total range of scores of 0-7. This indicates that the objective VIS/NIR method is able to distinguish between the well stunned and the less well stunned pigs, while the method cannot be said to be reliable for an exact estimate of the depth of stunning. But further investigation using more pigs at different slaughterhouses is required in order to confirm whether the VIS/NIR spectroscopic method is a solution for a rapid and objective estimate of the depth of CO_2 stunning in slaughter pigs.

Spectral pre-transformations like second derivative or Multiplicative Signal Correction (MSC) often help to eliminate interferences and to simplify the multivariate model to yield a simpler and more robust model (Geladi, MacDougall and Martens, 1985). Several pre-transformations were tested on the present data set, but none seemed to improve the modelling performance significantly compared to application of the raw mean-centred spectra. In Table 2, the results of PLSR based on second derivative of the spectra and on MSC-corrected spectra are shown. The MSC was applied piecewise (600-800 nm and 800-1400 nm) in an attempt to compensate for the shift in the spectra around 800 nm, which is most easily seen in Figure 1.

Table 2. The reflexes appearing during debleeding and the range of score for each parameter. Number of components (PC), correlation coefficient (r) and prediction error (RMSECV) of PLSR models based on raw VIS/NIR spectra (700-1300 nm) of pig blood versus reflex references, and of PLSR models based on second derivative (2nd) and piecewise MSC (MSC)-corrected VIS/NIR spectra (700-1300 nm) of pig blood versus ResponsTotal for the 145 pigs from the three slaughterhouses; S1 (45), S2 (49) and S3 (51).

Parameter	Possible score	All		
		PC	r	RMSECV
Corneal 0	0-2	6	0.64	0.76
Corneal 15	0-2	1	0.61	0.75
Breath 0	0-2	6	0.75	0.34
Breath 15	0-2	-	-	-
Excitation 0	0-4	8	0.67	0.74
Excitation 15	0-4	-	-	-
Respons0	0-8	6	0.74	0.94
Respons15	0-8	1	0.67	0.88
ResponsTotal	0-16	7	0.80	1.42
2nd	0-16	4	0.83	1.32
MSC	0-16	6	0.78	1.50

The plot of the predicted ResponsTotal from the PLSR of NIR spectra (700-1300 nm) versus the measured ResponsTotal is displayed in Figure 6, where the samples are labelled according to slaughterhouse, demonstrating the heterogeneous distribution of samples from well-stunned pigs and less well stunned pigs in relation to slaughterhouse. According to the regression coefficient from this PLSR model (Fig. 7), especially the haemoglobin peak at 760 nm and the water peak at 1190 nm show relationships to the ResponsTotal parameter. The sharp feature at 1100 nm is an artefact due to instrumental detector shift. Predictions of the depth of stunning inside each individual slaughterhouse was not possible, which underlines the strong confounding effect in VIS/NIR between stunning quality and the environment of the slaughterhouses. For this reason, conclusions about the applicability of the VIS/NIR method applied on this data set should be taken with precaution.

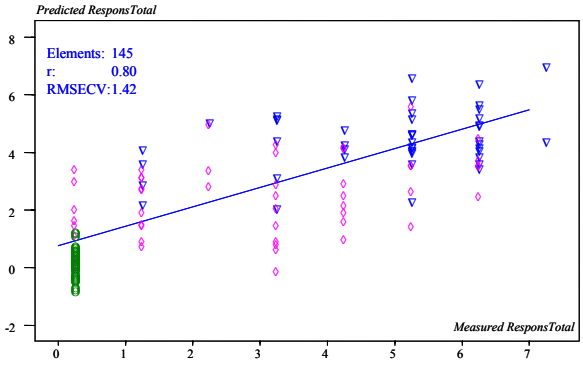

Figure 6. Predicted ResponsTotal of a PLSR based on VIS/NIR spectra (700-1300 nm) of blood (145 slaughter pigs from three slaughterhouses; S1(∇), S2(◊) and S3(O)) versus the assessed depth of CO_2 stunning (ResponsTotal).

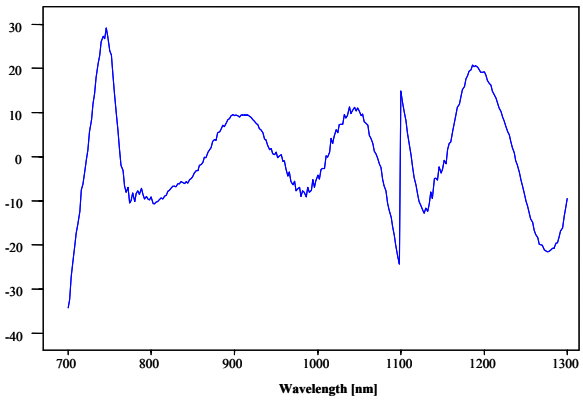

Figure 7. Regression coefficient for a 7 component PLSR of VIS/NIR spectra (700-1300 nm) of blood (145 slaughter pigs) versus the assessed depth of CO_2 stunning (ResponsTotal)

In order to find the most relevant parts of the spectra (700-1300 nm) interval PLSR (iPLSR) was applied. With the iPLSR algorithm PLSR is applied on subintervals of the spectra. The iPLSR predicting the ResponsTotal was validated by full cross validation and performed on 6 equally sized spectra intervals covering 100 nm each. The prediction errors (RMSECV) for the PLSR (5 components) of the 6 intervals are shown as bars in Figure 8. All intervals seem more or less to be able to predict the ResponsTotal with prediction errors between 1.4 and 1.5, almost as good but never

better than when full spectra are applied (RMSECV = 1.4). This holds for the individual slaughterhouses (S1 and S2) as well. This points out that the spectral information needed for prediction of the depth of stunning seems to be distributed over the whole region (700-1300 nm).

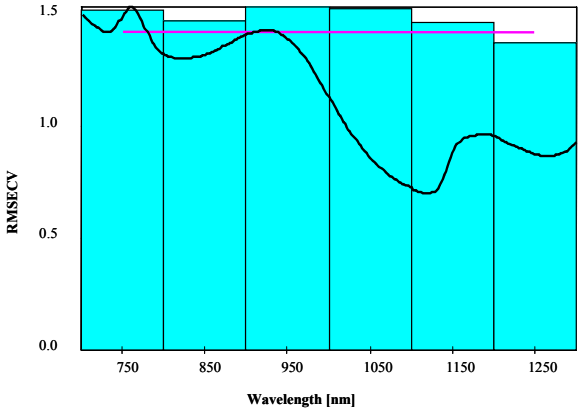

Figure 8. Prediction error (RMSECV), bars, for iPLSR models (5 components) of 6 subintervals of VIS/NIR spectra (700-1300 nm) of blood (145 slaughter pigs from three slaughterhouses; S1, S2 and S3) versus ResponsTotal (the depth of CO_2 stunning). The prediction error for the full spectrum PLSR model (6 components) is displayed as the horizontal line.

Another approach was to utilize information from the qualitative investigation of the blood spectra and use the assigned haemoglobin peak at 760 nm or the water bands at 940 nm or 1190 nm for predictions of the depth of stunning. PLSR of the spectral regions 725-800 nm (haemoglobin), 825-1100 nm (water) or 1100-1300 nm (water) yielded 5 or 6 component models with prediction errors of 1.4-1.5 and correlation coefficients of 0.8. These models equal the model using the full region of 700-1300 nm and the iPLSR models described above.

The applied reference measurements of this investigation must be considered to involve a certain amount of error. First, the quantitative graduation in the form of the scoring system was based on the estimated significance of the observed reflexes. Since these reference parameters were not natural characteristics of the samples, but

constructed and somewhat theoretical characteristics, this is considered to be a source of error. Even though the presence of the reflexes was assessed by a competent veterinarian, it was still based on subjective observations and for this reason provided a source of error. However, this systematic way of observation of reflexes in conjunction with stunning of slaughter pigs was developed as a monitoring tool for characterizing slaughterhouses and not meant for assessment of single animals. Nevertheless, this method was for the present considered the most promising method for rapid objective assessment of the depth of stunning.

Conclusions

In this study VIS/NIR spectra of blood were applied for multivariate predictions of the depth of CO_2 stunning assessed as presence or absence of reflexes during sticking and debleeding of 145 slaughter pigs from three slaughterhouses. Pigs from two of the slaughterhouses varied greatly according to presence of the assessed reflexes, while pigs from the third slaughterhouse all showed a total lack of reflexes because they were very deeply stunned or possibly dead during stunning.

The spectra contained gross features related to the water content of the samples and to the presence and level of oxygenated and deoxygenated haemoglobin. The spectra from the three slaughterhouses were quite similar in shape, but the spectra from the one slaughterhouse with no occurrence of reflexes differed from the spectra from the other two slaughterhouses in regions of the spectra that pointed in the direction of a more powerful CO_2 stunning. The spectra varied systematically according to different levels of the assessed reflexes and according to the CO_2 indicative peak at 760 nm. Besides the effect of stunning, the spectra also contain information on biological properties of the blood and environmental effects from the slaughterhouses. A more complete interpretation of the spectra in this study was regarded impossible as the relevant information concerning depth of stunning will be difficult to separate, especially because the level of influence of the interfering effects (biology and environment) was not assessed.

This study demonstrated that the spectra could be roughly classified according to slaughterhouse, and the spectral region of 1190-1390 nm was particularly capable of providing a good classification.

PLSR predictions by VIS/NIR spectra (700-1300 nm) of the assessed reflexes indicated that the objective instrumental method has the potential to detect the well stunned and the less well stunned pigs with prediction errors around 1.4 for the total range of 0-7 (quantitative scoring of the reflex assessments). The method might not be reliable for an exact estimate of the depth of stunning; but the VIS/NIR spectroscopic method still deserves further investigation for its potential as a rapid and objective estimate of the depth of CO_2 stunning in slaughter pigs. However, to establish a general useable method requires further investigations involving different slaughterhouses and control or measure of environmental and biological effects in order to compensate for them in the regressions.

Acknowledgements

The authors would like to thank Bo L. Jespersen for assistance during the slaughterhouse measurements. Danske Slagterier and the Ministry of Food, Agriculture and Fisheries are thanked for financial support through the project "Early post mortem measurement of WHC (water-holding capacity) and drip loss in fresh pork".

References

Appleby, M.C. & Huges B.O. (1997). Introduction. In M.C. Appleby, & B.O. Huges, *Animal Welfare* (pp. xi-xii). Wallingford: CAB International.

Baykut, D., Gebhard, M.M., Bölükoglu, H., Kadipasaoglu, K., Hennes, S., Frazier, O.H. & Krian, A. (2001). Online detection of myocardial ischemia by Near Infrared spectroscopy with a fiberoptic catheter. *Thoracic and Cardiovascular Surgeon*, 49, 162-166.

Blackmore, D.K. & Newhook, J.C. (1983). The assessment of insensibility in sheep, calves and pigs during slaughter. In G. Eikelenboom, *Stunning of Animals for Slaughter* (pp. 13-25). Dordrecht: Martinus Nijhoff Publishers.

Council Directive 93/119/EC of 22 December 1993. On the protection of animals at the time of slaughter or killing. *Official Journal of the European Communities*, No. L 340/21.

Geladi, P., MacDougall, D. & Martens, H. (1985). Linearization and scatter-correctiion for near-infrared reflectance spectra of meat. *Applied Spectroscopy*, 39, 491-500.

Gregory, N.G., Moss, B.W. & Leeson, R.H. (1987). An assessment of carbon dioxide stunning of pigs. *Veterinary Record*, 121, 517-518.

Hazen, K.H., Arnold, M.A. & Small, G.W. (1998). Measurement of glucose and other analytes in undiluted human serum with near-infrared transmission spectroscopy. *Analytica Chimica Acta*, 371, 255-267.

Holst, S. (2001). CO_2 stunning of pigs for slaughter. Practical guidelines for good animal welfare. In *Proceedings 47th International Congress of Meat Science and Technology* (pp. 48-54), August 26-31, Krakow, Poland.

Kim, Y.J., Kim, S., Kim, J.W. & Yoon, G. (2001). Data preprocessing and partial least squares regression analysis for reagentless determination of hemoglobin concentrations using conventional and total transmission spectroscopy. *Journal of Biomedical Optics*, 6, 177-182.

Kuenstner, J.T., Norris, K.H. & McCarthy, W.F. (1994). Measurement of hemoglobin in unlysed blood by near-infrared spectroscopy. *Applied Spectroscopy*, 48, 484-488.

Lafrance, D., Lands, L.C., Hornby, L. & Burns, D.H. (2000). Near-infrared spectroscopic measurement of lactate in human plasma. *Applied Spectroscopy* **54**: 300-304.

Martoft, L., Lomholt, L., Kolthoff, C., Rodriguez, B.E., Jensen, E.W., Jørgensen, P.F., Pedersen H.D. and Forslid A. (2002). Effects of CO2 anaesthesia on central nervous system activity in swine. *Laboratory Animals*, 36, 115-126.

Nørgaard, L. (2002). iPCA source code in Matlab available from www.models.kvl.dk

Nørgaard, L., Saudland, A., Wagner, J., Nielsen, J.P., Munck, L. & Engelsen, S.B. (2000). Interval partial least-squares regression (*i*PLS): A comparative chemometric study with an example from near-infrared spectroscopy. *Applied Spectroscopy*, 54, 413-419.

Osborne, B.G., Fearn, T. & Hindle, P.H. (1993). *Practical NIR spectroscopy with applications in food and beverage analysis*. Essex: Longman Scientific & Technical.

Peuchant, E., Salles, C. & Jensen, R. (1987). Determination of serum cholesterol by near-infrared reflectance spectrometry. *Analytical Chemistry*, 59, 1816-1819.

Raj, M. (1999). Behaviour of pigs exposed to mixtures of gases and the time required to stun and kill them: Welfare implications. *Veterinary Record*, 144, 165-168.

Thygesen, L.G. & Lundqvist, S.-O. (2000). NIR measurement of moisture content in wood under unstable temperature conditions. Part 1. Thermal effects in near infrared spectra of wood. Journal of Near Infrared Spectroscopy, 8, 183-189.

Vályi-Nagy, I., Kaffka, K.J., Jákó, J.M., Gönczöl, É. & Domján, G. (1997). Application of near infrared spectroscopy to the determinatin of haemoglobin. *Clinica Chimica Acta*, 264, 117-125.

van Toorenenbergen, A.W., Blijenberg, B.G. & Leijnse, B. (1988). Measurement of total serum protein by near-infrared reflectance spectroscopy. *Journal of Clinical Chemistry and Clinical Biochemistry*, 26, 209-211.

Wold, S., Esbensen, K. & Geladi, P. (1987). Principal Component Analysis. *Chemometrics and Intelligent Laboratory Systems*, 2, 37-52.

Wray, S., Cope, M., Delpy, D.T., Wyatt, J.S. & Reynolds, E.O.R. (1988). Characterization of the near infrared absorption spectra of cytochrome aa_3 and haemoglobin for the non-invasive monitoring of cerebral oxygenation. *Biochimica et Biophysica Acta*, 933, 184-192.

Wülfert, F., Kok, W.T. & Smilde, A.K. (1998). Influence of temperature on vibrational spectra and consequences for the predictive ability of multivariate models. *Analytical Chemistry*, 70, 1761-1767.

Zhang, S., Soller, B.R., Kaur, S., Perras, K. & van der Salm, T.J. (2000). Investigation of noninvasive *in vivo* blood hematocrit measurement using NIR reflectance spectroscopy and partial least-squares regression. *Applied Spectroscopy*, 54, 294-299.

Paper VII

Development of non-destructive screening methods for single kernel characterisation of wheat

J.P. Nielsen, D.K. Pedersen and L. Munck

Abstract

The development of non-destructive screening methods for single seed protein, vitreousness, density and hardness index has been studied for single kernels of European wheat. A single kernel procedure was applied involving, image analysis, Near Infrared Transmittance (NIT) spectroscopy, laboratory density determination, Single Kernel Characterization System (SKCS) and finally Kjeldahl protein determination on the crushed single kernels.

Single kernel NIT spectroscopy showed excellent ability to determine protein content, and some ability for determination of single kernel vitreousness. Non-destructive determination of single kernel density, either based on NIT spectroscopy or based on image analysis and kernel weight, needs to be further improved for practical use.

The use of SKCS hardness index as a true single kernel hardness reference in a NIT prediction model resulted in a poor predictability. However, by applying an averaging approach, in which single seed replicate measurements are mathematically simulated, a very good NIT prediction model was achieved. This suggests that the single seed NIT spectra contain hardness information, but that a single seed hardness method with higher accuracy is needed, in order to achieve a good NIT prediction model for single kernel hardness.

Key word index: Screening methods, single wheat kernels, protein content, vitreousness, hardness, density, non-destructive, multivariate data analysis

Introduction

The purpose of this paper is to apply a combinatory single seed approach involving several types of single seed measurements on the same individual seeds for an improved wheat characterisation, with special emphasis on single kernel protein, vitreousness, density and hardness.

Protein content, kernel density in terms of test weight, and kernel vitreousness by visual inspection are normally used in the miller's quality evaluation of wheat for milling. Protein content largely determines the end use quality, and premiums are often offered on high protein wheat. Test weight reflects kernel size and density, and should be above a certain level in order to secure a good flour yield. The vitreousness is used for evaluation of millability, even though the relationship between vitreousness and hardness is not straightforward. Vitreousness and/or hardness affects the milling processing of wheat, including tempering of the grains, flour yield and the end-use properties such as particle size distributions and the amount of damaged starch. Grain hardness is mainly determined by the degree of adhesion between the starch granules and the protein matrix, with a tight adhesion of the starch granules in the hard wheat and a weaker adhesion in soft wheat. To a certain extent this starch-protein matrix adhesion is genetically controlled involving the protein friabilin (Greenwell and Schofield, 1986) and is used for classification of wheat in hard and soft varieties. Even though wheat can be divided into genetically soft and hard, a substantial variation in texture is seen within the two classes, and the apparent vitreousness of the wheat is therefore used by the millers in their evaluation of millability. The genetically hard wheats are also generally high in protein content and flour from these wheats is usually used for bread making. The genetically soft wheats are generally low in protein and are usually used for cakes and biscuits.

Wheat quality evaluation has traditionally been performed on bulk samples, which implies that the characteristics of the individual kernels within the sample is lost, and thereby the opportunity to evaluate sample homogeneity. In seed sorting and grading by size, form and density for better and more uniform quality, the single seed is the functional unit to be investigated. Single seed quality analyses thus contribute to an increased understanding of the variation of the single seeds in a seed lot in order to evaluate sorting performance and thereby be able to optimise the choice of variety, grading conditions and end use.

New developments in instrumentation have made single kernel characterisation possible, and for some quality parameters rapid enough, to become a valuable tool for homogeneity evaluation in the cereal industry. The Single Kernel Characterization System (SKCS) 4100 (Perten Instruments Inc., Reno, NV, USA) is an example of such an instrument for rapid, albeit destructive, measurement of single kernel hardness, weight, diameter and moisture content (Martin et al., 1993). The single kernel measurements are normally conducted on 300 single kernels in a bulk sample in order to classify the sample into soft, hard or mixed wheat.

One of the limitations of destructive single seed analysis is that several readings on the same kernels are impossible. It therefore becomes difficult to differentiate between instrument variability and kernel-to-kernel variability. By using of non-destructive single seed analyses these problems could be circumvented. Additionally, fast and non-destructive single kernel quality analyses would be valuable tools in plant breeding for quality selection in early generations and for single kernel quality evaluation within the heads.

Near infrared spectroscopy on single kernels fulfils these requirements and the technique has been used for several single kernel applications. Near Infrared Transmittance (NIT) spectroscopy has been reported for determination of oil in maize (Orman and Schumann, 1992) and meadowfoam (Patrick and Jolliff, 1997), protein in wheat (Delwiche, 1995) and soybeans (Abe et al., 2000) and for wheat hardness (Delwiche, 1993). Near infrared reflectance spectroscopy has similarly been applied for wheat classification (Delwiche and Massie, 1996), for determination of single seed protein (Delwiche, 1998;Delwiche and Hruschka, 2000), for differentiation between vitreous and non-vitreous durum wheat kernels (Dowell, 2000) and for assessment of heat-damaged wheat kernels (Wang et al., 2001).

Image analysis is another method for fast non-destructive characterisation of kernels. Image analysis has been used for discrimination between kernels of different species (Chtioui et al., 1996), discrimination between wheat classes and varieties (Zayas et al., 1986) and, used in combination with physical measurements, for variety identification (Zayas et al., 1996). Berman et al. (1996) used the method for screening of flour milling yield in wheat breeding.

This investigation involves a combination of image analysis; NIT spectroscopy, hardness analysis (SKCS), protein analysis as well as a simple laboratory density analysis applied on single kernels of European wheats. The paper includes a survey of the use of non-destructive screening methods for prediction of single kernel protein, vitreousness, density and hardness.

Material and Methods

Samples:

Bulk samples of 43 different wheat cultivars or mixtures of cultivars from two different locations in Denmark (Jutland and Funen) were collected. These samples were screened on a 2.2 mm screen and the fractions above 2.2 mm were stored separately in plastic bags. Five kernels were randomly chosen from each of the 86 bulk samples to make up the calibration set (430 kernels in total). Another ten kernels from each of 11 of the 86 bulk samples (11 cultivars from Funen) were selected as the test set (110 kernels in total).

Single kernel measurements:

The single kernels were put through the following sequence of measuring steps. The kernels were analysed one by one with their identity retained during the whole measurement procedure.

GrainCheck:

Grain morphology was measured by digital image analysis using a GrainCheck^{TM} 310 instrument (FossTecator, Höganäs, Sweden). The instrument is specifically designed for automated purity analysis of grain samples based on the calculated morphological and color data. The instrument was used for single kernel characterisation by manually placing each kernel under the RGB camera from which the kernels were automatically imaged and from which several morphological and color characteristics were automatically assessed. In this investigation the following nine kernel characteristics were registered from the instrument and used in the data analysis: kernel width, kernel length, roundness, area, volume, red reflectance, green reflectance, blue reflectance, and total light reflectance.

NIT Spectra:

After the GrainCheck analysis, the single kernels were moved to an Infratec 1255 Food and Feed Analyzer (FossTecator, Höganäs, Sweden). Each kernel was placed in a single seed sample cassette with slots for 23 single kernels, and near infrared transmittance (NIT) spectra in the range 850-1050 nm were automatically recorded. A tungsten lamp (50 W) and a diffraction grating were used to create monochromatic light that passes through each of the kernels and reaches the silicon detector. Spectra were recorded three times on each kernel and the average of the three spectra was used. The position of the kernels in the sample cassette was manually changed between each of the three measurements. The time required for scanning (single scan) 23 single kernels in the cassette was about 90 s.

Single kernel density:

A laboratory single kernel density measurement was developed and applied to the 110 test set kernels prior to the SKCS analysis. The kernels were individually weighed to the nearest 0.1 mg using a Mettler/Toledo scale (Type AB204). The method for volume determination of the kernels is based on the principle of Archimedes. When immersing a wheat kernel in water, the weight of the displaced water divided by the density of the water equals the kernel volume. This measurement was carried out by using the equipment shown in Figure 1, which was specially designed for the purpose.

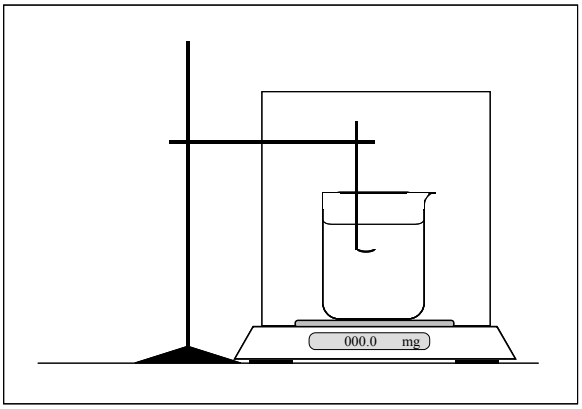

Figure 1. Illustration of the method for determination of single kernel volume

A beaker containing water at 20°C was placed on the Mettler/Toledo scale. A single kernel holder (modified sample spoon) was mounted on a rack outside the scale chamber (without touching the scale) with the kernel holder end immersed in the water. The scale was tared and the kernel (one at the time) was placed in the holder using a needle. The weight of the water displaced by the volume of the kernel was recorded immediately after, in order to avoid too much water uptake by the kernel. After the analysis, the kernels were dried for 16 hours at 30°C, and checked to have returned to the same weight as prior to the volume measurements.

Having determined the kernel volume from the weight of the displaced water, the single kernel density (in g/cm^3) is subsequently calculated by dividing the kernel weight (g) by the volume (cm^3). Prior to the single seed analyses the volume method was tested on 10 glass beads differing slightly in volume. The average deviation between the "real" volume and the volume determined using the method shown here was 0.0004 cm^3 for an average of 0.0142 cm^3, i.e. an error of 2.8 %.

Perten SKCS analysis:

The kernels were subsequently analysed using a Single Kernel Characterization System (SKCS) 4100 (Perten Instruments Inc., Reno, NV, USA). The SKCS measures a single kernel hardness index (HI), single kernel moisture content (%), single kernel diameter (mm) and single kernel weight (mg). A rotating vacuum wheel picks up the individual kernels and deposits them one at a time into a weighing boat. After the weighing, the kernel passes down an inclined crescent where the diameter is measured and the kernel is then crushed between the crescent and a toothed rotor. A load cell measures and records the crush force-time profile for each kernel and its hardness index is calculated. The hardness index values are based on algorithms that attempt to segregate wheats on a numeric scale on which hard wheats are forced toward an average value of 75, and soft wheats toward an average value of 25. The scale is similar to that used by the Near Infrared spectroscopy method (AACC 39-70A) for assessment of texture of bulk wheat samples. Normally, the SKCS analysis is carried out on a small bulk sample (300 kernels), but in this experiment the single kernels were fed one by one into the vacuum wheel in order to retain their identity. Thus, for each of the analysed kernels

we obtained four measurements, namely single kernel weight, moisture content, diameter and a hardness index.

The normal container for collecting the crushed kernels was removed, and the single kernel grist from the individual kernels was collected in a small container and used without further grinding for determination of single seed protein according to Kjeldahl.

Protein determination on single kernels:

Single kernel nitrogen content was finally determined directly by a modified Kjeldahl (1883) method according to the AACC Method 46-12. The nitrogen in single kernels was transformed into ammonium sulphate by digestion (410^{o}C for 1 hour) with 6 ml sulphuric acid (98%). The solution was then alkalized (25 ml 35% NaOH and 75 ml H_2O) and distilled into 25 ml boric acid (0.2%) with methyl red and bromcresol green indicator. The amount of ammonia produced was determined by titration (0,0050 M HCl). The protein content is reported as percent in dry matter calculated using the moisture content measured by the SKCS instrument.

Prior to the single kernel analysis, the method was tested on samples of 30-40 mg wheat flour. The analytical error in terms of standard deviation of 20 replications amounted to 0.16 % (percent protein content in dry matter).

GrainCheck data, NIT spectra, SKCS data and protein content were then recorded for each kernel, and single kernel density was determined on each of the kernels in the test set. One disadvantage of destructive single seed analysis is that if a measurement goes wrong, there is no sample left for a second analysis. Here, a few of the SKCS, protein and volume analyses went wrong and the following results and discussion are therefore based on a slightly reduced number of kernels. The calibration set consists of 415 out of the original 430 kernels, while the test set of 110 kernels gave valid data for 108 kernels, except for the density measurements where valid results were obtained for only 99 kernels.

The mean and range of all the 14 non-spectral single kernel characteristics for the calibration set kernels and the test set kernels are given in Table I.

Table I: Mean and range of the recorded single kernel characteristics.

Method	Parameter	Calibration set (n=415)			Test set (n=108)			Total (n=523)		
GrainCheck		Mean	Min	Max	Mean	Min	Max	Mean	Min	Max
	Width (mm)	3,7	2,3	5,0	3,8	2,5	4,7	3,7	2,3	5,0
	Length (mm)	6,2	5,0	7,5	6,1	5,0	7,2	6,2	5,0	7,5
	Roundness (AU)[a]	0,50	0,25	0,83	0,54	0,31	0,82	0,51	0,25	0,83
	Area (mm^2)	16,9	9,4	25,8	17,1	10,2	24,8	17,0	9,4	25,8
	Volumen (mm^3)	40,8	14,6	82,8	42,6	16,6	76,0	41,2	14,6	82,8
	Red	46,4	31,9	62,4	44,0	25,9	60,5	45,9	25,9	62,4
	Green	33,6	22,7	46,5	31,8	17,6	43,9	33,3	17,6	46,5
	Blue	24,4	17,4	34,0	23,2	14,8	31,1	24,1	14,8	34,0
	Intensity	34,8	24,2	47,4	33,0	19,5	44,9	34,4	19,5	47,4
SKCS										
	Weight (mg)	45,1	24,5	68,0	45,1	24,1	69,3	45,1	24,1	69,3
	Diameter (mm)	2,9	1,7	4,6	3,0	1,7	4,3	2,9	1,7	4,6
	Moisture (%)	11,9	10,4	13,3	11,0	10,0	11,6	11,7	10,0	13,3
	Hardness (HI)	44,0	-21,4	101,5	32,3	-28,8	82,2	41,6	-28,8	101,5
Reference										
	Protein (%DM)	10,0	6,8	15,2	9,8	7,0	17,0	10,0	6,8	17,0
	Density (g/cm^3)				1,16	0,99	1,25			

[a]: Values in the range of 0-1. A perfect circle has roundness=1, while a very narrow elongated object has roundness close to 0.

Data analysis:

Partial Least Squares Regressions (PLSR) (Martens H and Næs T, 1993) were performed using Unscrambler version 7.6 (CAMO A/S, Norway) in order to predict a given quality parameter (**y**) from fast acquirable **X** data. The multivariate prediction results are presented and discussed as correlation coefficients (r) between predicted and measured values, and prediction error in terms of Root Mean Square Error of Prediction (RMSEP) for true test set predictions, and Root Mean Square Error of Cross Validation (RMSECV) for cross-validated results. Relative predictions errors (RE) reported in percent are calculated by dividing the prediction errors (RMSECV or RMSEP) by the range (max. - min. value) of the given parameter.

Results and discussion

Single kernel protein:

The statistics of the Kjeldahl protein determination are listed in Table I. The single seed protein content ranges from 6.8% to 17.0% for all the analysed kernels, and thus in principle covers the whole range of end-use requirements from low-protein

wheat for crackers to high-protein wheat for bread making. In order to evaluate and utilise this single seed protein variation, a spectroscopic method would be appreciated. For this purpose, we use single seed NIT spectra recorded on each of the 523 wheat kernels in the spectral region 850-1050 nm. This region covers primarily the second overtones of O-H (carbohydrates and water), N-H (protein) stretching vibrations and the third overtone of the C-H (fat) stretching vibration. For most food related samples this spectral region is of importance as the most significant functional components are represented here.

The NIT spectra of the 523 single wheat kernels are shown in Figure 2 as both raw spectra (a) and scatter-corrected spectra (b), applying a combination of second derivative followed by Multiplicative Scatter Correction (MSC) (Geladi et al., 1985). This combined scatter correction has been discussed by de Noord (1994) and applied to single seed NIT spectra by Delwiche (1995). The raw spectra show large intensity offsets, as well as less clear multiplicative effects. These scatter effects are probably due to differences in kernel size and texture together with kernel orientation in the single seed cassette. With respect to the scatter-corrected spectra (Figure 2b), it is evident that the spectral scatter has been corrected for and thereby more spectral emphasis could be focused to represent chemical composition, e.g. the level of water, starch and protein content in the kernels.

Multivariate calibration techniques such as PLSR can to a certain extent compensate for different types of scatter effects by introducing more regression components. By doing this, however, a more complex and less robust model is built which furthermore can be difficult to interpret. When predicting chemical composition it is normally feasibly to eliminate the spectral scatter prior to the calibration. As discussed earlier, Delwiche (1995) has shown that the combination of second derivative of the single seed NIT spectra followed by MSC gave the best predictions. Our results are in agreement with this finding because raw spectra, first derivative spectra, second derivative, MSC or MSC followed by second derivative corrected spectra (data not shown) were less efficient in a prediction model. The issue of scatter in single seed NIT spectra, including suggestions for more general and powerful pre-transformations, is further investigated by Pedersen et al. (2002).

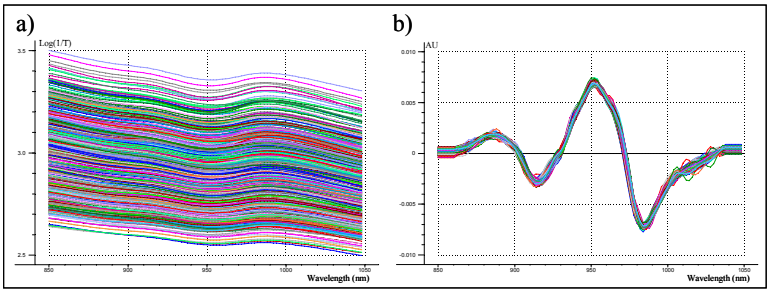

Figure 2. Single seed NIT spectra of 523 wheat kernels shown as (a) raw spectra and (b) corrected spectra using second derivative followed by MSC

A prediction model for protein content was developed based on single seed NIT spectra corrected by the second derivative followed by MSC. The cross-validated calibration model using 5 PLSR components including 415 single kernel spectra is shown in Figure 3a. This calibration model is used for independent prediction of the 108 test set kernels (Figure 3b).

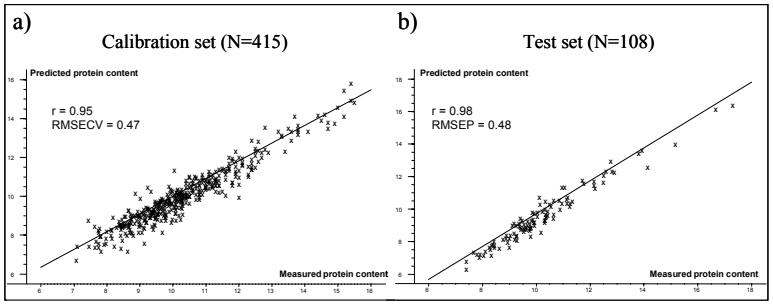

Figure 3. Predicted versus measured plot of a 5 PLSR component regression model for single seed protein using scatter-corrected NIT spectra for (a) the calibration set and (b) the subsequent prediction of the test set kernels

The relatively low number of PLSR components (5) as compared to other PLSR models in the near infrared range implies a simple and thus robust model. The prediction error (RMSEP) of 0.48 % protein when tested independently on 108 new kernels also indicates a good and robust calibration model. Our results for single

seed protein determination are comparable to results reported earlier using near infrared transmittance (850-1050 nm) (Delwiche, 1995) and near infrared reflectance (1100-2498 nm) (Delwiche, 1998).

Single kernel vitreousness:

Kernel vitreousness is normally determined by visual inspection, where vitreous kernels appear glassy and translucent whereas non-vitreous kernels appear starchy and opaque. Vitreouness is mainly controlled by nitrogen availability in the field as well as temperature during grain filling (Pomeranz and Williams, 1990). Vitreous kernels are often harder and have higher protein content. In this investigation we apply RGB image analysis by the GrainCheck instrument in order to provide a fast and objective analysis of vitreousness. As a pre-test to the current investigation we analysed vitreous and non-vitreous kernels (selected by visual inspection) on the image analyser (GrainCheck). Among the registered color data it was found that especially the red color reflectance differentiated well between vitreous and non-vitreous kernels. The red reflectance from GrainCheck was therefore selected as a quantitative measurement of vitreousness and denoted “GrainCheck vitreousness”. The more vitreous the kernel, the lower the red reflectance and vice versa, i.e. the higher the number, the more non-vitreous the kernel appears. A single seed correlation coefficient of -0.63 (Table II) between protein content and GrainCheck vitreousness shows that the kernels with high protein kernels tend to be more vitreous.

A PLSR model was computed using the raw NIT spectra for the prediction of GrainCheck vitreousness in order to see if the NIT spectra contained information regarding the GrainCheck vitreousness. A calibration model based on the 415 calibration kernels was developed using 6 PLSR components (not shown). The correlation coefficient between measured and predicted GrainCheck vitreousness was 0.76 with a prediction error of 4.5 AU. A subsequent test of this model on the 108 test kernels confirmed the calibration results (r=0.76, RMSEP=4.6 AU). Even though the NIT model is based on 6 PLSR components, most of the spectral NIT information is simply based on the level of absorbance. This can be concluded, since the first score from a Principal Component Analysis (not shown) on the raw NIT spectra (Figure 2), mainly representing differences in optical densities (offset)

correlates well (r=0.71) with GrainCheck vitreousness. The raw NIT spectra thus contain information regarding the GrainCheck vitreousness.

Table II. Correlations coefficients (r) between protein content, density, GrainCheck vitreousness and SKCS hardness

	Correlation coefficient (r)
Protein content vs. GrainCheck vitreousness[a]	(-) 0.63
Protein content vs. density[b]	0.65
Protein content vs. SKCS hardness[a]	0.38
SKCS hardness vs. GrainCheck vitreousness[a]	(-) 0.55
SKCS hardness vs. density[b]	0.34
Vitreousness vs. density[b]	(-) 0.53

[a]: N = 523 kernels

[b]: N = 99 kernels

Single kernel density:

Kernel density is an important parameter in the milling industry, which is normally determined on bulk samples as test weight. The test weight measurement is greatly influenced by kernel packing, kernel size and kernel density, without differentiation between those factors. Utilising differences in kernel density by grading for a better and more uniform quality on for example gravity tables, the link between single kernel density and other single kernel quality parameters is essential, in order to predict if a given sample is worthwhile sorting for density. For instance, there should be a link between single kernel density and single kernel protein in order to be able to sort for higher protein content by indirectly sorting for density.

The single kernel density in the test set of 99 kernels ranges from 0.99 g/cm^3 to 1.25 g/cm^3. In this material of European wheats, a correlation coefficient of 0.65 (Table II) between protein content and density and a correlation coefficient of -0.53 between GrainCheck vitreousness and density was seen (Table II). A single seed correlation coefficient of 0.65 between protein and density would probably be too low to be able to sort for protein by use of density grading on a gravity table.

The "Archimedes" procedure developed and used for single seed volume analysis in this investigation is rather tedious and it was of interest to investigate whether the much more rapidly acquirable NIT or GrainCheck data could be used for good volume and density determinations. The GrainCheck provides a calculated value on kernel volume based on a 2D-image. Densities derived from these calculated volumes gave, however, a poor correlation (r=0.07) to the real densities based on "Archimedes". This low correlation is most likely due to the approximation of a 3D-volume based on a 2D-image, which even if it gives a correlation coefficient of 0.9 to the "real" volume (Archimedes) is not sufficiently accurate to provide the basis for an accurate measurement of single kernel density.

A second approach, in which the nine GrainCheck variables (see Table I) plus the kernel weight were used as **X** in a PLSR model, gave a good prediction of the single kernel volume (Figure 4a).

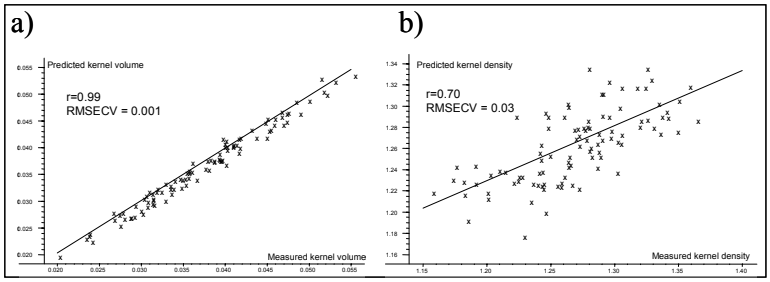

Figure 4. a) Predicted versus measured plot of a PLSR model for kernel volume using the nine GrainCheck variables plus single kernel weight. b) Predicted versus measured plot of a PLSR model for kernel density using the nine GrainCheck variables plus single kernel weight

This combination of image analysis data with kernel weight gives an excellent, rapidly acquirable estimate of the single kernel volume (r=0.99, RMSECV=0.001cm^3) using full cross-validation (N=99). The subsequent calculation of the single kernel density based on this predicted volume provides a considerably better estimate of kernel density, but still only a correlation coefficient of 0.68, as compared to the 0.07 above, with a prediction error of 0.04 g/cm^3 (plot not shown).

Thirdly, by directly using the nine GrainCheck variables plus the kernel weight for PLSR prediction of density, the results can be improved slightly, giving r=0.70 and a lower prediction error (RMSECV=0.03 g/cm^3) (Figure 4b).

In a final approach, it was investigated whether the NIT spectra contained information, which could be used for prediction of single kernel density. For a PLSR model using the raw NIT spectra for the prediction of the kernel density, the correlation between measured and predicted density gave 0.63 with a cross-validated prediction error of 0.035 g/cm^3. An attempt to combine GrainCheck and NIT data for an improved prediction of kernel density was not successful.

Single kernel hardness:

We have now provided data on the single kernel basis for protein content, kernel density and apparent vitreousness, the tools normally used by the miller for wheat quality evaluation. Hardness is also used for classification of wheats and its quality in relation to different end uses. It was of interest to investigate to what extent hardness added any further information to the structural characterisation of wheat in addition to kernel vitreousness and density. Hardness determination of wheat is normally conducted on a bulk sample by several different methods such as grinding-sieving (Particle Size Index), energy required for milling, or NIR (scattering) determination on ground material. None of these methods are easily applicable to single kernels. SKCS, however, offers a possibility to measure single kernel hardness index (HI).

In this investigation each kernel was fed separately into the SKCS in order to retain its identity and thereby explore the link between SKCS HI and other single kernel quality parameters. The range in SKCS HI for the analysed kernels is shown in Table I. The 108 test set kernels are considerably softer (mean HI=32.3) than the calibration kernels (mean HI=44.0). Figure 5 shows a scatter plot of single seed SKCS HI versus a) the protein content and b) the GrainCheck vitreousness. A low correlation (r=0.38) between protein content and SKCS HI indicates that the SKCS HI is nearly independent of the kernel protein content in this wheat material. This is surprising, as it is often assumed that high protein wheat kernels tend to be harder. The low correlation between single kernel Kjeldahl protein content and SKCS hardness might be explained by the fact that the kernels originate from a range of

genotypes, and that the link between seed protein and seed hardness is seen in some genotypes but not in others. The low number of kernels (10) within each variety in this experiment, however, does not allow for investigation of the correlations within each of the varieties.

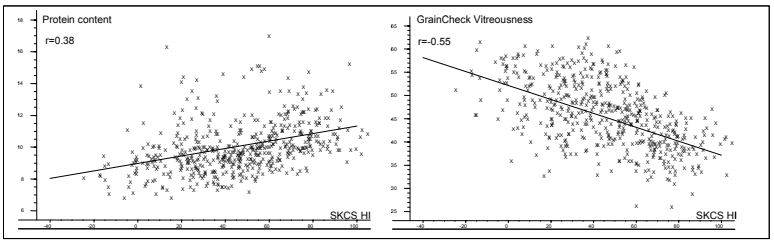

Figure 5. Scatter plots of (a) single seed (N=523) SKCS hardness versus protein content and (b) single seed SKCS hardness versus GrainCheck vitreousness

A higher, yet still low, correlation (r=-0.55) is seen between the GrainCheck vitreousness and the SKCS HI (Figure 5b). Table II summarises the correlations between protein content, density, GrainCheck vitreousness and SKCS HI. Only a small portion of the SKCS HI information seems to be explained in protein content, vitreousness or density as seen by the relatively low correlations. This suggests that the SKCS single kernel HI provides additional information not included in the traditional wheat evaluation tools.

In bulk, NIT has been successfully applied for prediction of texture in wheat. Williams (1991) concluded that a bulk NIT measurement was capable of predicting whole-wheat kernel texture with precision equal to that of the Particle Size Index (PSI) method and slightly better than the NIR method. Delwiche (1993) reported on the use of single kernel NIT measurements for hardness determination. When calibrating single seed NIT spectra against bulk hardness data, he found that NIT spectra of single seeds had some ability to determine wheat hardness.

Here we attempt to develop a PLSR model between single seed NIT spectra and true single seed hardness data, namely the SKCS hardness index. In general, we achieve better prediction models for kernel hardness using the raw NIT spectra compared to

scatter corrected spectra, which agrees with the findings of Delwiche (1993). Therefore, when attempting to predict the SKCS hardness it is important to utilise the scatter of the NIT spectra. This is thus an example of a case, where scatter correction should not be applied, unlike the protein models discussed earlier. A prediction model (6 PLSR components) for SKCS HI based on the raw single seed NIT spectra using segmented cross validation was performed on the calibration kernels. A reasonable calibration is achieved (r=0.74, RMSECV=17.6 HI) as shown in Figure 6a. This calibration was subsequently used for HI prediction of 107 of the original 108 test set kernels (Figure 6b). A low correlation coefficient of 0.59 and a high prediction error of 20.2 HI was achieved. This prediction error corresponds to 20% of the hardness range and thus limits the practical use. In Figure 6a and 6b the samples are labelled according to the hardness groups, where "A" is soft (HI<33), "B" is semi-soft (33<HI<46), "C" is semi-hard (46<HI<59) and "D" is hard (HI>59). It is apparent that the soft kernels (denoted “A”) give a more scattered picture in the plots, which means that the hardness index of these kernels are more difficult to predict. However, an exclusion of the soft “A” kernels did not improve the results.

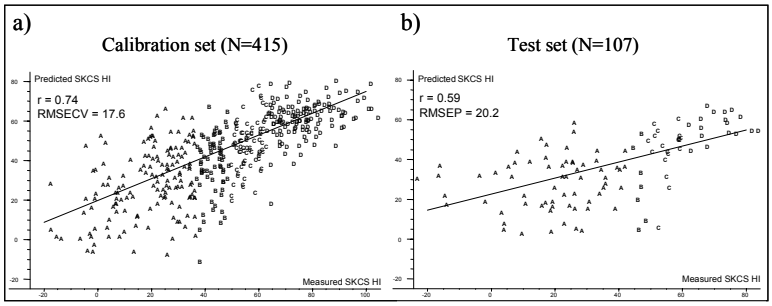

Figure 6. Predicted versus measured plot of a 6 PLSR component regression model for single seed SKCS hardness using (a) the raw NIT spectra for the calibration set and (b) the subsequent prediction of the test set kernels

Various aspects have been considered when interpreting the reason for the relatively poor NIT prediction of SKCS HI we achieve in this investigation. First, there might not be a link between single seed NIT spectra and single seed kernel hardness, but, as mentioned above, earlier reports have demonstrated the use of NIT spectroscopy

on whole-wheat kernels for hardness determination. Secondly, irrelevant noise in the NIT spectra (**X**) and the SKCS hardness data (**y**) might impair the model. Our single seed NIT spectra are averages of three spectra recorded on each kernel. As shown earlier, these spectra correlate very well with kernel protein, so the quality of the NIT spectra seems to be satisfactory. On the other hand, the single seed HI, as determined by the SKCS, might be too inaccurate and thereby problematic as y-values in a NIT prediction model. Since the SKCS HI measurement is destructive, multiple HI readings on the same kernel are not possible and an average of replicate readings is thereby impossible to obtain. This essential condition also makes it difficult to quantify the uncertainty of the instrument measurement.

One possible way to investigate this problem of uncertainty is to mathematically simulate replicate measurements by averaging across single kernels that are nearly identical.

First, we have applied such an averaging approach for the NIT model to protein content where we are certain of both the NIT spectra and the Kjeldahl protein content determinations. Since this method requires a great number of samples, we use all the 523 analysed kernels. The NIT spectra and corresponding protein content values are sorted according to protein content. As a start, a PLSR model is developed on the basis of all the 523 calibration kernels. Then, the sorted data are averaged across two kernels. Since the kernel data are sorted according to protein content, the two-kernel average is an average, which might be taken as an average of two duplicated analyses on one kernel. A subsequent PLSR model is then developed for the 262 averaged data objects (averaged kernels). This procedure is repeated another 4 times in which PLSR models are developed averaging across 1 (N=523), 2 (N=262), 4 (N=131), 8 (N=66), 16 (N=33) and 32 (N=17) kernels, respectively. For each model the percent of non-explained variation of the total variation is calculated. The trend of non-explained variation of the protein data for the different PLSR models can then be evaluated (Figure 7, dotted line). In an ideal situation i.e. with no noise in the NIT spectra and with determinations of Kjeldahl protein content without any errors, together with a perfect description of the protein content by the NIT spectra, a horizontal line at an ordinate value of 0 would have appeared. In a situation in which we only have model error, i.e. not perfect description of the protein content by the NIT spectra, but still with no noise in the NIT spectra and Kjeldahl protein content measurements, we would expect a horizontal line at a

certain level above an ordinate value of 0. The decrease in non-explained variation when averaging (moving from left to right in the plot) represents the noise and errors in the NIT spectra and in the Kjeldahl protein content determinations, reaching a horizontal level representing only model error as mentioned above. As seen from the dotted line, approximately 13% of the protein data variation is not explained by the NIT PLSR model using all kernel data (original single kernel data), but already after averaging over 4 kernels (2^2), a nearly horizontal line is appearing at approximately 4% non-explained variation. This means that after 4 simulated replicates, nearly all data noise and errors have been eliminated.

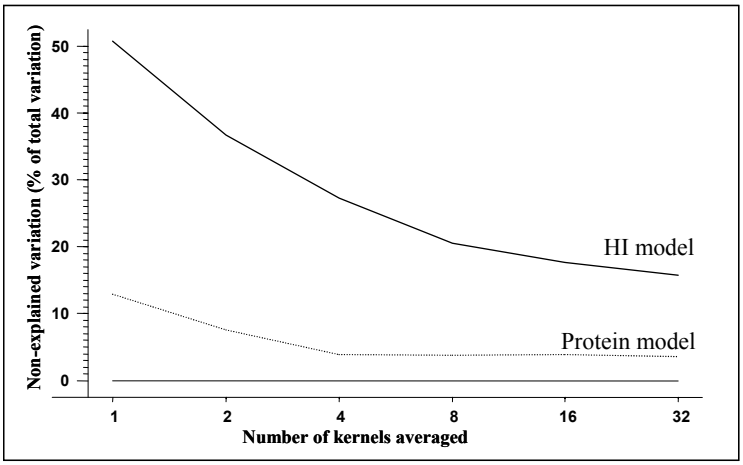

Figure 7. Plot of non-explained variation in percent of total variation versus levels of averaging for the NIT prediction model for hardness (solid line) and protein content (dotted line

The exact same strategy was applied to the NIT model for SKCS HI (only 522 out of the original 523 kernels had valid data and were used), but now the data were sorted according to SKCS HI values. The results are shown in Figure 7 (solid line). It is evident that the non-explained variation in the HI model is considerably higher than for the protein model. As much as 50% of the HI data variation is not explained by the NIT PLSR model using all kernel data, and even after averaging 32 kernels (2^5) the curve is still declining slightly, reaching a level around 15% non-explained variation. When comparing the two models which are based on the exact same NIT

spectra, it is apparent that the decrease in non-explained variation when averaging is much smaller for the protein model compared to the HI model, thus indicating considerably higher measurement errors in the HI measurement. Table III summarises the averaging approach in terms of correlation coefficients (r) and RMSECV for the protein content and SKCS HI prediction models. For the protein content model, a constant prediction error around 0.31% protein is reached after 4 averaging operations. For the SKCS HI model on the other hand, the prediction error never becomes constant. It is seen that by averaging 32 times a very good prediction model for HI is developed reaching a correlation coefficient of 0.93 and a prediction error of 10.4 HI, which corresponds to 10% of the range. This good model suggests that the raw NIT spectra can be used for single seed prediction of SKCS HI. However, the results also show that the single SKCS HI values are not sufficiently accurate to be used as reference values in a NIT-based prediction model.

Table III. Correlation coefficients (r) and prediction errors (RMSECV) of the replicate simulation by averaging kernels for the NIT prediction models for Kjeldahl protein content and SKCS hardness

Number of kernels averaged	Protein model		SKCS HI model	
	r	RMSECV	r	RMSECV
1	0.93	0.58	0.70	18.6
2	0.96	0.44	0.80	15.8
4	0.98	0.32	0.85	13.7
8	0.98	0.31	0.90	11.9
16	0.98	0.31	0.91	11.0
32	0.99	0.31	0.93	10.4

Conclusions

By applying a single kernel procedure in which the non-destructive analyses are conducted prior to the destructive ones, several single kernel characteristics can be linked directly to the same functional unit, the single seed, to be used in cereal processing and breeding. In this investigation, the development of non-destructive screening methods for single seed protein content, vitreousness, density and SKCS

hardness index for the same set of kernels has been studied by applying this type of procedure.

The results of the non-destructive prediction models for single kernel protein, vitreousness, hardness, volume and density are summarised in Table IV. NIT spectroscopy, in combination with multivariate analysis, shows excellent ability to determine protein content, and only shows some ability for determination of single kernel vitreousness. It is concluded that the non-destructive determination of kernel density, on the other hand, either based on NIT spectroscopy or a combination of kernel weight and image analysis, needs further improvement for practical use.

Table IV. Summary of the non-destructive screening methods on single kernels

Data (**X**)	Parameter (**y**)	r[a]	RMSEP[b]	RE[c]
NIT 850-1050 nm (scatter corrected)	Protein	0.98	0.48	4.7%
NIT 850-1050 nm (raw)	Vitreousness[d]	0.76	4.6	12.6%
NIT 850-1050 nm (raw)	Density	0.63	0.035 [e]	13,4%
GrainCheck data plus kernel weight	Volume	0.99	0.001[e]	2.9%
GrainCheck data plus kernel weight	Density	0.70	0.030 [e]	11.5%
NIT 850-1050 nm (raw)	Hardness	0.59	20.2	15.5%

[a]: r is the correlation coefficient between measured and predicted
[b]: RMSEP is the average prediction error
[c]: Relative error (RE); RMSECV or RMSECV divided by the range (max-min values); reported in percent
[d]: Determined using GrainCheck
[e]: Models are validated using cross-validation and RMSEP should be RMSECV

The use of a true single seed hardness determination, in terms of SKCS HI, as reference values in a NIT prediction model resulted in poor predictability. However, the results shown in Figure 7 and Table III suggest that raw NIT spectra actually contain more information about kernel texture than the poor prediction model in Figure 6 suggests. It seems that a single seed reference method for hardness determination with greater accuracy is needed in order to achieve a good and useful NIT prediction model. If this is possible, there seems to be a potential for the development of a model, which would allow the use of raw NIT spectra for a non-destructive single seed hardness analysis.

For practical use of single seed near infrared spectroscopy as an homogeneity tool, it is important that the measurements are automated, as in the new combined SKCS-NIR instrument (Delwiche and Hruschka, 2000;Dowell et al., 1999). The Infratec 1255 single seed measurements provides excellent single seed protein data that are much easier to obtained than the traditional Kjeldahl method, but the single seed handling is still not automated and the measurements are quite time consuming when analysing high number of kernels. When applied automatically, near infrared spectroscopy on single seeds, alone or in combination with other automated non-destructive techniques, has a great potential as routine homogeneity analysis. This might not only be limited to protein and hardness, but also for other quality parameters in cereals, as the method is used today on bulk samples.

Acknowledgments

The authors are grateful to The Directorate for Food, Fisheries and Agri Business for financial support through the Danish Cereal Network-B4. Karen Thomsen is thanked for development and testing of the single seed Kjeldahl method, and The Danish Institute of Agricultural Sciences for providing the wheat samples. Dr. Bo Löfqvist, BoMill AB, Sweden, is thanked for inspiring discussions regarding the manuscript.

Literature cited

Abe, H., Kusama, T. and Kawano, S. 1995. Non-destructive determination of protein content in a single kernel of wheat and soybean by near infrared spectroscopy. In: A. M. C. Davies and P. Williams (Eds.), Near Infrared Spectroscopy: The Future Waves. NIR Publications, Chichester, UK, pp. 457-461.

Berman, M., Bason, M. L., Ellison, F., Peden, G., and Wrigley, C. W. 1996. Image analysis of whole grains to screen for flour-milling yield in wheat breeding. Cereal Chem. 73(3):323-327.

Chtioui, Y., Bertrand, D., Dattée, Y. and Devaux, M.-F. 1996. Identification of seeds by colour imaging: Comparison of discriminant analysis and artificial neural network. J sci food agr 71:433-441.

de Noord, O. E. 1994. The influence of data preprocessing on the robustness and parismony of multivariate calibration models. Chemom Intell Lab Systems 23:65-70.

Delwiche,S.R., 1993. Measurement of single-kernel wheat hardness using near-infrared transmittance. Trans. ASAE 36(5):1431-1437.

Delwiche, S. R., 1995. Single wheat kernel analysis by near-infrared transmittance: protein content. Cereal Chem. 72(1):11-16.

Delwiche, S. R. 1998. Protein content of single kernels of wheat by near-infrared reflectance spectroscopy. J cereal sci 27: 241-254.

Delwiche, S. R. and Hruschka, W. R. 2000. Protein content of bulk wheat from near-infrared reflectance of individual kernels. Cereal Chem. 77(1):86-89.

Delwiche, S. R. and Massie, D. R. 1996. Classification of wheat by visible and near-infrared reflectace from single kernels. Cereal Chem. 73(3):399-405.

Dowell, F. E. 2000. Differentiating vitreous and nonvitreous durum wheat kernels by using near-infrared spectroscopy. Cereal Chem. 77(2):155-158.

Dowell, F. E., Ram, M. S. and Seitz, L. M. 1999. Predicting of scab, vomitoxin, and ergosterol in single wheat kernels using near-infrared spectroscopy. Cereal Chem. 76(4):573-576.

Geladi, P., MacDougall, D. and Martens, H. 1985. Linearization and scatter-correction for near-infrared reflectance spectra of meat. Appl. Spectroscopy 39(3):491-500.

Greenwell, P. and Schofield, J. D. 1986. A starch granule protein associated with endosperm softness in wheat. Cereal Chem. 63(4):379-380.

Martens H. and Næs T. 1993. Multivariate Calibration. Wiley, New York.

Martin, C., Rousser, R. and Brabec, D. 1993. Development of a single-kernel wheat characterization system. Trans. ASAE 36:1399-1404.

Orman, B. A. and Schumann, R. A. 1992. Nondestructive single-kernel oil determination of maize by near-infrared transmission spectroscopy. JAOCS 69(10):1036-1038.

Patrick, B. E. and Jolliff, G. D. 1997. Nondestructive single-seed oil determination of meadowfoam by near-infrared transmission spectroscopy. JAOCS 74(3):273-276.

Pedersen, D. K., Martens, H., Nielsen, J. P. and Engelsen, S. B. 2002. Light absorbance and light scattering separated by Extended Inverted Multiplicative Signal Correction (EIMSC). Analysis of NIT spectra of single wheat seeds. Appl Spectroscopy, submitted.

Pomeranz, Y. and Williams, P. C. 1990. Wheat hardness: Its genetic, structural and biochemical background, measurement and significance. Advances in Cereal Science and Technology 10:471-544.

Wang, D., Dowell, F. E. and Chung, D. S. 2001. Assessment of heat-damaged wheat kernels using near-infrared spectroscopy. Cereal Chem. 78(5):625-628.

Williams, P. C. 1991. Prediction of wheat texture in whole grains by near-infrared transmittance. Cereal Chem. 68(1): 112-114.

Zayas, I., Lai, F. S. and Pomeranz, Y. 1986. Discrimination between wheat classes and varieties by image analysis. Cereal Chem. 63(1):52-56.

Zayas, I., Martin, C. R., Steele, J. L. and Katsevich, A. 1996. Wheat classification using image analysis and crush-force parameters. Trans. ASAE 39(6):2199-2204.

Paper VIII

Screening for dioxin contamination in fish oil by PARAFAC and N-PLSR analysis of fluorescence landscapes

D.K. Pedersen, L. Munck and S.B. Engelsen

Abstract

A preliminary investigation of fish oils demonstrates that fluorescence excitation-emission landscapes evaluated by 3-way chemometric methods may be a candidate for an inexpensive screening method to indicate the level of contamination by dioxins and PCB's which are normally analysed with expensive and time-consuming physicochemical separation techniques such as GC-MS. Fluorescence landscapes of 88 fish oils have been investigated and showed great variation due to species, season and treatment, depicting a variation in natural fluorescent components. The fluorescence landscapes were analysed by PARAFAC. Samples with similar fluorescence fingerprints were selected from a PARAFAC score plot and local significant prediction models with PARAFAC/MLR, N-PLSR and PLSR were established with correlation coefficients in the range from r=0.69 (n=10) to r=0.97 (n=75) for dioxin and r=0.92 (n=12) for PCB. Application of PARAFAC/MLR and N-PLSR to fluorescence landscapes of fish oils resulted in local regression models for dioxin determination with prediction errors below 1 ng/kg, which is comparable to the reference method. In the PARAFAC model, two of the modes give the excitation and emission spectra of the pure underlying fluorophores and the third mode their individual concentrations. Excitation and emission optima for 3-4 PARAFAC components in each data set were identified, representing both positive and negative (quenching) correlation components. It is hypothesized that the quenching correlation may be effected by the joint contribution of chlorinated organic compounds in the fish oil, including dioxins and PCB's. Other explanations for the results are discussed.

Key Words: Dioxin, PCB, fluorescence, multi-way, PARAFAC, N-PLSR

1. Introduction

To an increasing extent food and feed contain residues of environmental contaminants. Monitoring programmes are required to analyse food and feed for the presence of trace amounts of toxic substances such as heavy metals, pesticides, polyaromatic hydrocarbons (PAH), polychlorinated biphenyls (PCB), dioxins, flame retardants as polybrominated diphenylethers (PBDE), and estrogenic compounds such as nonyl phenols and phathalates. Dioxins are widely encountered toxic substances. Dioxins is a short expression for polychlorinated dibenzo-*p*-dioxins (PCDD's) and polychlorinated dibenzofurans (PCDF's). Both are tricyclic, chlorine-substituted, aromatic organic compounds. Polychlorinated biphenyls (PCB's) is another class of environmental contaminants. In practice, dioxins appear as mixtures of various congeners with different concentrations and with extreme variations in toxicity. Dioxins are persistent and lipophilic compounds which bioaccumulate and bioconcentrate in the food chain. Dioxins are very toxic, acutely as well as chronically, and some dioxins might be carcinogens, immunotoxics, endocrine disruptors or teratogens. The number of chlorine substituents may range from one to eight, which means 75 possible PCDD congeners and 135 possible PCDF congeners [1]. Congeners with chlorine substitution in the 2,3,7,8-positions (TCDD) (Fig. 1) are very persistent, bioaccumulative and toxic [1].

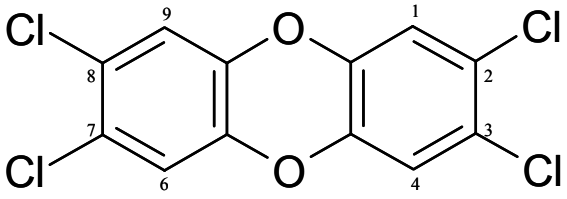

Figure 1. Structure formula of 2,3,7,8-tetrachlorodibenzo-*p*-dioxin: an example of a compound in the dioxin family

Dioxin is formed involuntarily as a by-product of many industrial processes involving chlorine, for example, in producing inflammable transformer oil. It is also

produced when chlorinated substances are burned in the presence of carbon and oxygen and thus released into the environment through air pollution, chemical waste and soil contamination [2]. However, a significant contribution to the dioxin level in the environment originates from natural sources such as forest fires and volcanic eruptions. PCDD and PCDF contamination of food is primarily caused by the deposit of emissions from various sources (e.g. waste incineration, production of chemicals) on farmland and water bodies followed by bioaccumulation in terrestrial and aquatic food chains [2].

Well-known examples of accidental extreme exposure of the local human population to PCDD's, PCDF's and PCB's include the incident at Seveso (Italy), and fires in PCB-filled electrical equipment. At the Seveso accident in 1976 in Northern Italy, a few kilograms of 2,3,7,8-tetrachloro-*p*-dioxin (TCDD) were spread to the surrounding areas by a blast from a chemical factory [1]. High exposure may also be caused by food items accidentally contaminated [2]. In the beginning of 1999 a case involving contamination of feed by transformer oil occurred in Belgium. The contamination caused an epidemic of intoxication of farm animals and resulted in high levels of PCB and dioxin in meat and food [3], which constituted a threat to human health.

In general, the dioxin levels found are very low (ppt-level), the detection of which requires sophisticated and hypersensitive (sub-ppb) physicochemical separation techniques such as high resolution GC-MS. In the case of complex organic molecules such methods are often laborious and very expensive; a typical dioxin analysis takes 2 weeks and costs approximately $1,000 [3]. For this reason, only limited environmental monitoring can be performed. For dioxin analysis the samples are extracted by organic solvents and spiked with isotopically labelled (^{13}C) internal standards before the chemical analysis with sample clean-up and determination with high-resolution gas chromatography/mass spectrometry (HRGC/MS) [1]. Clean-up procedures of complex samples for the subsequent analysis of compounds like PCDD's, PCDF's and PCB's are in most cases time-consuming and associated with problems concerning recovery of the compounds. Unwanted contaminants are usually present in much higher concentrations than the analytes and, in some cases, these are capable of completely hiding the signal from the dioxin analytes or giving false positive results on the analytical equipment used. The problems are in most cases associated with the removal of the unwanted contaminants without affecting

the recovery of the analytes [4]. An international intercalibration study with the participation of nine experienced laboratories measured dioxin in fly ash extracts. Results reported as ng I-TEQ/sample varied 20-23 % [1]. TEQ (Toxic Equivalents) is the total amount of dioxins converted into the most toxic 2,3,7,8 tetrachloro-*p*-dioxins (TCDDs). In this study the international WHO-TEQ standard is used.

Multivariate spectroscopic methods in combination with chemometric data analysis are applied widely for quality control of composition in the food and feed industries [5]. Fluorescence spectroscopy is a useful technique for analysing biological samples and food products due to its selectivity and high sensitivity [6-8]. Fluorescence spectroscopy measures transitions between electronic states, and the light emitted following excitation by monochromatic light is detected. Fluorescence spectroscopy has the potential to rapidly measure sub-ppm levels of complex organic molecules due to the normally low background fluorescence signal (few molecules exhibit fluorescence). Fluorescence spectra are measured as a function of two variables, the excitation and the emission wavelength. For each excitation wavelength a whole emission spectrum is recorded. Two-dimensional spectra (landscapes) are thereby generated for each sample. The landscape structure has the advantage that analytes or interferences emitting in different spectral areas are revealed, and unique resolvation of analytes is possible because of the trilinear data structure [9]. With the PARAFAC algorithm [10] it is possible to perform "mathematical chromatography" and resolve the complex fluorescence landscapes into excitation and emission profiles of the underlying fluorophores [11] and thus obtain their relative concentrations.

This paper outlines an attempt to develop a rapid approximate fluorescence spectroscopic determination of the dioxin content in fish oil. The fluorescence data are primarily investigated by the application of multi-way chemometric methods such as PARAFAC [10, 11] and N-PLSR [12, 13].

2. Materials and methods

2.1. Samples

Fish oils vary considerably with regard to species, fishing territory and season. For calibration purposes it is therefore very important to span the relative variance. As

mentioned previously, traditional dioxin analyses are very expensive, for which reason only a limited material was available for this investigation. The Danish fish industry delivered all fish oil samples, which represented different treatments and deliveries during the production season. The main sample set (set A) consisted of 65 samples that originated from one batch of primarily sand eel fish oil which was treated by different types (poresize) activated charcoal filters and using varying temperature and filter times in order to examine and optimise their potential to remove dioxin and dioxin-related contaminants. Additionally, 10 (set B) and 13 (set C) different untreated (non-filtered) fish oil samples were collected from the different companies in the fish industry. Sample sets A and B originated from the same company, while sample set C originated from another company with different extraction and sample processing. Sample sets A and B (75 samples) were employed for development of dioxin models, whereas set C was not included in these models due to large differences in spectral characteristics. Twelve of the samples from sample set A (A_{PCB}) were employed for PCB models.

2.2. Reference measurements - Dioxin

The dioxin concentration was measured for each of the fish oil samples. The analyses were performed by ERGO Forschungsgesellschaft mbH (Hamburg, Germany). In short, the samples were spiked with ^{13}C-UL-labeled internal standards (Underwriters Laboratories Inc.). The samples were extracted with appropriate solvents. Clean-up was done on multicolumn systems. The measurement was done by means of high-resolution gas chromatography and high-resolution mass spectrometry (HRGS/HRMS). 17 different PCDD's and PCDF's are reported, and the total dioxin content is calculated as WHO-TEQ. The uncertainty of the results is approximately 5 %.

2.3. Reference measurements - PCB

For 12 of the fish oils from sample set A, the PCB concentration was additionally measured. The analyses were performed by ERGO Forschungsgesellschaft mbH (Hamburg, Germany). The samples were spiked with ^{13}C-UL-labeled internal standards, then extracted with appropriate solvents and the clean-up was done on

multicolumn systems. The measurement was done by means of high-resolution gas chromatography and mass spectrometry (HRGS/MS). Twelve different "dioxin alike" coplanar non-ortho and mono-ortho PCB's are reported, and the total PCB content is calculated as WHO-TEQ.

2.4. Spectroscopic measurements

All spectroscopic measurements of the fish oils were performed without sample pre-treatment, and the measurements were made at room temperature.

Fluorescence landscapes were collected on an LS50B spectrofluorometer (Perkin-Elmer, Palo Alto, CA, USA). The excitation-emission landscapes were acquired on the spectrofluorometer using a quartz cuvette in a 90° excitation-emission arrangement. The excitation wavelengths 300, 330, 360, 390, 400, 410, 420, 430, 440 and 450 nm were employed. Emission spectra were recorded from the excitation wavelength plus 20 nm, to avoid Rayleigh scattering, and up to 700 nm in 1.0 nm steps. Excitation and emission slit widths were set to 10 nm [14]. A scan rate of 500 nm/min provided a spectral resolution of approximately 1 nm.

2.5. Chemometrics

Chemometric calculations were performed with Matlab ver. 5.3 (The MathWorks Inc., Natick, MA) installed with PLS Toolbox ver. 2.0.0b (Wise & Gallagher; Eigenvector Technologies, Manson, WA), N-way toolbox (www.models.kvl.dk) and The Unscrambler ver. 7.6 (CAMO ASA, Trondheim, Norway).

2.6. PLSR

Standard bilinear regression employing PLSR (Partial Least Squares Regression) [15] was performed relating fluorescence emission spectra to dioxin content. PLSR is a two-dimensional model (samples x emission wavelength) and the trilinear fluorescence landscape (samples x emission x excitation) cannot be used directly. Instead, the landscapes are unfolded into a two-dimensional sample set in which the emission spectra are arranged as one vector in ascending order with the excitation

wavelength. Full cross-validation was applied throughout this study and only validated results are presented.

2.7. PARAFAC

PARAFAC (PARAllel FACtor analysis) [10] is a multi-way method that facilitates the unique resolution of the underlying components. PARAFAC is a trilinear decomposition method, which conceptually can be regarded as the multi-way analog to the bilinear PCA (Principal Component Analysis) or, more precisely, to alternating least squares (ALS). Three loading matrices with elements a_{in}, b_{jn}, and c_{kn} give a PARAFAC model of a three-way array (x_{ijk}). The trilinear model is found to minimize the sum of squares of the residuals, e_{ijk} in the model, where n is the number of components:

$$x_{ijk} = \sum_{n=1}^{N} a_{in} b_{jn} c_{kn} + e_{ijk}$$

The reason for using PARAFAC instead of PCA was not to obtain a better fit, but rather to obtain a more adequate, robust and interpretable model due to its mathematically unique resolvation. If the data is indeed trilinear and providing the right number of components is used, the underlying spectra of fluorescent analytes including their relative concentration will be found [11]. Thus, the analyte concentration may be obtained directly after scaling, but without need for regression.

2.8. Multiple Linear Regression (MLR)

Multiple Linear Regression (MLR) is a method that combines a set of several independent variables in linear combinations which correlate as closely as possible to the corresponding single reference variable. MLR was applied for regression between PARAFAC fluorescence scores and dioxin reference values. As mentioned above, this regression procedure is not strictly required, if the analyte is directly measured. However, when screening for indirect correlation, we found it safer to use MLR.

2.9. Multi-way calibration

The general multi-way PLSR model (N-PLSR) is considered superior to the unfolded PLSR method owing to stabilisation of the decomposition respecting the original structure of the fluorescence data [13]. In the three-way version of PLSR, the three-way array of independent variables is decomposed into a trilinear model similar to the PARAFAC model. However, for N-PLSR the model is not a least squares fit of the independent data, but seeks in accordance with the philosophy of PLSR to maximise the covariance of the dependent and independent variables. The advantage of using N-PLSR instead of unfolding methods is that N-PLSR is more parsimonious, i.e. simple, and hence easier to interpret. N-PLSR will also be less prone to noise, because the information across all modes is used for the decomposition [13].

3. Results

3.1. Dioxin levels

Distribution of the dioxin concentration in the fish oils in the sample sets A, B and C is shown in Figure 2a.

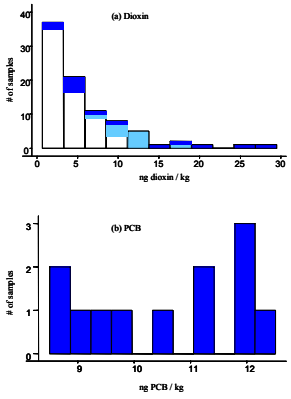

Figure 2. Distribution of dioxin concentration in the fish oils in the three sample sets; sample set A (white), sample set B (pattern) and sample set C (dark) (a) and of PCB concentration in the 12 fish oils in sample set A_{PCB} (b).

The original non-filtered dioxin content of the tobis fish oil used as a basis for set A was 9 ng/kg. Approximately 80 % of the samples from sample set A have a dioxin content less than 6 ng/kg (the total range is 0.7-8.9 ng/kg), while the samples from sets B and C have a mean dioxin content around 11-12 ng/kg (total range 7.4-17.5 ng/kg for set B and 1.0-29.5 ng/kg for set C).

3.2. PCB levels

Distribution of the PCB concentration in the fish oils is shown in Figure 2b. The 12 fish oil samples originate from sample set A. The concentration varies between 8.5 and 12.5 ng/kg. In the untreated sample the original PCB content was 12 ng/kg. The correlation (r) between dioxin concentration and PCB concentration for the 12 fish oil samples from set A_{PCB} is 0.94.

3.3. PARAFAC models for data overview

A 3-component PARAFAC model was generated from fluorescence landscapes of 88 fish oil samples (sample sets A, B and C). In order to get an overview of the data, PARAFAC scores were plotted in two-dimensional scatter plots. Figure 3 shows the plot of PARAFAC score 1 versus PARAFAC score 2. The figure reveals that the fluorescence data of the A samples are all closely related due to the fact that they originate from the same batch. In addition, the fluorescence data of the B samples appear to be related to the A samples, while the fluorescence data obtained from the C samples clearly are more scattered and less related to the A samples. A comparison of the A, B and C samples demonstrates that fish oils vary considerably with regard to, for example, species, fishing territories, season and treatment. Despite this variation, it is noteworthy that all samples from one fish oil company (A + B) fit into one simple PARAFAC model, whereas the samples from the second fish oil company introduce multiple new PARAFAC components. Possible explanations for the new variation found in the C-samples are:

- different sample processing

- addition of antioxidant (C6, C9, C10, C11) and

- oil made of deviant fish species, e.g. caprin (C5, C7, C8)

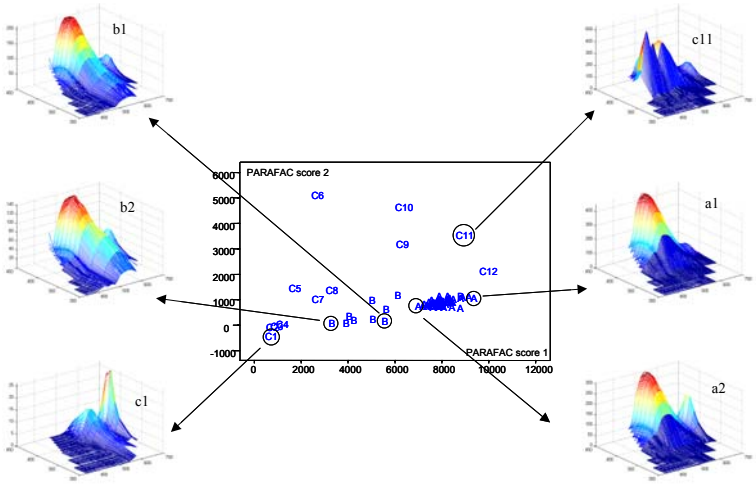

Figure 3. Score plot of PARAFAC component 1 versus component 2 from a 3-component PARAFAC model of sample sets A, B and C. Landscapes of two set A samples (a1 and a2), two set B samples (b1 and b2) and two set C samples (c1 and c2) are shown.

3.4. Comparison of fluorescence landscapes of fish oils

A fluorescence landscape of a fish oil with low dioxin content (a1) and a fish oil with higher dioxin content (a2), the original non-filtered fish oil, from sample set A are shown in Figure 3. The two landscapes express very marked differences in intensity. The high-dioxin oil shows two strong and distinct emission maxima at approximately 545 nm (excitation 435 nm) and 675 nm (excitation 420 nm). In the low-dioxin oil the broad emission maximum at approximately 545 nm (excitation 435 nm) has a higher intensity than the corresponding maximum for the high-dioxin oil, whereas the maximum at 675 nm (ex 420 nm) has almost vanished. This pattern dominates for all the 65 samples in set A. The landscape profiles for the set B samples (b1 and b2) are almost similar to the A set, except that the broad emission maxima vary between 445 nm and 450 nm and the corresponding excitation maxima vary between 430 nm and 440 nm, whereas the sharper emission maximum at

675 nm appears to have a more constant position. Examination of the landscapes (Fig. 3) of the C samples (c1 and c2) originating from other types of fish oil reveals that their profiles are profoundly different from the A and B samples. The fluorescence emission band at 675 nm has the characteristic position of chlorophyll and is most intense for fish oils made from fish at the lowest trophic level, namely tobis, which feed mainly on algae.

3.5. PARAFAC resolvation

PARAFAC models with 1 to 4 components were generated from the fluorescence landscapes of sample set A and from sample set B fish oils, and additional 1- to 4-component PARAFAC models were generated from a combination of sets A and B. The PARAFAC modelling estimates excitation (mode 3) and emission profiles (mode 2) of the measured fluorophores as well as a sample profile assumed to be the concentration of each fluorophore in the samples measured (mode 1). Figure 4 presents the emission profiles (left) and the excitation profiles (right) of the modelled components of a 4-component PARAFAC model of the fish oils from sets A and B.

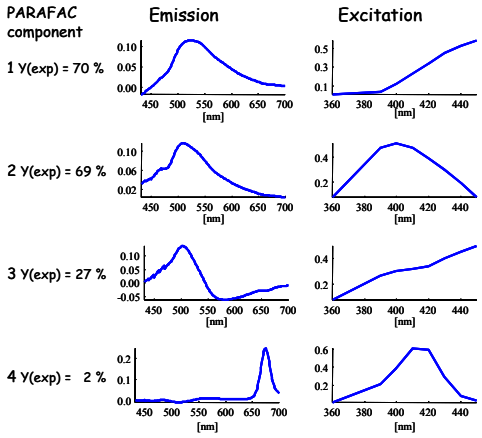

Figure 4. Loadings for the emission mode (left) and the excitation mode (right) of the 4-component PARAFAC model for the combination of sample sets A and B. The percentage of the explanation of the dioxin concentration (Y(exp)) is reported.

The components are displayed in the same order as they are modelled, depending on their contribution to the sample profiles. The found excitation/emission maxima are approximately 450 nm (or higher)/525 nm (component 1), 400 nm/510 nm (component 2), 450 nm (or higher)/505 nm (component 3) and 415 nm/675 nm (component 4). The 675 nm emission maximum is easily identified in the raw data (Fig. 3), while the 525 nm, 510 nm and 505 nm emission maxima are a part of the broad emission maximum measured in the raw data (Fig. 3). The emission maxima found for the PARAFAC loadings for the models of sample set A, sample set B, sample set A + B and sample set A_{PCB} are quite similar in the area of 510-555 nm and at 675 nm.

Multiple Linear Regression (MLR) was applied to the obtained PARAFAC score vectors (mode 1) in order to predict dioxin concentrations in the fish oils. Results are shown in Table 1. The 4-component PARAFAC model (Table 1) generated from set A fish oils provides a good prediction with a prediction error (RMSECV) of 0.7 ng dioxin/kg oil. PARAFAC components ideally reflect pure components and investigation of the single PARAFAC components is therefore of prime importance. Regression models employing one of the four components at a time (Table 2) show that PARAFAC component 4 contributes most to the prediction ability of dioxin for the set A fish oils. PARAFAC components 1 and 3 are negatively correlated to the dioxin concentration, while components 2 and 4 are positively correlated to the dioxin concentration.

The 3-component PARAFAC model (Table 1) generated from set B fish oils provides a poorer prediction with a RMSECV of 2.3 ng dioxin/kg. Data set B consists of only 10 samples and covers the dioxin concentration area from 7.4 to 17.5 ng/kg. For this reason the regression is expected to be less reliable than a regression including many samples. Regression models employing one of the three components at a time (Table 2) show that the individual PARAFAC components are less successful in explaining the dioxin content of the sample set B. PARAFAC components 1 and 3 are negatively correlated to the dioxin concentration, while component 2 has a weak positive correlation to the dioxin concentration. The intensity of the 675 nm maximum (component 3) does not seem to correlate as well with the dioxin concentration as for the A samples (Table 2).

Table 1. Correlation coefficients (*r*) and prediction errors (RMSECV) for regressions (MLR of PARAFAC scores, PLSR and N-PLSR) of dioxin and PCB concentrations in sample set A (dioxin), sample set B (dioxin), sample set A + B (dioxin) and sample set A_{PCB} (PCB).

Data set	Method	# of PC's	*r*	RMSECV [ng/kg]	Y-mean [ng/kg]	Y-range [ng/kg]
A	PARAFAC	1	0.69	1.7	3.6	0.7 - 8.9
	PARAFAC	2	0.71	1.6		
N=65	PARAFAC	3	0.92	0.9		
Dioxin	PARAFAC	4	0.95	0.7		
	PLSR	4	0.95	0.7		
	N-PLSR	4	0.95	0.7		
B	PARAFAC	1	0.12	2.9	11.7	7.4 – 17.5
	PARAFAC	2	0.19	3.1		
N=10	PARAFAC	3	0.62	2.3		
Dioxin	PARAFAC	4	0.53	2.5		
	PLSR	2	0.69	2.0		
	N-PLSR	3	0.63	2.2		
A+B	PARAFAC	1	0.86	1.8	4.7	0.7 – 17.5
	PARAFAC	2	0.85	1.9		
N=75	PARAFAC	3	0.88	1.7		
Dioxin	PARAFAC	4	0.93	1.3		
	PLSR	4	0.97	0.9		
	N-PLSR	4	0.96	1.0		
A_{PCB}	PARAFAC	1	0.69	1.0	10.6	8.5 – 12.5
	PARAFAC	2	0.77	0.9		
N=12	PARAFAC	3	0.93	0.5		
PCB	PARAFAC	4	0.88	0.7		
	PLSR	2	0.92	0.5		
	N-PLSR	2	0.92	0.5		

The 4-component PARAFAC model (Table 1) generated from the A and B samples also provides a good prediction with a RMSECV of 1.3 ng dioxin/kg. This regression covers the dioxin concentration area from 0.7 to 17.5 ng/kg with 75 samples, which is a large enough sample set to be regarded as reliable. Regressions employing one of the four components at a time (Table 2) show that

PARAFAC components 1 and 2 contribute most to the prediction ability for the combination of sets A and B. The combination of all 4 components in MLR provide the best model. PARAFAC components 1 and 2 are negatively correlated to the dioxin concentration, while components 3 and 4 have a weak positive correlation to the dioxin concentration.

Table 2. Excitation (Ex) and emission (Em) maxima for the PARAFAC profiles for sample set A, sample set B, sample set A + B and sample set A_{PCB}. Regression coefficients (r), quotation of negative or positive correlation to dioxin and PCB concentration respectively, explained dioxin or PCB concentration (Y(exp)) and prediction errors (RMSECV) for MLR regressions of PARAFAC scores 1, 2, 3 and 4 in sample set A (dioxin), sample set B (dioxin), sample set A + B (dioxin) and sample set A_{PCB} (PCB).

Data set	PARAFAC component	Ex Max. [nm]	Em Max. [nm]	R	Correlation	Y(exp) [%]	RMSECV [ng/kg]
A	1	435	550	0.69	Negative	48	1.7
	2	430	555	0.71	Positive	51	1.6
Dioxin	3	395	510+540	0.75	Negative	57	1.5
	4	415	675	0.89	Positive	78	1.1
B	1	>450	550	0.58	Negative	33	2.3
	2	395	510	0.02	Positive	0	3.0
Dioxin	3	410	675	0.51	Negative	26	2.5
A+B	1	>450	525	0.84	Negative	70	2.0
	2	400	510	0.83	Negative	69	2.0
Dioxin	3	>450	505	-0.52	Positive	27	3.8
	4	415	675	0.13	Positive	2	3.6
A_{PCB}	1	410	555+675	0.85	Positive	72	0.7
	2	410	555+675	0.80	Negative	64	0.8
PCB	3	430	525	0.85	Negative	72	0.7

PARAFAC models with 1 to 4 components were separately generated from the 12 PCB samples from sample set A_{PCB} fish oils. The obtained PARAFAC score vectors (mode 1) were applied in MLR in order to predict PCB concentrations in the fish oils. Results are shown in Table 1. The 3-component PARAFAC model (Table 1) provides a good prediction with a RMSECV of 0.5 ng PCB/kg. Regressions employing one of the three components at a time (Table 2) show that all the PARAFAC components contribute to the prediction ability. PARAFAC components

2 and 3 are negatively correlated to the PCB concentration, while component 1 is positively correlated to the PCB concentration.

3.6. PLSR results

Bilinear PLSR models were made for the dioxin and PCB references. The results, listed in Table 1, show that PLSR models based on the unfolded fluorescence spectra provide good correlations to the fish oil dioxin content when employing 4 components, especially for set A (r=0.95) and for the combination of set A and set B (r=0.97). Compared to the regression model of fish oil samples from set A (RMSECV=0.7 ng/kg), the added variation in set B leads to a higher prediction error (RMSECV=0.9 ng/kg), but the correlation remains good. Compared to the results reported from an international intercalibration study [1] with participation of nine experienced laboratories measuring dioxin in fly ash extracts as ng I-TEQ/sample with variations around 20-23 % corresponding on average to approximately ± 1 ng/kg in the collected samples, much better prediction errors should not be expected due to the reproducibility of the reference method and due to the fact that the reference value is a compound toxicity number and not a concentration value of a single analyte following beer's law of proportionality. The relatively poor results for set B modelling can be explained by the few (10) samples involved. The PCB results (Table 1) show that PLSR models of unfolded fluorescence spectra also provide good correlations to the fish oil PCB content when employing 2 components.

3.7. N-way regressions

N-PLSR modelling was applied to both sets (A and B) and to the combination of set A and set B. In the three-way version of N-PLSR the three-way array of spectroscopic measurements is decomposed into a trilinear model. The three modes are: 1) the sample mode, 2) the emission wavelengths and 3) the excitation wavelengths. In order to avoid too many missing data points in the three-way array, two emission (mode 3) spectra were left out: the emission spectra for excitation at 300 nm and at 330 nm. For the eight remaining excitation wavelengths only the emission area from 430-700 nm was used.

The correlation coefficient (r=0.95) and the prediction error (RMSECV=0.7 ng/kg) for data set A equal the results for the two-way PLSR of unfolded data (r=0.95 and RMSECV=0.7 ng/kg). The regression results are shown in Table 1. The results for data set B show a slightly higher prediction error in the three-way approach (RMSECV=2.2 ng/kg) than in the unfolded approach (RMSECV=2.0 ng/kg). Predicted dioxin concentration versus measured dioxin concentration for the N-PLSR model of data set A + data set B is shown in Figure 5. Even though N-PLSR models are supposed to be more parsimonious and easier to interpret, the predictive ability is rarely improved over the unfolded PLSR [13]. The reason for this is probably that fluorescence is correlated to chemical parameters with few emission wavelengths and that the potential added stability to the noise component is insignificant. The N-PLSR loadings for dioxin regression in data set A show expected maxima at 510 nm (loading 1), 675 nm (loading 2), 540 nm (loading 3) and 555 nm (loading 4). The emission maxima found for the N-PLSR loadings for the models of data set B and data set A + B are in the area of 510-555 nm and at 675 nm as well as found by the PARAFAC model.

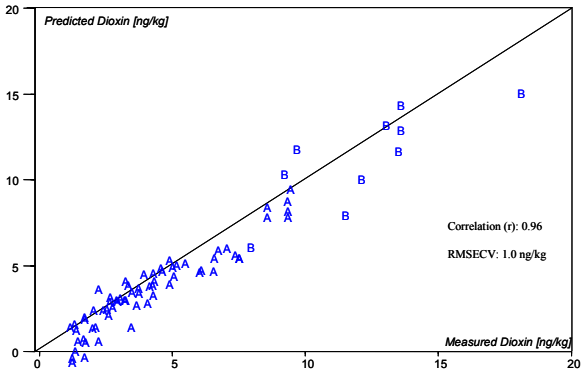

Figure 5. Predicted dioxin concentration versus measured dioxin concentration for the N-PLSR model (4 PC's) for sample set A (A) and sample set B (B) fish oil samples (75). The correlation coefficient (r) and the prediction error (RMSECV) are reported.

N-PLSR modelling was applied to the 12 PCB samples from data set A_{PCB}. The correlation coefficient (r=0.92) and the prediction error (RMSECV=0.5 ng/kg) equal

the results for the two-way PLSR of unfolded data (r=0.92 and RMSECV=0.5 ng/kg). The regression results are shown in Table 1.

4. Discussion

Fluorescence is a highly sensitive and chemically specific spectroscopic tool for screening, which yields unique spectra [7, 8]. One would think that matrices of biological origin with many different fluorophores and quenching substances might produce fluorescence landscapes which are too complex to be resolved. However, trilinear chemometric models such as PARAFAC are well suited for interpreting fluorescence landscapes, because the loadings give the excitation and emission spectra of the underlying fluorophores [11]. In an earlier example, when monitoring production streams and products from the sugar beet industry [6], it was demonstrated that PARAFAC is able to resolve four fluorophores from white sugar: two amino acids - tryptophane and tyrosine and two high molecular coloured reaction products between amino acids/phenoles and reducing sugars. The four fluorophores were confirmed by HPLC analysis [17]. It was concluded from that investigation that fluorescence spectroscopy and the PARAFAC algorithm are able to automatically select a covariate model in the form of four indicator substances which were able to predict colour as well as related process and quality parameters.

In the present study we attempt to trace fluorescence patterns in fish oil by three-way chemometric analysis and relate them to dioxin and PCB contamination. This is conceptually parallel to the sugar process example [6], although much less controlled. They are both examples of exploratory data analysis based on induction, where one measures first in a preliminary approach with a minimum of hard assumptions. This hypothesis-generating method has only become possible thanks to new instruments, the computer and chemometric software [6, 18].

The high price of the dioxin and PCB analyses limits this preliminary fish oil study. Information about species prevalence, catch site, fish storage conditions and time as well as raw material analyses and process parameters in the fish oil/meals company would have been helpful in interpreting the results. Different fish species are prevalent at different times of the year in the industry. Feeding conditions for the fish are also seasonal and dependent on fishing territory. When studying

fluorescence fingerprints in fish meals we have previously been able to pick up such seasonal fluctuations through principal component analysis of the spectra [19].

The heterogeneity of the origin of the present fish oil collection of the 88 samples is illustrated in the PARAFAC fluorescence score plot and indicated by the fluorescence landscapes in Figure 3. The different correlation analyses in Table 2 indicate that sample set consistency is of prime importance, for which reason local modelling is needed. The local model with sample set A (n=65) is based on an experiment which with various degrees of success was able to remove dioxins and PCB's with chemical and physical filters, yielding correlation models up to r=0.95 (RMSECV=0.7 ng dioxin/kg). Sample set B with different unfiltered fish oils (n=10) with similar fluorescence landscapes shows a less satisfying, but significant correlation (up to r=0.69 RMSECV=2.0 ng dioxin/kg). A combination of these samples (A+B) in an N-PLSR analysis (Figure 5) gives a linear correlation of r=0.96 and RMSECV=1.0 ng dioxin/kg. If the outlier sample set C originating from another factory is included, the N-PLSR correlation is reduced to r=0.42. The importance of local models is in accordance with the experience of chemometric modelling in the agricultural industry [5] where Near InfraRed (NIR) and InfraRed (IR) spectroscopy is widely employed based on inductive PLSR models. Global models need time and great effort to catch and include all possible extreme samples which at first are treated as outliers and include them in the calibration model. They should be able to cover the whole problem space evenly in the calibration mode. The different fluorescence landscapes from the 88 fish oil samples, which in this investigation are represented in a PARAFAC score plot, are too diverse and scattered in order to form a viable global model for dioxin. Prediction models should, of course, be based on data sets without significant outliers.

The multivariate approach, which in fluorescence – 3-way analysis, allows for very precise automatic identification of outliers with unique patterns, which is the essence of a scientific basis for inductive analysis [6]. However, the fluorescence and PARAFAC resolution has its limits. As seen in Figure 4, two of the excitation spectra proposed by the model do not have discernable optima, as do all emission spectra. This is because the resolution of the excitation dimension in the fluorescence landscape, due to time restrictions, has been selected to be roughly 30 nm, while it is 1 nm on the emission side. The resolved emission spectra in Figure 4 are therefore more reliable than the excitation spectra.

In the present investigation it is found that the group of fluorophores that are causing the broad emission maxima in the area of 510-555 nm are negatively correlated to the dioxin concentration. This suggests that the fluorescence in this area is quenched as the dioxin concentration rises, or rather when the total amount of chlorinated aromatic compounds rises. The sharper emission maximum at 675 nm was found to be positively correlated with the dioxin concentration for the set A samples. This implies that the fluorophore causing the 675 nm maximum (probably chlorophyll – it has the typical dual peak behaviour with excitation maxima at approximately 420 nm and 510 nm) follows the dioxin through the filtering treatments. The results demonstrate that fluorescence spectroscopy could serve as a guide in exploring how fluorophores covariate in fish oil, which could be indicative of the level of lipophilic pollutants. The composition of fish oils directly mimics the diet of the fish, containing several natural fluorophores like vitamin E and xanthines. Non-fluorescencent compounds can also be detected due to their ability to quench fluorescence [7, 8]. It is clear from this investigation that PARAFAC components of the fluorescence analysis contain positive as well as negative elements (Table 2), the latter being indicative of quenchers. Chlorinated lipophilic pollutants like dioxins and PCB's are not likely to fluoresce, because the chlorine atom is a strong quencher [7, 8]. Nor is it likely that dioxins could be directly detected in the ecological production chains due to very low sub-ppb levels.

The present results should be taken with precaution. Dioxins do not fluoresce, so the correlations must be related to complex chemical covariate objects in the fish oil matrix. However, from our experience in fluorescence spectroscopy we take the liberty to generate a few fresh hypotheses regarding the fluorescence screening method for dioxin to be further tested. **Hypothesis 1)** The combined total of chlorinated hydrocarbons may be causing the negative correlation with dioxin due to quenching. A positive correlation (r=0.94) was found between dioxin and coplanar PCBs in the fish oil material. Against this hypothesis may be the fact that inter-molecular quenching is magnitudes less than intra-molecular quenching. **Hypothesis 2)** Natural lipophilic fluorescent chemical compounds generated, for example, by plankton may be accumulated in fish oil and could be used as indicators for establishing the level of a fish oil sample in the ecological feeding pyramid indirectly correlated to dioxin. They could both have the potential to indicate the trophic level of the fish catch in the ecological feeding pyramid. **Hypothesis 3)** By

removing dioxins with chemical filters, fluorescent indicator substances are proportionally absorbed. Thus, fluorescence analysis could be a candidate for monitoring the efficiency of the cleaning procedure. **Hypothesis 4)** Man-made fluorescent chemical compounds could also serve as similar indicators for dioxin, preferably if they are produced together with the dioxin and PCB.

Further research could give profitable results based on the hypotheses generated in this explorative investigation. It is concluded that a holistic exploratory approach to environmental chemistry is needed coupled with sensitive, specific and economical screening methods evaluated by chemometrics in a dialogue with classical analytical methods. Thus, screening methods could be developed that are operational under field conditions and in industry. The scientific basis of this inductive approach is the high precision of the fluorescence/multi-way approach [6] in characterising the uniqueness of and the relationships between the fish oil samples. Such methods would allow direct chemical fingerprinting of a range of natural and polluting molecules which are concomitant in the ecological production chains and which can be introduced as markers. Fluorescence spectroscopy combined with three-way chemometric analysis is such a candidate screening method with a great potential because of its sensitivity and specificity.

Acknowledgements

The authors are indebted to Foreningen for Danmarks Fiskemel- og Fiskeolieindustri (DK), 999 TripleNine (Fiskerihavnsgade 35, DK-6701 Esbjerg) and FF of Denmark (Havnevagtvej 12, DK-9990 Skagen) for supplying the fish oil samples with the corresponding chemical reference data. The authors wish to thank the Ministry of Food, Agriculture and Fisheries for financial support during the projects “Early post mortem measurement of WHC (water-holding capacity) and drip loss in fresh pork “ and “Novel type of unique mathematical identification of spectral components from hyphenated spectroscopic methods applied to food samples”. Associate professor Rasmus Bro and Ph.D. student Charlotte Møller Andersen are acknowledged for help with the data analysis and interpretation, and Gilda Kischinovsky is acknowledged for assistance with the manuscript.

References

[1] Jensen A.A. *Dioxins. Sources, levels and exposures in Denmark*. Danish Environmental Protection Agency. 1997.

[2] WHO Consultation. *Assessment of the health risk of dioxins: Re-evaluation of the Tolerable Daily Intake*. May 25-29 1998, Geneva, Switzerland.

[3] Belgian Government, Federal Ministry of Agriculture and Federal Ministry of Health. PCB and dioxin contamination in the feed and food chain in Belgium. http://dioxin.fgov.be/pe/ene00.htm. 1999.

[4] Zebühr Y., Näf C., Bandh C., Broman D., Ishaq R. and Pettersen H. An automated HPLC separation method with two coupled columns for the analysis of PCDD/Fs, PCBs and PACs. *Chemosphere* 1993, **27**(7): 1211-1219.

[5] Munck L., Nørgaard L., Bro R., Andersson C.A., Wittrup C. and Hansen P.W. New chemometric multivariate method for an overview of food processes. *Dairy Science and Technology. Proceedings of 25th International Dairy Congress*, Aarhus, Denmark 1998: 372-382.

[6] Munck L., Nørgaard L., Engelsen S.B., Bro R. and Andersson C.A. Chemometrics in food science - a demonstration of the feasibility of a highly exploratory, inductive evaluation strategy of fundamental scientific significance. *Chemometric Intell. Lab. Syst.* 1998, **44**(1): 31-60.

[7] Rettig W., Strehmel B., Schrader S. and Seifert H. *Applied Fluorescence in Chemistry, Biology and Medicine*. Springer-Verlag, Berlin. 1999.

[8] Munck L. *Fluorescence Analysis in Foods*. Longman Singapore Publishers Ltd., Singapore. 1989.

[9] Ho C.N., Christian G.D. and Davidson E.R. Application of the method of rank annihilation to quantitative analyses of multicomponent fluorescence data from the video fluorometer. *Anal. Chem.* 1978, **50**: 1108-1113.

[10] Harshman R.A. Foundations of the PARAFAC procedure: models and conditions for an 'explanatory' multi-modal factor analysis. *UCLA Working Paper. Phonetics* 1970, **16**: 1-84.

[11] Bro R. PARAFAC. Tutorial and applications. *Chemometric Intell. Lab. Syst.* 1997, **38**: 149-171.

[12] Stahle L. Aspects of the analysis of 3-way data, *Chemometric Intell. Lab. Syst.* 1989, **7**: 95-100.

[13] Bro R. Multiway calibration. Multi-linear PLS. *J. Chemometrics* 1996, **10**: 47-61.

[14] Nørgaard L. Spectral resolution and prediction of slit widths in fluorescence spectroscopy by two- and three-way methods. *J. Chemometrics* 1996, **10** (5-6): 615-630.

[15] Martens H. & Næs T. *Multivariate Calibration*. Wiley, UK. 1989.

[16] Bro R. Exploratory study of sugar production using fluorescence spectroscopy and multi-way analysis. *Chemometric Intell. Lab. Syst.* 1999. **46**: 133 -147.

[17] Baunsgaard D., Andersson C.A., Arndal A. and Munck L. Multi-way chemometrics for mathematical separation of fluorescent colorants and color precursors from spectrofluorimetry of beet sugar and beet sugar juice as validated by HPLC analysis. *Food Chem.* 2000. **70**: 113-121.

[18] Andersson C.A. *Exploratory Multivariate Data Analysis with applications in Food Technology*. PhD Thesis, 2000. The Royal Veterinary and Agricultural University. Food Technology. Rolighedsvej 30 DK-1958 Frederiksberg, Denmark pp. 202.

[19] Dahl P.L., Christensen B.M., Munck L., Larsen E.P. and Engelsen S.B. Can spectroscopy in combination with chemometrics replace minks in digestibility tests?, *J. Sci. Food Agr.* 2000, **80:** 365-374.